THE UNIVERSITY OF OKLAHOMA

GRADUATE COLLEGE

STUDIES OF THE COMPLEXATION REACTIONS OF POLYETHER IONOPHORE ANTIBIOTICS NIGERICIN AND SALINOMYCIN WITH LEAD(II), ZINC, CALCIUM, MAGNESIUM, SODIUM AND POTASSIUM CATIONS.

A Dissertation

SUBMITTED TO THE GRADUATE FACULTY

In partial fulfillment of the requirements for the degree of

DOCTOR OF PHILOSOPHY

By

BO TAN

Norman, Oklahoma

2005

Downloaded from SHAREOK. Persistent Handle URL: https://hdl.handle.net/11244/832

UMI Number: 3161638



UMI Microform 3161638

Copyright 2005 by ProQuest Information and Learning Company.
All rights reserved. This microform edition is protected against unauthorized copying under Title 17, United States Code.

ProQuest Information and Learning Company
300 North Zeeb Road
P.O. Box 1346
Ann Arbor, MI 48106-1346

STUDIES OF THE COMPLEXATION REACTIONS OF POLYETHER IONOPHORE ANTIBIOTICS NIGERICIN AND SALINOMYCIN WITH LEAD (II), ZINC, CALCIUM, MAGNESIUM, SODIUM AND POTASSIUM CATIONS

A Dissertation APPROVED FOR THE

DEPARTMENT OF CHEMISTRY AND BIOCHEMISTRY

By

_____

Dr. Richard W. Taylor

_____

Dr. C. LeRoy Blank

_____

Dr. Robert L. White

_____

Dr. Robert P. Houser

_____

Dr. Lance L. Lobban

© Copyright by BO TAN 2005
All Rights Reserved

ACKNOWLEDGMENTS

Without many people's help I could not have finished this project. First, I would like to express great gratitude to my mentor Dr. Richard W. Taylor. He not only inspired me to seek chemistry knowledge but also taught me to write in proper scientific English. I would like to extend my appreciation to the members of my advisory committee: Dr. C. LeRoy Blank, Dr. Robert L. White, Dr. Robert P. Houser, and Dr. Lance L. Lobban for their valuable suggestions, encouragement, and cooperation in scheduling committee meetings.

I owe my achievement to my parents. Their teaching made me who I am today. I would like to thank my husband Huaxing Pei for his emotional support and confidence in my ability to complete this project. I would like to thank all the members in my family for their unconditional love and care through my life.

I acknowledge the help of Dr. Susan Alguindigue for her meticulous training on the NMR machine. I would like to thank Dr. Li Zhang in obtaining the mass-spectrometry data.

I truly thank all my friends and colleagues among the students and the personnel of the Department of Chemistry and Biochemistry. We spent so many days together laughing. Their great friendship made my experience at OU a wonderful memory. I especially thank my lab mates Dr. Olga Shimelis, Kendra Cox and Gary Smith. We share the knowledge of chemistry and our own cultures.

All the teachers in my life not only provided me knowledge but also taught me how to learn. The last acknowledgement is for them.

Financial support for this work was provided by the University of Oklahoma Department of Chemistry and Biochemistry in the form of Teaching Assistantship. Part of this project is also funded by the National Institutes of Health and OCAST.

TABLE OF CONTENTS

Page

LIST OF TABLES……...viii

LIST OF FIGURES……..xii

ABSTRACT…….xxi

CHAPTER I. INTRODUCTION…….1

A. Introduction…….1

B. Nigericin complexes, literature overview……..15

C. Salinomycin complexes, literature overview…….22

References……32

CHAPTER II. EXPERIMENTAL…….36

A. Reagents…….36

B. Stability of salinomycin 80% methanol-water solutions……44

C. Preparation of lead-salinomycin (1:2) and lead-nigericin (1:2) complexes……...47

D. pH* measurements…….50

E. Determination of CO_2 percentage in tetramethylammonium hydroxide titrant solutions……..……...56

F. Measurement of protonation constants and metal complexation constants of nigericin and salinomycin……..……58

G. Nuclear Magnetic Resonance (NMR) studies of nigericin-lead and salinomycin-lead complexes……..…….61

References……62

CHAPTER III. CD STUDIES OF IONOPHORE-METAL BINDING..……...64

References……..……...83

CHAPTER IV. STUDIES OF LEAD NIGERICIN-COMPLEXES……84

A. Elemental analysis of lead-nigericin complexes……...84

B. Characterization of lead-nigericin complexes by mass-spectrometry……...86

C. UV spectrophotometric studies of lead-nigericin complexation reactions……...88

D. The protonation constant for nigericin in 80% methanol-water determined using potentiometric titrations……95

E. Potentiometric studies of metal binding……98

F. NMR studies of free nigericin and nigericin complexes……130

References……163

CHAPTER V. STUDIES OF LEAD-SALINOMYCIN COMPLEXES

……..164

A. Elemental analysis of lead-salinomycin complex……...……..164

B. Characterization of the lead-salinomycin complex by ESI-MS……...……166

C. UV spectrophotometric studies of lead-salinomycin complexation reactions……..169

D. The protonation constant for salinomycin in 80% methanol-water determined using potentiometric titrations……173

E. Potentiometric studies of metal binding……178

F. NMR studies of free salinomycin and salinomycin complexes…….207

References……...235

CHAPTER VI. DISCUSSION…….236

A. Isolation and characterization of the lead complexes with the polyether ionophores nigericin and salinomycin……..237

B. Protonation constants of salinomycin and nigericin…….239

C. Complexation constants of metal ions with nigericin and salinomycin……241

D. NMR Studies of ligand conformation and binding in lead complexes having 1:2 lead-ionophore stoichiometry……247

E. Discussion of the lead transport data and the results of the present study compared with monensin and ionomycin……...250

References……...259

LIST OF TABLES

Page

Table I.1. Stoichiometries reported for complexes of carboxylic acid ionophores with mono- and divalent cations and the associated modes of transport……6

Table I.2. Polyether antibiotics and their cation selectivities……..9

Table I.3. Literature values of the protonation constants of nigericin in various organic solvents and heterogeneous media……16

Table I.4. Literature values of the complex formation constants of nigericin with monovalent cations in various organic solvents and heterogeneous media..17

Table I.5. Identities of donor atoms of nigericin and grisoxin salts in different states..18

Table I.6. Values of the complex formation constants of salinomycin and narasin with monovalent cations……...23

Table II.1. Autoprotolysis constants for 80% methanol-water (I = 0.05 M)……..54

Table III.1. CD spectra characteristic and stoichiometry of ionophore lead complexes in 80% methanol-water…….66

Table IV.1. Experimental and calculated elemental composition of lead-nigericin (1:2) complexes…….84

Table IV.2 Calculated values of the protonation constant for nigericin in 80% methanol-water…….96

Table IV.3 Log β_X values obtained from potentiometric titrations of nigericin acid (HL) and sodium……..100

Table IV.4 Log β_X values obtained from potentiometric titrations of nigericin acid (HL) and potassium……..105

Table IV.5 Log β_X values obtained from potentiometric titrations of nigericin acid (HL) and calcium (II)……...108

Table IV.6. Log β_X values obtained from potentiometric titrations of nigericin acid (HL) and Zn (II)……...112

Table IV.7. Log β_X values obtained from potentiometric titrations of nigericin acid (HL) and Mg (II)……..116

Table IV.8. Log β_X values obtained from potentiometric titrations of nigericin acid (HL) and lead (II) in 80% methanol-water……..122

Table IV.9. Average values of cumulative equilibrium constants (log β_X) for nigericin with various ions in 80% methanol-water……..129

Table IV.10 The three-bond and two-bond coupling in the HMBC spectrum of the tetraethylammonium salt of nigericin in $CDCl_3$ at 25 ^oC……...139

Table IV.11. ^1H and ^{13}C NMR chemical shifts of the sodium salt of nigericin at 25 ^oC ……..141

Table IV.12. ^1H and ^{13}C NMR chemical shifts (ppm) of the sodium salt of nigericin in CD_3OD at 25^oC…….142

Table IV.13. ^1H and ^{13}C NMR chemical shifts (ppm) of the free acid form of nigericin in $CDCl_3$ at25^oC……...143

Table IV.14. ^1H and ^{13}C NMR chemical shifts (ppm) of the free acid form of nigericin in CD_3OD and C_6D_6 at 25^oC…….144

Table IV.15. ^1H and ^{13}C NMR chemical shifts (ppm) of the tetraethylammonium salt of nigericin in CD_3OD and $CDCl_3$ at 25^oC……...145

Table IV.16. ^1H and ^{13}C NMR chemical shifts (ppm) of nigericin-lead (2:1) complexes in CD_3OD and $CDCl_3$ at 25^oC using a Varian 300 MHz spectrometer……155

Table V.1. Experimental and calculated elemental composition of lead-salinomycin (1:2) complexes……...164

Table V.2. Calculated values of the protonation constant for salinomycin in 80% methanol-water……...173

Table V.3. Log β_X values obtained from potentiometric titrations of salinomycin acid (HL) and potassium…….181

Table V.4. Log β_X values obtained from potentiometric titrations of salinomycin acid (HL) and calcium (II)……..186

Table V.5. Log β_X values obtained from potentiometric titrations of salinomycin acid (HL) and zinc (II)……191

Table V.6. Log β_X values obtained from potentiometric titrations of salinomycin acid (HL) and Mg (II)……196

Table V.7. Log β_X values obtained from potentiometric titrations of salinomycin acid (HL) and lead (II) in 80% methanol-water……199

Table V.8. Average values of cumulative equilibrium constants (log β_X) for salinomycin with various ions in 80% methanol-water……..206

Table V.9. Different C-H coupling behavior shown in HMBC spectrum (Figure V.35) of the tetraethylammonium salt of salinomycin in $CDCl_3$ at 25 ^oC……213

Table V.10. ^1H and ^{13}C NMR chemical shifts (ppm) of sodium salinomycin in $CDCl_3$ using a Varian 500 MHz spectrometer and literature values at 25 ^oC……214

Table V.11. ^1H and ^{13}C chemical shifts (ppm) of sodium salinomycin using a Varian 300 MHz spectrometer and literature values using a 500 MHz spectrometer at 25^oC……215

Table V.12. ^1H and ^{13}C experimental chemical shifts (ppm) of the free acid form of salinomycin using a Varian 500 MHz spectrometer and literature values in $CDCl_3$……..216

Table V.13. ^1H and ^{13}C experimental chemical shifts (ppm) of the free acid form of salinomycin using a Varian 500 MHz spectrometer in CD_3OD…….217

Table V.14. ^1H and ^{13}C NMR chemical shifts (ppm) of tetraethylammonium salt of salinomycin in CD_3OD and $CDCl_3$ at 25 ^oC (experimental values)……...218

Table V.15. ^1H and ^{13}C NMR chemical shifts (ppm) of the lead-salinomycin (1:2) complex in CD_3OD and $CDCl_3$ at 25 ^oC (experimental values) using a Varian 300-MHz spectrometer…….228

Table VI.1. Literature values of the protonation constants of nigericin in various organic solvents and heterogeneous media at 25.^oC……...…….239

Table VI.2. Protonation constants of ionophore antibiotics and acetic acid in different solvent systems at 25.^oC (ionic strength = 0 M)…….240

Table VI.3. Average values of overall complexation constants of nigericin with metal ions in 80% methanol-water at 25.^oC…..……. 242

Table VI.4. Values of the complex formation constants of nigericin with monovalent cations in various organic solvents and heterogeneous media at 25 ^oC…..243

Table VI.5. Average values for overall complexation constants of salinomycin with metal ions in 80% methanol-water…….244

Table VI.6. The protonation constants and overall formation constants for nigericin, salinomycin and monensin[2] with several metals obtained in 80% methanol-water……245

LIST OF FIGURES

Page

Figure I.1. Structures of representative polyether carboxylic acid ionophores……3

Figure I.2. Illustration of metal-oxygen and hydrogen bonding scheme in the potassium salt of nigericin, as inferred from the X-ray structure……5

Figure I.3. Examples of transport modes and reactions involved in cation transport across a lipophilic membrane……7

Figure I.4. The transport scheme in a system using 1-palmitoyl-2-oleoyl-*sn*-glycerophosphatidylcholine (POPC) vesicles loaded with Quin-2 as the indicator in a buffered medium……10

Figure I.5. Selectivity trends for membrane transport of divalent cations by salinomycin and nigericin at pH 7.0 from studies using phospholipid vesicles……11

Figure I.6. Structure of nigericin with numbering schemes for carbon (plain) and oxygen (bold italic) atoms……15

Figure I.7. Structure of grisorixin with numbering schemes for carbon (plain) and oxygen (bold italic) atoms……16

Figure I.8. Structure of salinomycin with numbering schemes for carbon (plain) and oxygen (bold italic) atoms……22

Figure II.1. ESI-MS of Na salinomycin salt from Sigma and Na nigericin salt from Fluka, recorded in the positive ion mode……38

Figure II.2. Plot of activity coefficients[23] vs. molal ionic strength for HCl in 80% methanol-water……52

Figure II.3. Gran plot for a titration of perchloric acid with tetramethylammonium hydroxide……57

Figure III.1. CD spectra from the titration of Na salinomycin with $Pb(ClO_4)_2$ in 80% methanol-water at 25^{o}C……68

Figure III.2. CD spectra from the titration of NaSal with $Pb(ClO_4)_2$ in 80% methanol-water at 25^{o}C after being smoothed using the Aviv CD program……69

Figure III.3. Plot of the ellipticity at 293 nm versus the concentration ratio $[Pb]_{Total}$:$[salinomycin]_{Total}$ for the titration of NaSal with $Pb(ClO_4)_2$ in 80% methanol-water……70

Figure III.4. CD spectra from the titration of Na narasin with $Pb(ClO_4)_2$ in 80% methanol-water at 25°C……..71

Figure III.5. Plot of the ellipticity at 294 nm versus the concentration ratio $[Pb]_{Total}$:$[narasin]_{Total}$ for the titration of Na narasin with $Pb(ClO_4)_2$ in 80% methanol-water……72

Figure III.6. CD spectra from the titration of sodium lasalocid with $Pb(ClO_4)_2$ in 80% methanol-water at 25°C……..73

Figure III.7. Plot of the ellipticity at 296 nm versus the concentration ratio $[Pb]_{Total}$:$[lasalocid]_{Total}$ for the titration of Na lasalocid with $Pb(ClO_4)_2$ in 80% methanol-water……74

Figure III.8. CD spectra from the titration of Na nigericin with $Pb(ClO_4)_2$ in 80% methanol-water at 25°C……..75

Figure III.9. CD spectra from the titration of Na nigericin with $Pb(ClO_4)_2$ in 80% methanol-water at 25°C after being smoothed using the program Aviv CD……76

Figure III.10.Plot of the ellipticity at 238 nm versus the concentration ratio $[Pb]_{Total}$:$[nigericin]_{Total}$ for the titration of NaNi with $Pb(ClO_4)_2$ in 80% methanol-water……77

Figure III.11.CD spectra from the titration of ammonium maduramicin with $Pb(ClO_4)_2$ in 80% methanol-water at 25°C……78

Figure III.12.Plot of the ellipticity at 239 nm versus the concentration ratio $[Pb]_{Total}$:$[maduramicin]_{Total}$ for the titration of Na maduramicin with $Pb(ClO_4)_2$ in 80% methanol-water……79

Figure III.13.CD spectra from the titration of sodium monensin with $Pb(ClO_4)_2$ in 80% methanol-water at 25°C……..80

Figure III.14.CD spectra of the free acid form of salinomycin (0.1 mM) with addition of different metal solutions in 80% methanol-water as indicated in the graph. ……...82

Figure IV.1. A. Part of the positive ion ESI-MS for the 1:1 nigericin-lead complex. B. The calculated isotopic pattern for $C_{40}H_{67}O_{11}Pb$……..87

Figure IV.2. UV-Vis spectra from the titration of lead perchlorate with nigericin in 80% methanol-water at 25°C……89

Figure IV.3. Plot of the absorbance resulting from each aliquot of 0.0129 M sodium nigericin added versus the ratio of the total nigericin to total lead concentrations……...90

Figure IV.4. Change in absorbance at 248 nm as a function of [Hnigericin] at pH* 3.361 ……...94

Figure IV.5. A potentiometric titration curve for 6.00 mL of a solution containing 0.846 mM the free acid form of nigericin at an ionic strength of 0.05 M (TEAP) in 80% methanol-water at 25 ^{o}C……...97

Figure IV.6. Potentiometric titration curves for various stoichiometric ratios of sodium-nigericin in 80% methanol-water at 25 ^{o}C……..101

Figure IV.7. A potentiometric titration curve for 6.22 mL of a solution containing 1.29 mM nigericin acid and 1.29 mM sodium chloride at an ionic strength of 0.05 M Et_4NCl (25 ^{o}C)……102

Figure IV.8. A potentiometric titration curve for 8.2 mL of a solution containing 0.64 mM nigericin acid and 2.52 mM sodium chloride at an ionic strength of 0.05 M Et_4NCl (25 ^{o}C)……103

Figure IV.9 A species distribution curve for sodium-nigericin complexes in 80% methanol-water solution as a function of p[H]……...104

Figure IV.10. A potentiometric titration curve for 6.1 mL of a solution containing 0.85 mM nigericin acid and 1.15 mM potassium chloride at an ionic strength of 0.05 M Et_4NCl (25 ^{o}C)……106

Figure IV.11. Species distribution curves for potassium-nigericin complexes in 80% methanol-water solution as a function of p[H]……...107

Figure IV.12. Potentiometric titration curves for various stoichiometric ratios of calcium-nigericin in 80% methanol-water at 25 ^{o}C……..109

Figure IV.13. A potentiometric titration curve for 6.15 mL of a solution containing 0.93 mM nigericin acid and 2.42 mM calcium chloride at an ionic strength of 0.05 M Et_4NCl (25 ^{o}C)……110

Figure IV.14. Species distribution curves for calcium-nigericin complexes in solution as a function of p[H]……..111

Figure IV.15. Potentiometric titration curves for various stoichiometric ratios of zinc-nigericin in 80% methanol-water at 25 ^{o}C……..113

Figure IV.16. A potentiometric titration curve for 7.70 mL of a solution containing 0.80 mM nigericin acid and 1.79 mM zinc perchlorate at an ionic strength of 0.05 M TEAP (25 ^{o}C)…….114

Figure IV.17. Species distribution curves for zinc-nigericin complexes in 80% methanol-water as a function of p[H]…….115

Figure IV.18. Potentiometric titration curves for various stoichiometric ratios of magnesium-nigericin in 80% methanol-water at 25 ^{o}C……..117

Figure IV.19. A potentiometric titration curve for 6.10 mL of a solution containing 0.99 mM nigericin acid and 2.41 mM magnesium perchlorate at an ionic strength of 0.05 M TEAP (25 ^{o}C)…….118

Figure IV.20. Species distribution curves for zinc-nigericin complexes in 80% methanol-water solution as a function of p[H]……...119

Figure IV.21. Plot of thermodynamic solvent autoprotolysis constants as a function of methanol-water solvent composition……..121

Figure IV.22. Potentiometric titration curves for various stoichiometric ratios of lead-nigericin in 80% methanol-water at 25 ^{o}C……..123

Figure IV.23. A potentiometric titration curve for 6.08 mL of a solution containing 0.77 mM nigericin acid and 0.41 mM lead perchlorate in 80% methanol-water at an ionic strength of 0.05 M TEAP (25 ^{o}C)…….124

Figure IV.24. A potentiometric titration curve for 5.10 mL of a solution containing 0.6 mM nigericin acid and 0.61 mM lead perchlorate at an ionic strength of 0.05 M TEAP (25 ^{o}C)…….125

Figure IV.25. Species distribution curves for lead (II)-nigericin complexes in 80% methanol-water solution as a function of p[H]……...126

Figure IV.26. Species distribution curves for lead (II)-nigericin complexes in 80% methanol-water solution as a function of p[H]……...127

Figure IV.27. Potentiometric titration curves for 6.00 mL of a solution containing 0.7 mM nigericin acid and various metals at the specified stoichiometric ratios and an ionic strength of 0.05 M (25^{o}C)…….……..128

Figure IV.28. Structure of nigericin with numbering schemes for carbon (plain) and oxygen (bold italic) atoms……..131

Figure IV.29. ^{1}H NMR spectrum of the sodium-nigericin complex in CD_3OD at 25^{o}C …….134

Figure IV.30. ^{13}C NMR spectrum of sodium-nigericin complex in CD_3OD at 25°C…..135

Figure IV.31. DEPT spectrum of the free acid form of nigericin in $CDCl_3$ at 25°C…...136

Figure IV.32. HSQC spectrum of the tetraethylammonium salt of nigericin in CD_3OD at 25°C……137

Figure IV.33. HMBC spectrum of the tetraethylammonium salt of nigericin in $CDCl_3$ at 25°C…….138

Figure IV.34. Schematic representation of the W type bond conformation……139

Figure IV.35. ^{1}H NMR spectrum of the lead-nigericin (1:2) complex in $CDCl_3$ at 25°C……..147

Figure IV.36. ^{13}C NMR spectrum of the lead-nigericin (1:2) complex in $CDCl_3$ at 25°C……..148

Figure IV.37. HMBC spectrum of the lead-nigericin (1:2) complex in $CDCl_3$ at 25°C..149

Figure IV.38. HSQC spectrum of the lead-nigericin (1:2) complex in $CDCl_3$ at 25°C…150

Figure IV.39. ^{1}H NMR spectrum of the lead-nigericin (1:2) complex in CD_3OD at 25°C…….151

Figure IV.40. ^{13}C NMR spectrum of the lead-nigericin (1:2) complex in CD_3OD at 25°C…….152

Figure IV.41. HSQC spectrum of the lead-nigericin (1:2) complex in CD_3OD at 25°C …….153

Figure IV.42. HMBC spectrum of the lead-nigericin (1:2) complex in CD_3OD at 25°C ……..154

Figure IV.43. Plots of the difference in ^{13}C chemical shifts, $\Delta\delta^{13}C$, between the free acid or complexed forms and the anionic form of nigericin for each carbon atom in $CDCl_3$……..159

Figure IV.44. Plots of the difference in ^{13}C chemical shifts, $\Delta\delta^{13}C$, between the free acid or complexed forms and the anionic form of nigericin for each carbon atom in CD_3OD……162

Figure V.1. A. Part of the positive ion ESI-MS for lead-salinomycin complex……166

Figure V.2. A. Peaks for the 1:1 lead-salinomycin molecular ion in positive ion ESI-MS. B. The calculated isotopic pattern for $C_{42}H_{69}O_{11}Pb$……...167

Figure V.3. A. Peaks for the 1:2 lead-salinomycin molecular ion in positive ion ESI-MS. B. The calculated isotopic pattern for $C_{84}H_{139}O_{22}Pb$……..168

Figure V.4. A. Peaks for the 2:2 lead-salinomycin molecular ion in positive ion ESI-MS. B. The calculated isotopic pattern for $C_{84}H_{137}O_{22}Pb_2$…….168

Figure V.5. UV-Vis spectra from the titration of lead perchlorate with salinomycin in 80% methanol-water at 25^{o}C……..170

Figure V.6. Plot of the absorbance resulting from each aliquot of sodium salinomycin added versus the ratio of the total salinomycin to total lead concentrations…….171

Figure V.7. Change in absorbance at 248 nm as a function of [Hsalinomycin] at pH* 3.177……172

Figure V.8. A potentiometric titration curve for 10.00 mL of a solution containing 1.01 mM salinomycin acid at an ionic strength of 0.05 M TEAP in 80% methanol-water (25 ^{o}C)……...174

Figure V.9. CD spectra for a solution of 2.7 mL 0.647 mM salinomycin acid containing 5 mM MES and 5 mM HEPES in 80% methanol-water at different pHs using 0.1 M $HClO_4$ and 0.1 M Et_4NOH…….176

Figure V.10. Plot of the ellipticity values at 215 nm as a function of p[H]…….177

FigureV.11. A potentiometric titration curve for 10.05 mL of a solution containing 1.01 mM salinomycin acid and 0.982 mM NaCl at an ionic strength of 0.05 M (TEAP) in 80% methanol-water (25 ^{o}C)…….180

Figure V.12. Potentiometric titration curves for various stoichiometric ratios of potassium-salinomycin in 80% methanol-water at 25 ^{o}C……...182

Figure V.13. A potentiometric titration curve for 5.08 mL of a solution containing 3.2 mM salinomycin acid and 1.81 mM potassium chloride at an ionic strength of 0.05 M Et_4NCl (25 ^{o}C)……...183

Figure V.14. A potentiometric titration curve for 5.05 mL of a solution containing 1.2 mM salinomycin acid and 1.12 mM potassium chloride at an ionic strength of 0.05 M Et_4NCl (25 ^{o}C)……...184

Figure V.15. Species distribution curves for potassium-salinomycin complexes in 80% methanol-water solution as a function of p[H]……..185

Figure V.16. Potentiometric titration curves for various stoichiometric ratios of calcium-salinomycin in 80% methanol-water at 25 ^{o}C……187

Figure V.17. A potentiometric titration curve for 10.06 mL of a solution containing 1.24 mM salinomycin acid and 0.53 mM calcium at an ionic strength of 0.05 M TEAP (25 ^{o}C)……..188

Figure V.18. A potentiometric titration curve for 5.25 mL of a solution containing 1.14 mM salinomycin acid and 4.59 mM calcium at an ionic strength of 0.05 M TEAP (25 ^{o}C)……..189

Figure V.19. Species distribution curves for calcium-salinomycin complexes in 80% methanol-water solution as a function of p[H]……...190

Figure V.20. Potentiometric titration curves for various stoichiometric ratios of zinc-salinomycin in 80% methanol-water at 25 ^{o}C……192

Figure V.21. A potentiometric titration curve for 10.63 mL of a solution containing 1.15 mM salinomycin acid and 1.288 mM zinc perchlorate at an ionic strength of 0.05 M TEAP (25 ^{o}C)…….193

Figure V.22. A potentiometric titration curve for 6.50 mL of a solution containing 0.938 mM salinomycin acid and 1.95 mM zinc perchlorate at an ionic strength of 0.05 M TEAP (25 ^{o}C)…….194

Figure V.23. Species distribution curves for zinc-salinomycin complexes in 80% methanol-water solution as a function of p[H]……...195

Figure V.24. A potentiometric titration curve for 6.93 mL of a solution containing 1.09 mM salinomycin acid and 3.54 mM magnesium perchlorate at an ionic strength of 0.05 M TEAP (25 ^{o}C)……...197

Figure V.25. Species distribution curves for magnesium-salinomycin complexes in 80% methanol-water solution as a function of p[H]……..198

Figure V.26. Potentiometric titration curves for various stoichiometric ratios of lead-salinomycin in 80% methanol-water at 25 ^{o}C……200

Figure V.27. A potentiometric titration curve for 10.40 mL of a solution containing 0.90 mM salinomycin acid and 0.49 mM lead perchlorate at an ionic strength of 0.05 M TEAp (25 ^{o}C)…….201

Figure V.28. A potentiometric titration curve for 5.62 mL of a solution containing 0.916 mM salinomycin acid and 1.35 mM lead perchlorate at an ionic strength of 0.05 M TEAP (25 ^{o}C)…….202

Figure V.29. Species distribution curves for salinomycin-lead (II) complexes as a function of p[H] in 80% methanol-water……203

Figure V.30. Species distribution curves for lead (II)-salinomycin complexes in 80% methanol-water solution as a function of p[H]……...204

Figure V.31. Potentiometric titration curves for 10.00 mL of a solution containing 0.9 mM salinomycin acid and various metals at an ionic strength of 0.05 M at 25^{o}C……205

Figure V.32. Structure of salinomycin and narasin molecules with numbering schemes for carbon (plain style) and oxygen (bold italic) atoms……..207

Figure V.33. ^{1}H NMR spectrum of the sodium salt of salinomycin in $CDCl_3$ at 25^{o}C..209

Figure V.34. ^{13}C NMR spectrum of the free acid form of salinomycin in $CDCl_3$ at 25^{o}C……210

Figure V.35. HMBC spectrum of the tetraethylammonium salt of salinomycin in $CDCl_3$ at 25^{o}C……211

Figure V.36. HSQC spectrum of the free acid form of salinomycin in CD_3OD at 25^{o}C ……212

Figure V.37. ^{1}H NMR spectrum of the lead-salinomycin (1:2) complex in $CDCl_3$……220

Figure V.38. ^{13}C NMR spectrum of the lead-salinomycin (1:2) complex in $CDCl_3$…...221

Figure V.39. HMBC spectrum of the lead-salinomycin (1:2) complex in $CDCl_3$……..222

Figure V.40. HSQC spectrum of the lead-salinomycin (1:2) complex in $CDCl_3$……223

Figure V.41. ^{1}H NMR spectrum of the lead-salinomycin (1:2) complex in CD_3OD…..224

Figure V.42. ^{13}C NMR spectrum of the lead-salinomycin (1:2) complex in CD_3OD….225

Figure V.43. HMBC spectrum of the lead-salinomycin (1:2) complex in CD_3OD…….226

Figure V.44. HSQC spectrum of the lead-salinomycin (1:2) complex in CD_3OD……..227

Figure V.45. Plots of the difference in ^{13}C chemical shifts, $\Delta\delta^{13}C$, between the free acid or complexed forms and the anionic form of salinomycin for each carbon atom in CD_3OD……...231

Figure V.46. Plots of the difference in ^{13}C chemical shifts, $\Delta\delta^{13}C$, between the free acid or complexed forms and the anionic form of salinomycin for each carbon atom in $CDCl_3$…….234

Figure VI.1. Schematic diagram of possible nigericin coordination in the lead (II) complex in methanol based on ^{13}C chemical shift data……..248

Figure VI.2. Schematic diagram of possible salinomycin coordination in the lead(II) complex in chloroform based on 13C chemical shift data……..249

Figure VI.3. Selectivity trends for membrane transport of divalent cations by nigericin, monensin and ionomycin at pH 7.0 using phospholipid vesicles……...250

Figure VI.4. Dependence of Pb^{2+} transport across POPC membranes by three ionophores on the concentrations of ionophores using phospholipid vesicles……..252

Figure VI.5. Dependence of Pb^{2+} transport across POPC membranes by three ionophores on the concentration of free Pb^{2+} using phospholipid vesicles……...252

Figure VI.6. Dependence of Pb^{2+} transport by nigericin on external pH……253

Figure VI.7. Species distribution curves for lead-nigericin complexes as a function of p[H] in 80% methanol-water…….255

Figure VI.8. Selectivity trends for membrane transport of divalent cations by salinomycin at pH 7.0 using phospholipid vesicles……257

Figure VI.9. Species distribution curves for lead-salinomycin complexes as a function of p[H] in 80% methanol-water……..258

ABSTRACT

Salinomycin and nigericin are members of polyether carboxylic acid ionophores. Recent studies using phospholipid vesicles show that these compounds transport Pb^{2+} with high selectivity relative to other divalent cations. The purpose of this work is to help explain the high selectivity of these ionophores for lead over other metal ions.

CD studies in 80% methanol-water indicate that Pb^{2+} forms 1:1 complexes almost quantitatively with monensin, nigericin, narasin, maduramicin, and salinomycin. UV-Vis titrations in 80% methanol-water showed the same result for nigericin and salinomycin.

The lead complexes of nigericin and salinomycin were prepared and were subjected to elemental and MS analysis. Equilibrium constants are determined in this work. The protonation constants of salinomycin (log K_H 6.49) and nigericin (log K_H 7.02) were determined in 80% methanol-water using potentiometric titrations. For a better comparison of the complexation behavior of the ionophores with lead and other metal ions, potentiometric titrations were done in the presence of metal ions. Complex formation constants, K_{ML}, were determined in 80% methanol-water for H^+, Pb^{2+}, Na^+, K^+, Ca^{2+}, Mg^{2+}, and Zn^{2+} by potentiometric titrations. The values of K_{PbL} are 5 x 10^2 to 10^4 larger than the corresponding constants, K_{ML}, for the other metals tested. These studies also show that a substantial fraction of complexed ionophores exist as the neutral PbL(OH) species at pH 7-8. Information about the binding sites and conformation of ionophore-metal complexes was obtained using NMR. All the information obtained in this work was used to explain the lead transport data from the vesicle studies of ionophores.

Chapter I

Introduction

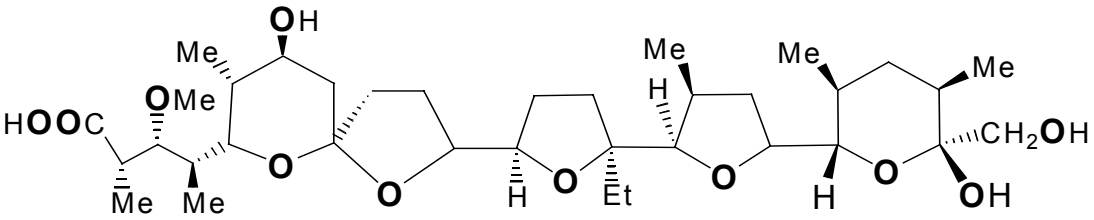
Ionophores are defined as compounds that can efficiently transport metal ions across phospholipid bilayer membranes, such as the plasma and subcellular membranes of cells. These compounds can be made synthetically or occur as natural products. The latter group can be divided into two classes; the so-called electrogenic and electroneutral ionophores. Valinomycin, a neutral dodecadepsipeptide, is a good example of the electrogenic class. The major feature of this group is the absence of ionizable functional groups with the result that charged ionophore complexes are formed with metal ions. When those complexes are transported across a membrane, a net positive charge will be built up in one side of the membrane. In this case the cation transport is determined by the transmembrane potential. Members of the electroneutral class possess a carboxylic acid group that can produce neutral ionophore-metal complexes. There is no charge build up during metal ion transport across the membrane. The transmembrane pH gradients and the cation distribution affect the cation transport. All the ionophores studied in this dissertation belong to the electroneutral class.

In 1951 antibiotics X-206, X-464 (nigericin), and lasalocid A were reported by Berger et al.[1,2], which is the first report on the electroneutral compounds. In the same year, nigericin was isolated independently by another group[1,2]. It was discovered that all those acidic compounds possessing antimicrobial activity are very soluble in organic solvents. At that time scientists were not able to elucidate the structures of the antibiotics, and because of their toxicity they were considered to be useless as medicinal agents. There were few reports about the electroneutral compounds in 16 years, however,

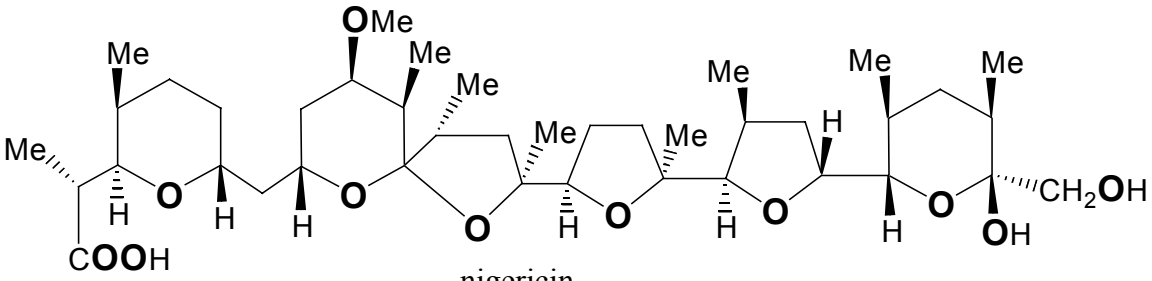
in 1967 the structure of the polyether antibiotic, monensin, was reported[3]. The anticoccidial activity of nigericin and monensin was reported[4], which has great potential utility in the poultry industry and motivated the search for new polyether antibiotics. More than 100 polyether ionophores have been discovered since that year[5]. These compounds are produced primarily by soil bacteria of the *Streptomyces* genus[6]. It was suggest that their biological function was contributed by dissipation of the metal cation gradient (such as K^+) in the membranes[7].

Comparison of the structures of several polyether ionophores shown in Figure I.1 reveals that there are some common features distinctive for this group. They are acyclic molecules with a carboxyl group at one end and a tertiary hydroxyl group at the other end, except A23187. Because of a hydrogen bond between these two functional groups, ionophores maintain a pseudo-cyclic conformation in nonpolar solvents[8-11]. Multiple tetrahydrofuran and tetrahydropyran rings provide ether functions throughout the carbon chain and many methyl or ethyl groups are present along the hydrocarbon backbone. Due to the existence of ether groups, those ionophores are also called polyether ionophores. Many of them have a characteristic mono- or dispiroketal system.

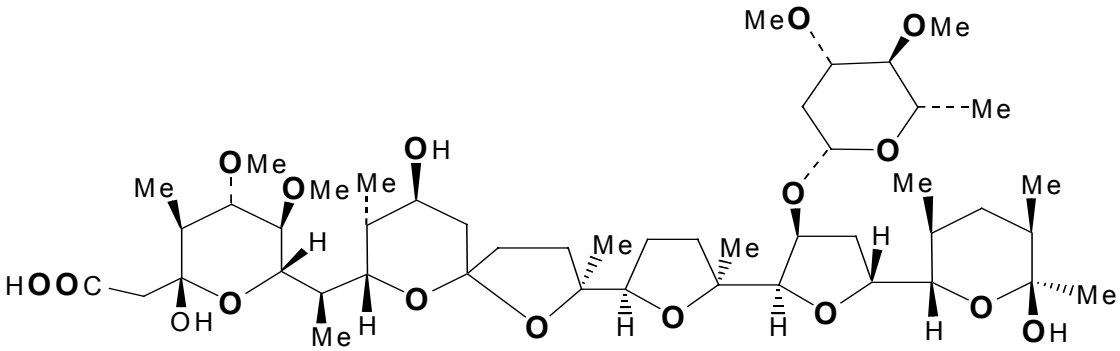
Upon complexation, most of oxygen atoms are oriented inward to bind with a cation, as shown in Figure I.2. The hydrophilic moieties are in the interior and the hydrophobic ones are in the exterior. These structural features enable polyether ionophores to transport ions by passive diffusion.



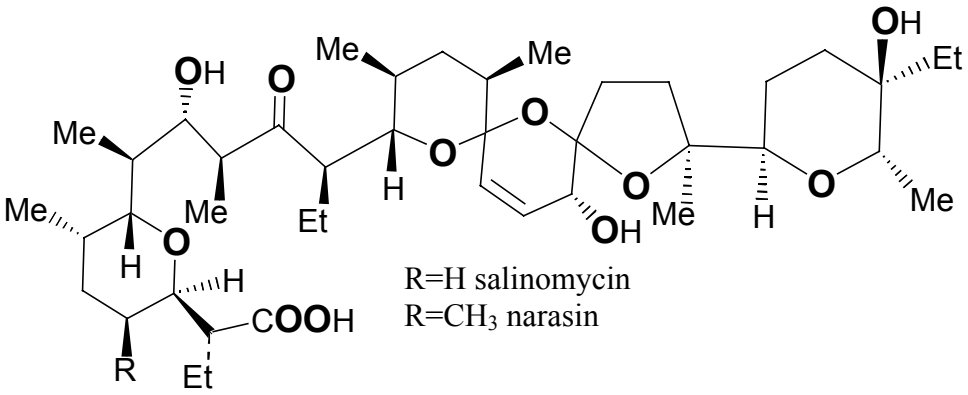
monensin



nigericin

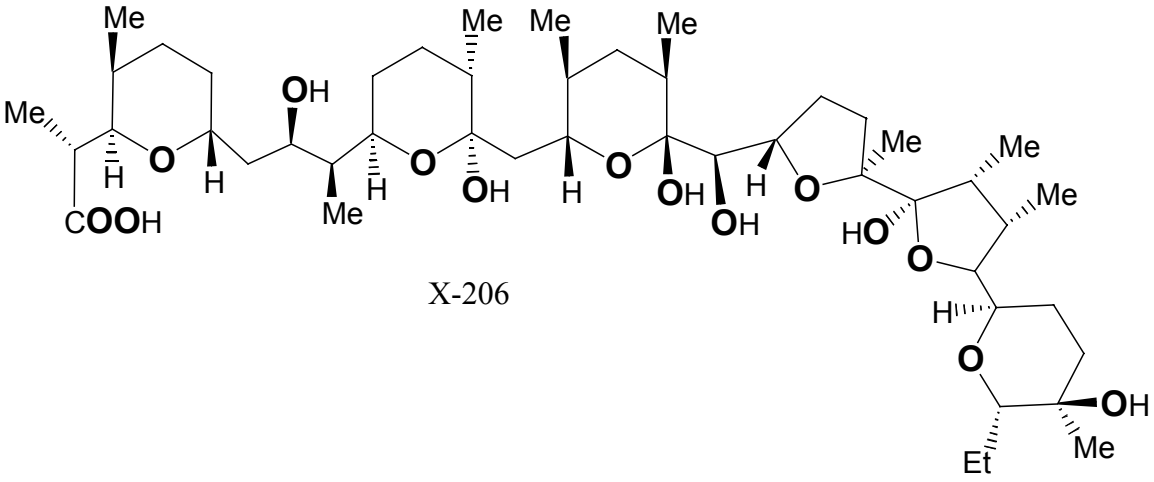


maduramicin

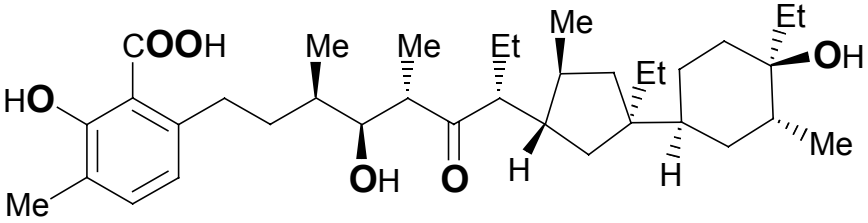


R=H salinomycin
R=CH_3 narasin

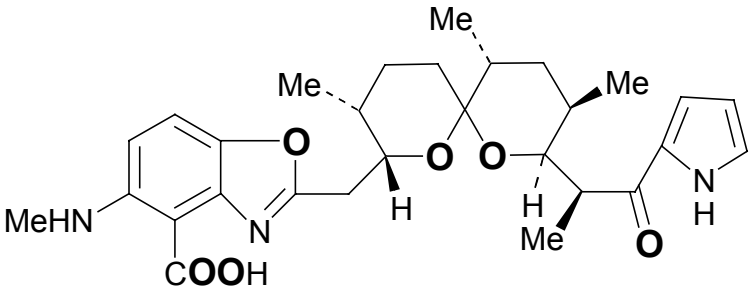
Figure I.1. Structures of representative polyether carboxylic acid ionophores.



X-206



lasalocid



A23187

Figure I.1. (continued) Structures of representative polyether carboxylic acid ionophores.

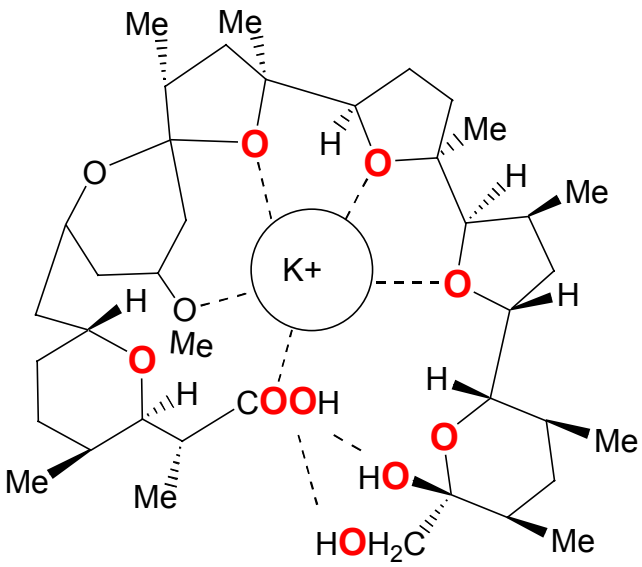


Figure I.2. Illustration of metal-oxygen and hydrogen bonding scheme in the potassium salt of nigericin, as inferred from the X-ray structure[12].

The popular model of transport was proposed by Painter and Pressman[13]. Ionophores partition near or at the surface of the membrane with the hydrophilic moieties (e.g. COO^-) oriented outward. Initially, the carboxylate group captures the solvated metal ion, then the other polar groups replace the solvent molecules in a stepwise fashion and eventually wrap around the metal ion after the structural reorientation. The complex then diffuses through the membrane. On the other side of membrane the reverse process takes place and the metal ion is revealed. Another ion or proton is picked up by the ionophore to allow completion of the transport cycle[13]. Those are the major steps and reactions involved in cation-ionophore transport although the details maybe differ from one system to another. It was found that diffusion is not the rate-limiting step at high cation concentrations in this model based on ^{23}Na and ^{39}K NMR studies of nigericin[14]. Efficient transport in this process requires moderately stable ionophore-metal complexes, so that the ionophore is able to release the metal ion after transport.

There are two transport modes based on the form of the complexes that conduct ions through the membranes. For the electroneutral mode there is no net movement of charge across the membrane because complexes are usually neutral. The transport is driven by pH and the concentration gradients of ions. For the electrogenic mode there is a net movement of charge across the membrane. Usually the ligand is neutral, and the complex is charged. The transport is driven by a potential gradient across the membrane. Polyether carboxylic acid ionophores are found to use both transport modes[15,16]. Table I.1 provides the overall reactions reported for both modes and Figure I.3 shows the transport cycle for the different modes. It is generally believed that the electroneutral mode accounts for most cation transport by carboxylic acid ionophores such as sodium and potassium transport by monensin[17] and calcium transport by A23183 and ionomycin[18,19].

Table I.1. Stoichiometries reported for complexes of carboxylic acid ionophores with mono- and divalent cations[15,16] and the associated modes of transport.[a]

class of carboxylic acid ionophores	overall reaction of complex formation	transport mode
monovalent (L^-) (e.g., salinomycin and nigericin)	$M^+ + L^- \rightleftharpoons ML$ $M^+ + L^- + H^+ \rightleftharpoons MLH^+$ $M^+ + 2L^- + H^+ \rightleftharpoons ML_2H$	electroneutral electrogenic electroneutral
divalent (L^-) (e.g., A23187)	$M^{2+} + L^- \rightleftharpoons ML^+$ $M^{2+} + 2L^- \rightleftharpoons ML_2$ $M^+ + L^- + X^- \rightleftharpoons MLX^+$	electrogenic electroneutral electrogenic
divalent (L^{2-}) ionomycin	$M^{2+} + L^{2-} \rightleftharpoons ML$ $M^+ + L^{2-} + H^+ \rightleftharpoons MLH^+$	electroneutral electrogenic

[a] M represents metal ions and X represents anions.

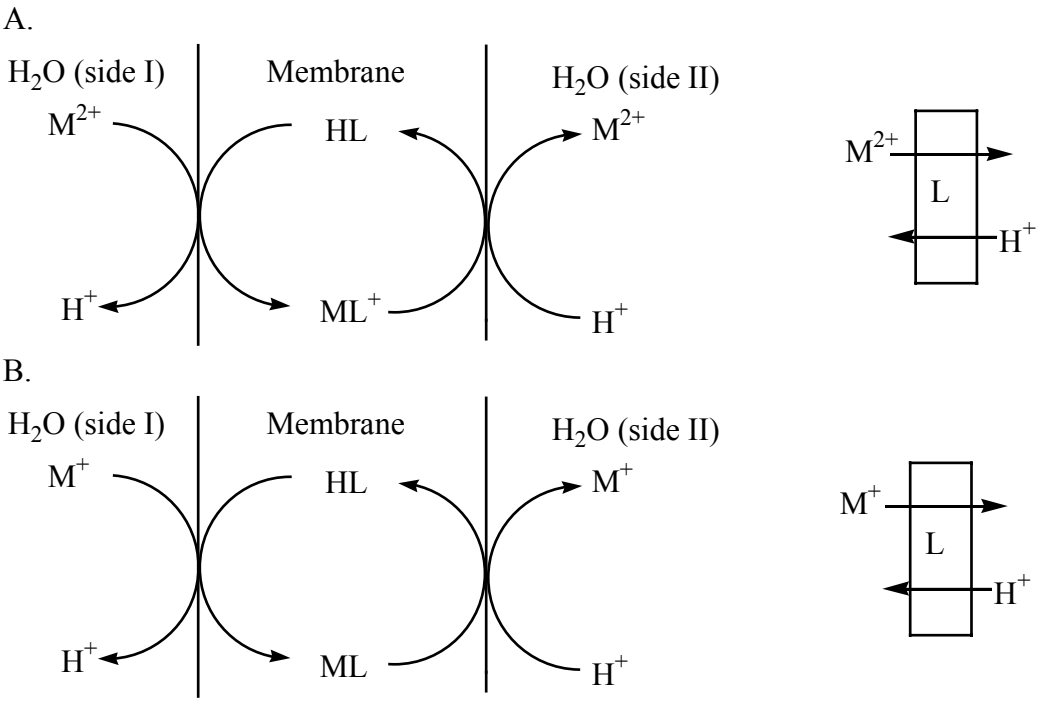


Figure I.3. Examples of transport modes and reactions involved in cation transport across a lipophilic membrane. The net results are shown in the smaller diagrams on the right. A. electrogenic transport; L = lasalocid, M = Ba; B. electroneutral transport; L = nigericin, M = K.

Identification of the transport mode requires knowledge of transporting species. At physiological pH, the carboxylic acid group in most polyether ionophores is partially or completely ionized. Due to limitations of the cavity size polyether ionophores can only host one metal ion at maximum. The ratio of ionophore to metal can be 1:1, or 2:1 for smaller ionophores such as lasalocid and A23187[15,16]. Higher or lower ratios were thought to be not stable enough to carry across the membranes. Protons and small anions can be attached to the complexes, as shown in Table I.1. Ionomycin with its higher charge (-2) is distinguished from other ionophores. It forms 1:1 neutral complexes with divalent cations[15]. Therefore, the overall charge of the complexes is determined by the stoichiometry of complexes and the charges of the ionophores and metal ion. Other

anions, such OH^- and Cl^-, may have some role in forming neutral compounds with ionophores and cations, as shown in Table I.1.

Polyether ionophores have been widely used in many important fields besides to prevent coccidiosis in poultry and as feed additives to increase the efficiency of feed utilization in ruminant animals. Monensin, salinomycin, and lasalocid are FDA approved and widely utilized as growth promoters for cattle, sheep, and goats because they can kill some bacteria. These antibiotics interfere with the alkali metal cation transport of the bacteria in the stomach of ruminant animals[7], which leads to the disruption of cell structures followed by the death of cells. That was the explanation for the accumulation of long carbon chain products and the depression of acetate, butyrate and methane production[20-22]. From the agricultural point of view, the weight of animals is increased in a shorter time. Because of their high efficiency of metal ion transport, ionophores have been employed to manipulate transmembrane ion gradients (e.g., Ca^{2+}, Mg^{2+}, Na^+ and K^+) to study the role of metal ions in cell signaling systems[23]. In a fashion similar to crown ethers, many ionophores are able to distinguish between metal ions with different sizes, which is the principle used to develop ion selective membrane electrodes containing ionophores (nigericin for K^+, monensin for Na^+, and salinomycin and lasalocid for Ba^{2+})[24,25].

To understand the behavior of polyether ionophores, the metal ion transport selectivity of ionophores was studied in various systems. Biological systems such as mitochondria cells were the first systems[26] used but are hard to manipulate to provide detailed information because of the limits on pH, temperature, cation concentrations and toxicity. The complexity of the cell systems resulted in many uncertainties in the data

analysis. Endogenous ion channels and pumps interfere with metal ion transport caused by ionophores. Therefore, suitable model systems are extremely important for ionophore studies. The earliest version is a U-shaped tube with the aqueous layers in each arm separated by chloroform layer[27]. The metal ion conducted through the organic layer is measured by ion selective electrodes or spectroscopic methods such as UV or atomic absorption. The shortcoming of this method is that the organic layer is greatly different from biological membranes in terms of thickness, membrane potential, and the structural properties of the membrane surface. Table I.2 lists some results of studies about metal selectivity of ionophores in various systems.

Table I.2. Polyether antibiotics and their cation selectivities

Antibiotic	Reference	Cation selectivity (method)
lasalocid	28	$Ba^{2+}>>Cs^{+}>Rb^{+}$, $K^{+}>Na^{+}$, Ca^{2+}, $Mg^{2+}>Li^{+}$ (two phase distribution)
monensin	28 29	$Na^{+}>>K^{+}>Rb^{+}>Li^{+}>Ca^{2+}$ (two phase distribution) $Na^{+}>K^{+}$, $Li^{+}>Rb^{+}>Cs^{+}$ (erythrocytes)
nigericin	28 29	$K^{+}>Rb^{+}>Na^{+}>Cs^{+}>Li^{+}$ (two phase distribution) $K^{+}\sim Rb^{+}>Na^{+}>Cs^{+}>Li^{+}$ (erythrocytes)
salinomycin	28 30	$K^{+}>Na^{+}>Cs^{+}>>Ca^{2+}$ (two phase distribution) $K^{+}>Na^{+}>Cs^{+}>>Ca^{2+}>Mg^{2+}$ (two phase distribution)
grisorixin	31	$Ag^{+}>Tl^{+}\sim K^{+}>NH_4^{+}>Rb^{+}>Na^{+}>Cs^{+}>>Li^{+}$ (electrochemical cells)
X-206	28	$K^{+}>Rb^{+}>Na^{+}>Cs^{+}>Li^{+}$ (two phase distribution)

Only lasalocid can conduct divalent cations with comparable efficiency with monovalent cation transport. A planar bilayer lipid membrane is a further step towards a model for biological membranes[27-29]. The lipid and ionophores mixed in decane are dropped into a pin-hole and a thin layer is formed after evaporation of decane. The problem still lies with the uncertain character of these membranes that may not be a true unilamellar bilayer[27]. The most successful model system employs unilamellar

phospholipid vesicles with a defined size that use lipids commonly found in biological membranes as shown in Figure I.4. The properties of the vesicles are well studied[18,19,30,31]. Different techniques such as fluorescene, UV-Vis, and NMR were used to measure ions transported into the solutions trapped inside vesicles.

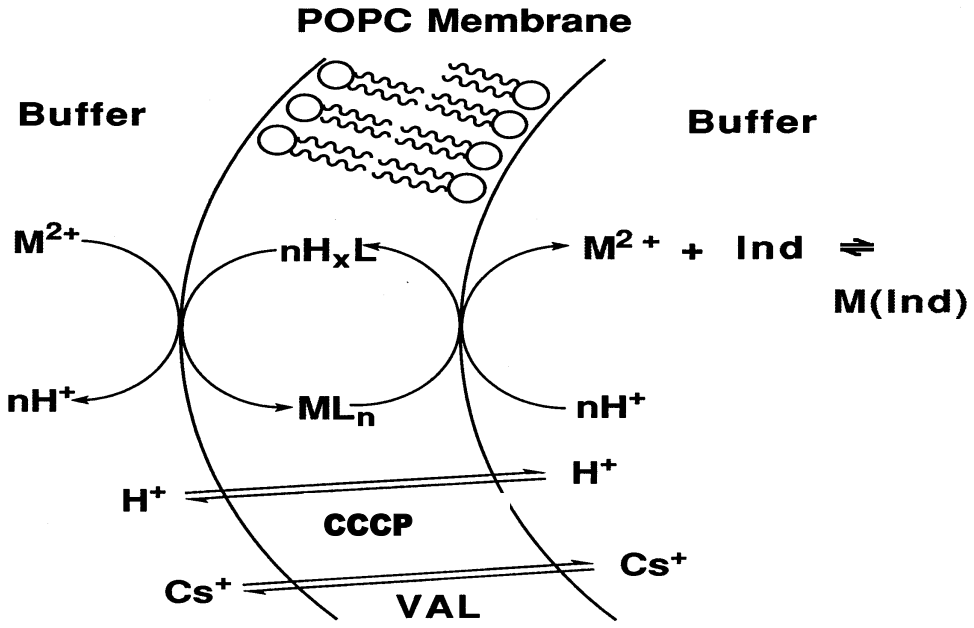


Figure I.4. The transport scheme in a system using 1-palmitoyl-2-oleoyl-*sn*-glycerophosphatidylcholine (POPC) vesicles loaded with Quin-2 as the indicator in a buffered medium. VAL and CCP represent valinomycin and carbonyl cyanide *m*-chlorophenylhydrazone that dissipate transmembrane electrical potential)[32].

Based on earlier selectivity studies it was generally accepted that salinomycin, nigericin, monensin act as monovalent ionophores for Na^+ and K^+ and lasalocid acts as divalent cation ionophore. However, recent membrane transport studies of divalent cations with polyether ionophores (salinomycin, nigericin, monensin, ionomycin, and lasalocid) show that this is not accurate[32-35]. These ionophores have surprisingly higher selectivity for transport of lead compared to other divalent cations, as shown in Figure I.5.

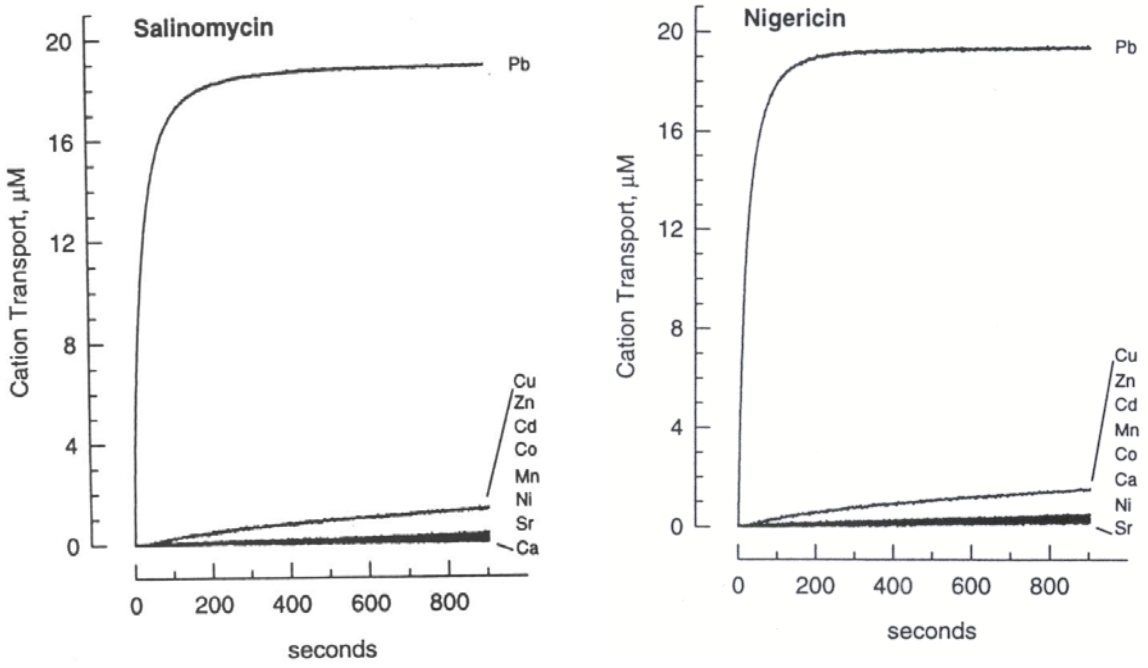


Figure I.5. Selectivity trends for membrane transport of divalent cations by salinomycin and nigericin at pH 7.0 from studies using phospholipid vesicles[32,35].

Monensin, salinomycin, and nigericin have a transport selectivity of about 3000-fold for lead compared to the transport of calcium (selectivity is defined as the ratio of initial transport rates for lead over other metal ions). The transport selectivity for lead over the other divalent cations follows a similar order for both ionophores, with copper displaying the highest transport rate among these cations. Ionomycin, well known as an ionophore for Ca^{2+}, transports lead about 100 times faster than calcium[34]. Transport selectivity for lead over calcium for lasalocid is around 250-fold. A23187 is the only ionophore that transports some divalent cations more efficiently than lead, but lead is still among the list of metal ions transported with high efficiency[32,33,35]. Nigericin catalyzed lead transport is not inhibited by physiological concentrations of Ca^{2+} or Mg^{2+} and is only modestly affected by K^+ and Na^+ for concentrations in the range of 0-100 mM[35]. Similar to nigericin, monensin catalyzed lead transport is little effected by the concentrations of

Ca^{2+}, Mg^{2+}, or K^{+} encountered in living systems[33]. It was found that salinomycin, nigericin and monensin formed 1:1 complexes with lead during transport and that mixtures of 1:1 and 2:1 lead complexes are involved with lasalocid[32,33,35].

Such high selectivity for lead raises concerns over the public health. Salinomycin, monensin and lasalocid are the most common feed additives[36]. There is some evidence showing that they are carried into the human diet[37,38]. Ionophore residues were detected in meat[38-40], milk[41], and eggs[42]. Chickens fed monensin accumulate lead more readily and show more signs of lead intoxication than do chickens fed lead without monensin[43-45]. Although nigericin and ionomycin are not used as feed additives they are utilized in basic research to control the concentrations of K^{+} and Ca^{2+}, respectively[12,46-48].

Lead is the second highest among toxic substances according to the harm done to the society[49]. Most of organs and systems in humans are affected by lead because lead has high affinity for many functional groups in proteins such as sulfhydryl, amine, phosphate, and carboxylate groups and can replace some metal ion that centers in proteins. Lead toxicity in adults causes hypertension, damage to the kidneys and brain, and shortens life span[50]. One famous example of lead toxicity happened during the period of the Roman Empire. Human skeletons from the time of the Roman Empire contain 10-100 fold more lead than those before Roman Empire[51]. Containers, water systems, coins and coffins from this period of the Roman Empire were often made of lead[51]. Romans even added lead oxide powder into wine for a better taste. All of these factors are suspected causes of many unexplainable diseases at that time.

The modern origins of lead contamination are gasoline containing lead antiknocking agents (such as tetraethyllead) and paints containing lead oxide. Although

both lead applications are banned in USA, they are used in many poor countries around the world. Lead is still circulating in the environment due to previous applications.

Children have a greater chance of exposure to lead because lead tends to be retained in the surface of soil and children tend to put dirt in their mouth[52]. Damage to the brains of children due to lead toxicity will cause poor cognitive ability and low IQ[50], and affects the whole life of children. It is easy to remove lead from blood for a short time but a significant part of lead accumulates in bones or brains that are hard to reach[53]. Available lead chelating agents require long periods for chelation therapy. This is a problem for young children who are in a rapid growth and development period. The high selectivity of certain ionophores for lead suggests that they may be applied as biomedical agents. They have the potential to increase the lead transport rate into blood where chelating agents take lead out of the body. That reduces the treatment time for lead toxicity, with no significant change in the levels of other essential cations (Ca^{2+}, Mg^{2+}, Zn^{2+}, Fe^{2+}, and Cu^{2+})[33].

For the reasons listed above, studies of the lead transport mechanism by ionophores are needed to explain their high selectivity for lead transport and to provide important information for medical applications. The mechanism for transport proposed by Painter and Pressman[13] mentioned previously indicates the individual steps that may be involved in a single transport cycle. These individual steps and reactions have their own equilibrium constants and kinetic rate constants for both directions. It is known that for the electroneutral mode the transport direction and extent is controlled by the concentrations of cations, ionophores, and pH on both sides of membranes, not directly by the membrane potential[15]. Therefore, the solution equilibria involved will be

investigated in this dissertation, which provides not only the prediction of the transport selectively, but also the stoichiometric information about the transporting species. The equilibrium constants and the structures of the complexes obtained in this dissertation can be used to explain transport data obtained using a phospholipid vesicle model system[33-35].

Conformation and complexation studies of salinomycin and nigericin by various methods are described in detail in the next section.

Nigericin complexes, literature overview.

Nigericin, shown in Figure I.6, was the second polyether antibiotic to be structurally elucidated[54,55], and is also known as duamycin, helixin C, azalomycin M, X-464, K-178, and polyetherin A.

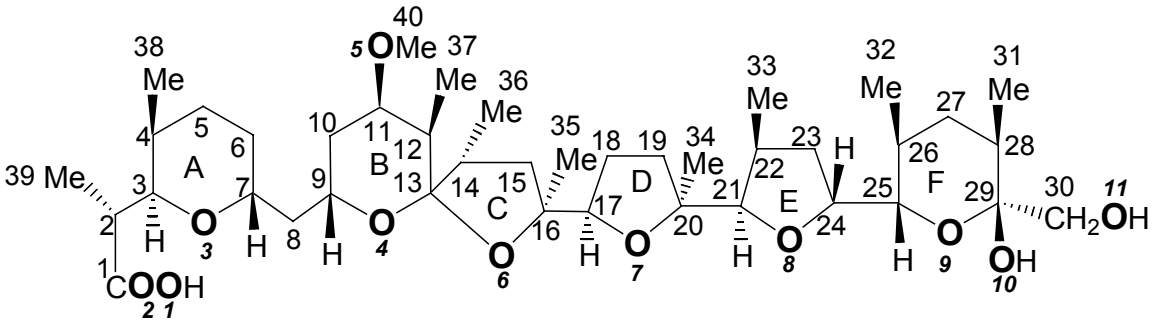


Figure I.6 Structure of nigericin with numbering schemes for carbon (plain) and oxygen (bold italic) atoms.

Several polyether antibiotics have structures similar to nigericin. Epinigericin has the same structure as nigericin except that the stereochemistry at C28 is different. TLC can separate epinigericin and nigericin using a methanol-chloroform solvent system. It was reported that Na epinigericin was transformed into the free acid form of nigericin using 0.1M HCl because epinigericin was less stable than nigericin[56]. Under acidic conditions, ring F opens and forms a ketonic intermediate. After bond rotation, the intermediate closes ring F to produce nigericin[56]. Little research about epinigericin has been reported probably because it is not very stable. Grisorixin, 30-deoxy nigericin, only has one hydroxyl group at the end of the carbon chain, as shown in Figure I.7. It has high complexation selectivity for K^+ among alkali cations in methanol as determined from conductmetric measurements[57]. Due to their structural similarity, studies about nigericin and grisorxin are described below.

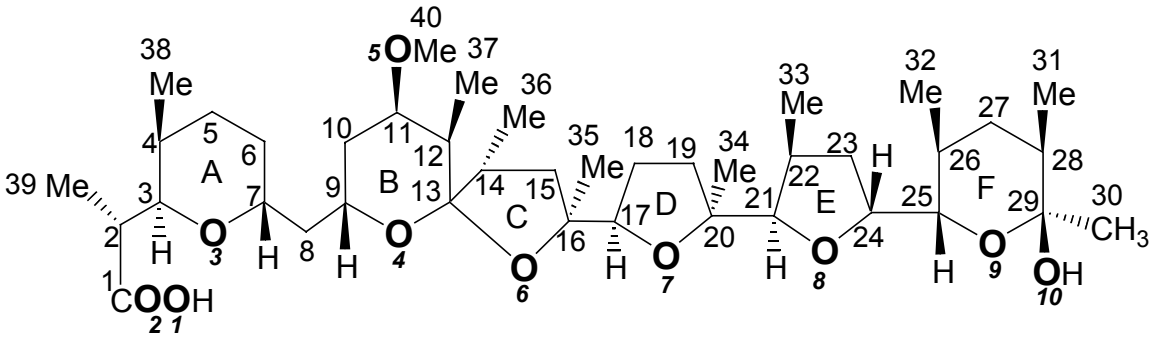


Figure I.7. Structure of grisorixin with numbering schemes for carbon (plain) and oxygen (bold italic) atoms.

Extraction and transport selectivities of nigericin were determined using two different methods. The trends obtained from the two methods matched each other very well, as shown in Table I.2. To explain the trends requires complexation and conformation studies of nigericin and its complexes. The protonation constants and complexation constants of nigericin with monovalent cations in homogeneous solutions and in phospholipid bilayer membranes are listed in Tables I.3 and I.4.

Table I.3. Literature values of the protonation constants of nigericin in various organic solvents and heterogeneous media[a]

log K_H	method	solvent system
6.93	potentiometry	dioxane-H_2O 30% (v/v)[58]
8.45	potentiometry	ethanol 90% (v/v)[58]
7.76	potentiometry	dioxane-H_2O 45% (v/v) [58]
10.2	voltammetry	methanol[59]
6.25	potentiometry	bilayer lipid vesicles[60]

[a] 25 ^{o}C, molar scale of concentrations.

Protonation constants obtained from different systems vary from each other. Complexation constants range from 1.34 to 6.39. But the order of stability is the same as the complexation trend (K^+>Na^+) except that in two cases the complexation constants of K^+ and Na^+ are almost the same, as shown in Table I.2. Because nigericin was considered to be a monovalent ionophore there is only one study on the complexation

between nigericin and divalent cations. The complexation constants were obtained in ethanol by a competitive method using the fluorescent signal of Tl^{+}[11]. The values of log K_{ML} (5.53 for Mg^{2+}, 5.43 for Ca^{2+}, 5.14 for Sr^{2+}, and 5.66 for Ba^{2+}) vary by only a factor of ~3 and are about the same as values for K^+ (6.14), Rb^+ (6.08), and Cs^+ (5.97).

Table I.4. Literature values of the complex formation constants of nigericin with monovalent cations in various organic solvents and heterogeneous media[a]

solvent	method	Log K_{ML}					
		Li^+	Na^+	K^+	Rb^+	Cs^+	Tl^+
methanol[61]	potentiometry		4.38	5.17			
dioxane/H_2O 45%(v/v)[62]	potentiometry	4.16	3.91	3.70	3.70	3.82	
bilayer lipid vesicles[63]	NMR		1.34	1.98			
methanol[64]	calorimetry		4.66	5.64	5.08		
ethanol[11]	kinetics		6.17	6.14	6.08	5.977	6.39

[a] 25 °C, molar scale of concentrations

Mass spectra of complexed monensin, nigericin[65] and grisorxin [66] showed a different pattern from the free acid form of these ionophores, especially in the high m/z area. The most important difference is absence of the peak due to loss of CO_2 in the spectra of complexed ionophores because the carboxylic group is bound with the metal tightly enough to prevent the decarboxylation reaction.

For a complete picture of the conformation of nigericin, IR, crystallography, and NMR were used to provide detailed information. The absorption band (~1705 cm^{-1}) in IR studies showed that the carboxylic acid groups in monensin and nigericin were linked with hydroxy groups by a hydrogen bond[61].

Among the nigericin salts, the silver salt of nigericin is the earliest one whose solid-state structure was resolved because silver is a heavy metal. X-ray study of its crystal revealed an envelope conformation of rings D and E, a half chair conformation of ring C, and a chair conformation for the three tetrahydropyran rings (A, B, and F). Five oxygen atoms (O2, O5, O6, O7, and O8) are coordinated with silver as listed in Table I.5

that also includes identities of donor atoms involved in metal complexation for nigericin and grisoxin salts of different atoms. The distance between O2 and silver is a little larger than those for any other oxygen atoms complexed with silver. The head to tail hydrogen bond is O1H-O10[67].

Table I.5. Identities of donor atoms of nigericin and grisoxin salts in different states.

compounds	oxygen atoms complexed with metal	state
silver-nigericin[67]	O2, O5, O6, O7, O8	solid-state
potassium-nigericin[12]	O1, O5, O6, O7, O8	solid-state
sodium-nigericin[68]	O2, O5, O6, O7, O8	solid-state
thallium[69] and silver[70] salts-grisorixin	O2, O5, O6, O7, O8	solid-state
sodium-nigericin[71]	O1, O5, O6, O7, (O8), O11	solution

In the crystal structure of the potassium salt of nigericin, five oxygen atoms (O1, O5, O6, O7, and O8) are coordinated with potassium and there are two hydrogen bonds (O10H-O2 and O11H-O2). The distances between the oxygen atoms and potassium are greater than those in the silver salt of nigericin[12]. The X-ray structure of sodium-nigericin showed that sodium is coordinated with five oxygen atoms (O2, O5, O6, O7, and O8). Considering that the bond C1-C2 can rotate freely, O1 and O2 are hard to distinguish from each other. So the oxygen atoms complexed with sodium ion were the same ones complexed with the metal ion in the solid-state structure of the potassium and silver salts of nigericin. The distance between sodium ion and O2 is the shortest one indicating a stronger bond. There are two head-tail hydrogen bonds (O10H-O1, O11H-O2)[68], as in the potassium salt.

Crystal structures of the thallium[69] and silver salts[70] of grisorixin are similar to the crystal structures of the silver salt of nigericin. The head-tail hydrogen bond is O10H-O1. Five oxygen atoms (O2, O5, O6, O7, and O8) are coordinated with metal ions, which are the same oxygen atoms involved in the silver salt of nigericin. The difference

between the thallium and silver salts is that the former has larger ionic radius and longer oxygen to metal bonds.

To investigate the conformation of both the free acid and sodium salt of nigericin in solution, experiments were done to obtain ^{1}H NMR spectra in C_6D_6 and $CDCl_3$[71]. The ^{1}H NMR chemical shifts and coupling constants of the acid form and sodium salt of nigericin in those two solvents were obtained. The chemical shift changes of protons ranged –0.28-0.346 ppm. The coupling constants varied from 1 to 13.5 Hz. It is evident from Karplus equation[72] that the coupling constants are related to the dihedral angle ϕ. Strong coupling occurs at the synperiplanar (ϕ = 0°-30°) and antiperiplanar (ϕ = 150°-180°) geometries. Weak couplings take place when the orbitals are not parallel (ϕ = 60°-120°). When cyclohexane is in a chair formation, J_{aa} is large (8-13 Hz) because the dihedral angle is close to 180°, whereas J_{ee} (0-5 Hz) and J_{ae} (1-6 Hz) are small because the angles are close to 60°. The presence of ~2 or 10 Hz of coupling constants is the strong evidence of a chair conformation in a six-membered ring. Based on the coupling constants ring A is in a chair formation with C7 sticking out a little and C38 and C8 in axial positions. Ring B is also in a chair formation with the bonds C11-OMe and C13-O5 turning outward. The methoxyl group on C11 and proton on C9 are in axial positions and methyl group on C12 is in equatorial position. There is no information about ring C and E. Ring D is a half chair form. Ring F is in a chair form with protons on C25 and C26 in axial positions[71]. It was believed that both hydrogen atoms from O10H and O11H have a role in hydrogen bonding. In the sodium form, the head-tail hydrogen bond only involves O10H. In the acid form of nigericin, O10H and O11H interact with the carboxylic group.

Sodium is coordinated with O1, O5, O6, O7, and O11 but there is uncertainty about the participation of O8[71].

NOE spectra of the sodium and potassium salts of nigericin in chloroform provided distances of those oxygen atoms that matched well with the distances in the crystal structure. The NOE distances for the potassium salt were 15% greater than for the sodium salt, which mirrored the percentage of the distance increase between the two crystal structures. Calculations based on the NOE distances of two salts revealed a more compacted and rigid structure of the sodium salt compared to that of the potassium salt. Solution structures for both complexes[9] are in consistent with the solid state structures.

^{1}H NMR chemical shifts and coupling constants of the free acid form of nigericin in CD_3OD and $CDCl_3$ were obtained[73]. Coupling constants for H7-H8 and H8-H9 decreased significantly going from $CDCl_3$ to CD_3OD because the C7-C8 and C8-C9 bonds rotate more freely in CD_3OD and the coupling constants are average values for several conformations. Ring C was found to be in an envelope form with H14 antiperiplanar to H15[73].

The structure of nigericin is the foundation of the ion selectivity and transport. The transformation of the C-1 carboxyl group into an alcohol group produced nigericin derivatives with complexation constants for Na^+ and K^+ close to those of nigericin, which indicates that the carboxylic group does not play a major role in metal complexation. To the contrary, theoretical calculations show that carboxylic groups secure the conformation of metal complex[74]. After any changes in C1 and C29 of nigericin that destroyed the head-tail hydrogen bond, the molecule was not able to close and the complexation ability was affected[74]. Although ring F does not participate in metal

complexation by nigericin[68], opening of ring F by $NaBH_4$ took away the ion selectivity of nigericin although the nigericin derivative had two extra hydroxy groups. After formation of a different ring F by $NaIO_4$, the selectivity was regained although the ion binding ability was weaker than the original nigericin[75]. Grisorixin metabolites with an extra carboxylic acid group in ring E can complex metal ions well but lose transport ability because the overall negative charge on the metal ion complex prevents diffusion through the membrane[76].

Salinomycin complexes, literature overview.

Salinomycin was discovered in 1973[77]. Its production, isolation, biological properties were reported in 1974[78] and the structure was elucidated in 1975[79] and is shown in Figure I.8.

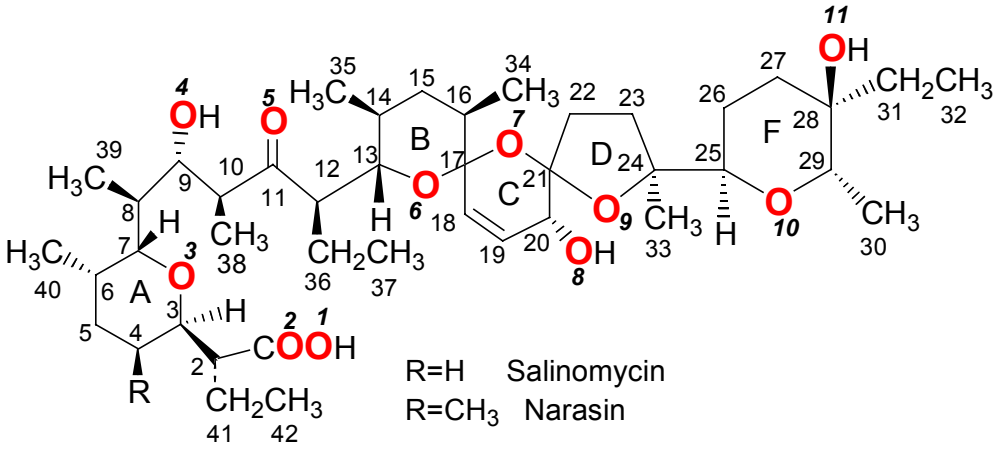


Figure I.8. Structure of salinomycin with numbering schemes for carbon (plain) and oxygen (bold italic) atoms.

Salinomycin is a monocarboxylic polyether antibiotic with a unique tricyclic spiroketal ring system (B-C-D) and an unsaturated six-membered ring (C) in the molecule. Narasin (or A-28086B) isolated and characterized in 1976[80] has the exactly same structure except an extra methyl group on the ring A. It is an equally effective antibiotic and a potent coccidiostate in poultry. Due to the structural similarity of salinomycin and narasin, all reports about narasin are included in this dissertation. Although the backbone chains of nigericin, salinomycin and narasin are of similar length, the presence of trispiroketal moiety gives the latter two ionophores less conformation freedom.

Although salinomycin is an FDA approved feed additive for agricultural use along with monensin and lasalocid, there are only a few reports about the complexation

constants of salinomycin or narasin, compared to the extensive literature for monensin and lasalocid. The values of the complexation constants of Na^+ and K^+ with salinomycin and narasin are listed in Table I.6. There are no reports about the protonation constants of salinomycin or narasin and complexation constants with divalent cations.

Table I.6. Values of the complex formation constants of salinomycin and narasin with monovalent cations.

Reactions	solvent	logK_f
$Na^+ + sal^- \rightleftharpoons$ Nasal	bilayer lipid vesicle[63]	0.78
$K^+ + sal^- \rightleftharpoons$ Ksal	bilayer lipid vesicle[63]	1.31
$Na^+ + narasin^- \rightleftharpoons$ Nanarasin	bilayer lipid vesicle[63]	1.04
$K^+ + narasin^- \rightleftharpoons$ Knarasin	bilayer lipid vesicle[63]	0.94
$Na^+ + narasin^- \rightleftharpoons$ Nanarasin	methanol[10]	3.64
$Na^+ + narasin^- \rightleftharpoons$ Nanarasin	20% methanol-water[10]	2.51
$K^+ + narasin^- \rightleftharpoons$ Knarasin	methanol[10]	5.52
$K^+ + narasin^- \rightleftharpoons$ Knarasin	20% methanol-water[10]	4.03

In contrast to the few complexation studies, there are some important reportes regarding the conformation of salinomycin and narasin. In early studies it proved difficult to obtain suitable crystals of salinomycin so derivatives of salinomycin were prepared for X-ray studies. The X-ray crystal structure for the *p*-iodophenacyl ester of salinomycin shows that there is a large distance between the terminal hydroxy and the ester carboxyl groups of salinomycin. Therefore, there should be no intramolecular hydrogen bonding to stabilize a cyclic conformation of the molecule[77], which explains why esterification of the carboxylic acid group resulted in loss of K^+ transport ability. Derivatives of salinomycin where the terminal hydroxyl group is converted to a methoxyl group transport K^+ as well as the parent molecule because the methoxy group can form an intramolecular hydrogen bond with the carboxylic acid group to form a cavity[81].

Crystals of sodium salinomycin obtained from water-acetonitrile solvent systems disclosed two different conformers. The same oxygen atoms from salinomycin (O1, O5, O9, and O10) and some water molecules were coordinated to sodium in both conformers. The carboxylate group participated in sodium ion coordination. One conformer containing a single complexed water molecule possessed a flat shape with two different sides (hydrophilic and hydrophobic). The other conformer with two complexed water molecules formed a sphere. All oxygen atoms were involved in hydrogen bonding. There are two important hydrogen bonds (O11H-O1 and O4H-O1). The first one is the head-tail bond. All these hydroxyl groups form V-shape hydrogen bonds with adjacent oxygen atoms, such as O8H-O9. There are no hydrogen bonds between the conformers[82].

CD and NMR methods were used to obtain information about the conformation of salinomycin in solution. Most of the polyether ionophores do not have absorption bans in the UV. However, almost all have substantial peaks in circular dichroism (CD) spectra. CD spectra are sensitive to the structural differences between different forms of the ionophores. They can be used in the study of cation complexation and can provide kinetic information. This is especially true for ionophores with carbonyl groups in the backbone, such as salinomycin, narasin, and lasalocid. The carbonyl group gives CD peaks at 280-295 nm. Narasin has a larger signal at 290 nm than salinomycin and thus has been the subject of more CD studies. The complexation selectivity of narasin was determined in methanol and 20% methanol-water solutions based on changes in the CD spectra. The order is $K^+ > Na^+$ and the complexation constants are listed in Table I.6[10,83]. A large change was observed in CD spectra between the anionic form of narasin and the complexed form, and there was little difference among different metal ion complexes

(K^+, Na^+, and NH_4^+) or the protonated ionophore. Interaction of these cations with narasin brought about conformation changes similar to protonation because the linear form of the narasin anion was transformed into a pseudocyclic form with the formation of a head-tail hydrogen bond in all those compounds. The hinge region around C11 went through a conformational change, which produced the CD signal change at 290 nm[83].

NMR studies on the conformations of narasin and salinomycin require peak assignment in ^{1}H NMR and the coupling constants of hydrogen atoms. In the early stages of ionophore studies, high power NMR instruments were still under development and most spectra were assigned based on comparisons with those for simpler compounds[55], or using doubly labeled derivatives[84]. It was extremely time-consuming to assign every hydrogen peak and to obtain the coupling constants. Using 2D NMR techniques and higher power instruments[56], it was observed that ^{1}H NMR chemical shifts for several protons adjacent to oxygen atoms increased upon complexation with potassium[58].

NMR studies on the solution structure of the sodium salt of salinomycin were not consistent to each other. The first important one was reported by Anteunis et al. in 1981[8], where chemical shifts and coupling constants for most of protons were obtained. The effect of complexation on ^{1}H NMR chemical shifts was observed for the sodium salts of salinomycin and narasin in $CDCl_3$. Based on the stereoscopic information from the vicinal coupling constants, sodium ion is proposed to coordinate with seven oxygen atoms (O4, O5, O6, O8, O9, O10, and O11) in the sodium salts of narasin and salinomycin. The carboxylate group was found not to complex with sodium. There are two hydrogen bonds (O8H-O4 and O11H-O1). The former stabilizes the conformation of the backbone C9-C20 and the latter for the pseudocyclic conformation of the molecule.

Alkali metal salts (Na^+, K^+, Cs^+, and Rb^+) of salinomycin and narasin were prepared in $CDCl_3$ and the ^1H and ^{13}C chemical shifts were assigned using COSY NMR[85]. Large chemical shift changes were found between the acid form and the salts while small chemical shift changes occurred when the sizes of metal ions were changed[85].

Mronga et al. calculated the solution conformation of the sodium salt of salinomycin using the coupling constants from ^1H NMR and COSY and hydrogen distances from NOE spectra (600 Hz)[86]. The beginning model was based on the crystal structure of the p-iodophenylacyl ester derivative of salinomycin where the ionophore has a noncyclic form. Two hydrogen bonds were suggested to be O11H-O1 and O8H-O2. Both oxygen atoms in the carboxylate group are involved in hydrogen bonding, which is different from what the Anteunis group[8] reported and agrees with the solid state structure[82]. Chair conformations of ring A and ring E aided the formation of the head-tail hydrogen bond. The sodium ion was coordinated with six oxygen atoms (O2, O4, O5, O9, O10, and O11). All oxygen-ion distances were about 230 pm[86]. O6 and O8, previously reported to be coordinated with sodium[8], were missing. A plane was formed by O2, O4, O5, and O10 with O9 and O11 on either side of the plane.

^1H chemical shifts of narasin free acid in C_6D_{12}, $CDCl_3$, $(CD_3)_2CO$, and CD_3OD were assigned using 600 MHz NMR[87]. The chemical shifts in different solvents were compared to correlate the conformational changes of narasin with the changes in solvent polarity. Protons 10, 12, 13,14 and 25 showed significant chemical shift changes when the solvent was changed from the nonpolar solvent (C_6D_{12}) to the polar solvent (CD_3OD). This finding supported the hypothesis that the flexible hinge regions (C10-C13 and C24-C25) between the highly constrained rings will rotate readily, as proposed by Anteunis et

al[8]. Conformational changes in C10-C13 also lead to changes in dihedral coupling constants. Similar results were found for salinomycin[87].

The hinge regions can play an important role in accommodating ions with different sizes, and therefore on the ion selectivity. But there is disagreement about the identity of the hinge regions. C9-C10-C11-C12, C10-C11-C12-C13 and C23-C24-C25-C26 were proposed as hinge regions by Anteunis and Rodios[8]. The dihedral angle fluctuations expected in those regions were not found in a study by Monga and coworkers, where the major change occurred at C10-C11-C12-C13 and C6-C7-C8-C9[86]. X-ray data and calculations for $CDCl_3$ and DMSO[82] strongly supported the first theory. A large dihedral angle changes occurred in those hinge regions defined by Anteunis and Rodios between the crystal structure of sodium salinomycin and the open chain conformation of salinomycin based on the crystal structure of p-iodophenacyl salinomycin ester[82]. All reports agreed on the existence of two important hydrogen bonds. The head-tail bond (O11H-O1) was defined in the same way in every report. But the identity of the other hydrogen bond was totally different. Anteunis and Rodios[8] proposed O8H-O4 and Mronga et al.[86] claimed O8H-O2 as the second hydrogen bond. Another major difference in the reports was the number of oxygen atoms complexed with sodium. Anteunis and Rodios proposed that seven oxygen atoms were coordinated with sodium[8], calculations showed only six were involved[86], while the X-ray structure revealed that only four oxygen atoms of salinomycin and one or two water molecules were coordinated to sodium. These water molecules were not observed in the NMR studies or predicted by calculation[82]. Analysis of the ring conformations agreed well with each other.

Degradation of salinomycin and narasin was carried out with 96% formic acid at 25 ^{o}C[88], however, concentrated formic acid is not used in this work. One report describes the degradation of the sodium salts of salinomycin and narasin in 2% methanol-water (v/v) solutions at room temperature and at 4^{o}C. After 11 days at room temperature HPLC-Ms analysis showed that the tricyclic spiroketal ring system (rings B, C, and D) was opened and that a new furan ring was formed. Mass spectral studies indicated existence of several intermediates and the structure of the isomer was identified by NMR[89]. This result indicated that extra care was needed in experiments using salinomycin and solutions of salinomycin containing water are not safe for long-term storage.

Summary of studies

The purpose of this work is to provide an explanation for the high selectivity of salinomycin and nigericin for lead. This requires a detailed characterization of the reactions between lead and ionophores and the identities of possible transport species. Salinomycin and nigericin are chosen as subjects of this study because of the widespread application of salinomycin in agriculture, the routine use of nigericin in basic research and, most of all, their extremely high selectivity for transport of lead over other divalent cations by both ionophores.

The lead complexes of nigericin and salinomycin were prepared and were subjected to elemental analysis. Solutions of ionophore-lead complexes were injected into ESI-MS, and the species observed suggest the identity of possible lead-ionophore species involved in membrane transport.

The model of metal ion transport proposed by Painter and Pressman[13] pictured the individual steps that make up the overall transport process in membranes. The major steps are deprotonation of ionophores, complexation with metal ions, diffusion through membrane, dissociation of the complex, and protonation of ionophores. Equilibrium and kinetic constants for each step determine the direction and the extent of transport. The equilibrium constants were obtained in this work. The protonation constants of salinomycin and nigericin were determined in 80% methanol using potentiometric titrations. Stoichiometric information for the major lead species of several important ionophores (nigericin, salinomycin, narasin, monensin, lasalocid, maduramicin, and X-206) was obtained using CD titrations. UV-Vis titrations in 80% methanol were also applied to obtain information about the stoichiometry and complexation constants of

ionophore-lead complexes for nigericin and salinomycin. For a better comparison of the complexation behavior of the ionophores with lead and other metal ions, potentiometric titrations were done in the presence of these metal ions. The metal ions chosen for the titrations are sodium, potassium, lead, calcium, zinc, and magnesium. Sodium and potassium are generally believed to be transported well by nigericin and exist at relatively high concentrations in biological systems. Calcium is important in biological systems because of its role in controlling metabolic pathways and its well-known structural functions. The ionic radius of lead is close to that of calcium. Comparison between lead complexes and calcium complexes may reveal more about the mechanism of high selectivity for lead. Zinc and magnesium also were chosen due to their biological importance. Zinc is the most common trace metal ion in the cytoplasm and is required by many enzymes. Magnesium is the vital component in phosphate metabolism and other enzymes[90]. Both zinc and magnesium are found to be in low concentration range in biological systems. Small changes in concentrations for these two elements could have serious biological effects. Complexation information for all these metal ions is necessary to evaluate potential applications of ionophores in the medical field.

The conformation and structure of ionophore-metal complexes can affect the metal ion transport through membranes. Changes in the conformation of the ionophore upon complexation cause substantial changes in the ^{13}C NMR chemical shifts. Therefore, NMR was used in this work to obtain information about the binding sites and conformation of the ionophore-metal complexes. Chemical shifts from the ^{13}C NMR of ionophore-lead complexes were compared with those for tetraethylammonium salts of ionophores in the uncomplexed form.

The information obtained in this work will be used to help explain the results of transport studies using phospholipid vesicles. The results should be used to develop a transport model for lead with nigericin and salinomycin and provide information for the future design of strategies and for improved treatment of lead-intoxication. Nigericin and salinomycin, which show high selectivity for lead transport, also have great potential in lead selective electrodes.

References

(1) Berger, J.; Rachlin, A. I.; Scott, W. E.; Sternbach, L. H.; Goldberg, M. W. *J. Am. Chem. Soc.* **1951**, *73*, 5295-5298.

(2) Harned, R. L.; Hidy, P. H.; Corum, C. J.; Jones, K. L. *Antibiot. Chemother.* **1951**, *I*, 594-596.

(3) Agtarap, A.; Chamberlin, J. W.; Pinkerton, M.; Steinrauf, L. *J. Am. Chem. Soc.* **1967**, *89*, 5737-5739.

(4) Shumard, R. F.; Callender, M. E. *Antimicrob. Agents Chemther.* **1968**, *1967*, 369-377.

(5) Dutton, C. J.; Banks, B. J.; Cooper, C. B. *Nat. Prod. Rep.* **1995**, *12*, 165-181.

(6) Prosser, B. L. T.; Palleroni, N. J. in Polyether Antibiotics: Naturally Occurring Acid Ionophores, Volume 1: Biology; Marcel Dekker, Inc.: New York, **1982**, 21-42.

(7) Estrada-O, S.; Rightmire, B.; Lardy, H. A. *Antimicrob. Agents Chemther.* **1968**, *1967*, 279-288.

(8) Anteunis, M. J. O.; Rodios, N. A. *Bull. Soc. Chim. Belg.* **1981**, *90*, 715-735.

(9) Beloeil, J.-C.; Biou, V.; Dauphin, G.; Garnier, J.; Morellet, N.; Vaufrey, F. *Magn. Res. Chem.* **1994**, *32*, 83-86.

(10) Caughey, B.; Painter, G.; Drake, A. F.; Gibbons, W. A. *Biochim. Biophys. Acta* **1986**, *854*, 109-116.

(11) Cornelius, G.; Gartner, W.; Haynes, D. H. *Biochemistry* **1974**, *13*, 3052-3057.

(12) Geddes, A. J.; Sheldrick, B.; Stevenson, W. T. J.; Steinrauf, L. K. *Biochem. Biophys. Res. Commun.* **1974**, *60*, 1245-1251.

(13) Painter, G. R.; Pressman, B. C. *Top. Curr. Chem.* **1982**, *101*, 84-110.

(14) Riddell, F. G.; Arumugam, S.; Brophy, P. J.; Cox, B. G.; Payne, M. C. H.; Southon, T. E. *J. Am. Chem. Soc.* **1988**, *110*, 734-738.

(15) Taylor, R. W.; Kauffman, R. F.; Pfeiffer, D. R. in Polyether Antibiotics: Naturally Occuring Acid Ionophores, Volume 1: Biology; Marcel Dekker, Inc.: New York, **1982**, 103-184.

(16) Hilgenfeld, R.; Saenger, W. *Topics in Current Chemistry: Host Guest Complex Chemistry 2:* **1982**, *101*, 3-82.

(17) Sandeaux, R.; Seta, P.; Jeminet, G.; Alleaume, M.; Gavach, C. *Biochim. Biophys. Acta* **1978**, *511*, 499-508.

(18) Erdahl, W. L.; Chapman, C. J.; Taylor, R. W.; Pfeiffer, D. R. *Biophys. J.* **1994**, *66*, 1678-1693.

(19) Erdahl, W. L.; Chapman, C. J.; Taylor, R. W.; Pfeiffer, D. R. *Biophys. J.* **1995**, *69*, 2350-2363.

(20) Harold, F. M.; Baarda, J. R. *J. Bacteriol.* **1968**, *95*, 816-823.

(21) Harold, F. M. Advances in Microbial Physiology; Academic Press: New York, **1970**, 45-104.

(22) Lubin, M. *Fed. Proc.* **1964**, *23*, 994-1001.

(23) Reed, P. W. in Polyether Antibiotics: Naturally Occurring Acid Ionophores, Volume 1: Biology; Marcel Dekker, Inc.: New York, **1982**, 185-302.

(24) Suzuki, K.; Tohda, K.; Aruga, H.; Matsuzoe, M.; Inoue, H.; Shirai, T. *Anal. Chem.* **1988**, *60*, 1714-1721.

(25) Suzuki, K.; Tohda, K. *Trends Anal. Chem.* **1993**, *12*, 287-296.

(26) Pressman, B. C. *Fed. Proc.* **1968**, *27*, 1283-1288.
(27) Riddell, F. G. *Chem. Br.* **1992**, 533-537.
(28) Celis, H.; Estrada-O, S.; Montal, M. *J. Membr. Biol.* **1974**, *18*, 187-199.
(29) Estrada-O, S.; Celis, H.; Calderon, E.; Gallo, G.; Montal, M. *J. Membr. Biol.* **1974**, *18*, 201-218.
(30) Thomas, T. P.; Wang, E.; Pfeiffer, D. R.; Taylor, R. W. *Arch. Biochem. Biophys.* **1997**, *342*, 351-361.
(31) Erdahl, W. L.; Chapman, C. J.; Wang, E.; Taylor, R. W.; Pfeiffer, D. R. *Biochemistry* **1996**, *35*, 13817-13825.
(32) Pfeiffer, D. R. Ohio State University, Columbus, OH; Taylor, R. W. University of Oklahoma, Norman, OK *Personal Communications* **1999-2005**.
(33) Hamidinia, S. A.; Shimelis, O. I.; Tan, B.; Erdahl, W. L.; Chapman, C. J.; Renkes, G. D.; Taylor, R. W.; Pfeiffer, D. R. *J. Biol. Chem.* **2002**, *277*, 38111-38120.
(34) Erdahl, W. L.; Chapman, C. J.; Taylor, R. W.; Pfeiffer, D. R. *J. Biol. Chem.* **2000**, *275*, 7071-7079.
(35) Hamidinia, S. A.; Tan, B.; Erdahl, W. L.; Chapman, C. J.; Taylor, R. W.; Pfeiffer, D. R. *Biochemistry* **2004**, *43*, 15956-15965.
(36) Asukabe, H.; Harada, K.-I. *AOAC International* **1995**, 121-163.
(37) Pressman, B. C.; Fahim, M. *Ann. Rev. Pharmacol. Toxicol.* **1982**, *22*, 465-490.
(38) Salisbury, C. D. C.; Rigby, C. E.; Chan, W. *J. Agric. Food. Chem.* **1989**, *37*, 105-108.
(39) Martinez, E. E.; Shimoda, W. *J. Assoc. Off. Anal. Chem.* **1985**, *68*, 1149-1153.
(40) Takatsuki, K.; Suzuki, S.; Ushizawa, I. *J. Assoc. Off. Anal. Chem.* **1986**, *69*, 443-448.
(41) Moran, J. W.; Turner, J. M.; Coleman, M. R. *J. AOAC Int.* **1995**, *78*.
(42) Kennedy, D. G.; Hughes, P. J.; Blanchflower, W. J. *Food Addit. Contamin.* **1998**, *15*, 535-541.
(43) Khan, M. Z.; Szarek, J.; Markiewicz, K.; Markiewicz, E. *J. Vet. Med. A* **1993**, *40*, 466-475.
(44) Khan, M. Z.; Szarek, J.; Konicicki, A.; Kransnodebska-Depta, A. *Acta Vet. Hung.* **1994**, *42*, 111-120.
(45) Khan, M. Z.; Szarek, J. *J. Vet. Med. B* **1994**, *41*, 77-82.
(46) Kauffman, R. F.; Taylor, R. W.; Pfeiffer, D. R. *J. Biol. Chem.* **1980**, *255*, 2735-2739.
(47) Ferguson, S. M. F.; Estrada-O., S.; Lardy, H. A. *J. Biol. Chem.* **1971**, *246*, 5645-5652.
(48) Toepilitz, B. K.; Cohen, A. I.; Funke, P. T.; Parker, W. L.; Gougoutas, T. Z. *J. Am. Chem. Soc.* **1979**, *101*, 3344-3353.
(49) "Hazardous Substances Fact Sheets: Appendix B," USA, Agency of toxic Substance Registry, 2004.
(50) "Hazardous Substances Fact Sheets: Appendix B," USA, Agency of toxic Substance Registry, 1999.
(51) Nriagu, J. O. *Lead and Lead Poisoning in Antiquity*; John Wiley & Sons, Inc.: New York, **1983**,
(52) U.S. Environmental Protection Agency, **www.epa.gov/ttn/atw/hlthef/lead.html.**; March 11, 2005.

(53) Kalia, K.; Flora, S. J. S. *J. Occup. Health* **2005**, *47*, 1-21.
(54) Steinrauf, L. K.; Pinkerton, M.; Chamberlin, J. W. *Biochem. Biophys. Res. Commun.* **1968**, *33*, 29-31.
(55) Kubota, T.; Matsutani, S.; Shiro, M.; Koyama, H. *Chem. Commun.* **1968**, *1968*, 1541-1543.
(56) Berrada, R.; Dauphin, G.; David, L. *J. Org. Chem.* **1987**, *52*, 2388-2391.
(57) Cuer, A.; Dauphin, G.; G., J.; Beleil, J. C.; Y., L. J. *Nouv. J. Chim.* **1985**, *9*, 437-441.
(58) Toro, M.; Arzt, E.; Cerbon, J.; Alegria, G.; Alva, R.; Meas, Y.; Estrada-O, S. *J. Membr. Biol.* **1987**, *95*, 1-8.
(59) Sabela, A.; Koryta, J.; Valent, O. *J. Electroanal. Chem.* **1986**, *204*, 267-272.
(60) Antonenko, Y. N.; Yaguzhinsky, L. S. *Biol. Membr.* **1988**, *5*, 718-727.
(61) Lutz, W. K.; Wipf, H. K.; Simon, W. *Helv. Chim. Acta.* **1970**, *53*, 1741-1746.
(62) Alva, R.; Lugo-R., J. A.; Arzt, E.; Cerbon, J.; Rivera, B., E.; Toro, M.; Estrada-O *J. Bioenerg. Biomembr.* **1992**, *24*, 125-129.
(63) Riddell, F. G.; Tompsett, S. T. *Biochim. Biophys. Acta* **1990**, *1024*, 193-197.
(64) Pointud, Y.; Tissier, M.; Juillard, J. *J. Solution Chem.* **1983**, *12*, 473-483.
(65) Chamberlin, J. W.; Agtarap, A. *Org. Mass Spectrum.* **1970**, *3*, 271-285.
(66) Gachon, P.; Kergomard, A. *J. Antibiot.* **1975**, *28*, 351-357.
(67) Shiro, M.; Koyama, H. *J. Chem. Soc. B* **1970**, *2*, 243-253.
(68) Barrans, P. Y.; Alleaume, M. *Acta Crystallogr., Sect. B* **1980**, *36*, 936-938.
(69) Alleaume, M.; Hickel, D. *J. Chem. Soc., Chem. Commun.* **1972**, *3*, 175-176.
(70) Alleaume, M.; Hickel, D. *J. Chem. Soc., Chem. Commun.* **1970**, *1*, 1422-1423.
(71) Rodios, N. A.; Anteunis, M. J. O. *Bull. Soc. Chim. Belg.* **1977**, *86*, 917-929.
(72) Karplus, M. J. *J. Chem. Phys.* **1955**, *30*, 11-15.
(73) Rodios, N. A.; Anteunis, M. J. O. *Bull. Soc. Chim. Belg.* **1980**, *89*, 537-550.
(74) Grabley, S.; Hammann, P.; Klein, R.; Magerstadt, M. *Heterocycles* **1990**, *31*, 1907-1913.
(75) David, A. L.; Chapel, M.; Gandreuil, J.; Jeminet, G.; Durand, R. *Experientia* **1979**, *35*, 1562-1563.
(76) Cuer, A.; Dauphin, G. *J. Chem. Soc., Perkin Trans. II* **1986**, *2*, 295-281.
(77) Kinashi, H.; Otake, N.; Yonehara, H.; Sato, S.; Saito, Y. *Tetrahedron Lett.* **1973**, *1973*, 4955-4958.
(78) Miyazaki, Y.; Shibuya, M.; Sugawara, H.; Kawaguchi, O.; Hirose, C.; Nagatsu, J.; Esumi, S. *J. Antibiot.* **1974**, *27*, 814-821.
(79) Westley, J. W. *Ann. Rep. Med. Chem.* **1975**, *10*, 246-256.
(80) Occolowitz, J. L.; Berg, D. H.; Dobono, M.; Hamill, R. L. *Biomed. Mass Spectrosc.* **1976**, *3*, 272-277.
(81) Mitani, M.; Yamanish, T.; Miyazaki, Y. *Biochem. Biophys. Res. Commun.* **1975**, *66*, 1231-1236.
(82) Paulus, E. F.; Kurz, M.; Matter, H.; Vertesy, L. *J. Am. Chem. Soc.* **1998**, *120*, 8209-8221.
(83) Caughey, B.; Painter, G.; Gibbons, W. A. *Biochem. Pharmacol.* **1986**, *35*, 4103-4105.
(84) Seto, H.; Miyazaki, Y.; Fujita, K.-I.; Otake, N. *Tetrahedron Lett.* **1977**, *28*, 2417-2420.

(85) Riddell, F. G.; Tompsett, S. T. *Tetrahedron Lett.* **1991**, *47*, 10109-10118.
(86) Mronga, S.; Muller, G.; Fischer, J.; Riddell, F. G. *J. Am. Chem. Soc.* **1993**, *115*, 8418-8420.
(87) Caughey, B.; Painter, G.; Pressman, B. C.; Gibbons, W. A. *Biochem. Biophys. Res. Commun.* **1983**, *113*, 832-838.
(88) Well, J. L.; Bordner, J.; Bowles, P.; Mcfarland, J. W. *J. Med. Chem.* **1988**, *31*, 274-276.
(89) David, A. L.; Harris, J. S.; Russell, C. A.; Wilkins, J. P. G. *Analyst* **1999**, *124*, 251-256.
(90) Frausto da Silva, J. J. R.; Williams, R. J. P. *The Biological Chemistry of the Elements: the Inorganic Chemistry of Life*; Oxford University Press Inc.: New York, **2001**,

Chapter II

Experimental

A. Reagents

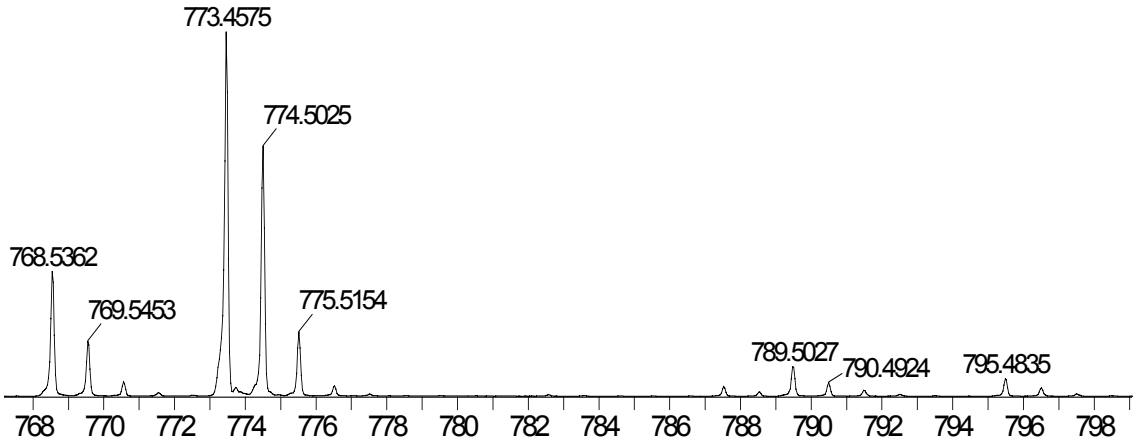
Salinomycin. Salinomycin, sodium salt, was purchased from Sigma, Fluka, CalbioChem, and Zhejiang Shenghua Biok Biology Co., Ltd. (P. R. China). The purity was reported to be 98% (by TLC analysis). The salt was analyzed using thin layer chromatography (TLC) and electrospray ionization mass spectrometry (ESI-MS). Results showed the presence of two compounds: sodium salinomycin and an impurity. The R_f values are 0.333 for sodium salinomycin and 0.41 for the impurity using silica gel TLC with 50% ethyl acetate/hexane (v/v). The formula of the impurity was determined using the positive mode of ESI-MS. The internal standard chosen for high resolution MS was spiromycin (MW 875.9) because its peaks are close to, but do not overlap with those of salinomycin. The formula $C_{43}H_{72}O_{10}Na^+$ provided a molecular weight (771.5022) that is closest to the experimental value (771.4598) of the molecular ion peak for the impurity with the same isotopic pattern. This molecular formula matched that of two polyether antibiotics: 20-deoxynarasin and 17-epi-20-deoxynarasin[1]. It was not possible to identify which one is the impurity in this study because the amount of the impurity confirmed by MS was not sufficient to prepare NMR samples.

Sodium salinomycin was purified using silica gel column chromatography with ethyl acetate/hexane 1:1 (v/v) as the eluting solvent. TLC (silica gel IB-F plates, Baker-flex) was used to monitor the eluting fractions in liquid chromatography. After being developed in 1:1 ethyl acetate/hexane (v/v), TLC plates were dipped into 5% phosphomolybdic acid/ethanol (v/v) and heated using a hot air gun because TLC spots of

sodium salinomycin were not visualized with a UV lamp or in an iodine chamber. The purity of sodium salinomycin was confirmed using NMR and electrospray ionization mass spectrometry (ESI-MS). Chemical shifts in ^{1}H NMR and ^{13}C NMR were compared with literature values[2] and the identity of sodium salinomycin was confirmed. The largest peak cluster in the ESI-MS of sodium salinomycin was $C_{42}H_{70}O_{11}Na^{+}$ (m/z 73.5). Other significant peaks were $C_{42}H_{69}O_{11}Na_2^{+}$ (m/z 795.5), ($C_{42}H_{70}O_{11}K^{+}$ (m/z 789.5), $C_{42}H_{69}O_{11}KNa^{+}$ (m/z 811.5), $C_{42}H_{70}O_{11}$-H_3O^{+} (m/z 768.5), and $C_{42}H_{70}O_{11}Na_2^{2+}$ (m/z 398.3) as shown in Figure II.1. In the negative mode of ESI-MS, there was only one peak cluster, $C_{42}H_{69}O_{11}$ (m/z 749.5). Only the purified salinomycin was used in the experiments described in this dissertation. Due to concerns about degradation, all ionophore solutions were freshly prepared. The concentrations of ionophore sodium salt solutions were determined by weighing. The concentrations of solutions of the ionophore in the acid form were determined by potentiometric titrations.

Nigericin. Nigericin, sodium salt, was purchased from Sigma, CalbioChem, Fluka, and Fermentek (Israel). The purity was reported to be 99% (by TLC analysis). The salt was analyzed using TLC and ESI-MS. Results showed only one compound (sodium nigericin) except the TLC for one sample from Fermentek. In the exceptional sample two spots were observed on the silica gel TLC plate (5% methanol in chloroform) with R_f values of 0.57 for the impurity and 0.70 for nigericin. No impurity peak showed in MS but two sets of ^{13}C peaks were found in NMR. Among all the compounds reported in literature, epinigericin was the only one consistent with this data. It has the same structure as nigericin shown in Figure I.6 except the different stereochemistry at C28 and

A. salinomycin



B. nigericin

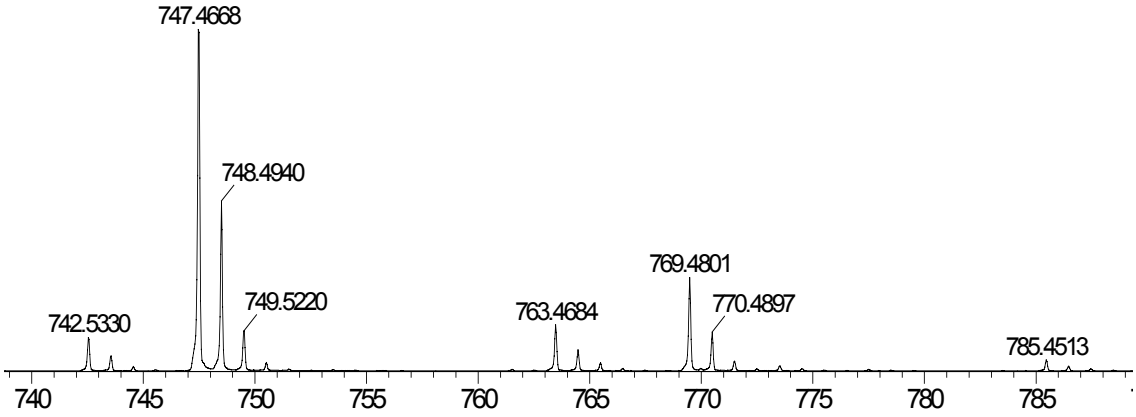


Figure II.1. ESI-MS of Na salinomycin salt from Sigma and Na nigericin salt from Fluka, recorded in the positive ion mode. The samples were prepared by dissolving the compounds of interest (1.0-10.0 μM) in methanol.

its R_f value was 0.57 (5% methanol in chloroform)[3]. It was reported that epinigericin was less stable than nigericin and the sodium salt of epinigericin was transformed into the acid form of nigericin using 0.1M HCl. Under acidic conditions, ring F opened and formed a ketonic intermediate. After bond rotation, the intermediate closed ring F to produce nigericin[3]. Based on this information, back extraction was done to test whether epinigericin was indeed our impurity. A sample in chloroform was extracted with 0.1 N HCl in water to isolate the free acid form of the ionophore. The ^{13}C NMR spectrum of

this product showed the exact same ^{13}C NMR spectra as the free acid form of nigericin obtained from pure sodium nigericin. That proved that the impurity was epinigercin and could be transformed into nigericin using back extraction from 0.1 M HCl. Although no other impurity was found in most of samples, all nigericin samples were purified by the same chromatographic method used for salinomycin. The purity of nigericin was checked using NMR and electrospray ionization mass spectrometry (ESI-MS). For the sodium salt of nigericin the largest peak cluster was $C_{40}H_{68}O_{11}Na^+$ (m/z 747.5) in ESI-MS. Other significant peaks were $C_{40}H_{67}O_{11}Na_2^+$ (m/z 769.5), $C_{40}H_{68}O_{11}K^+$ (m/z 763.5), $C_{40}H_{67}O_{11}KNa^+$ (m/z 785.5), $C_{40}H_{68}O_{11}\cdot H_3O^+$ (m/z 743.5), and $C_{40}H_{68}O_{11}Na_2^{2+}$ (m/z 385.3) as shown in Figure II.1. In the negative mode of ESI-MS, there was only one peak cluster ($C_{40}H_{67}O_{11}$, m/z 723.5). Only purified nigericin was used in the experiments described in this dissertation.

Salinomycin Acid (HSal). The sodium salt of salinomycin was transformed into the protonated form using back extraction. 20 mg of the sodium salt in 2-3 mL distilled chloroform was washed using 2-3 mL 1M hydrochloric acid three times and then using 2-3 mL double-distilled water three times[4]. The chloroform phase was dried under N_2, redissolved with acetone, and evaporated to help remove water in the product. The solid was dried under vacuum for 6 hours and stored in a freezer. Sodium content in the free acid form was checked by flame atomic emission and found to be lower than 0.05% (w/w). NMR spectra of free acid form in chloroform were compared with those in literature to confirm the identity of the product[5,6]. Due to the contamination by sodium

ions, the free acid form of salinomycin revealed the same spectra in ESI-MS as the sodium salt.

Nigericin Acid (HNi). Nigericin, sodium salt, was transformed into the acidic form by the same method used for salinomycin. HNi in CD_3OD was stored at 4°C for two weeks. No impurity peaks appeared in ^{13}C NMR after that period. That means HNi was stable at least two weeks in alcohol solvent at 4°C. The free acid form of nigericin behaved in the same way as nigericin, sodium salt in ESI-MS.

Tetraethylammonium salinomycin (Et_4NSal). The free acid form of salinomycin was neutralized by addition of a stoichiometric amount (1:1) of tetraethylammonium hydroxide in methanol. The completion of the reaction was indicated by the pH of the solution (pH 9). The product was dried under N_2 and then under vacuum for 6 hours. The tetraethylammonium ion is too big to bind strongly to salinomycin in ESI-MS; therefore sodium and potassium ions in MS replaced tetraethylammonium ions. Therefore, no peaks for Et_4Nsal^+ were observed. The tetraethylammonium salt of salinomycin behaved in the same way as the sodium salt of salinomycin except for the presence of the tetraethylammonium ion peak cluster (m/z 130.0). In the negative mode of ESI-MS only the anion peak cluster of salinomycin (m/z 749.5) was present. Similar behavior was observed previously for the ESI-MS study of tetraethylammonium monensin[7].

Tetraethylammonium nigericin (Et_4NNi). This salt was prepared using the method described for salinomycin. The ESI-MS spectrum showed tetraethylammonium ion and the same sodium and potassium clusters as those observed for sodium nigericin MS (m/z 130.0, 747.5, and 763.5).

Lasalocid A. Lasalocid, sodium salt ($C_{34}H_{53}O_8Na$), was purchased from Aldrich and its purity was reported to be 95%. It was used without further purification.

Maduramicin. Maduramicin, ammonium salt ($C_{47}H_{49}O_{17}NH_4$), was purchased from Sequoia Research Products Ltd. (the United Kingdom) and its purity was reported to be 97%. It was used without further purification.

Narasin. Narasin, sodium salt ($C_{43}H_{71}O_{11}Na$), was purchased from Sigma and its purity was reported to be 97%. It was used without further purification.

X-206. X-206 ($C_{42}H_{82}O_{14}$) was purchased from Alexis Biochemicals and its purity was reported to be 97%. It was used without further purification.

Lead Oxide and Lead Carbonate. PbO and $PbCO_3$ were obtained from Alfa Aesar in 99.9995% (metals basis) purity (Puratronic). There was no further purification.

Lead Perchorate. Ultra pure PbO (Alfa Aesar, 99.9995%) was reacted with 70% distilled perchloric acid (GFS Chemicals, Inc.) with a molar ratio of 1:1.01. The solution was diluted and standardized by titration with EDTA using methylthymol blue as the indicator and 10% hexamethylenetetramine as a buffer[8] (pH 6).

Zinc Perchlorate. ZnO (Alfa Aesar, 99.9995%) was dissolved in 70% perchloric acid (GFS Chemicals, Inc.) with a molar ratio of 1: 1.01. After crystallization from water the product was washed with diethyl ether and dried under vacuum. $Zn(ClO_4)_2$ solutions

were standardized by EDTA titrations with Eriochrome Black T (EBT) as the indicator and ammonia/ammonium chloride as a buffer (pH 10)[8].

Tetraethylammonium perchlorate (TEAP). Distilled perchloric acid (GFS Chemicals, Inc., 70%) was added dropwise into a solution of tetraethylammonium hydroxide (Aldrich, 20% in water). The completeness of the reaction was indicated by pH of the reaction mixture. The product was filtered and recrystallized three times from double distilled water. The final product was dried under vacuum for six hours.

Tetramethylammonium hydroxide. $(CH_3)_4NOH$ (Fluka, crystalline form, 97% purity) was stored under argon gas to reduce CO_2 contamination. Tetramethylammonium hydroxide solutions were stored under the same condition.

Tetraethylammonium hydroxide. $(C_2H_5)_4NOH$ 20% water solution (purum) was purchased from Fluka and was stored under argon gas to reduce CO_2 contamination.

Ethylenediaminetetraacetic acid disodium salt (EDTA). EDTA (Fisher, Certified A.C.S. grade) was used to standardize metal solutions. EDTA stock solutions were standardized using calcium carbonate (Mallinckrodt, primary standard grade) with EBT as an indicator and ammonia/ammonium chloride as a buffer (pH = 10)[8].

Sodium Chloride. NaCl (Aldrich, 99.999%, metals basis) was dried in the oven at 110^{o}C overnight. Solutions were prepared by weight.

Potassium Chloride. KCl (Aldrich, 99.999%, metals basis) was dried in the oven at 110^{o}C overnight. Solutions were prepared by weight.

Calcium Chloride. $CaCl_2 \cdot x$H2O (Aldrich, 99.999%, metals basis) was used to prepare solutions and was standardized by titration with EDTA using EBT as an indicator and ammonia/ammonium chloride (pH 10) as a buffer[8].

Magnesium Chloride. $MgCl_2$ (Alfa Aesar, Puratronic, 99.999%, metals basis) was using to prepare solutions and was standardized by titration with EDTA using EBT as an indicator and ammonia/ammonium chloride as a buffer[8].

Acetic Acid. Concentrated acid (Fisher, glacial, ≥99%) was diluted to give ~0.01M solutions. The solutions were titrated using tetramethylammonium hydroxide to determine pH correction factors in 80% methanol/water solutions that will be described in section I.D.

2-(*N*-morpholino) ethanesulfonic acid. MES (Sigma) was used without further purification.

Solvents. Methanol (Fisher, reagent grade) and chloroform (Fisher, reagent grade) were distilled before using. The drying agents are $CaSO_4$ for methanol and $CaCl_2$ for chloroform. Double distilled water was prepared using Corning Megapure (model MP-3A) glass distillation apparatus. Hexane (Fisher, reagent grade) and ethyl acetate (Fisher, reagent grade) were used without purification. Deuterated solvents (CD_3OD and $CDCl_3$, atom 99.8% D) for NMR were purchased from Cambridge Isotope Laboratories.

Glassware Cleaning. All glassware used for studies with salinomycin and nigericin was soaked in an acid bath (3:1 v/v sulfuric acid-nitric acid) for overnight and were rinsed thoroughly with distilled water.

B. Stability of salinomycin 80% methanol-water solutions

Several previous reports described the degradation of polyether ionophores under highly acidic and basic conditions[9,10]. However, there is one report about degradation of salinomycin in 2% methanol/water (v/v) solutions at room temperature and at 4°C[11]. In this study salinomycin solutions were stored at different temperatures and were checked periodically using HPLC-MS. Most of salinomycin turns into an isomer after 11 days at room temperature. MS spectra indicated existence of several intermediates. The structure of the isomer was identified by NMR[11]. This result indicated that extra care was needed in salinomycin experiments and only the dry powder form for any salinomycin was safe for long-term storage.

In this work it was found that salinomycin degraded readily even under mild conditions. Fresh salinomycin solutions in 80% methanol-water showed only a small peak (less than 0.2 absorbance for 0.1 mM salinomycin 80% methanol-water) at 210 nm in UV. After 11 days at room temperature, two large peaks with absorbance ~2 were found at 290 nm and at 210 nm. This behavior contrasts that found for monensin and lasalocid studied previously, where no signs of degradation were observed under conditions similar to those used in this work.

UV and CD spectroscopy were used to study the stability of salinomycin in 80% methanol-water. Spectra for salinomycin solutions in 80% methanol-water at different pHs and with different concentrations were recorded periodically. The presence of a peak at 290 nm in the UV spectra was adopted as the sign of degradation because emergence of that peak took place earlier than the increase in absorbance at 210 nm. It was found that the degradation rate of salinomycin in 80% methanol-water increased at

lower pH and higher concentrations. No peak appeared at 290 nm in the UV spectra of salinomycin (0.01 M) solutions at pH 4.0-8.0 for at least two days at 4 ^{o}C and in the UV spectra of 0.01M solutions (pH 3.0) stored overnight at 4 ^{o}C. Salinomycin solutions (0.01 M and 0.1 mM) at pH 3.0 did not show signs of degradation in the UV for three hours at room temperature. The same behavior was found for salinomycin (0.1 mM) at pH 4.461 for nine hours at room temperature. CD spectra for 0.1 mM salinomycin solutions at pH 5.0-8.0 showed that the absorbance at 208 nm started to decrease and the peak intensity at 290 nm changed less than 2% even after a day, indicating those solutions was stable for at least 20 hours at room temperature.

Based on these studies, experiments were carefully designed to prevent degradation of salinomycin. Salinomycin solutions were made fresh, stored at 4 ^{o}C immediately or used in less than an hour. Salinomycin solutions were made using a dry powder of salinomycin in the acid form. The pH values for those solutions were higher than 4.0 and the solutions should be stable for nine hours at room temperature. In some cases, lower initial pH values were used in UV titrations and lead potentiometric titrations; however, all potentiometric titrations were completed in an hour or less, so the solutions were at pH 3.0-4.0 for less than half an hour. The only concern was about UV titrations of salinomycin with pH ~4.0, although there was no obvious peak at 290 nm in UV spectra. Degradation studies were done under the conditions used for the UV titrations. A solution was freshly prepared with the same concentrations of components (Pb^{2+}, salinomycin, buffer, and TEAP) and the same pH value as the final sample in UV titrations of salinomycin. UV spectra were obtained immediately after mixing and after 25 minutes, the typical period required for UV titrations. These two spectra were

compared with the UV spectrum for the corresponding final sample from UV titrations. There was no obvious difference in those three spectra indicating that degradation was minimal during the time required for the UV titrations. A peak at 290 nm was found in the UV spectra of UV titration samples after five hours at room temperature. When compared to salinomycin solutions with the same concentrations at pH 3.0 that were stable only for three hours at room temperature, it appears that lead complexation decreased the degradation rate of salinomycin.

During the back extraction salinomycin was partitioned to the chloroform phase where it was more stable than in 80% methanol-water. For the free acid form of salinomycin prepared by back extraction, then dissolved in 80% methanol-water, no peak at 290 nm was observed in UV spectra. The stability of salinomycin under strongly basic conditions (pH >9.0) was not investigated because such high pH conditions were never used in this work.

The stability of nigericin in 80% methanol-water was not investigated because there was no evidence of degradation in the UV spectra of nigericin solutions at pH 3.0-4.0 maintained at 25 ^{o}C for a day.

C. Preparation of lead-salinomycin (1:2) and lead-nigericin (1:2) complexes.

Lead-salinomycin (1:2) and lead-nigericin (1:2) complexes were prepared by several methods. In the first method the acid forms of salinomycin or nigericin (40–25 mg) were reacted with lead oxide or lead carbonate at a 2:1 molar ratio (ligand/Pb) in 20 mL of methanol, as shown in eqs II.1 and II.2.

$$2HSal_{(MeOH)} + PbO_{(s)} \longrightarrow PbSal_{2\,(MeOH)} + H_2O \qquad (II.1)$$

$$2HNi_{(MeOH)} + PbO_{(s)} \longrightarrow PbNi_{2\,(MeOH)} + H_2O \qquad (II.2)$$

Polytetrafluoroethylene (PTFE) beakers were used as containers to diminish the contamination by sodium or potassium ions from glassware. The solutions were stirred for 24-36 hours and then centrifuged. The supernatant was dried under N_2 and then under vacuum for 6 hours and the product was characterized by mass spectrometry and ^1H and ^{13}C NMR. Combustion analysis and atomic absorption measurements were done to obtain the elemental compositions of the lead complexes. The details will be discussed later.

The second method is the back extraction of tetraethylammonium nigericin (or salinomycin) with aqueous solutions of lead nitrate, as shown in eqs II.3 and II.4.

$$Et_4NNi_{(CHCl_3)} \xrightarrow{\text{excess } Pb(NO_3)_{2\,(aq)}} Pb(Ni)_{2\,(CHCl_3)} + Et_4NClO_{4\,(aq)} \qquad (II.3)$$

$$Et_4NSal_{(CHCl_3)} \xrightarrow{\text{excess } Pb(NO_3)_{2\,(aq)}} Pb(Sal)_{2\,(CHCl_3)} + Et_4NClO_{4\,(aq)} \qquad (II.4)$$

40 mg tetraethylammonium nigericin was dissolved in 4 mL chloroform. That solution was extracted three times with 4 mL of aqueous 0.1 M lead nitrate (pH 4.3). The chloroform phase was evaporated under N_2 and dried under vacuum for 6 hours. The product was characterized by mass spectrometry and ^1H and ^{13}C NMR. Combustion

analysis and atomic absorption measurements were done to obtain the elemental compositions of the lead complexes. The details will be discussed later.

Another method was tried where lead carbonate was mixed with the free acid form of nigericin at a 2:1 molar ratio (ligand/Pb) in methanol. The reactions were shown in eqs II.5 and II.6.

$$2HSal_{(MeOH)} + PbCO_{3\,(s)} \longrightarrow PbSal_{2\,(MeOH)} + H_2O + CO_{2\,(g)} \quad \text{(II.5)}$$

$$2HNi_{(MeOH)} + PbCO_{3\,(s)} \longrightarrow PbNi_{2\,(MeOH)} + H_2O + CO_{2\,(g)} \quad \text{(II.6)}$$

About 16 mg of the acid form of nigericin or salinomycin was dissolved in about 20 mL methanol and 3.3 mg solid lead carbonate was added. A polytetrafluororoethylene (PTFE) beaker was used to prevent contamination by sodium or potassium ions. The mixture was stirred for 48 hours and then centrifuged. The methanol supernatant was dried under N_2 and then under vacuum for 6 hours. Analysis using atomic absorption showed that only one third of the lead ions reacted with nigericin or salinomycin.

For lead nigericin 2:1 complex another method has been tried. The free acid form of nigericin was reacted with lead acetate at a 2:1 molar ratio (ligand/Pb) in methanol. 12 mg of the acid form of nigericin was dissolved in 10 mL acetone. 7 mg lead acetate trihydrate, insoluble in acetone, was added into the solution. Solids disappeared after two hours' stirring and stirring was continued for one day. The acetone solution was separated into two parts. 5 mL chloroform and then 5 mL double stilled water was added into one part. In the second part 5 mL water and then 5 mL chloroform was added to wash off the acetic acid. Both solutions were stirred for five minutes. The aqueous phase was separated from the organic phase by centrifugation. The chloroform phase was washed with double distilled water three times, dried under N_2 and under vacuum for 6

hours. Lead percentages in these two samples were measured using AA. The samples were also submitted for MS analysis. There was no lead signal in the AA and only small signals in MS spectra for nigericin-lead complexes. For the purpose of excluding errors from MS, the mixture of 10^{-4} M nigericin acid form and lead nitrate at a 1:1 molar ratio in methanol (pH 7.2) was submitted to MS analysis. A strong signal for lead-nigericin complexes was shown in MS spectra. The hypothesis was that the acetone solution is so acidic that lead cannot bind with nigericin efficiently and was extracted to the water phase. The lead percentage in the aqueous phase was checked by AA. The result was consistent with the theory.

D. pH* measurements

The solvent system used for all the ionophore titrations in this work is 80% methanol-water, which is proposed to have polarity similar to the aqueous-lipid interfaces of biological membranes or phospholipid vesicles[12]. The protonation constants and complexation constants of ionophore A23187 in the presence of mono- and divalent cations in 80% methanol-water agree with the corresponding values obtained in phospholipid vesicles[13-16]. Those results provide support for the validity of replacement of phospholipid vesicle systems with 80% methanol-water systems for the titrations of polyether ionophores. This is required for nigericin and salinomycin because these ionophores do not have suitable chromophores for spectroscopic titrations used in studies with vesicles.

In this mixed solvent system there is a great difference in acidity measurements from those done in water system. Acidity measurements were studied by de Ligny et al.[17] and Gelsema et al.[18,19] who invented a convenient pH^* scale for the methanol/water system used in this work. An asterisk indicates quantities measured in the 80% methanol/water system. The symbol pH*, defined in eqs II.7 and II.8, represents acidity in 80% methanol/water solutions, analogous to pH for aqueous solutions.

$$pH^* = -\log \alpha^*_{H+} = pH_{obs} - \delta \qquad \text{(II.7)}$$

$$\delta = E_j - \log_m \gamma_H \qquad \text{(II.8)}$$

In these equations α^*_{H+} is the activity of hydrogen ion in the mixed solvent, pH_{obs} is the observed pH-meter reading, and δ is a correction factor. Theoretically, δ is defined as the difference between the liquid junction potential, E_j and the medium effect, $\log_m \gamma_H$. Because both of these quantities are difficult to measure, a convenient method has been

adopted where δ is obtained by measuring the difference between values of the experimental ($\log K^{m*}_{H,exp}$) and the reference ($\log K^{m*}_{H,ref}$) mixed-mode protonation constants for acetic acid in 80% methanol-water, according to eq II.9.

$$\delta = \log K^{m*}_{H,exp} - \log K^{m*}_{H,ref} \tag{II.9}$$

The mixed-mode constant is defined by eq II.10 below

$$L^- + H^+ \rightleftharpoons HL \qquad K^{m*}_H = \frac{[HL]}{\alpha^*_H [L^-]} \tag{II.10}$$

where $[HL]$ and $[L^-]$ are molar concentrations of the protonated and deprotonated forms of acetic acid, respectively. The value of $\log K^{m*}_{H,ref}$ was calculated from the thermodynamic protonation constant $\log K^{t*}_H$, because no mixed-mode constants for our experimental conditions were available in the literature. The relationships used in this calculation are given in eq II.11

$$\log K^{t*}_H = \frac{\alpha^*_{HL}}{\alpha^*_H \alpha^*_L} = \log K^{m*}_H \frac{\gamma^*_{HL}}{\gamma^*_L} = \log K^{c*}_H \frac{\gamma^*_{HL}}{\gamma^*_H \gamma^*_L} \tag{II.11}$$

where α^*_X is ion activity for a given specis, γ^*_X is the corresponding activity coefficient, and $\log K^{c*}_H$ is the concentration mode protonation constant in 80% methanol-water. The values of $\log K^{t*}_H$ for acetic acid reported are 6.50[20], 6.64[21], and 6.57[22].

Oiwa reported the values for the activity coefficients of hydrochloric acid in 80% methanol-water[23]. Due to the use of the molal concentration scale and lack of values for the condition (I = 0.05 M), several calculations have been done to obtain activity coefficient values for the experimental conditions used in this work.

Mark Craig[24] fitted the available activity coefficient values with a quadratic function[25] derived from the Pitzer equation and then applied the values of each parameter from the curve fitting into the Pitzer equation to calculate $\gamma_{\pm}$ for the ionic strength used in this work. According to the experimental conditions used in this work the Pitzer equation was simplified[26] and was transformed as shown in eq II.12 so that the non-linear least-squares program could be used to fit the curve and provide the Pitzer parameters, B_{MX}^{γ} and C_{MX}^{γ}. The curve fitting is shown in Figure II.2.

$$\ln \gamma_{\pm} - f_{\gamma} = IB_{MX}^{\gamma} + I^2 C_{MX}^{\gamma} \qquad \text{(II.12)}$$

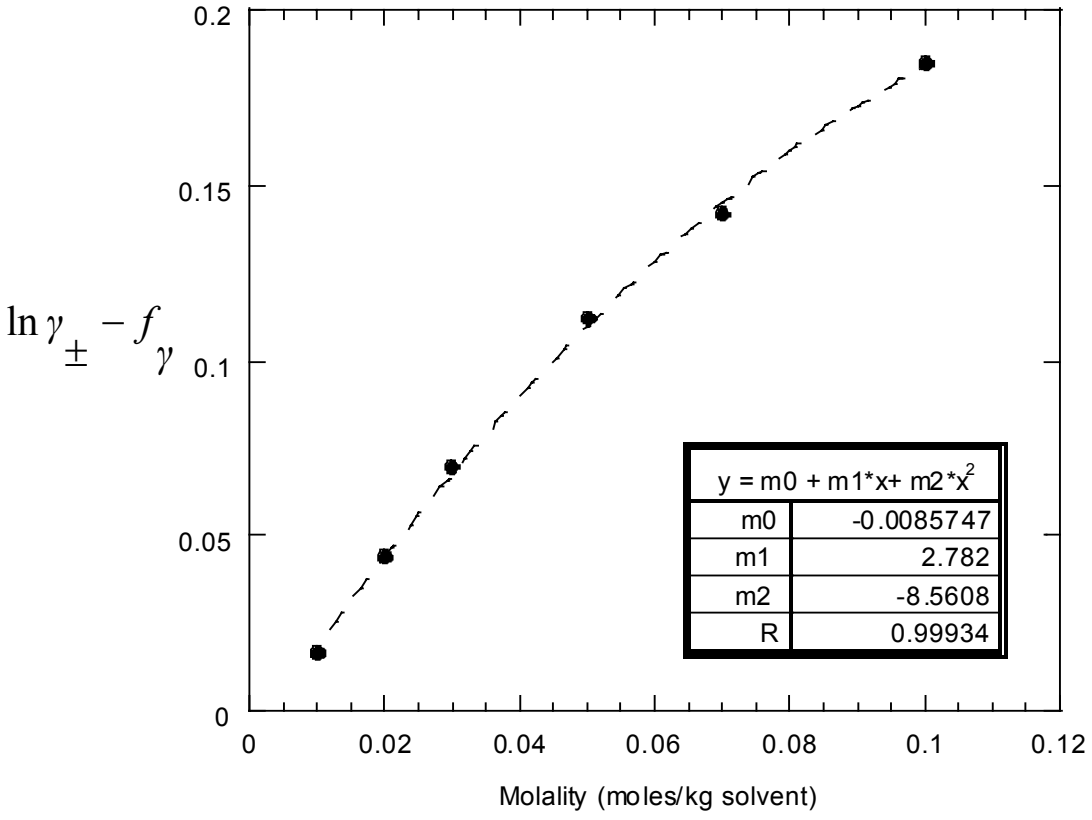


Figure II.2. Plot of activity coefficients[23] vs. molal ionic strength for HCl in 80% methanol-water. The dotted line is the result of curve fitting using the modified Pitzer equation (eq II.12). The insert table shows the parameters (m1 = B_{MX}^{γ}, m2 = C_{MX}^{γ}).

The value of $\log \gamma_{\pm}$ for experimental conditions in this work (I = 0.05 M, monovalent ions) was determined to be –0.187 ($\gamma_{\pm}$ = 0.650).

Equations II.13 and II.14 are used for conversion between the molal (m) and molar concentration (M) scales.

$$M = \frac{md}{1-(0.001 \times m \times MW)} \qquad \text{(II. 13)}$$

$$m = \frac{M}{d+(0.001 \times M \times MW)} \qquad \text{(II. 14)}$$

where MW is the molecular weight of electrolyte ($(C_2H_5)_4NClO_4$, 229.7), and d is the density of 80% methanol in this work (0.8425 g/mL)[20]. For 0.05 M TEAP in 80% methanol-water, the molar concentration is 0.059 molal. The molar concentration scale is applied in this work, unless indicated otherwise.

The protonation constant of acetic acid obtained by conductance measurements[21] was thought more accurate by Rorabacher et al. due to absence of such errors as in pH* measurements[22]. The mean of this value (6.64) and Rorabacher's value (6.57) was used in the calculation of $\log K^{m*}_{H,ref}$ that was found to be 6.42 (I = 0.05 M). The experimental value $\log K^{m*}_{H,\text{exp}}$ was determined by potentiometric titrations of 0.01-0.02 M acetic acid with 0.01 M tetramethylammonium hydroxide (I = 0.05 M) in 80% methanol-water followed by data analysis using the program PKAS[27].

The solvent autoprotolysis constant was required in the programs PKAS and BEST[27] used to fit the data from potentiometric titrations. The chemical equation and

equilibrium expressions for the mixed-mode autoprotolysis constant, K_S^{m*} , and the concentration autoprotolysis constant, K_S^{c*} , are shown eqs II.15, II.16, and II.17.

$$ROH \rightleftharpoons RO^- + H^- \quad \text{(II.15)}$$

$$K_S^{m*} = \alpha_H^* [RO^-] \quad \text{(II.16)}$$

$$K_S^{c*} = [H^+][RO^-] \quad \text{(II.17)}$$

The values of these two constants were calculated using the relationship involving the thermodynamic autoprotolysis constant, K_S^{t*} , and calculated activity coefficient, ${\gamma_\pm}^*$, as shown in eq II.18.

$$K_S^{t*} = \alpha_{H^+}^* \alpha_{OH^-}^* = K_S^{m*} \ {\gamma_\pm}^* = K_S^{c*} \ ({\gamma_\pm}^*)^2 \quad \text{(II.18)}$$

The values of different autoprotolysis constants for 80% methanol-water are listed in Table II.1.

Table II.1. Autoprotolysis constants for 80% methanol-water (I = 0.05 M)[28]

	$\log K_S^{x*}$
$\log K_S^{t*}$	-14.42 (I = 0.0 M)
$\log K_S^{m*}$	-14.23
$\log K_S^{c*}$	-14.05

The value of $\log K_S^{m*}$ (-14.23) was used in the PKAS program for the calculation of $\log K_{H,\ \exp}^{m*}$ for acetic acid. Based on the value obtained for $\log K_{H,\ \exp}^{m*}$, the electrode solvent correction factor in 80% methanol-water mixtures (δ) can be determined.

The method for pH* measurements in methanol solutions was based on the procedures described by de Ligny and coworkers[18,19]. Electrodes were calibrated in aqueous buffer solutions and then soaked in the methanol-water solvent to be used for experimental measurements. The procedure used in this work involves soaking the electrodes (Sensorex Phase, model S1021CD; Orion model 8103 Ross) in the desired solvent for at least 2 hours. The electrodes are then calibrated in aqueous buffer solutions (Gram-Pac, Fisher: pH 4.01, 6.86, and 9.18). These two procedures produce the same result. High pH buffer solutions (pH 6.86 and 9.18) were covered with argon gas to minimize CO_2 contamination. The internal filling solutions of electrodes are 0.1 M tetraethylammonium perchlorate in 20% methanol (for titrations involving lead, zinc and magnesium ions) and 3 M tetraethylammonium chloride in 20% methanol (for titrations involving sodium, potassium, and calcium ions). Tetraethylammonium perchlorate and tetraethylammonium chloride were used for the cations indicated to prevent clogging of the electrode glass frit junction by precipitation. Fisher pH meters, model 825MP, or model AR15 were used in electrode calibration and pH* measurements.

E. Determination of CO_2 percentage in tetramethylammonium hydroxide titrant solutions.

Contamination from CO_2 changes the concentrations of tetramethylammonium hydroxide solutions greatly, which would cause severe problems in the potentiometric titrations. A standard procedure was performed to decrease the CO_2 percentage in tetramethylammonium hydroxide titrant solutions. The mixed solvent was made using freshly boiled methanol and freshly boiled water. All containers used for preparation or storage of 80% methanol-water and tetramethylammonium hydroxide solutions were filled with argon gas before and after solutions were poured in. It was sufficient to blow argon gas into the bottles for five minutes.

The method of testing for the CO_2 percentage employs the titration of 10-20 mM $HClO_4$ in 80% methanol with tetramethylammonium hydroxide solutions. Based on the titration data and eq II.19, the Gran function[29], f, was plotted versus the titrant volume

$$f = (V_0 + V_b)10^{\pm pH^*} \qquad \text{(II. 19)}$$

where V_0 is the initial volume, V_b is the titrant volume, pH* is –log α_H^* in 80% methanol-water, and "+" or "-" are used in the basic or acidic regions of the titration data, respectively. A linear least-squares function in the program Kaleidagraph[30] was applied to fit acidic and basic regions of the plot, individually. The intersections of the fitted lines with the x-axis were represented as V_- in the acidic region and as V_+ in the basic region. The percentage CO_2 in the tetramethylammonium hydroxide solutions was calculated based on eq II.20.

$$\%CO_2 = \frac{(V_- - V_+)}{2V_-}100\% \qquad \text{(II. 20)}$$

Solutions of Me_4NOH with a percentage CO_2 greater than 2% were not used in potentiometric titrations[27]. An example of the plot with fitted lines is shown in Figure II.3 ($V_+ = 4.040$, $V_- = 4.117$, and $\%CO_2 = 0.94$).

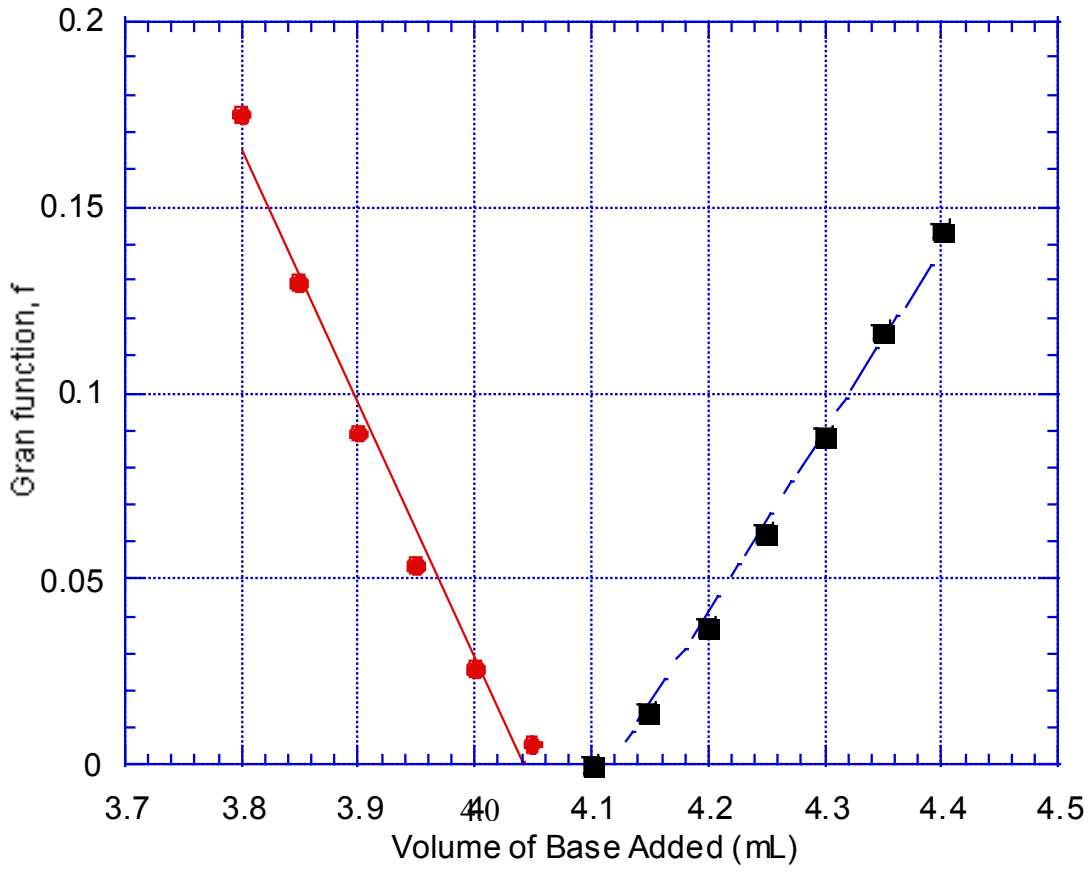


Figure II.3. Gran plot for a titration of perchloric acid with tetramethylammonium hydroxide.

F. Measurement of protonation constants and metal complexation constants of nigericin and salinomycin.

Potentiometric titrations

Different concentrations of ionophore in free acid form (0.4-3.2 mM) were titrated with 20 mM tetramethylammonium hydroxide in 80% methanol-water at 25 ^{o}C, using the autotitrator system that consists of a Metrohm model 655 digital buret, a Fisher 825MP pH meter, the electrodes described in section II.C, and a Zenith 158-42 computer[31]. The ionic strength of the solutions was adjusted to 0.05 M using tetraethylammonium perchlorate. If there are potassium ions in the solutions, tetraethylammonium chloride is used to avoid precipitation of potassium perchlorate. Due to concerns about degradation, all ionophore solutions were prepared freshly and then stored at 4 ^{o}C. N_2 gas saturated with 80% methanol-water is bubbled into the solutions to minimize CO_2 contamination during the titrations. The amount of excess strong acid in the solutions was minimized because some ionophores are not stable in a strongly acidic environment[32]. The titrant (Me_4NOH) was standardized against 0.01M KHP solution, followed by titration with $HClO_4$ to check CO_2 percentage (section II.E). For titrations in the presence of metal ions, various ratios of ionophore to metal concentration were used. Metal salt solutions of lead perchlorate, sodium chloride, calcium chloride, zinc perchlorate, potassium chloride or magnesium perchlorate were added into a solution of the free acid form of the ionophore in 80% methanol-water. The solution was stirred for 5 minutes to allow the components to reach equilibrium. The concentrations of the metal salt solutions were standardized by titration with EDTA except NaCl and KCl. The titration data were analyzed using the programs PKAS[27] to

obtain the mixed-mode protonation constants and BEST[27] for complexation constants. Based on eqs II.21 and II.22 below, the concentration mode protonation constants were calculated.

$$K_H^{c^*} = \frac{[HA]}{[H^+][A^-]} = \frac{\gamma_H^*[HA]}{\alpha_H^*[A^-]} = \gamma_\pm{}^* K_H^{m^*} \qquad \text{(II.21)}$$

$$\log K_H^{c^*} = \log K_H^{m^*} + \log \gamma_\pm{}^* \qquad \text{(II.22)}$$

In 80% methanol-water at 0.05 M ionic strength $\log \gamma_\pm{}^*$ is 0.187, thus

$$\log K_H^{c^*} = \log K_H^{m^*} - 0.187 \qquad \text{(II.23)}$$

UV-Vis Spectrophotometric studies

Most nigericin or salinomycin complexes don't show any significant UV peaks while their lead complexes have strong absorbance around 240 nm, which makes UV studies of these ionophores feasible. Titrations were carried out in two different pH ranges. At pH 6, 2.7 mL lead perchlorate (0.1 mM) solutions in 80% methanol-water (I = 0.05 M, TEAP) were titrated by addition of small aliquots (3-10 μL) of 0.01 M solutions of the ionophore (sodium salt) in 80% methanol-water buffered by 3 mM MES. The opposite titration order (ionophore solutions titrated with lead solutions) was not used in UV titrations because of the strong interference by the UV peak for lead around 230 nm. The sodium salts of ionophores were chosen for convenience because the weak binding by sodium ion does not compete with the interaction between lead and ionophores. Titrations at lower pH (pH 3.0-4.0) were done to estimate the stability constants of ionophore-lead (1:1) complexes. Small aliquots (3-10 μL) of a 10 mM solution of

ionophore sodium salt were used to titrate 2.7 mL of a solution containing 0.1 mM lead perchlorate in 80% methanol-water at 25 ^{o}C with an ionic strength of 0.05 M (TEAP). More than 99% of nigericin and salinomycin exist in free acid form at pH 4. No suitable buffer was found to be soluble enough at pH ~3.5. Aliquots (2 μL) of 0.04 M tetraethylammonium hydroxide in 80% methanol-water were added three times to control the pH. The pH value was measured at the end of UV titrations. The difference between the initial pH and the final pH was less than 0.1, indicating a stable pH value during the reaction.

In both types of experiments, the pH adjustment was done using 1 M perchloric acid and 1 M tetraethylammonium hydroxide 80% methanol-water solutions. The reaction took place in a 1 cm cuvette containing a micro stir bar for mixing. For better mixing, the cuvette was inverted at least four times and placed in the thermostated holder controlled at 25 ^{o}C. After each addition of ionophore solution the UV spectra were recorded using a Hewlett-Packard 8452A diode array spectrophotometer.

Circular Dichroism spectrophotometric studies

Circular dichroism spectra were recorded using an Aviv circular dichroism spectrometer, model 202-01. Concentrated 80% methanol-water solutions (metals, ionophores, buffers, and TEAP) were mixed and diluted into desired concentrations. All the solutions were placed in a 1 cm cuvette, inverted at least four times and placed in the thermostated holder controlled at 25 ^{o}C. UV spectra of comparable solutions were recorded to ensure the completion of reactions before any CD spectra were taken.

G. Nuclear Magnetic Resonance (NMR) studies of nigericin-lead and salinomycin-lead complexes

NMR studies were performed on a Varian VXR-500X 500 MHz spectrometer with a 3 mm 2-nuclei auto-NMR gradient probe, a Varian VMX-400 Unity Plus 400 MHz spectrometer with a Varian 5 mm 4-nuclei auto-NMR probe, and a VXR-300 (300 MHz proton) with a Varian 5 mm 3-nuclei auto-NMR gradient probe. The NMR experiments employed are ^{1}H NMR, ^{13}C NMR, DEPT (Distortionless Enhancement by Polarization Transfer, HMQC (Heteronuclear Multiple Quantum Coherence), HSQC (Heteronuclear Single Quantum Correlation), and HMBC (Heteronuclear Multiple Bond Coherence). All the NMR spectra were recorded in CD_3OD and $CDCl_3$ at 25 ^{o}C. Chemicals used in NMR experiments are sodium nigericin, tetraethylammonium nigericin, nigericin in the free acid form, the lead-nigericin (1:2) complex, sodium salinomycin, tetraethylammonium salinomycin, salinomycin in the free acid form and the lead-salinomycin (1:2) complex. These compounds (10-40 mg) were dissolved in 0.7 mL (for the 5 mm probe) or 0.3 mL of the appropriate deuterated solvent (for the 3 mm probe) and were recorded on the same day or stored at $-4^{o}C$ for NMR experiments carried out at a later date.

References

(1) Westley, J. W. In *Polyether Antibiotics: Naturally Occurring Ionophores, Volume 2: Chemistry*; Marcel Dekker, INC: New York, **1983**,
(2) Riddell, F. G.; Tompsett, S. T. *Tetrahedron Lett.* **1991**, *47*, 10109-10118.
(3) Berrada, R.; Dauphin, G.; David, L. *J. Org. Chem.* **1987**, *52*, 2388-2391.
(4) Cox, B. D.; Van Truong, N.; Rzeszotarska, J.; Schneider, H. *J. Am. Chem. Soc.* **1984**, *106*, 5965-5969.
(5) Seto, H.; Yahagi, T.; Miyazaki, Y.; Ôtake, N. *J. Antibiot.* **1977**, *30*, 530-532.
(6) Anteunis, M. J. O.; Rodios, N. A. *Bull. Soc. Chim. Belg.* **1981**, *90*, 715-735.
(7) Ivanova, O. G., University of Oklahoma, **2000**.
(8) Vogel, A. I. *Vogel's Text Book of Quantitative Chemical Analysis,* 5 ed.; Longman Scientific & Technical: Essex, **1989**,
(9) Well, J. L.; bordner, J.; bowles, P.; Mcfarland, J. W. *J. Med. Chem.* **1988**, *31*, 274-276.
(10) Gachon, P.; Kergomard, A. *J. Antibiot.* **1975**, *28*, 351-357.
(11) David, A. L.; Harris, J. S.; Russell, C. A.; Wilkins, J. P. G. *Analyst* **1999**, *124*, 251-256.
(12) Fernandes, M. S.; Fromherz, P. *J. Phys. Chem.* **1977**, *81*, 1755-1761.
(13) Kauffman, R. F.; Taylor, R. W.; Pfeiffer, D. R. *Biochemistry* **1982**, *21*, 2426-2435.
(14) Taylor, R. W.; Pfeiffer, D. R.; Chapman, C. J.; Craig, M. E.; Thomas, T. P. *Pure Appl. Chem.* **1993**, *65*, 579-584.
(15) Chapman, C. J.; Puri, A. K.; Taylor, R. W.; Pfeiffer, D. R. *Biochemistry* **1987**, *26*, 5009-5018.
(16) Taylor, R. W.; Chapman, C. J.; Pfeiffer, D. R. *Biochemistry* **1985**, *24*, 4852-4859.
(17) De Ligny, C. L.; Luykx, P. F. M.; Rehbach, M.; Wieneke, A. A. *Recl. Trav. Chim. Pay. B.* **1960**, *79*, 699-712.
(18) Gelsema, W. J.; de Ligny, C. L.; Remijnse, A. G.; Blijleven, H. A. *Recl. Trav. Chim. Pay. B.* **1966**, *85*, 647-660.
(19) Gelsema, W. J.; de Ligny, C. L.; Blijleven, H. A. *Recl. Trav. Chim. Pay. B.* **1967**, *86*, 852-864.
(20) Bacarella, A. L.; Grunwald, E.; Marshall, H. P.; Purlee, E. L. *J. Org. Chem.* **1955**, *20*, 747-762.
(21) Shedlovsky, T.; Kay, R. L. *J. Phys. Chem.* **1956**, *60*, 151-155.
(22) Rorabacher, D. B.; MacKellar, W. J.; Shu, F. R.; Bonavita, M. *Anal. Chem.* **1971**, *43*, 561-573.
(23) Oiwa, I. T. *J. Phys. Chem.* **1956**, *60*, 754-759.
(24) Craig, M. E. Ph.D., University of Oklahoma, **1990**.
(25) Pitzer, K. S. *J. Phys. Chem.* **1973**, *77*, 268-277.
(26) Pitzer, K. S.; Mayroga, G. J. *J. Phys. Chem.* **1973**, *77*, 2300-2308.
(27) Martell, A. E.; Motekaitis, R. J. *Determination and Use of Stability Constants,* 2nd ed.; VCH Publishers: New York, **1992**,
(28) Taylor, R. W. Ph.D., Wayne State University, **1973**.
(29) Gran, G. *Analyst* **1952**, *77*, 661-671.
(30) KaleidaGraph; 3.5 ed.; Synergy Software, **1990**.

(31) Stiles, M. K.; Craig, M. E.; Gunnell, S. L. N.; Pfeiffer, D. R.; Taylor, R. W. *J. Biol. Chem.* **1991**, *266*, 8336-8342.
(32) Anteunis, M. J. O. In *Polyether Antibiotics: Naturally Occurring Ionophores, Volume 2: Chemistry*; Westley, J. W., Ed.; Marcel Dekker: New York, **1983**.

Chapter III

CD studies of ionophore-metal binding

CD spectroscopy has been employed to study the protonation, metal complexation and conformational equilibria of polyether ionophores in solutions[1] and in suspensions of phospholipid vesicles[2]. The naturally occurring polyether antibiotic ionophores are amendable to this technique because these molecules contain one or more chiral centers. Furthermore, the CD spectra are sensitive to the environmental and conformational changes of the ionophore. In many cases the conformation of the ionophore will be altered by protonation or metal complexation resulting in changes in the CD spectra. These changes can be utilized to obtain information about the stoichiometry of the metal-ionophore complexes and under suitable conditions the corresponding equilibrium constants. The following section describes studies carried out using CD spectroscopy to investigate the reactions of Pb^{2+} with nigericin, salinomycin and several related ionophores as well as reactions of salinomycin with other metal ions. The additional ionophores selected for study include monensin, narasin, maduramicin, lasalocid, and X-206. Their structures are shown in Figure I.1. Previous studies have shown that monensin and lasalocid transport Pb^{2+} with high selectivity[3]. Narasin differs from salinomycin by the presence of one additional methyl group and has been studied using CD spectroscopy[1]. Maduramicin is similar to nigericin except for the addition of a pendent glycoside moiety to the ionophore backbone. X-206 differs from the other monovalent cation ionophores in that it does not contain any spiroketal subunits and has a longer backbone chain.

The complexation of Pb^{2+} was investigated by titrations of solutions of the ionophore with $Pb(ClO_4)_2$ at a controlled pH*. Solutions of the ionophores (~0.1 mM) in 80% methanol-water were prepared and buffered using 3 mM MES (pH* ~6.5) and the ionic strength was adjusted to 0.05 M using TEAP. Aliquots of a 0.01 M lead perchlorate solution in 80% methanol-water were added to the ionophore solutions to reach desired molar ratios of total lead over total ionophore concentrations. UV spectra were taken periodically to ensure the completion of reactions. All reactions reached equilibrium in less than a minute. The CD spectra were recorded as described in Section II.F. The exact concentrations of all components and pH* values are described in the corresponding figure captions. CD spectra of salinomycin, narasin, lasalocid, nigericin, maduramicin, and monensin with addition of lead solutions are shown in Figures III.1, III.4, III.6, III.8, III.11, and III.13, respectively.

The polyether ionophores studied in this chapter are divided into two groups. In the first group salinomycin, narasin and lasalocid have negative CD signals due to the carbonyl chromophore[1]. The second group, which includes nigericin, monensin, maduramicin, and X-206, has no inherent CD peaks. The addition of Pb^{2+} increased the intensity of the negative peak at ~295 nm in CD spectra, which is a distinct feature for the first group. Each of the three ionophores in the first group also showed its own pattern. For salinomycin the negative peak at 215 nm disappeared and a new small negative peak emerged at 238 nm that corresponds with the positive peak at 238 nm used in UV analysis. The lead-narasin system possessed similar features as the lead-salinomycin system but with larger signals and absence of the peak at 238 nm. In the lead-lasalocid system a small positive signal occurred at 255 nm.

CD spectra for the second group after addition of Pb^{2+} show significant peaks in the wavelength range 225-240 nm. For nigericin a negative peak at 239 nm grows with addition of Pb^{2+}. There was no clear pattern for the positive peak at 220 nm because the peak was close to the noise region and affected greatly. For the maduramicin-lead mixture CD spectra showed formation of a large positive peak at 239 nm and a small positive peak at 280 nm. Only one positive peak at 228 nm appeared in the CD spectra of the monensin-lead system and was affected greatly by the background noise produced by the high concentration of lead. Therefore in the case of monensin no clear pattern appeared with addition of lead. X-206-lead system didn't show any obvious CD peaks. Table III.1 summarizes the information about CD peaks from all CD titrations.

Table III.1. CD spectra characteristic and stoichiometry of ionophore lead complexes in 80% methanol-water.

	Major peak, λ (sign)	Minor peak, λ (sign)	(Pb:L) stoichiometry[a]
Pb-salinomycin	293 nm (-)	238 nm (-), 215 nm (-)	1:1
Pb-narasin	294 nm (-)	215 nm (-)	1.15:1
Pb-lasalocid	296 nm (-)	255 nm (+)	1.5:1
Pb-nigericin	238 nm (-)	220 nm (+)	1:1
Pb-maduramicin	239 nm (+)	280 nm (+)	1.2:1
Pb-monensin	228 nm (+)	none	-
Pb-X-206	none	none	-

[a] defined by intersection of linear segments of plots in Figures III.3, III.5, III.7, III.10, and III.12.

Comparison of the two groups of ionophores show that peaks associated with carbonyl groups, such as the peaks at ~295 nm in the first group, are more intense than the other peaks. When pH* values were adjusted to about 2, the CD peak intensities decreased dramatically for all ionophores in both groups. These spectra were different from the initial spectra recorded at higher pH*. This is due to differences in the spectra of the protonated ionophore and ionized ionophore.

For each ionophore except X-206 and monensin the ellipticity at the peak with the largest amplitude was plotted versus the ratio of the total concentration of lead over the total ionophore as shown in Figures III.3, III.5, III.7, III.10, and III.12. The wavelength used for each ionophore is noted in the corresponding figure caption. The intersection of the linear segment of each plot provides an estimate of the Pb-ionophore stoichiometry. For the ionophores studied, these intersections occur for ratios of lead over ionophore in the range of 1-1.5 and are summarized in Table III.1. This suggests that the predominant stoichiometry is 1:1 in the concentration and pH range studied. The titrations of lead with nigericin and salinomycin were carried out with more steps as shown in Figures III.2 and 9 and concentrations of salinomycin and nigericin were determined using potentiometric titrations before applied to the ellipticity plotting. In these cases, the intersection occurred at the 1:1 ratio of lead over ionophore. For the other ionophores, the titrations were less thorough and the [Pb]:[Ionophore] ratios obtained at the intersections are more qualitative.

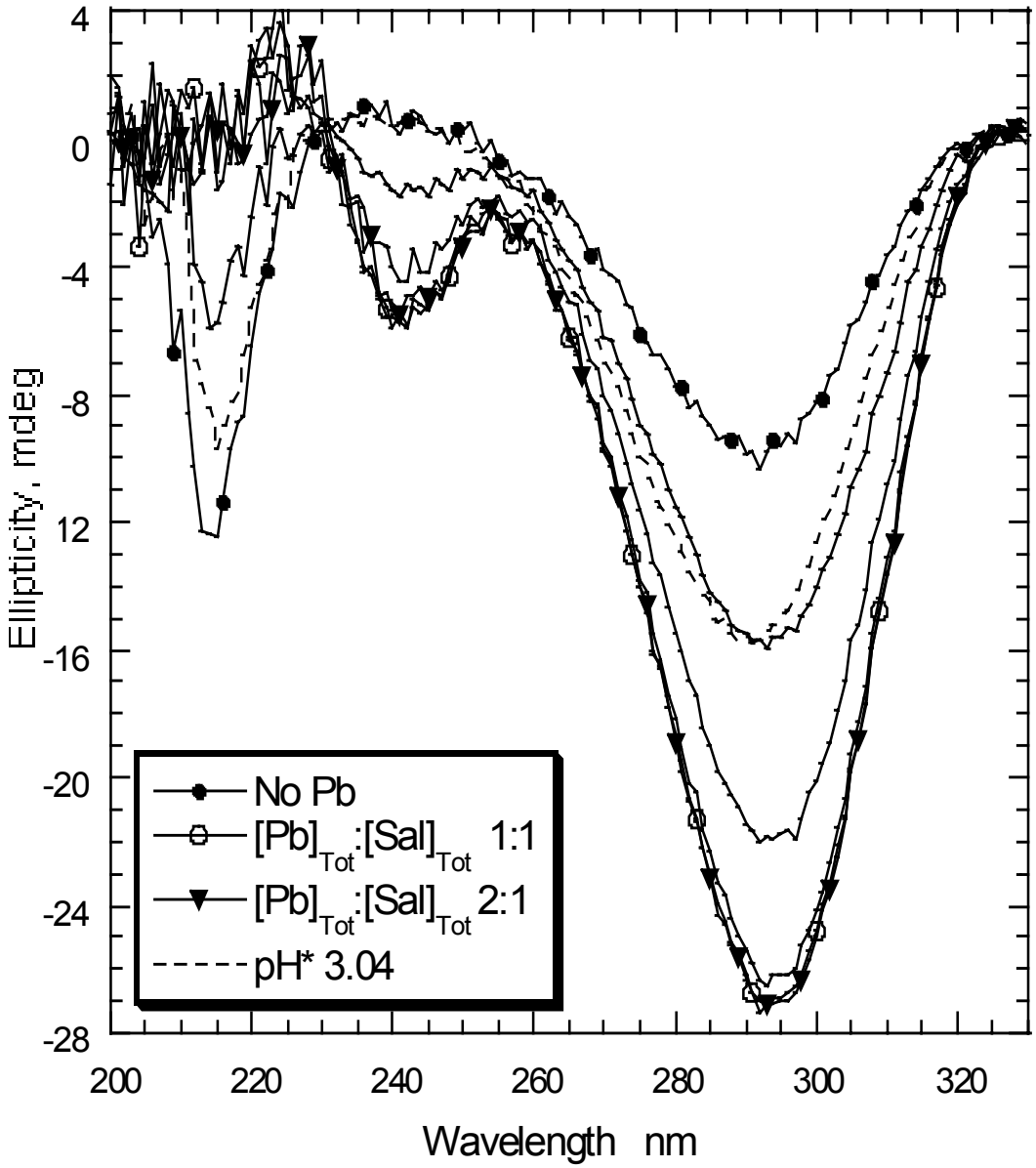


Figure III.1. CD spectra from the titration of Na salinomycin with $Pb(ClO_4)_2$ in 80% methanol-water at 25 ^{o}C. Aliquots of 0.01 M $Pb(ClO_4)_2$ were used to titrate 2.5 mL of a solution containing 0.0984 mM Na salinomycin, buffered at pH* 6.36 with 3 mM MES buffer, at an ionic strength of 0.05 M (TEAP). The dotted line represents the solution containing lead and salinomycin at a ratio of 2:1 after pH* was adjusted to 3.04.

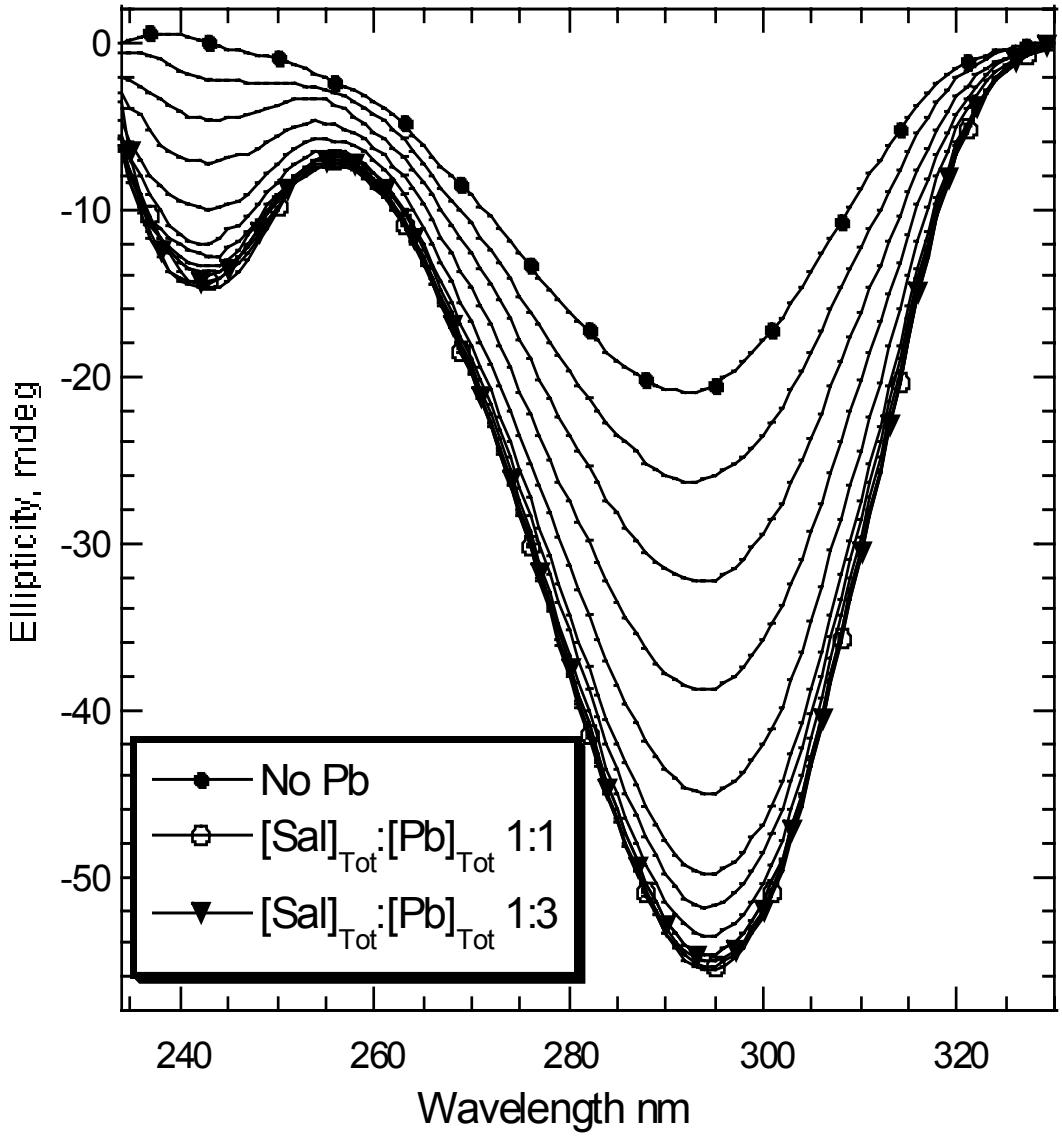


Figure III.2. CD spectra from the titration of NaSal with $Pb(ClO_4)_2$ in 80% methanol-water at 25 ^{o}C after being smoothed using the Aviv CD program. Aliquots of 0.01 M $Pb(ClO_4)_2$ were used to titrated 2.7 mL of a solution containing 0.118 mM NaSal, buffered at pH* 6.20 with 3 mM MES buffer, at an ionic strength of 0.05 M (TEAP). Spectra data at <234 nm was discarded because of the strong background noise from the high concentration of lead.

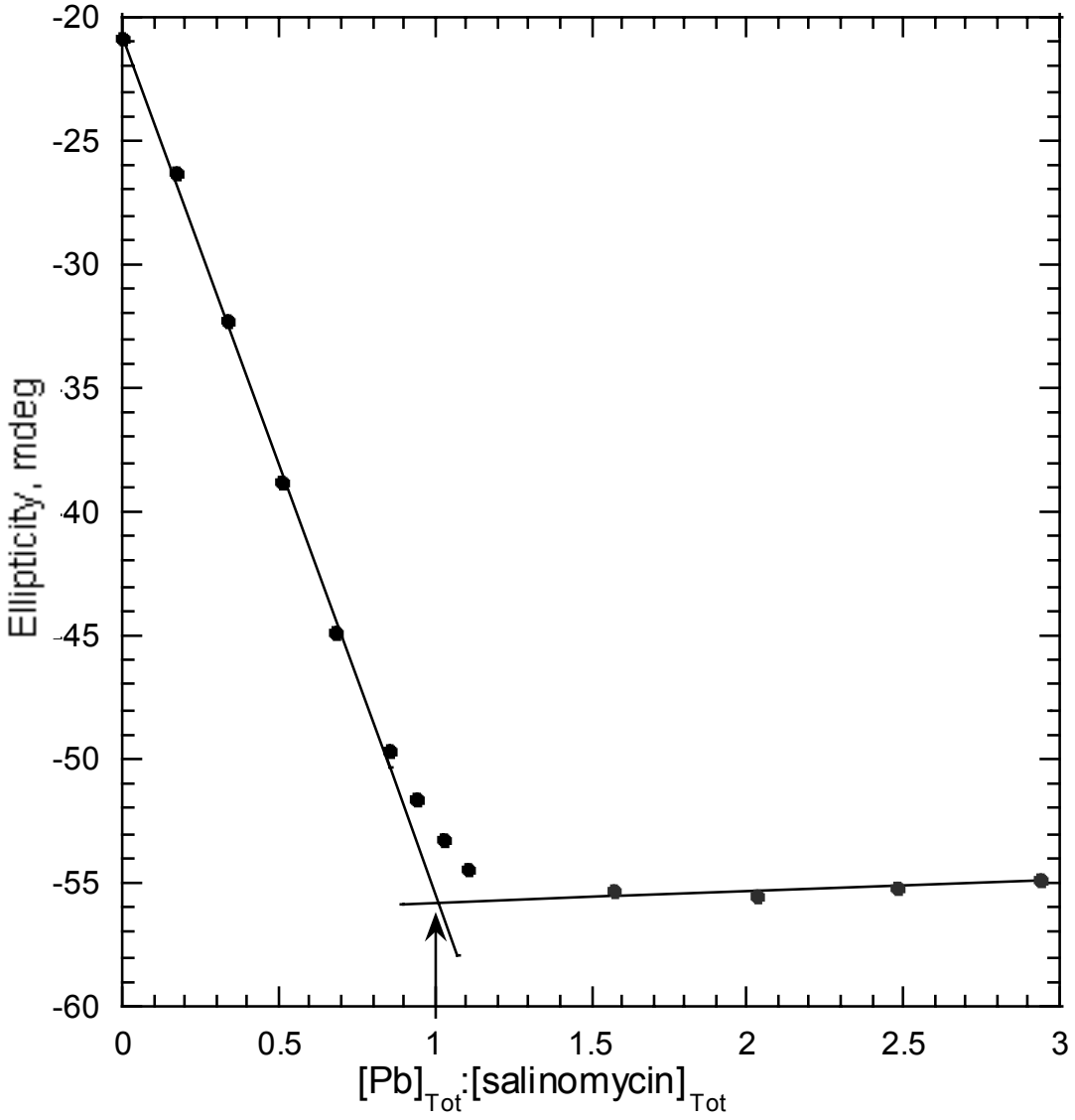


Figure III.3. Plot of the ellipticity at 293 nm versus the concentration ratio $[Pb]_{Total}$:$[salinomycin]_{Total}$ for the titration of NaSal with $Pb(ClO_4)_2$ in 80% methanol-water.

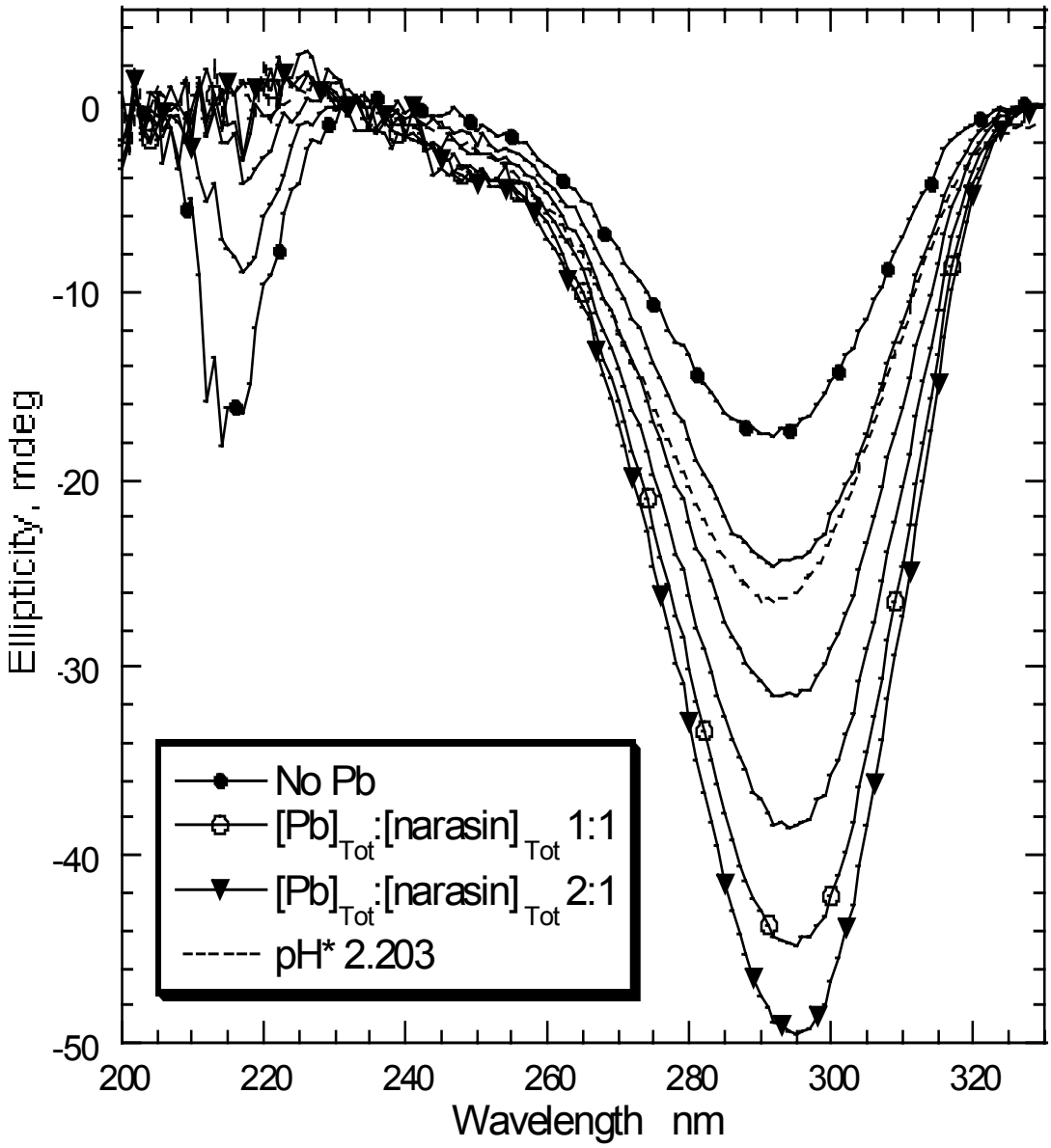


Figure III.4. CD spectra from the titration of Na narasin with $Pb(ClO_4)_2$ in 80% methanol-water at 25 ^{o}C. Aliquots of 0.01 M $Pb(ClO_4)_2$ were used to titrated 2.5 mL of a solution containing 0.0984 mM Na narasin, buffered at pH* 6.36 with 3 mM MES buffer, at an ionic strength of 0.05 M (TEAP). The dotted line represents the solution containing lead and narasin at a ratio of 2:1 after pH* was adjusted to 2.203.

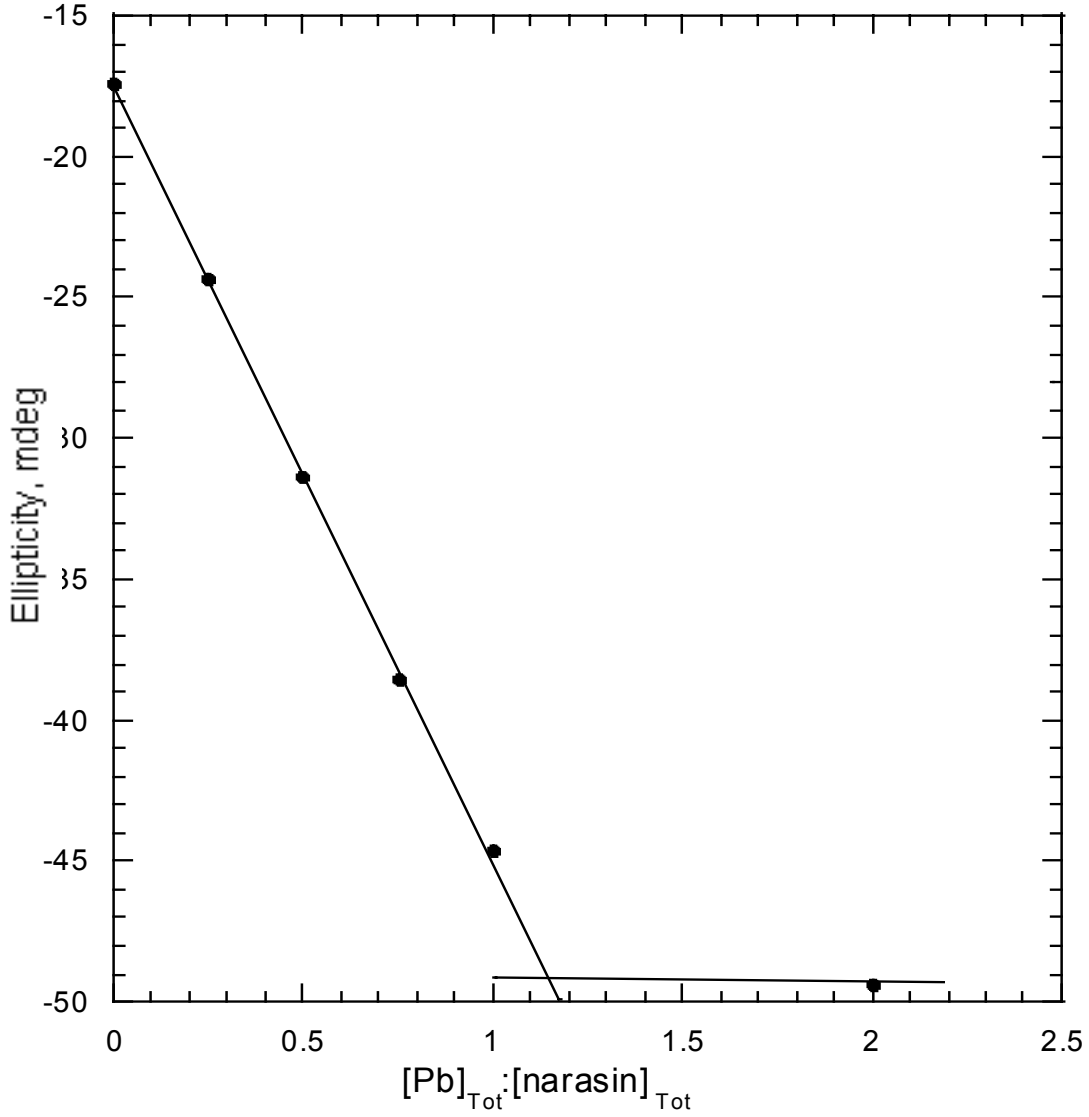


Figure III.5. Plot of the ellipticity at 294 nm versus the concentration ratio $[Pb]_{Total}$:$[narasin]_{Total}$ for the titration of Na narasin with $Pb(ClO_4)_2$ in 80% methanol-water.

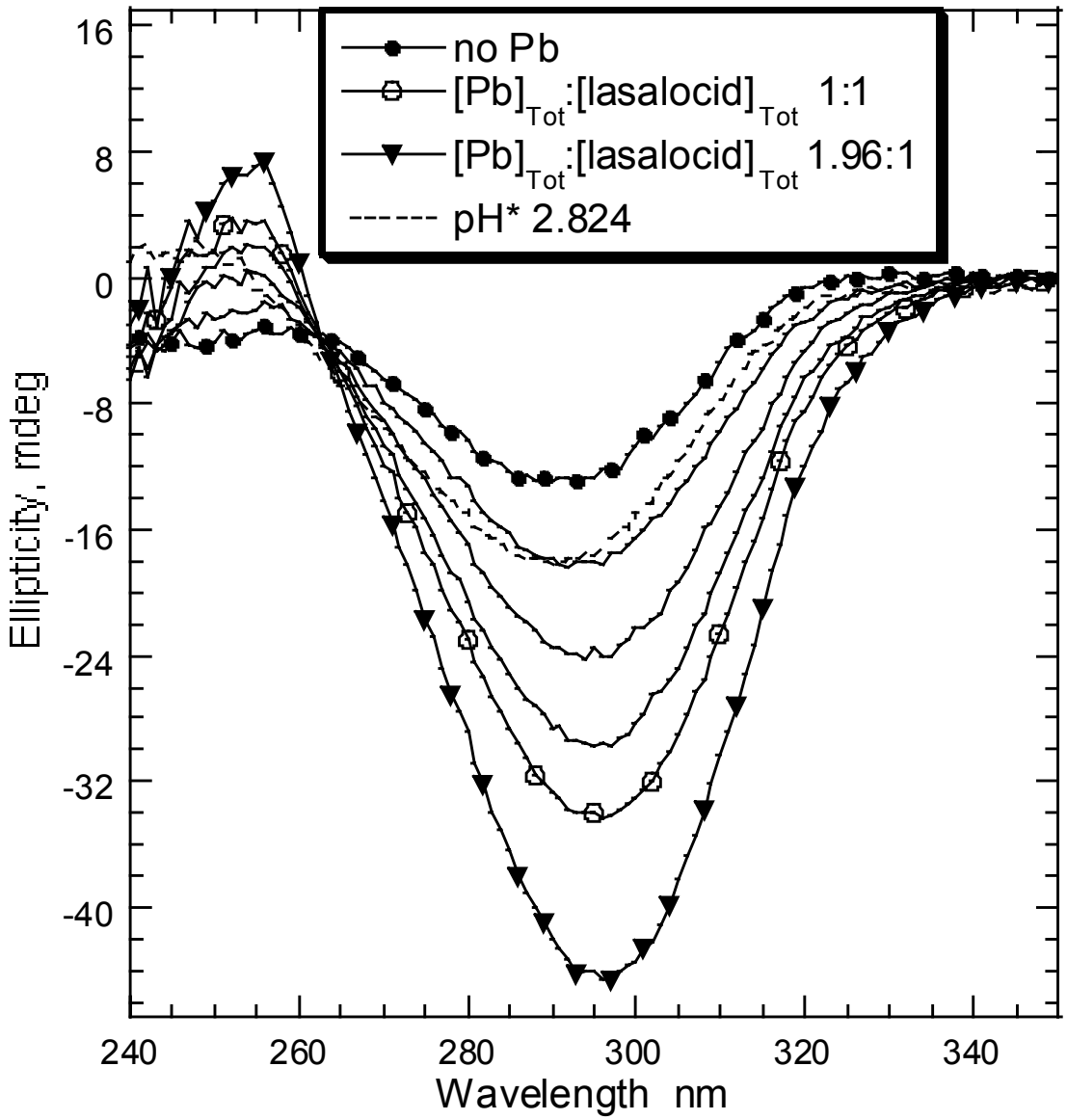


Figure III.6. CD spectra from the titration of sodium lasalocid with $Pb(ClO_4)_2$ in 80% methanol-water at 25 ^{o}C. Aliquots of 0.01 M $Pb(ClO_4)_2$ were used to titrate 2.5 mL of a solution containing 0.1633 mM sodium lasalocid, buffered at pH* 6.174 with 3 mM MES buffer, at an ionic strength of 0.05 M (TEAP). The dotted line represents the solution containing lead and lasalocid at a ratio of 1.96:1 after pH* was adjusted to 2.824.

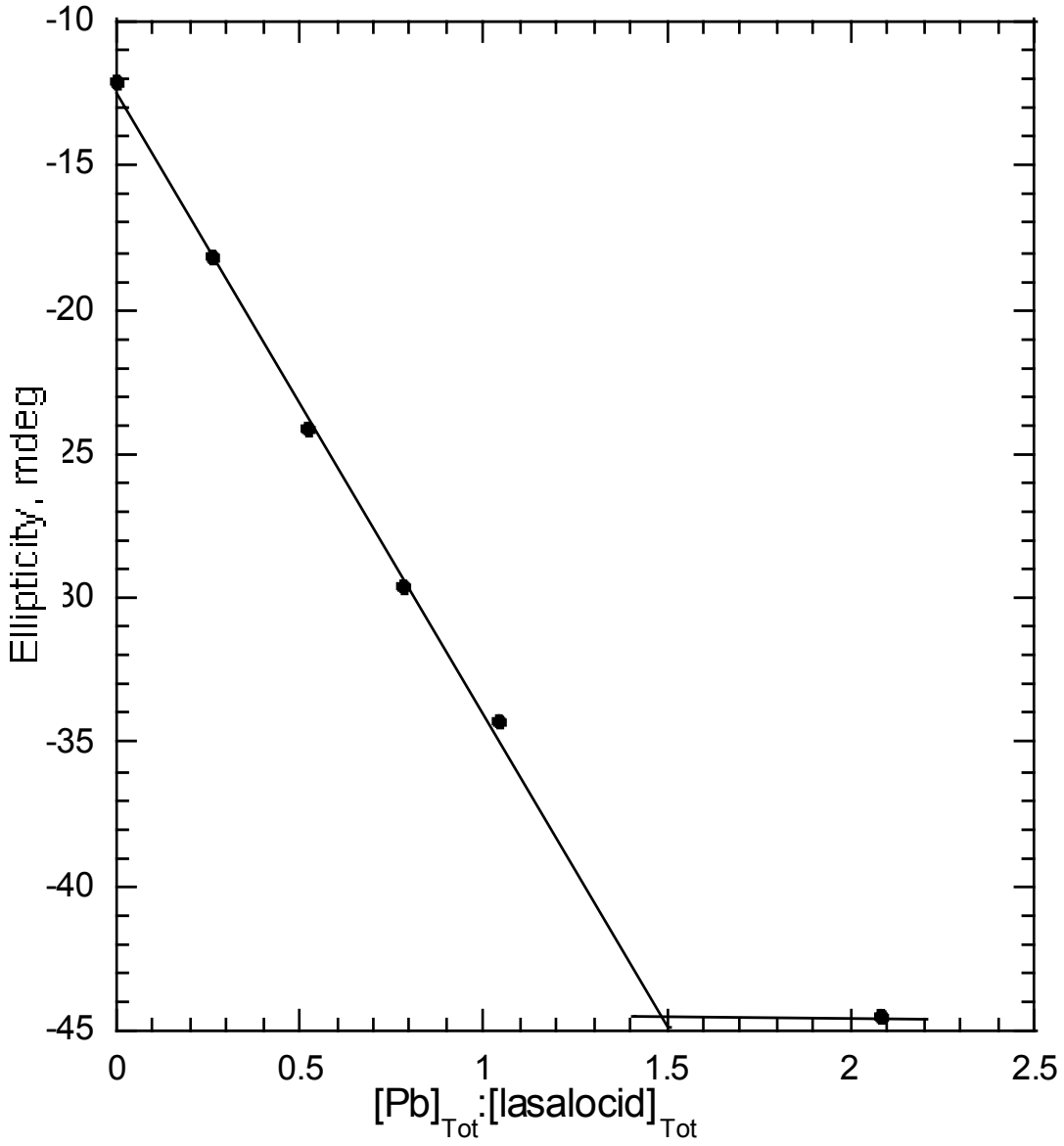


Figure III.7. Plot of the ellipticity at 296 nm versus the concentration ratio $[Pb]_{Total}$:$[lasalocid]_{Total}$ for the titration of Na lasalocid with $Pb(ClO_4)_2$ in 80% methanol-water.

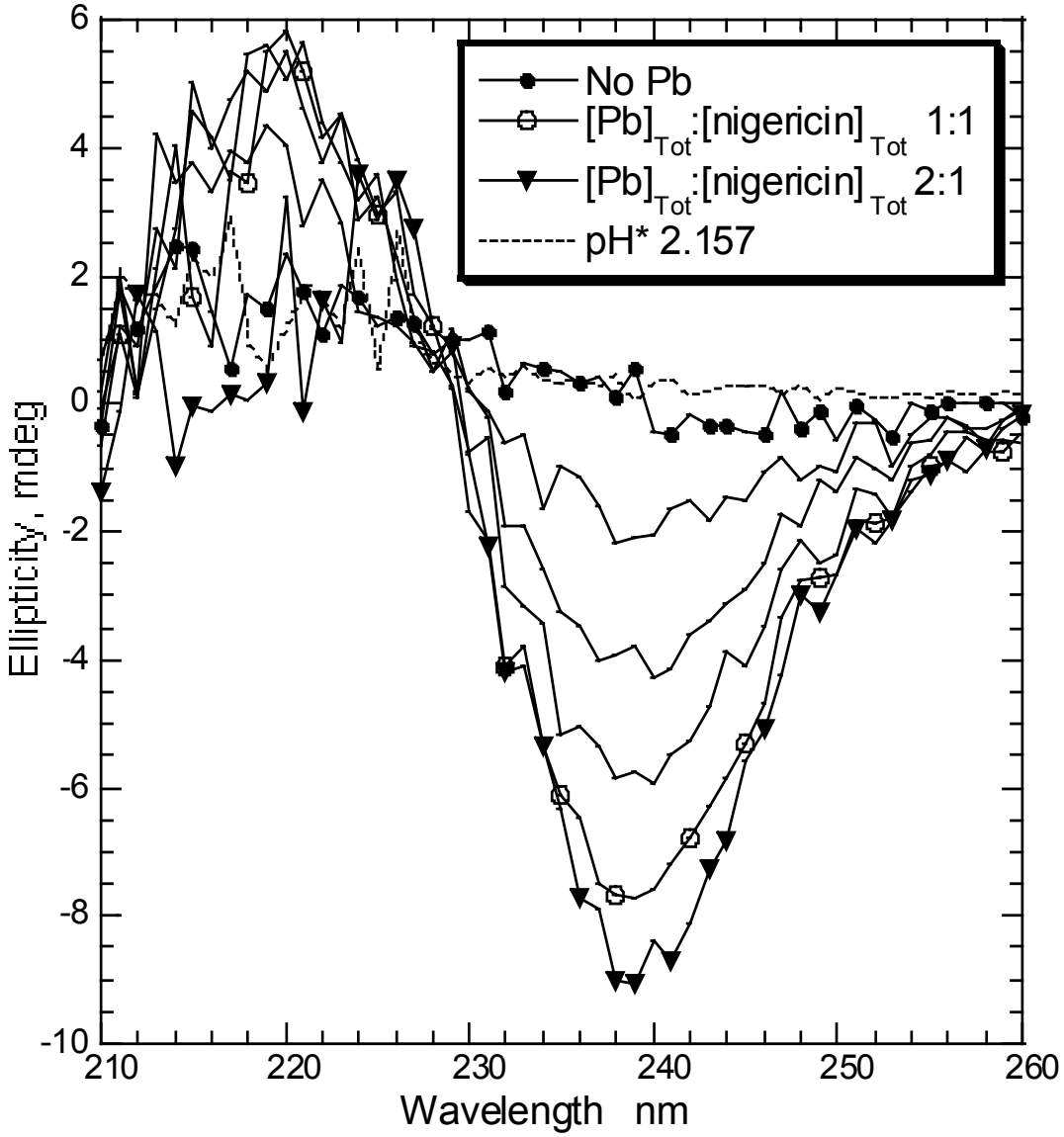


Figure III.8. CD spectra from the titration of Na nigericin with $Pb(ClO_4)_2$ in 80% methanol-water at 25 ^{o}C. Aliquots of 0.01 M $Pb(ClO_4)_2$ were used to titrate 2.7 mL of a solution containing 0.0885 mM Na nigericin, buffered at pH* 6.32 with 3 mM MES buffer, at an ionic strength of 0.05 M (TEAP). The dotted line represents the solution containing lead and nigericin at a ratio of 2:1 after pH* was adjusted to 2.157.

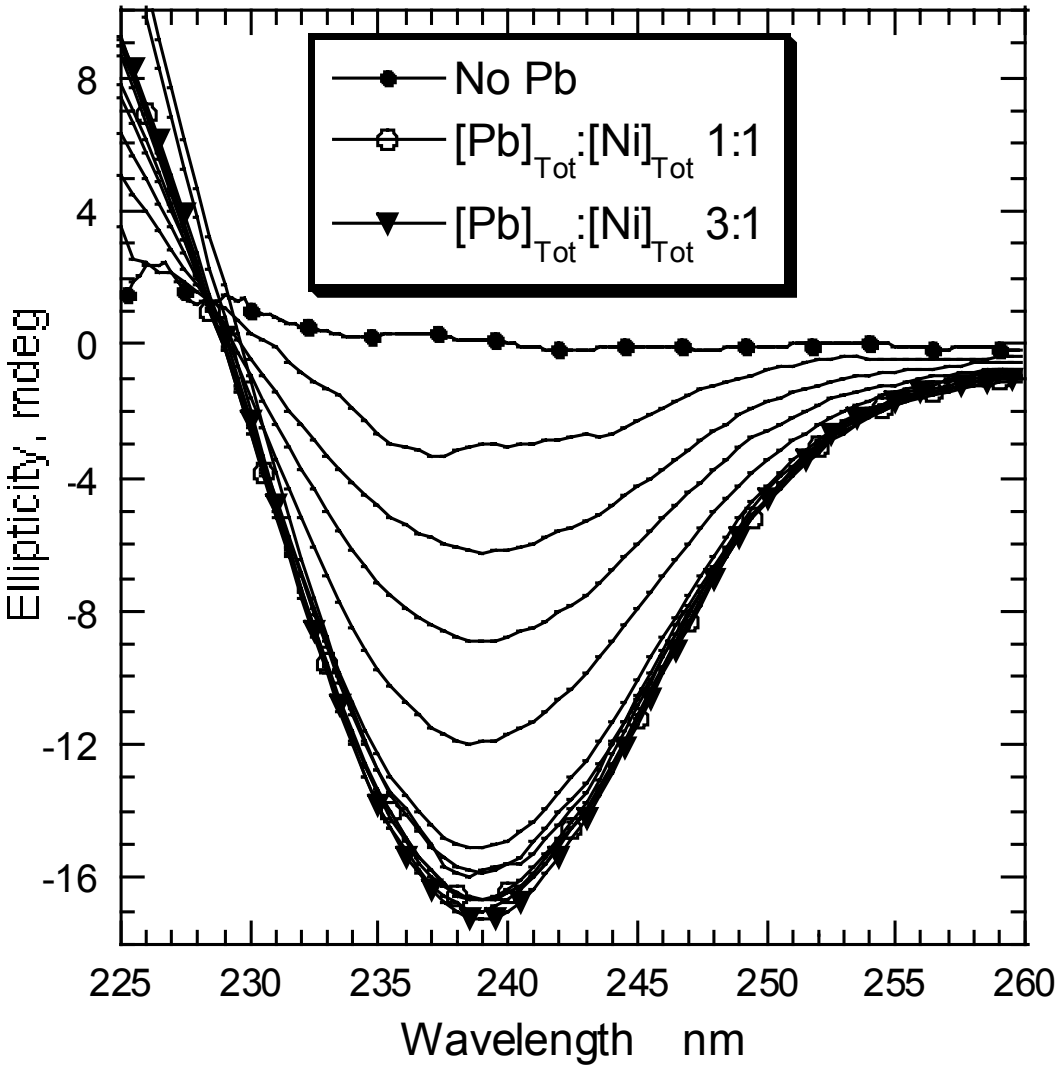


Figure III.9. CD spectra from the titration of Na nigericin with $Pb(ClO_4)_2$ in 80% methanol-water at 25 ^{o}C after being smoothed using the program Aviv CD. Aliquots of 0.01 M $Pb(ClO_4)_2$ were used to titrated 2.7 mL of a solution containing 0.18 mM NaNi, buffered at pH* 6.04 with 3 mM MES buffer, at an ionic strength of 0.05 M (TEAP). Spectra data at <225 nm was discarded because of the strong background noise from the high concentration of lead.

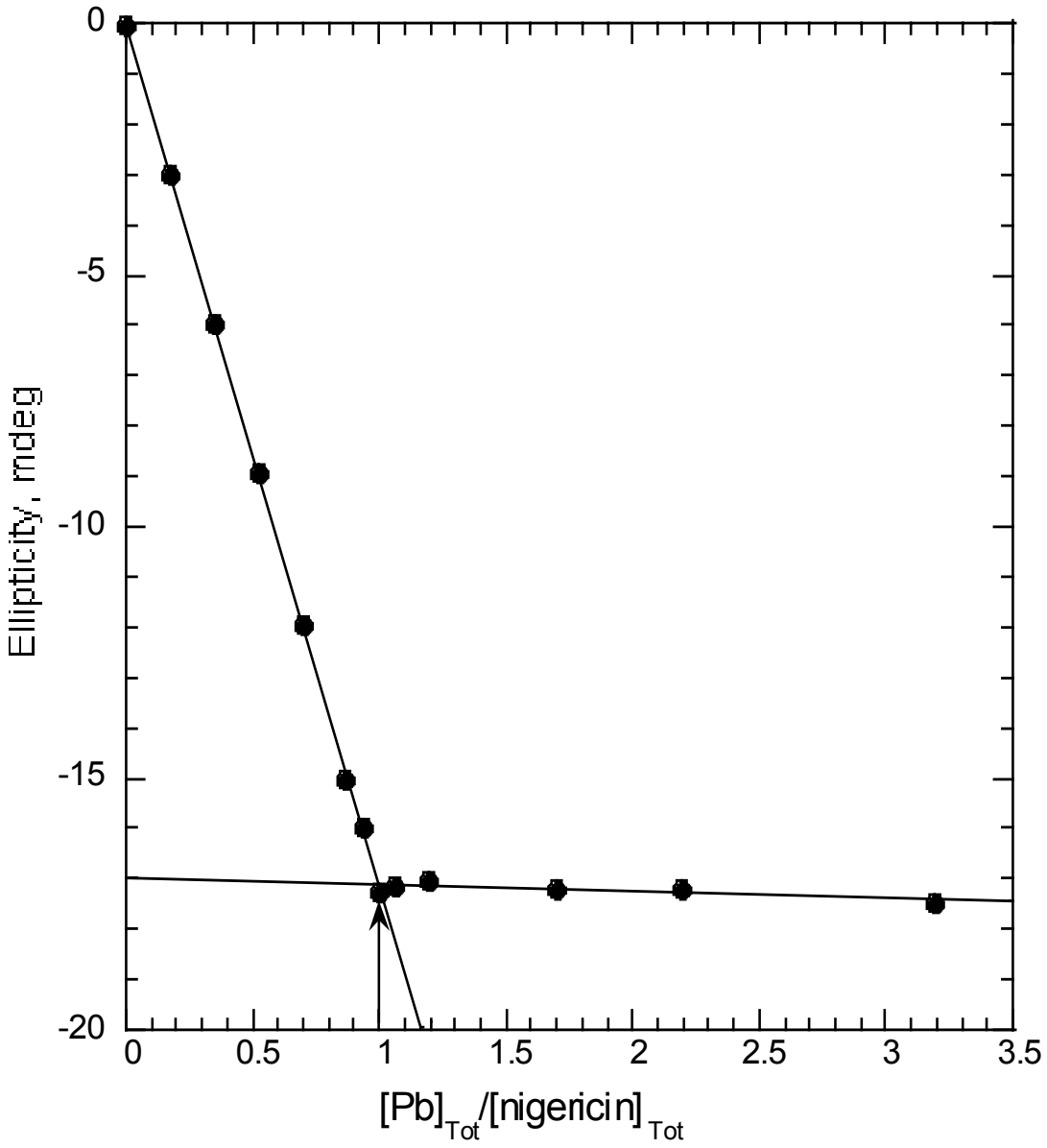


Figure III.10. Plot of the ellipticity at 238 nm versus the concentration ratio $[Pb]_{Total}$:$[nigericin]_{Total}$ for the titration of NaNi with $Pb(ClO_4)_2$ in 80% methanol-water.

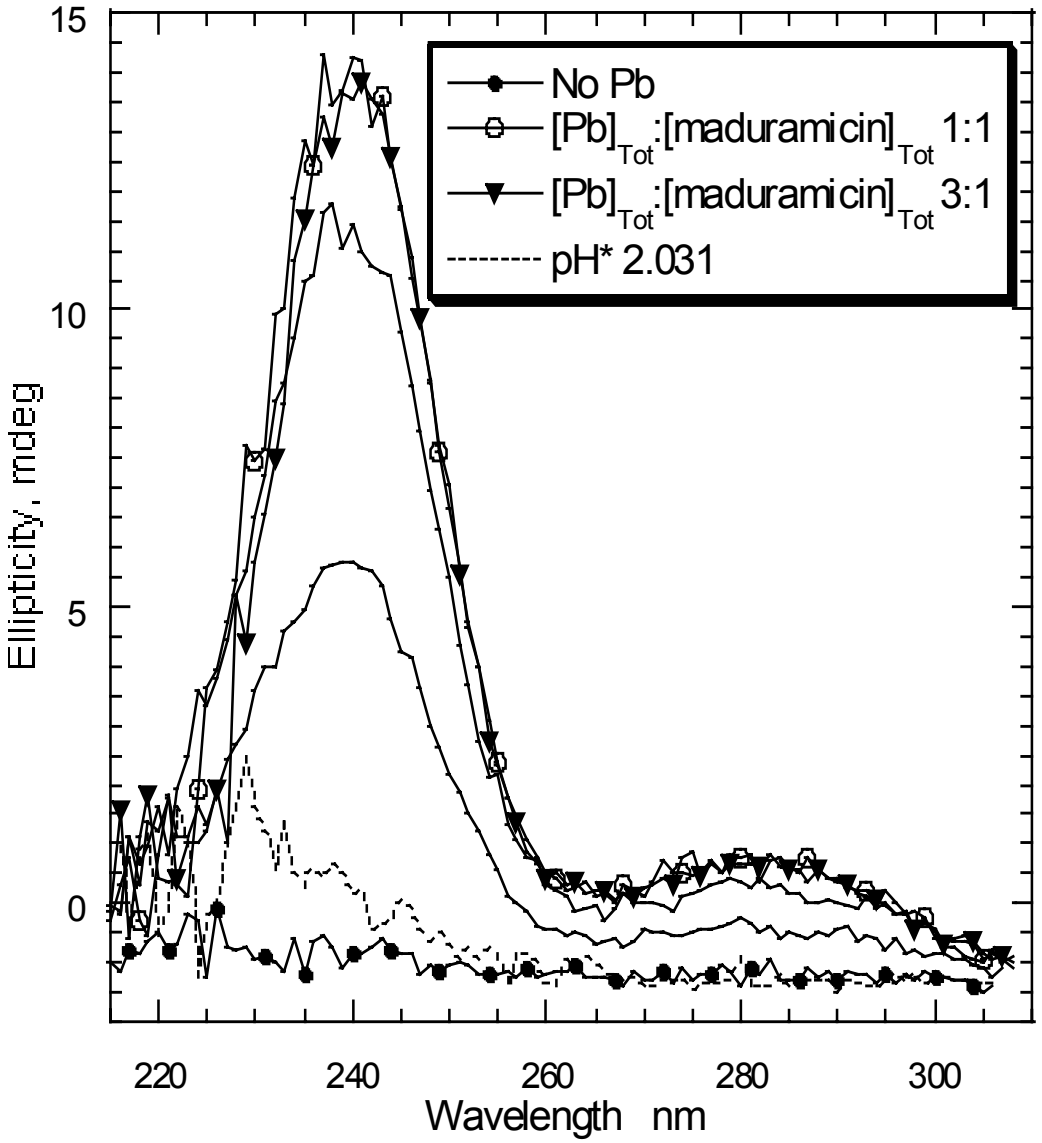


Figure III.11. CD spectra from the titration of ammonium maduramicin with $Pb(ClO_4)_2$ in 80% methanol-water at 25 ^{o}C. Aliquots of 0.01 M $Pb(ClO_4)_2$ were used to titrated 2.6 mL of a solution containing 0.107 mM ammonium maduramicin, buffered at pH* 6.10 with 3 mM MES buffer, at an ionic strength of 0.05 M (TEAP). The dotted line represents the solution containing lead and maduramicin at a ratio of 3:1 after pH* was adjusted to 2.031.

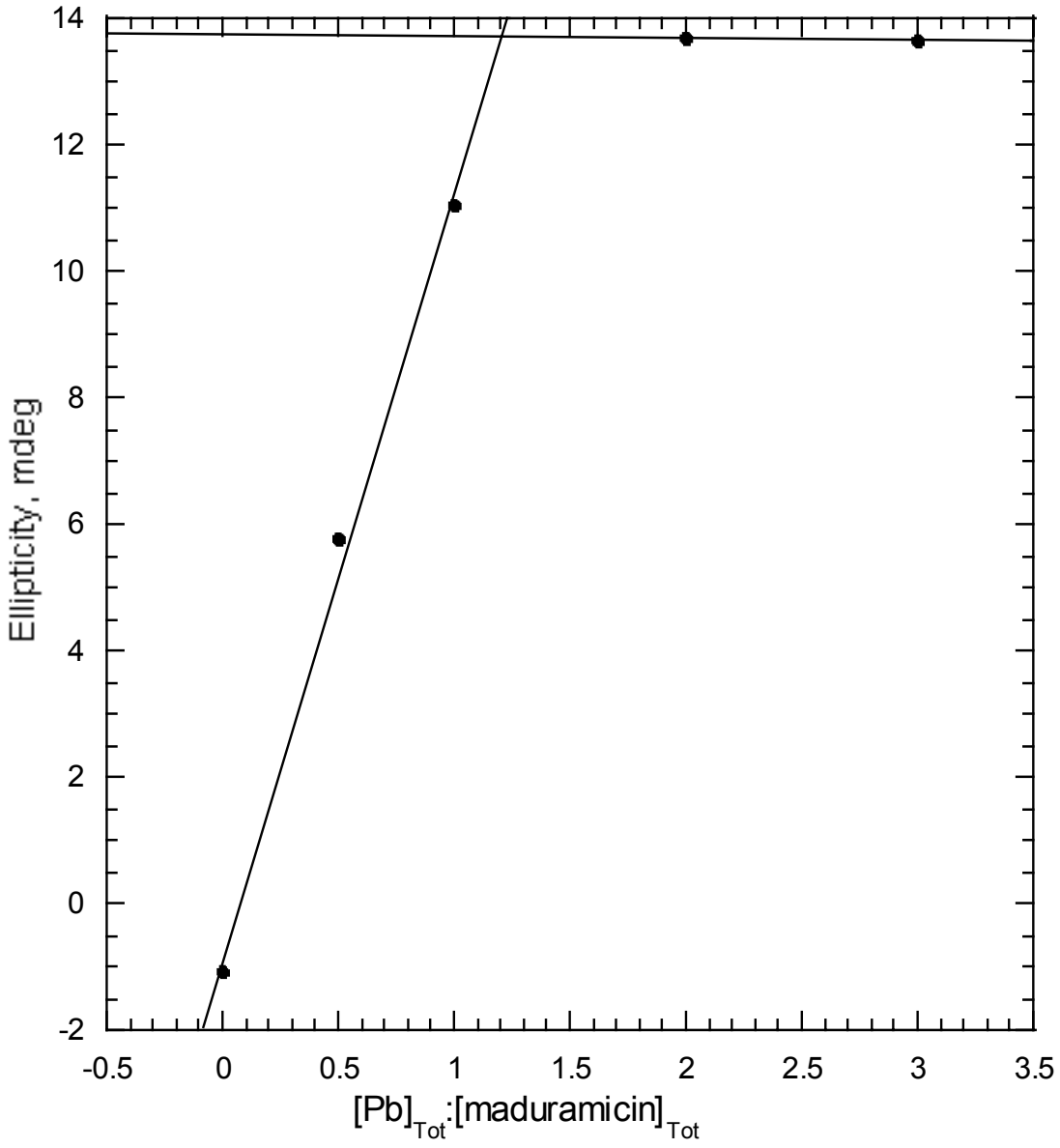


Figure III.12. Plot of the ellipticity at 239 nm versus the concentration ratio $[Pb]_{Total}$:$[maduramicin]_{Total}$ for the titration of Na maduramicin with $Pb(ClO_4)_2$ in 80% methanol-water.

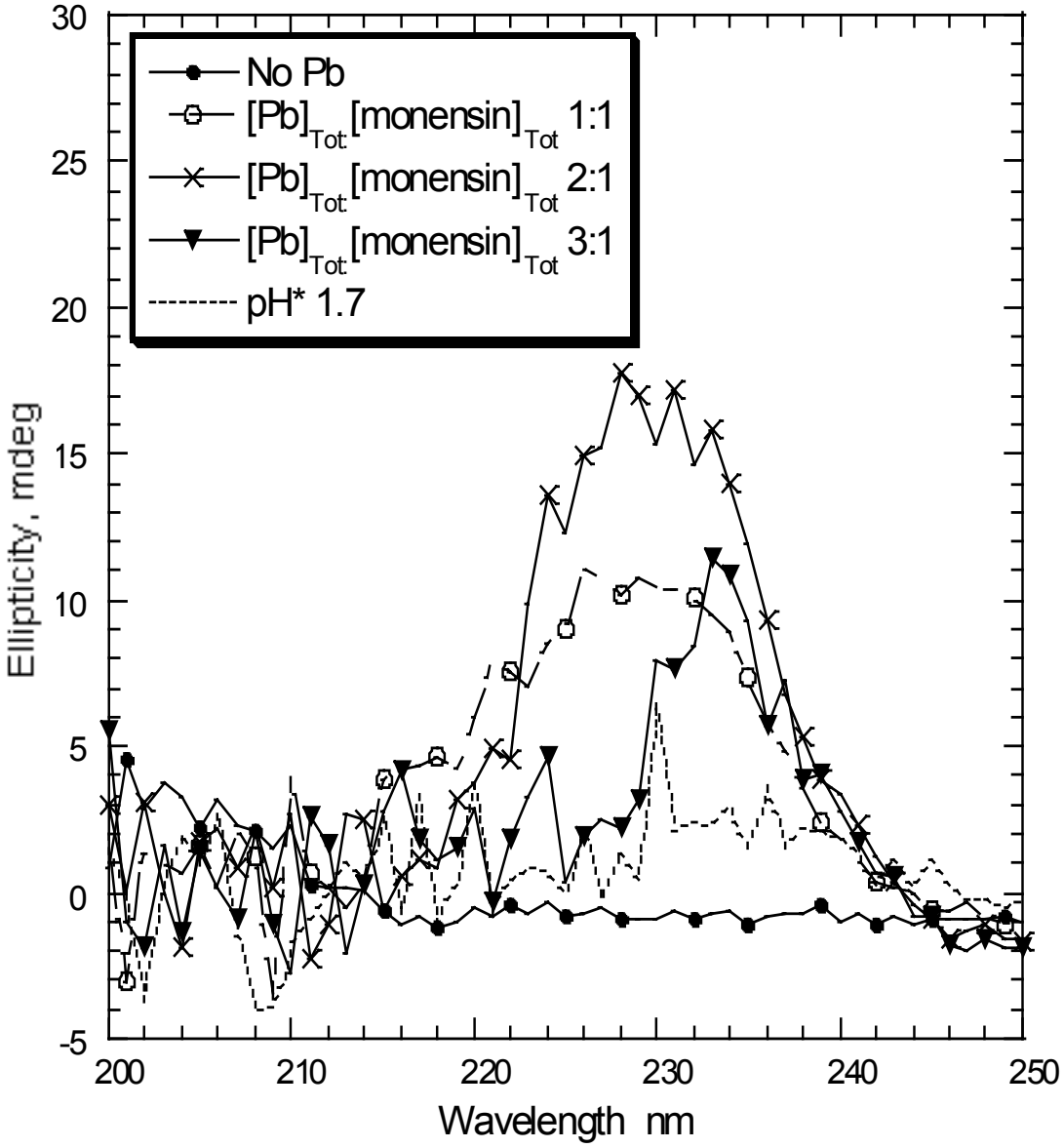


Figure III.13. CD spectra from the titration of sodium monensin with $Pb(ClO_4)_2$ in 80% methanol-water at 25 ^{o}C. Aliquots of 0.01 M $Pb(ClO_4)_2$ were used to titrated 2.5 mL of a solution containing 0.133 mM sodium monensin, buffered at pH* 5.01 with 3 mM MES buffer, at an ionic strength of 0.05 M (TEAP). The dotted line represents the solution containing lead and monensin at a ratio of 3:1 after pH* was adjusted to 1.7.

CD titrations of salinomycin sodium with other metals such as Zn^{2+}, K^{+}, Na^{+}, and Ca^{2+} were carried out at pH ~6.0. High concentrations (1 M) of salts (NaCl, KCl, $ZnCl_2$, and $CaCl_2$) were used because of the weak interaction between salinomycin and those metal ions. 27 μL of a 1 M solution containing required salt was added into 2.7 mL of a solution containing 0.1 mM HSal in 80% methanol-water. UV and CD spectra were taken as described in the beginning of this chapter. The CD spectra obtained after addition of the different metal salt solutions are similar to the one for the free acid form of salinomycin except that there is no peak at 210 nm after addition of Zn^{2+}. Increasing the concentrations of metal ions further did not lead to larger changes at 290 nm after initial small increases in the signal intensities. Addition of K^{+} shows a larger change than other cations at pH* ~6.0.

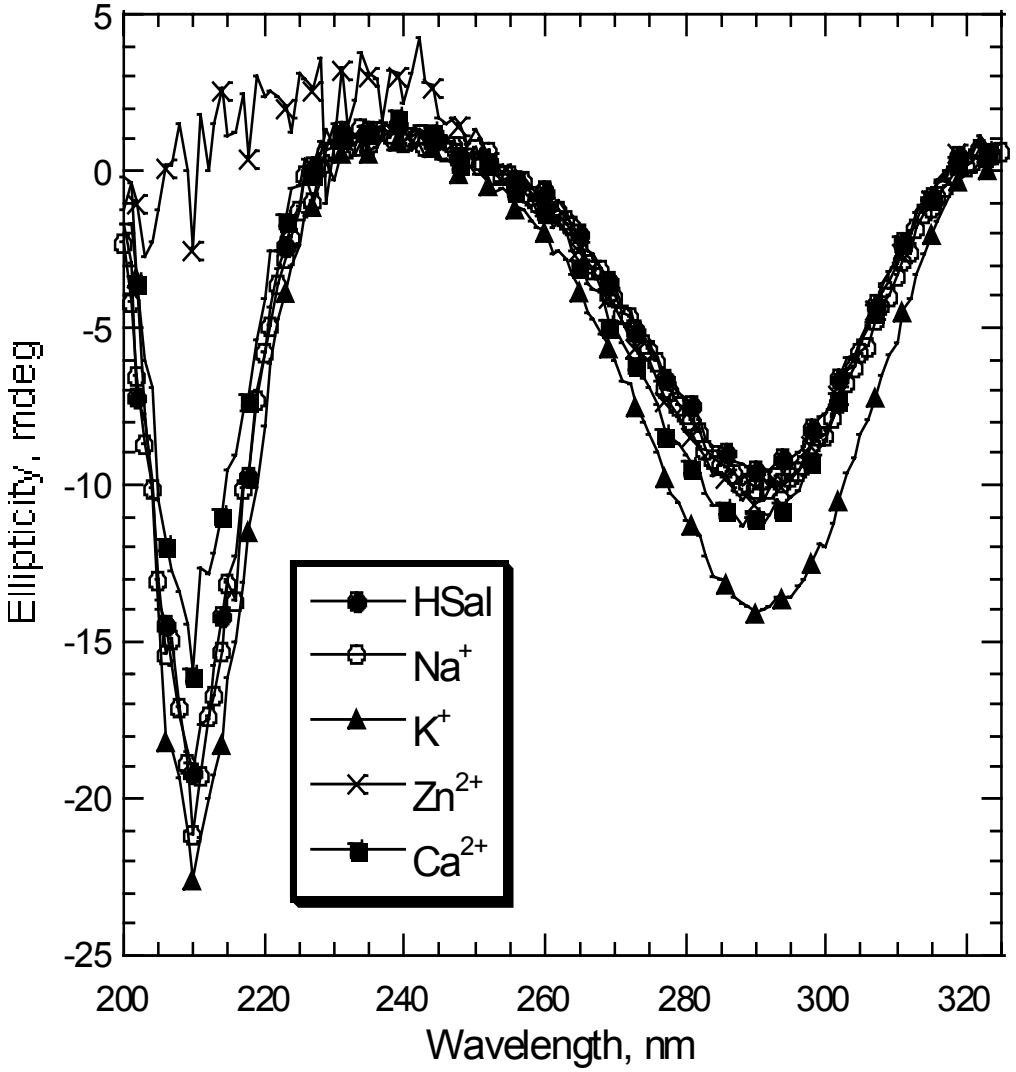


Figure III.14. CD spectra of the free acid form of salinomycin (0.1 mM) with addition of different metal solutions in 80% methanol-water as indicated in the graph.

References

(1) Painter, G. R.; Pressman, B. C. *Top. Curr. Chem.* **1982**, *101*, 84-110.
(2) Thomas, T. P., Ph. D. Thesis, University of Oklahoma, Norman, OK, **1991**.
(3) Hamidinia, S. A.; Shimelis, O. I.; Tan, B.; Erdahl, W. L.; Chapman, C. J.; Renkes, G. D.; Taylor, R. W.; Pfeiffer, D. R. *J. Biol. Chem.* **2002**, *277*, 38111-38120.

Chapter IV

Results

Studies of lead-nigericin complexes

IV.A Elemental analysis of lead-nigericin complexes.

Samples of lead-nigericin complexes, prepared using methods described in Section II.B, were submitted to a commercial firm for elemental analysis. The experimental percentages of carbon, hydrogen, and lead obtained are listed in Table IV.1 along with the corresponding theoretical values calculated for complexes with varying composition.

Table IV.1. Experimental and calculated elemental composition of lead-nigericin (1:2) complexes[a].

Compound/method	%Pb	%C	%H	%O
Experimentally obtained				
$PbNi_2$ by reaction of PbO with HNi	12.88	55.22	8.26	23.64
$PbNi_2$ by back extraction	9.36	53.55	7.94	29.15
Calculated from the specified molecular stoichiometries				
1Pb:2Ni	12.52	58.06	8.16	21.26
1Pb:2Ni:1H_2O	12.38	57.43	8.19	22.00
1Pb:2Ni:2H_2O	12.25	56.81	8.23	22.71
1Pb:2Ni:3H_2O	12.12	56.22	8.26	23.40
1Pb:2Ni:1HNO_3	12.06	55.92	7.92	24.10[b]

[a] Weight percentage scale (wt/wt) is used. The contents of lead, C and H were determined by Desert Analytics Company. The compounds are considered to only contain Pb, H, C, and O. The equation for %O calculation is (100 - %Pb - %C - %H).
[b] This value is the sum of oxygen and nitrogen percentages.

The lead percentage for the lead-nigericin compound prepared by the reaction of lead oxide and the free acid form of nigericin is higher than the calculated values but close to that for the model (1Pb:2Ni). The carbon percentage for the same compound is close to the number for the model containing three waters of hydration. The values for the last model are not compared with the elemental percentages for the compound made

from lead oxide because there is no possibility for the presence of nitrate ion in that compound. The experimental hydrogen percentage matches up well with the values from all four models and is equal to the value for the model (1Pb:2Ni:3H_2O). The experimental oxygen percentage is only 0.24% higher than the value for the model with three additional waters of hydration. Considering all experimental percentages, the model with three additional waters of hydration seems best to describe the composition of nigericin-lead complexes made by reaction of lead-oxide and the free acid form of nigericin. One explanation for the high lead percentage is that centrifugation was not sufficient to remove all the fine powder of lead oxide from the lead-nigericin methanol solutions.

The compound made by back extraction contains significantly less lead than any of the theoretical models. The experimental carbon and oxygen percentages show deviation from the theoretical values. The hydrogen percentage corresponds with the value for the model containing one molecule of nitric acid. None of the models considered were close to the experimental value for lead. The pH (4.6) for the aqueous lead nitrate solution (0.01 M) may not be high enough for quantitative extraction of the lead complexes. Experiments at higher pH values were unsuccessful because lead precipitated after addition of base. The material obtained by back extraction was not used for studies of lead-nigericin complexes.

IV.B Characterization of lead-nigericin complexes by mass-spectrometry.

Electrospray ionization-mass spectrometry (ESI-MS) has been widely used to analyze biomolecules, polymers, and inorganic and organometallic complexes. It possesses a soft ionization method and produces little fragmentation. The spectra are dominated by molecular ion peaks. ESI-MS studies on ionophore-lead complexes provided information about species possibly existing in the solution. The identity of the various species associated with a specific set of peaks is determined by comparison of the experimental peak intensities in the cluster to the calculated isotopic pattern.

The lead-nigericin (1:2) complex was dissolved in methanol and injected into MicroMass Q-TOF. MS data were collected under the positive mode using the program Masslynx 3.5. Only one set of peak cluster (931.5 m/z) was observed in the ESI-MS spectra shown in Figure IV.1. That cluster contained five peaks due to four isotopes of lead and two important isotopes of carbon elements and was identified as lead-nigericin (1:1), which indicates the strong interaction of lead and nigericin. The theoretical isotopic pattern based on that model is shown in Figure IV.1 (panel B) and matched well with the experimental pattern. Other peaks with different stoichiometries were too weak to show.

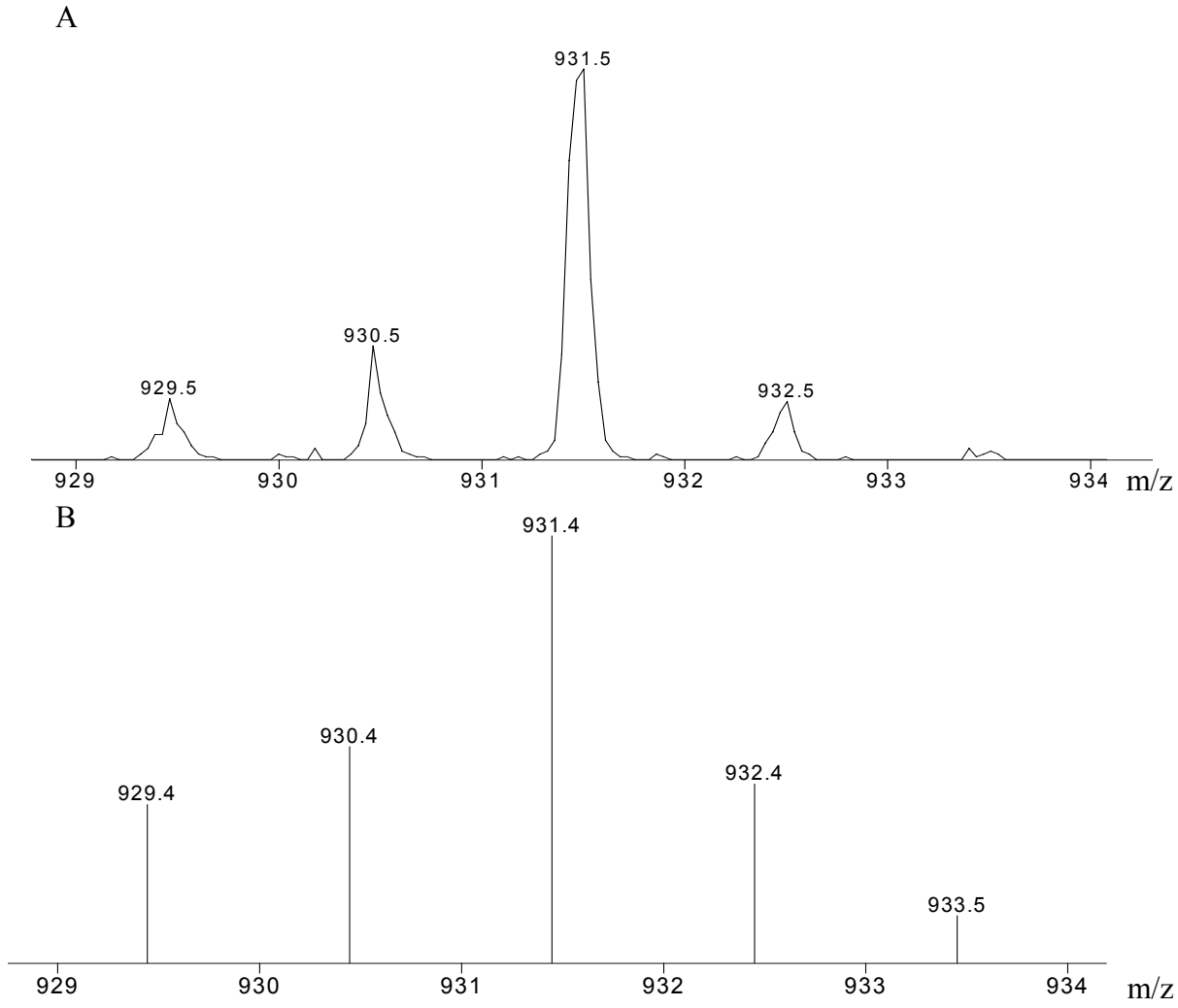


Figure IV.1. A. Part of the positive ion ESI-MS for the 1:1 nigericin-lead complex. B. The calculated isotopic pattern for $C_{40}H_{67}O_{11}Pb$.

IV.C UV spectrophotometric studies of lead-nigericin complexation reactions

Although uncomplexed nigericin and salinomycin do not absorb in the UV region, the lead-ionophore complexes show strong signals due to Pb-O charge transfer bands[1,2], which makes UV studies possible for these ionophores. The experimental details of ionophore UV studies were described in Section II.E. Titrations of the ionophores with Pb^{2+} were carried at two different pHs. The complexation constants of lead-ionophore (1:1) complexes were calculated based on experiments at low pH. Stoichiometry information was obtained from experiments at high pH where side reactions of salinomycin and nigericin with protons were negligible. According to eq IV.1, pH should be about 9 so that ~99% of nigericin is not protonated.

$$K_H^{m^*} = 10^{7.20} = \frac{[HMon]}{\alpha_H^* [Mon^-]} = \frac{1}{\alpha_H^* 99} \qquad \text{(IV.1)}$$

Lead perchlorate (0.1 mM) in 80% methanol-water will precipitate around pH 7. Due to the strong complexation of lead by nigericin, there is no strong interference from the protonation reaction of nigericin in the experiment carried out at pH ~6. The UV spectra for nigericin-lead titrations are shown in Figure IV.2. The largest UV absorbance change occurred at the wavelength 252 nm. The absorbance at 252 nm leveled off after the total concentration of nigericin was equal to the total concentration of lead, as shown in Figure IV.3. It is clear that the complexation reaction with 1:1 stoichiometry is the dominant reaction and is almost quantitative at this pH.

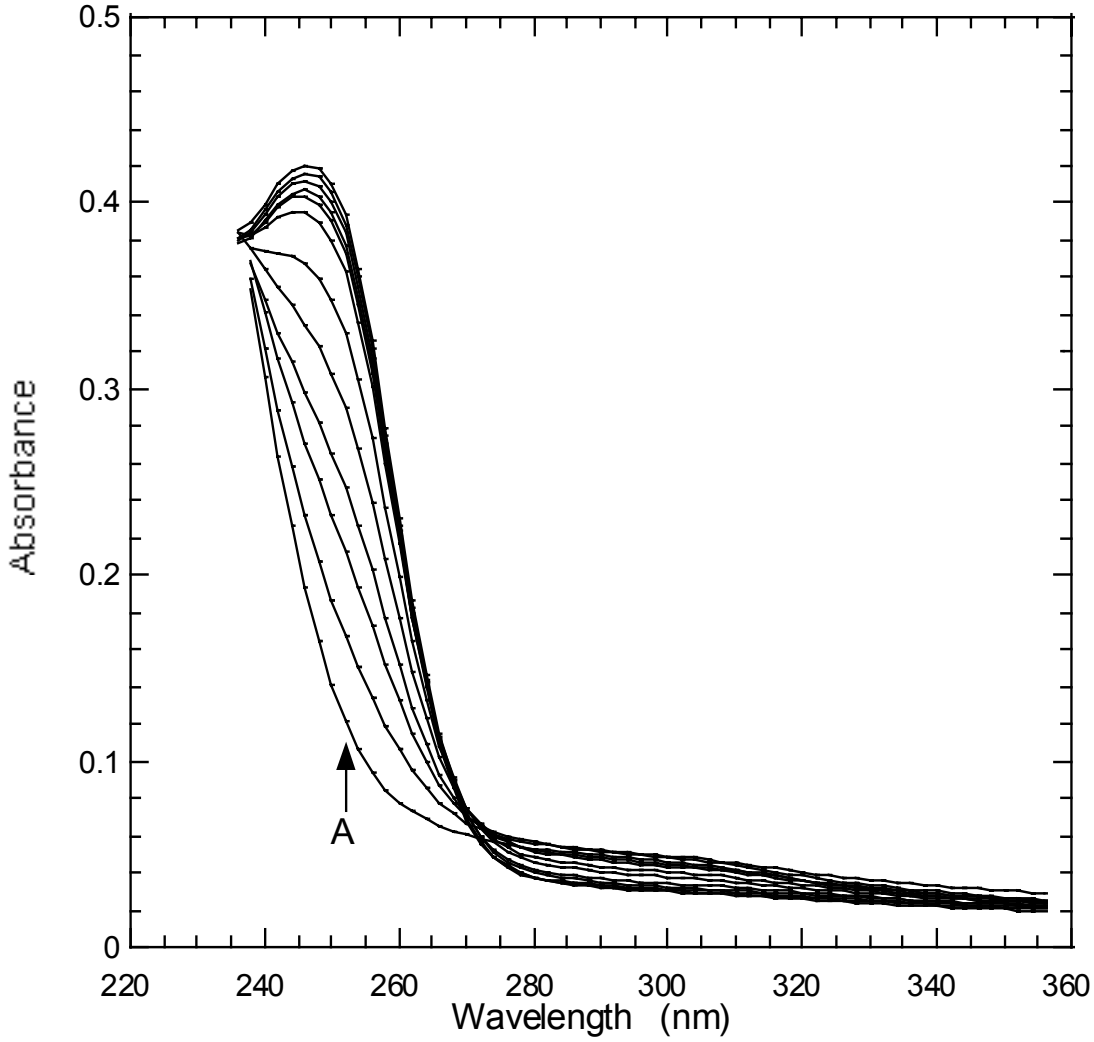


Figure IV.2. UV-Vis spectra from the titration of lead perchlorate with nigericin in 80% methanol-water at 25 ^{o}C. Aliquots (3 or 10 μL) of 0.0129 M sodium nigericin were used to titrate 2.7 mL of a solution containing 0.1 Mm lead perchlorate, buffered at pH* 6.43 with 3 mM MES, at an ionic strength of 0.05 M (TEAP). Curve A-$Pb(ClO_4)_2$ alone, no salinomycin added.

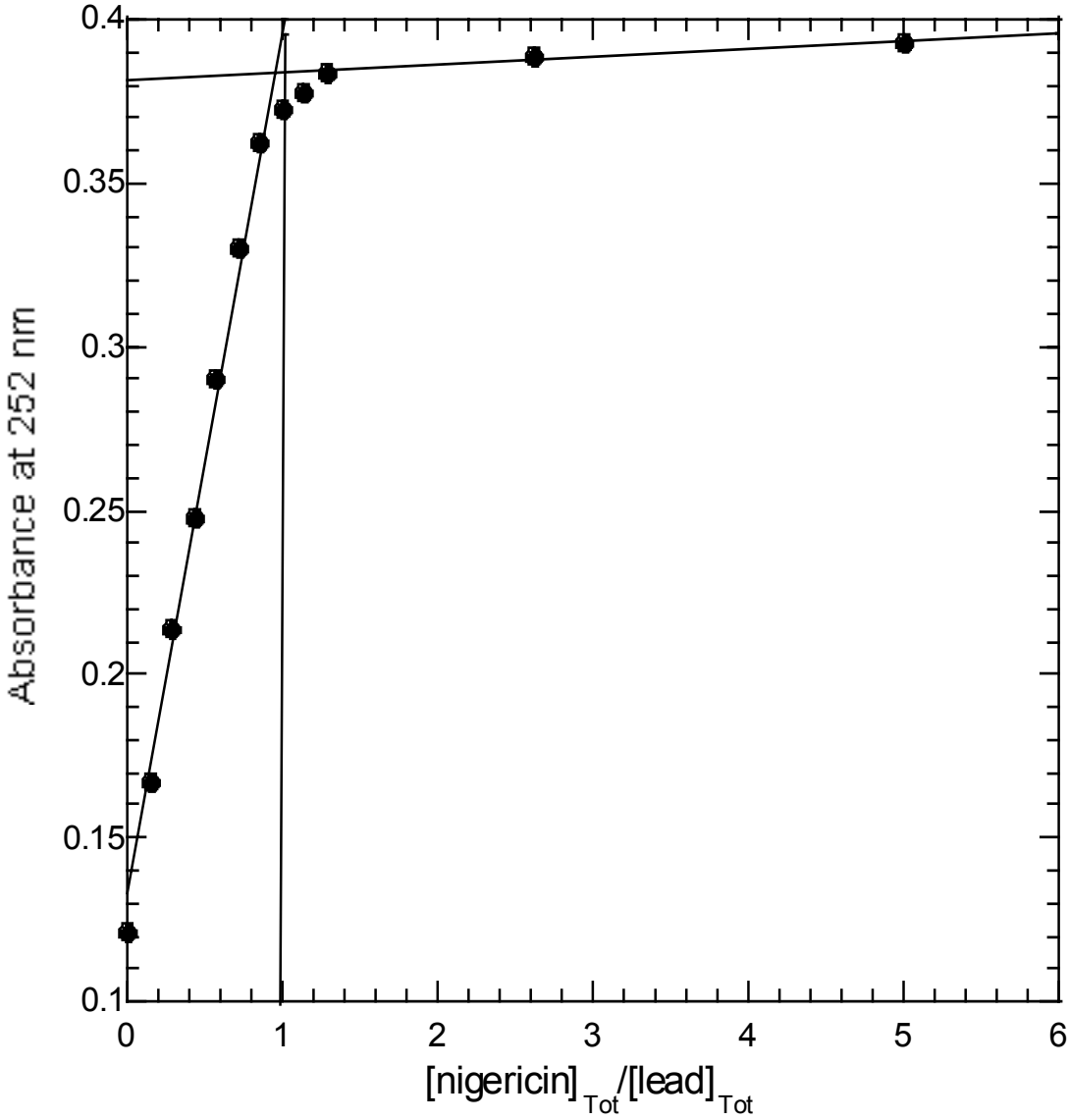


Figure IV.3. Plot of the absorbance resulting from each aliquot of 0.0129 M sodium nigericin added versus the ratio of the total nigericin to total lead concentrations.

The conditional stability constant of the lead-nigericin (1:1) complex was obtained at pH* 3.361. The two major reactions in solution are shown in eqs IV.2 and IV.3, where L represents nigericin.

$$H^+ + L^- \rightleftharpoons HL \qquad \text{(IV.2)}$$

$$Pb^{2+} + L^- \rightleftharpoons PbL^+ \qquad \text{(IV.3)}$$

The value of stability constants measured under these conditions is expressed in eq IV.4 and the definition of α_L is shown in eq IV.5

$$\log K_{PbL} = \log K'_{PbL} - \log \alpha_L \qquad \text{(IV.4)}$$

$$\alpha_L = \frac{[L^-]}{([L^-]+[HL])} = (1 + K_H^{m^*} \alpha_H^*)^{-1} \qquad \text{(IV.5)}$$

where $\log K'_{PbL}$ is the apparent formation constant obtained at low pH* and $K_H^{m^*}$ is the mixed-mode protonation constant. For pH* values lower than 4, the product of $K_H^{m^*} \alpha_H^*$ is larger than 100, and $\alpha_L \approx (K_H^{m^*} \alpha_H^*)^{-1}$. Under this condition, the expression of stability constant is given by eq IV.6.

$$\log K_{PbL} = \log K'_{PbL} + \log K_H^{m^*} - pH^* \qquad \text{(IV.6)}$$

The definition of the apparent formation constant, K'_{PbL}, is shown by eq IV.7.

$$K'_{PbL} = \frac{[PbL^+]}{[Pb^{2+}][HL]'} \qquad \text{(IV.7)}$$

The concentrations of free lead ions, $[Pb^{2+}]$, and conditional free acid form of ionophore, $[HL]'$, are related to the total concentrations of lead ions and ionophores as shown in eqs IV.8 and IV.9.

$$[Pb^{2+}]_{tot} = [Pb^{2+}] + [PbL^{+}] \quad \text{(IV.8)}$$

$$[L]_{tot} = [HL]' + [PbL^{+}] \quad \text{(IV.9)}$$

The apparent formation constant was first estimated based on the absorbance at the point where the total concentrations of lead ion ($[Pb^{2+}]_{tot}$) and ionophore ($[L]_{tot}$) were equal. Equation IV.10 shows the relationship of the absorbance at that point and the concentration of the lead complex.

$$\frac{\Delta Abs_i}{\Delta Abs_\infty} = \frac{[PbL^{+}]}{[Pb^{2+}]_{tot}} = \chi \quad \text{(IV.10)}$$

Combining eqs IV.7-IV.10, an initial estimate of, K'_{PbL}, can be calculated as shown in eq IV.11 for the condition where $[Pb^{2+}] = [HL]'$

$$K'_{PbL} = \frac{[PbL^{+}]}{[Pb^{2+}][HL]'} = \frac{\chi[Pb^{2+}]_{tot}}{((1-\chi)[Pb^{2+}]_{tot})^2} = \frac{\chi}{[Pb^{2+}]_{tot}(1-\chi)^2} \quad \text{(IV.11)}$$

This initial value of K'_{PbL} is used with eq IV.12 to fit the absorbances at a desired wavelength as a function of the concentration of the free acid form of ionophore ($[HL]$)

$$\Delta Abs_i = \frac{\Delta Abs_\infty K'_{PbL}[HL]}{1 + [HL]K'_{PbL}} \quad \text{(IV.12)}$$

where ΔAbs_i is the difference between the absorbance at each point and the initial absorbance, ΔAbs_∞ is the difference between the limiting and initial absorbance which is estimated from the plot, and the initial values of the free acid form of ionophore are the total concentrations of ionophore at every point. After the data was fitted to eq IV.12 using the nonlinear least-squares function of the program Kaleidagraph, a new apparent formation constant K'_{PbL} was generated and inserted into eq IV.13 to calculate the

concentration of free protonated nigericin at each point and these were then used in a new cycle of calculation.

$$[HL] = \frac{-(K'_{PbL}([Pb^{2+}]_{tot} - [HL]_{tot}) + 1) + \sqrt{(K'_{PbL}([Pb^{2+}]_{tot} - [HL]_{tot}) + 1)^2 - 4K'_{PbL}[HL]_{tot}}}{2K'_{PbL}} \quad \text{(IV.13)}$$

The calculations were repeated until the difference of the parameters between two cycles was less than 2%. Normally six cycles are enough to meet this criterion. The plot resulting from the last cycle of calculation for lead-nigericin UV titration is shown in Figure IV.4. The resulting log value of stability constant for lead-nigericin (1:1) complex $\log K_{PbL}$ is 7.58 based on the calculated apparent formation constant K'_{PbL}.

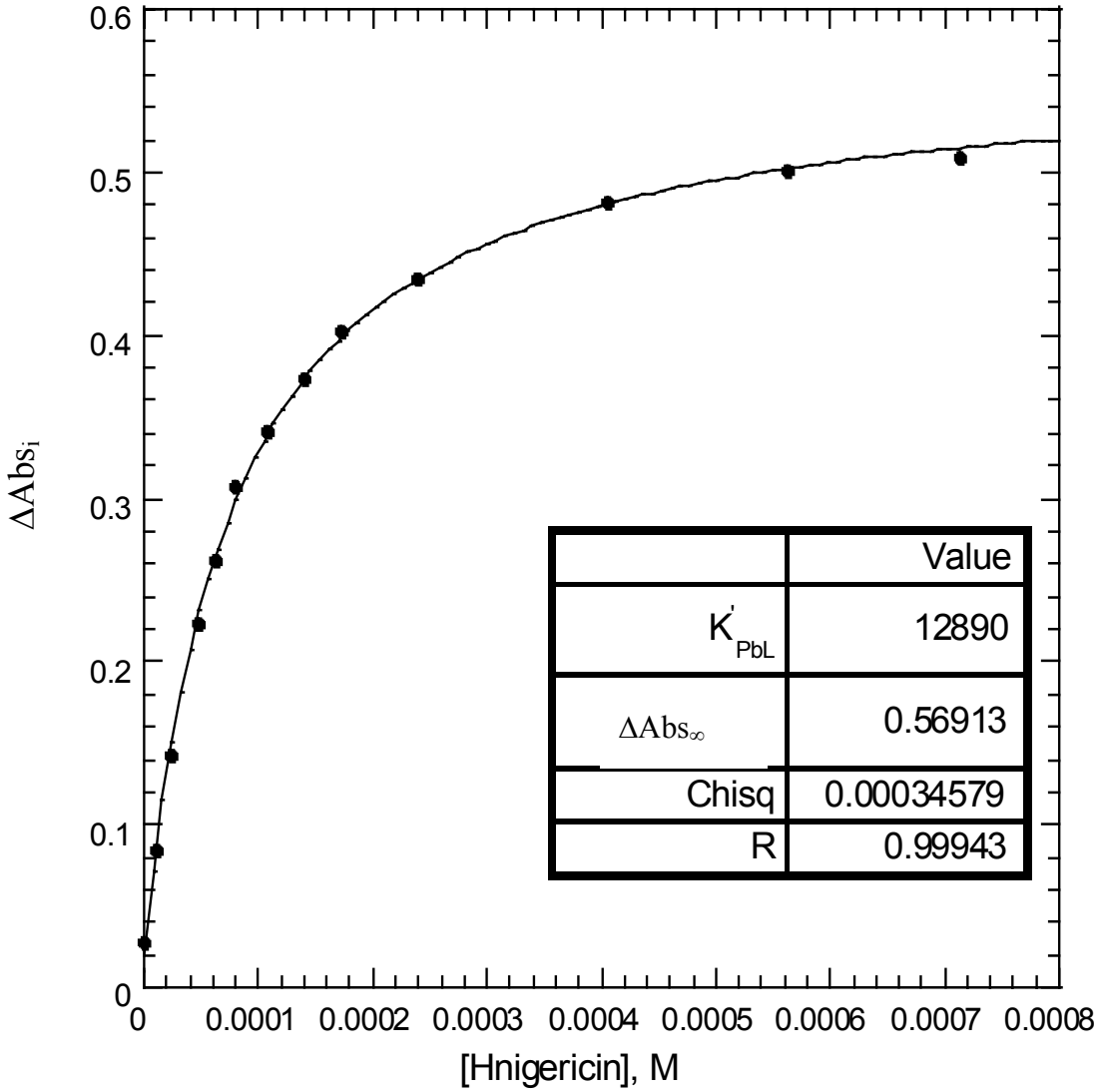


Figure IV.4. Change in absorbance at 248 nm as a function of [Hnigericin] at pH* 3.361. Aliquots (6 or 10 μL) of 0.0129 M nigericin acid were used to titrate 2.7 mL of a solution containing 0.1mM lead perchlorate in 80% methanol-water. The titration was done at 25 ^{o}C at an ionic strength of 0.05 M (TEAP). The solid line was calculated from eq IV.12 using the derived parameters listed in the inset table.

IV.D The protonation constant for nigericin in 80% methanol-water determined using potentiometric titrations

The protonation constant for nigericin was determined using potentiometric titrations. The free acid form of nigericin solution in 80% methanol-water was titrated with a solution of tetramethylammonium hydroxide (I = 0.05 M) at 25 ^{o}C as described in Section II.E. A single buffer region appeared in the titration curves indicating only one protonation site in nigericin. The titration data was first analyzed using the program PKAS[3], which requires the initial millimoles of the ligand, the initial volume of the ligand, the base concentration, the value of the solvent autoprotolysis constant, and the number of dissociable protons[3]. This information was used to calculate the p[H] value at every titration point based on volume of base added. The calculated p[H] values were determined using mass balance equations and an estimate of the protonation constant. The parameter used to measure the difference between the calculated p[H] values and the experimental p[H] values is defined in eqs IV.14 and IV.15.

$$U = \sum w_i(\mathrm{p[H]}_{exp} - \mathrm{p[H]}_{cal})^2 \qquad \text{(IV.14)}$$

$$w_i = \frac{1}{(\mathrm{p[H]}_{i+1} - \mathrm{p[H]}_{i-1})^2} \qquad \text{(IV.15)}$$

The protonation constant is refined to minimize the value of U. The standard deviation value of the titration curve is defined as

$$\delta_{fit} = \left(\frac{U}{N}\right)^{1/2} \qquad \text{(IV.16)}$$

where $N = \sum w_i$ (IV.17)

The program BEST[3] was also used in the titration data analysis. A similar algorithm is used in BEST, but the constants are expressed as overall constants, β. For

the protonation constant of nigericin, the overall constant is equal to the step-wise constant, K_H, as shown in eqs IV.18 and IV.19.

$$H^+ + L^- \rightleftharpoons HL \quad \text{(IV.18)} \qquad \beta_{HL} = K_H^C = \frac{[HL]}{[H^+][L^-]} \quad \text{(IV.19)}$$

The p[H] and volume of base data for a typical titration curve along with the theoretical curve obtained using the program BEST are shown in Figure IV.5. The individual values of K_H, for nigericin obtained using the program BEST, are listed in Table IV.2. The average value of log protonation constant of nigericin is 7.02 ± 0.03 for seven titrations.

Table IV.2 Calculated values of the protonation constant for nigericin in 80% methanol-water[a].

Nigericin concentration (mM)	Log K_H^C [b]	σ_{fit} [c]
0.69	7.06	0.050
0.85	6.98	0.015
0.83	7.07	0.051
1.61	7.01	0.021
1.61	7.00	0.023
1.61	7.00	0.022
1.61	7.01	0.021

[a] 25 °C, ionic strength 0.05 M (TEAP). [b] The value was refined using the program BEST. [C] $\sigma_{Fit} = (U/N)^{1/2}$

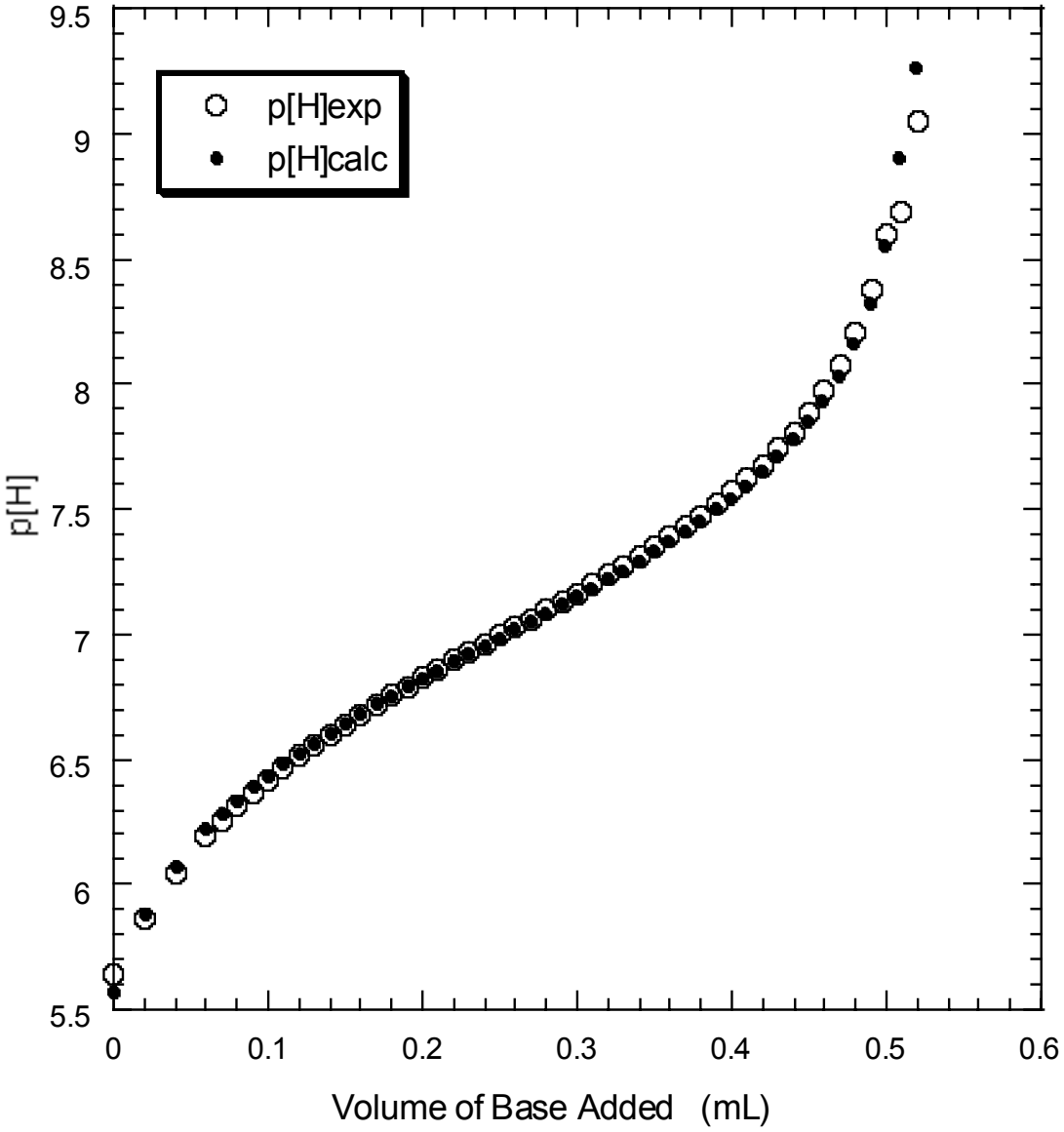


Figure IV.5. A potentiometric titration curve for 6.00 mL of a solution containing 0.846 mM the free acid form of nigericin at an ionic strength of 0.05 M (TEAP) in 80% methanol-water at 25 ^{o}C. The titrant is 9.6 mM Me_4NOH with ionic strength maintained at 0.05 M with TEAP. The calculated p[H] values were obtained using the program BEST.

IV.E Potentiometric studies of metal binding

Complexation constants in 80% methanol-water were determined by titration of solutions containing a mixture of nigericin acid (HNi) and the metal ion of interest with tetramethylammonium hydroxide, as described in Section II.E. Different ratios of nigericin and the metal ion were used to investigate the possible existence of complexes with different stoichiometries. The stability constants of the nigericin complexes of potassium, calcium, zinc, magnesium, and lead were calculated from the titration data using the program BEST. The input file required by the program BEST contains the complexation model, the electrode solvent correction factor, the base concentration, the initial volume of the test solution, and the initial millimoles of ligands, metal ions, and protons in that solution. The program BEST automatically transforms the titration pH* data into p[H] using the hydrogen ion activity coefficient and the electrode solvent correction factor, as described in Section II.C. Based on the complexation model, the p[H] data were refined to find the stability constants. Expressions of protonation constants and stability constants for all the reactions considered in the models are listed below. As required by the program BEST, all the constants are expressed as overall complexation constants (log β values), as shown in eqs IV.20-IV.28. The stability constants for metal hydroxide complexes (CaOH, ZnOH, $Zn(OH)_2$, MgOH, and PbOH)[4] in aqueous solution were corrected to 0.05 M ionic strength and expressed as acid dissociation constants using the 80% methanol-water autoprotolysis constants as explained in detail in the section describing lead-nigericin titrations.

$$H^+ + L^- \rightleftharpoons HL \qquad \beta_{HL} = K_H = \frac{[HL]}{[H^+][L^-]} \qquad \text{(IV.20)}$$

$$M^{n+} + L^{-} \rightleftharpoons ML^{n-1} \qquad \beta_{ML} = \frac{[ML^{n-1}]}{[M^{n+}][L^{-}]} \qquad \text{(IV.21)}$$

$$M^{n+} + 2L^{-} \rightleftharpoons ML_2^{n-2} \qquad \beta_{ML2} = \frac{[ML_2^{n-2}]}{[M^{n+}][L^{-}]^2} \qquad \text{(IV.22)}$$

$$M^{n+} + L^{-} + H^{+} \rightleftharpoons MLH^{n+} \qquad \beta_{MLH} = \frac{[MLH^{+}]}{[M^{n+}][L^{-}][H^{+}]} \qquad \text{(IV.23)}$$

$$M^{n+} + 2L^{-} + H^{+} \rightleftharpoons ML_2H^{n-1} \qquad \beta_{ML_2H} = \frac{[ML_2H^{n-1}]}{[M^{n+}][L^{-}]^2[H^{+}]} \qquad \text{(IV.24)}$$

$$M^{n+} + L^{-} + H_2O \rightleftharpoons MLOH^{n-2} + H^{+} \qquad \beta_{MLOH} = \frac{[MLOH^{n-2}][H^{+}]}{[M^{n+}][L^{-}]} \qquad \text{(IV.25)}$$

$$M^{n+} + H_2O \rightleftharpoons MOH^{n-1} + H^{+} \qquad \beta_{MOH} = \frac{[MOH^{n-1}][H^{+}]}{[M^{n+}]} \qquad \text{(IV.26)}$$

$$M^{n+} + 2H_2O \rightleftharpoons M(OH)_2^{n-2} + 2H^{+} \qquad \beta_{M(OH)_2} = \frac{[M(OH)^{n-2}][H^{+}]^2}{[M^{n+}]} \qquad \text{(IV.27)}$$

$$2M^{n+} + L^{-} \rightleftharpoons M_2L^{2n-1} \qquad \beta_{M_2L} = \frac{[M_2L^{2n-1}]}{[M^{n+}]^2[L^{-}]} \qquad \text{(IV.28)}$$

The protonation constants and the metal hydroxide constants were held at fixed values during the refinement and nigericin-metal complexation constants were obtained from the refinement. A simple model with only the nigericin protonation and nigericin-metal (1:1) complexation equilibria was used for the first stage of stability constant refinements. Each of the reactions listed above was added individually to the model to see if the fitting improved. When the sigma fit (eq IV.16) is improved by adding a species, that species will be kept in the model. The values of stability constants obtained

from the program BEST were input to the program Comics[5] to calculate the concentrations for every species as a function of pH. Species were deleted from the model when they accounted for less than 5% of the total ligand or metal concentration.

Sodium-nigericin

A weighed amount of dry sodium chloride was dissolved in 80% methanol-water and was diluted to the desired concentration. Different volumes of sodium chloride solutions were added to a solution containing a known concentration of nigericin acid (HNi) to provide ligand-metal ratios ranging from 0.25 to 1. The titration procedure was described in Section II. E. During data analysis using the program BEST[3], species such as Na_2Ni, HNa_2Ni, $NaNi_2$, $HNaNi_2$, and NaNi were tested. None of these except NaNi produce reasonable constants. Figure IV.6 shows the raw titration data with different Ni/Na ratios. Individual titrations with calculated curves obtained using the program BEST are shown in Figures IV.7 and IV.8. The average value of the stability constant for NaNi was input into the program Comics to generate the species distribution curve shown in Figure IV.9. The calculated values for the stability constant of the 1:1 sodium-nigericin complex are listed in Table IV.3.

Table IV.3 Log β_X values obtained from potentiometric titrations of nigericin acid (HL) and sodium[a]

Exp. No.	HL-Na ratio	Identity of complex species X		σ_{fit}[d]
		HL[b]	NaL[c]	
1	0.25	7.02	2.93	.011
2	0.30	7.02	2.84	.010
3	0.50	7.02	2.83	.020
4	1	7.02	2.96	.007

[a] 25 °C, ionic strength 0.05 M (TEAC). [b] The value of log β was fixed during refinement. [c] The value was refined using the program BEST. [d] $\sigma_{Fit} = (U/N)^{1/2}$, eq IV.16.

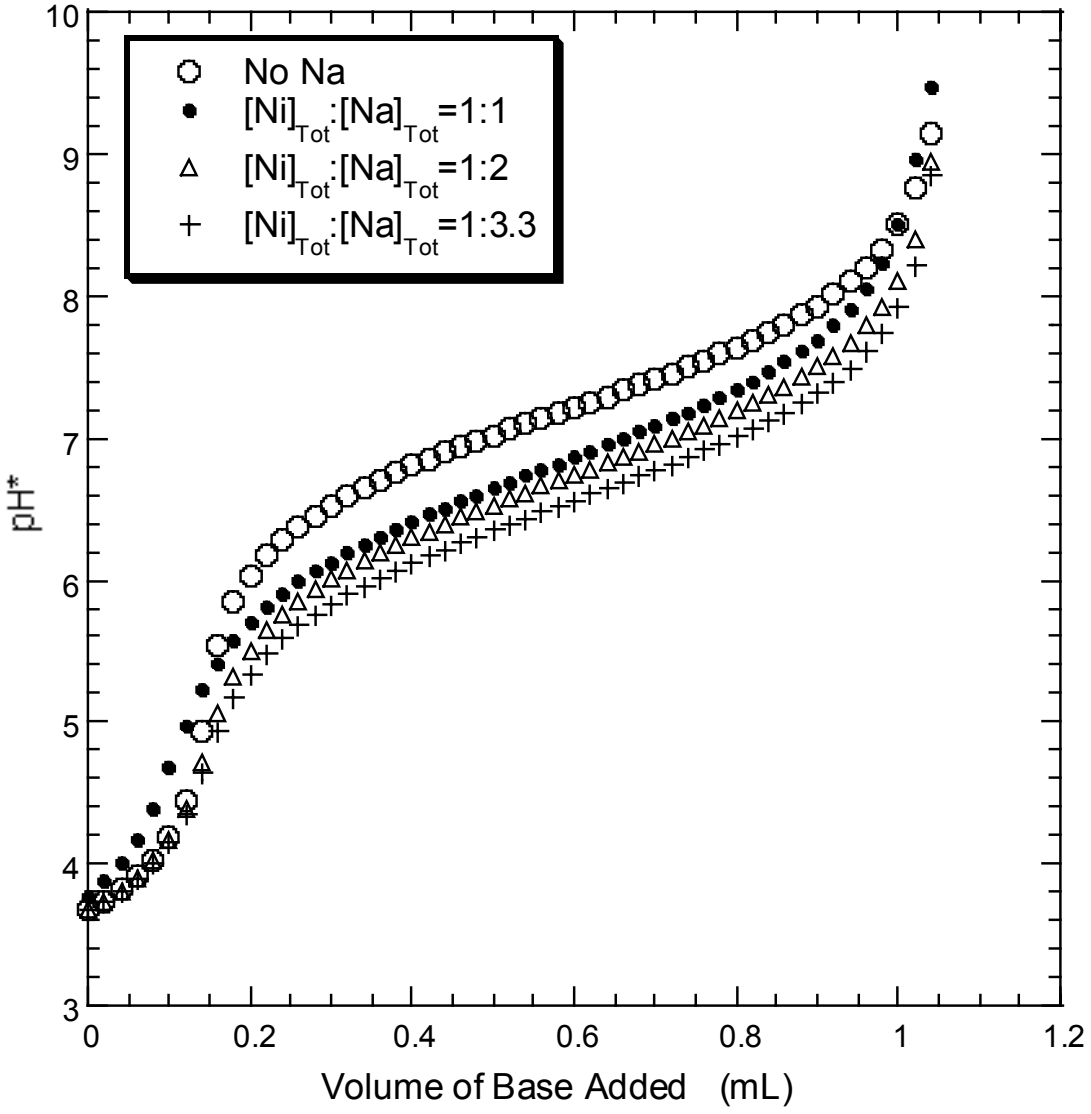


Figure IV.6. Potentiometric titration curves for various stoichiometric ratios of sodium-nigericin in 80% methanol-water at 25 ^{o}C. Each solution contained 6.22 mL of 1.29 mM nigericin acid at an ionic strength of 0.05 M Et_4NCl at 25 ^{o}C. The titrant is 9.3 mM Me_4NOH with ionic strength maintained at 0.05 M with Et_4NCl. A solution of 0.1 M sodium chloride was added in the required amount to obtain the indicated stoichiometric ratio.

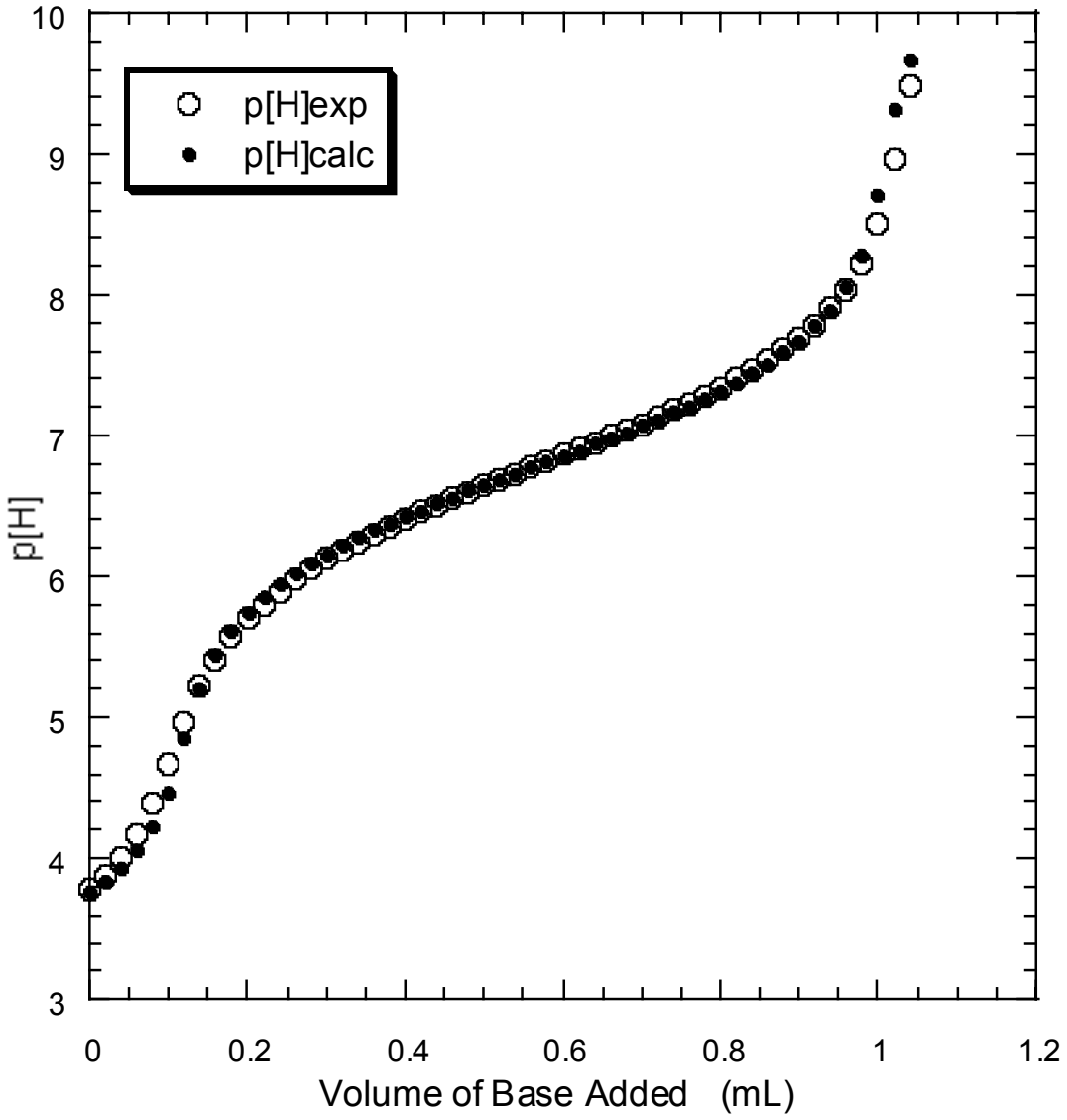


Figure IV.7. A potentiometric titration curve for 6.22 mL of a solution containing 1.29 mM nigericin acid and 1.29 mM sodium chloride at an ionic strength of 0.05 M Et_4NCl (25 ^oC). The titrant is 9.0 mM Me_4NOH at an ionic strength maintained at 0.05 M with Et_4NCl. The calculated p[H] values were obtained using the program BEST and values of equilibrium constants for the model containing the species listed in Table IV.3.

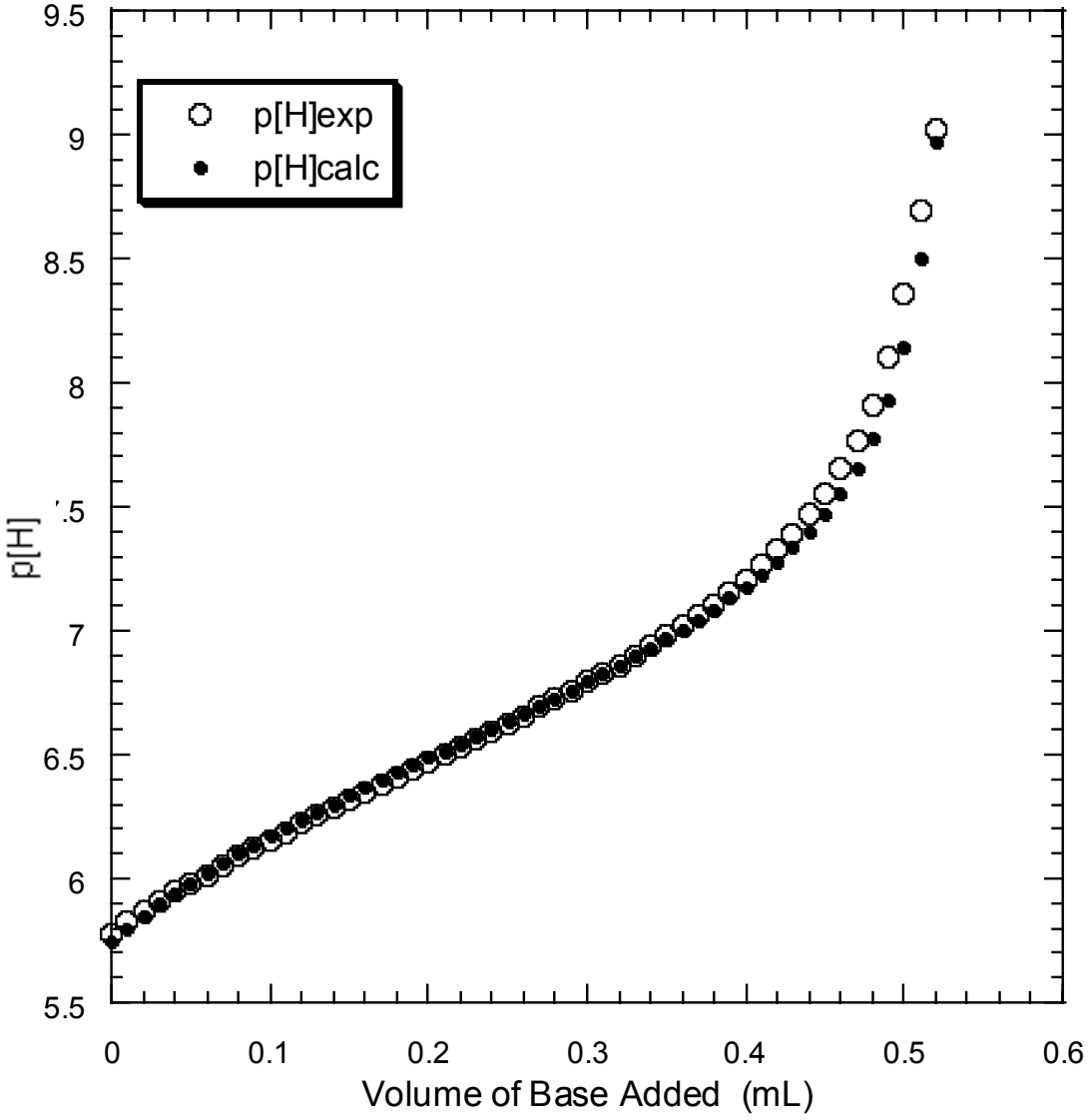


Figure IV.8. A potentiometric titration curve for 8.2 mL of a solution containing 0.64 mM nigericin acid and 2.52 mM sodium chloride at an ionic strength of 0.05 M Et_4NCl (25 ^oC). The titrant is 8.66 mM Me_4NOH at an ionic strength maintained at 0.05 M with Et_4NCl. The calculated p[H] values were obtained using the program BEST and values of equilibrium constants for the model containing the species listed in Table IV.3.

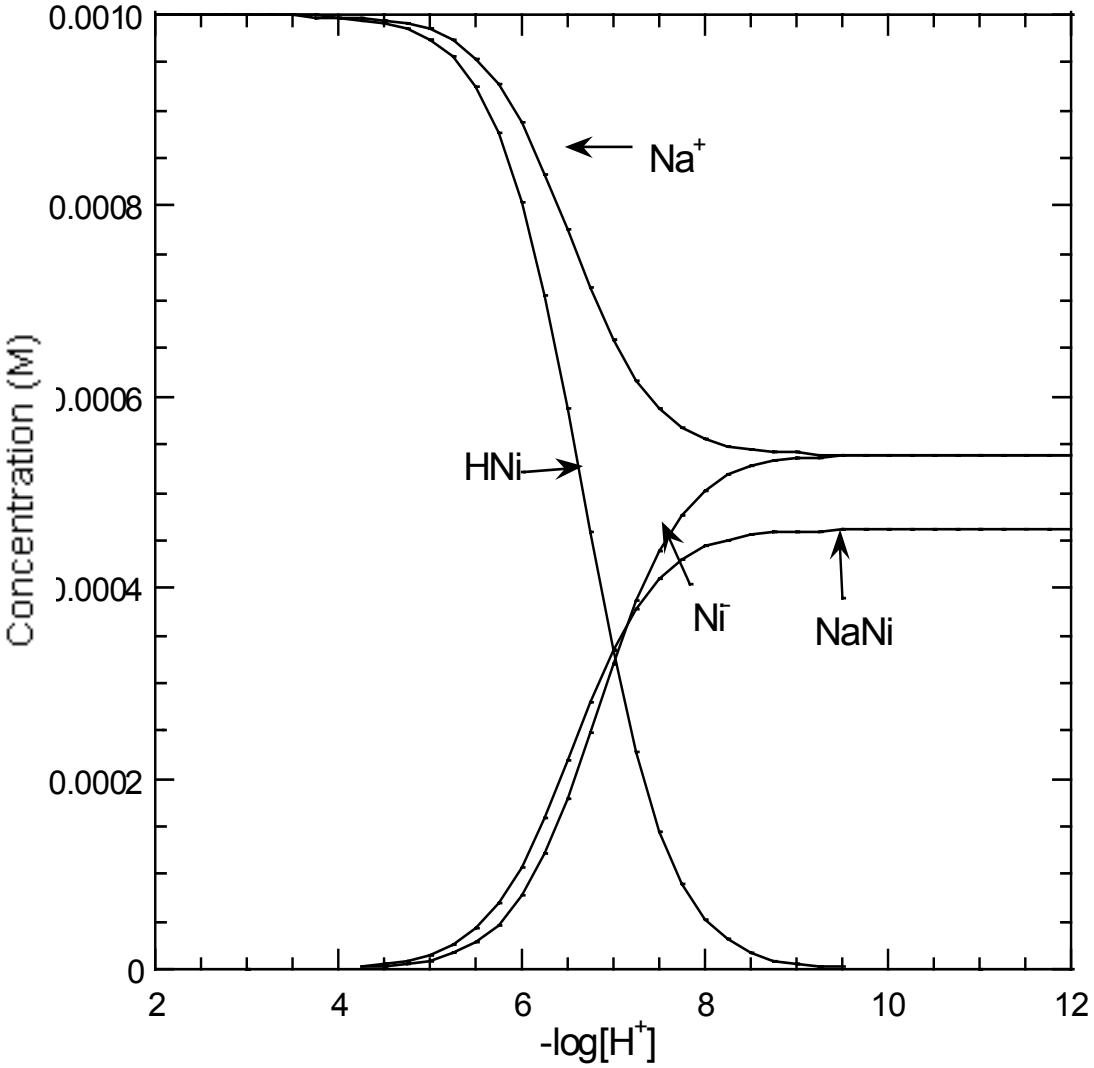


Figure IV.9 A species distribution curve for sodium-nigericin complexes in 80% methanol-water solution as a function of p[H]. Species concentrations were calculated using the program Comics for 1.0 mM nigericin and 1.0 mM sodium and the average value of the equilibrium constants listed in Table IV.3.

Potassium-nigericin

A weighed amount of dry potassium chloride was dissolved in 80% methanol-water and was diluted to the desired concentration. That potassium chloride solution was added to a solution containing with a known concentration of nigericin acid (HNi) to provide a desired metal-ligand ratio. The titration procedure was described in Section II.E. During data analysis using the program BEST[3], species such as K_2Ni, HK_2Ni, KNi_2, $HKNi_2$, and KNi were tested. None of these except KNi and $HKNi_2$ produce reasonable constants. A titration with the calculated curve obtained using the program BEST is shown in Figure IV.10. The average values of the stability constants for potassium-nigericin complexes were input into the program Comics to generate the species distribution curve shown in Figure IV.11. The calculated stability values from potentiometric titrations of nigericin acid (HNi) and potassium are listed in Table IV.4.

Table IV.4 Log β_X values obtained from potentiometric titrations of nigericin acid (HL) and potassium[a]

Exp. No.	HL-K ratio	Identity of complex species X			σ_{fit}[d]
		HL[b]	KL[c]	HKL_2[c]	
1	0.50	7.02	3.59	13.78	0.018
2	0.50	7.02	3.98	13.62	0.023
3	0.50	7.02	3.96	13.29	0.032
4	0.50	7.02	3.58	13.76	0.014

[a] 25 ^oC, ionic strength 0.05 M (TEAC). [b] The value of log β was fixed during refinement. [c] The value was refined using the program BEST. [d] $\sigma_{Fit} = (U/N)^{1/2}$, eq IV.16.

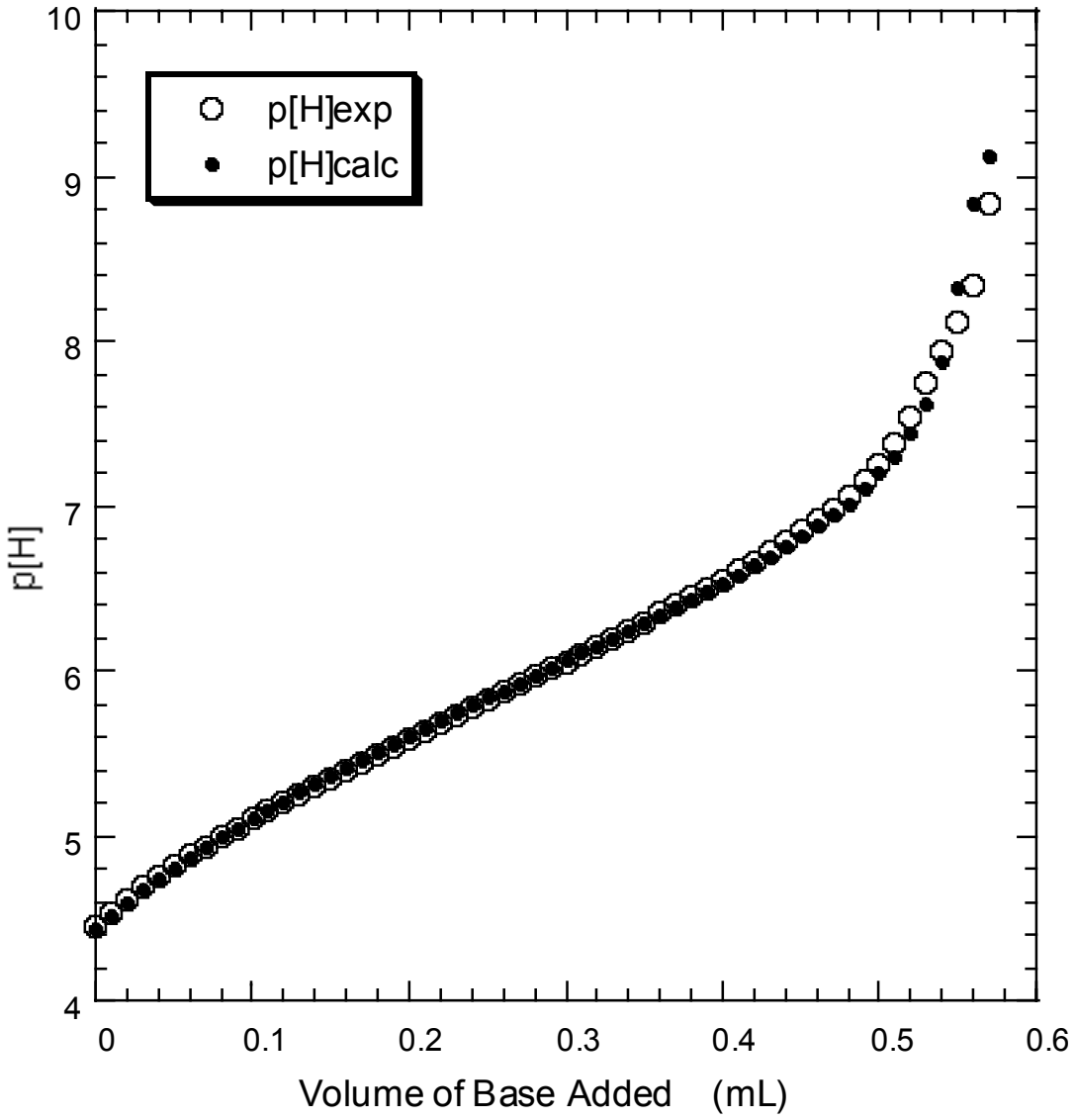


Figure IV.10. A potentiometric titration curve for 6.1 mL of a solution containing 0.85 mM nigericin acid and 1.15 mM potassium chloride at an ionic strength of 0.05 M Et_4NCl (25 ^{o}C). The titrant is 9.6 mM Me_4NOH with an ionic strength maintained at 0.05 M with Et_4NCl. The calculated p[H] values were obtained using the program BEST and refined values of equilibrium constants for the model containing the species listed in Table IV.4.

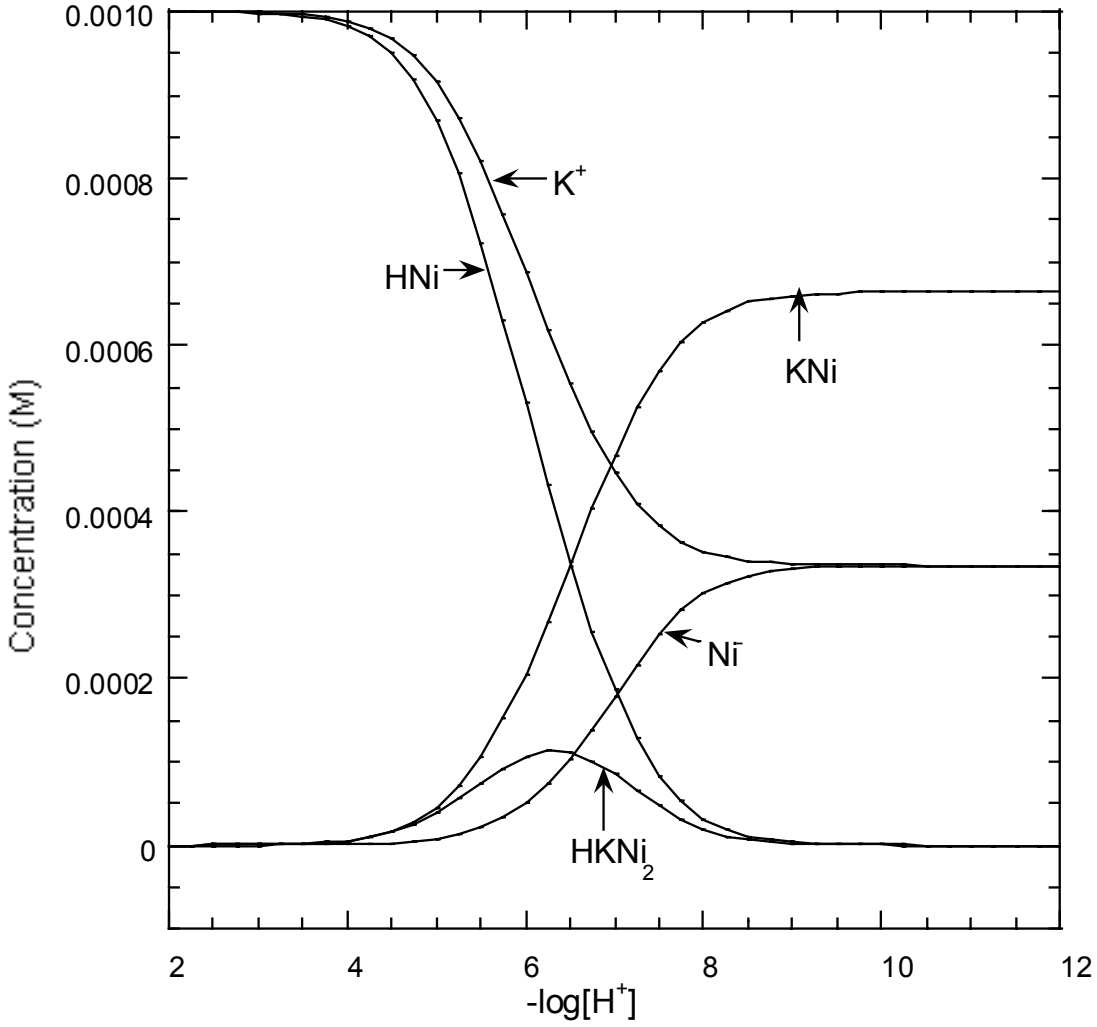


Figure IV.11. Species distribution curves for potassium-nigericin complexes in 80% methanol-water solution as a function of p[H]. Species concentrations were calculated using the program Comics for 1.0 mM nigericin and 1.0 mM potassium using the average values of the equilibrium constants listed in Table IV.4.

Calcium-nigericin

Different volumes of a solution of standardized calcium chloride in 80% methanol-water were added to a solution containing a known concentration of nigericin acid (HNi) to provide ligand-metal ratios ranging from 0.1 to 0.42. The titration procedure was described in Section II.E. During data analysis using the program BEST[3], species such as Ca_2Ni, HCa_2Ni, $CaNi_2$, $HCaNi_2$, CaNiOH, and CaNi were tested. None of these except CaNi produce reasonable constants. Figure IV.12 shows the raw titration data with different Ni/Ca ratios. A titration with the calculated curve obtained using the program BEST is shown in Figure IV.13. The average value of the stability constant for CaNi was input into the program Comics to generate the species distribution curve shown in Figure IV.14. The calculated values for the stability constant of calcium-nigericin are listed in Table IV.5.

Table IV.5 Log β_X values obtained from potentiometric titrations of nigericin acid (HL) and calcium (II)[a]

Exp. No.	HL-Ca ratio	Identity of complex species X			σ_{fit}[e]
		HL[b]	CaL[c]	CaOH[d]	
1	0.39	7.02	2.59	-13.11	0.016
2	0.39	7.02	2.54	-13.11	0.007
3	0.42	7.02	2.86	-13.11	0.020
4	0.1	7.02	2.38	-13.11	0.021

[a] 25 ^oC, ionic strength 0.05 M (TEAC). [b] The value of log β was fixed during refinement. [c] The value was refined using the program BEST. [d] Value was fixed during refinement; it was estimated for 80% methanol-water and corrected to 0.05 M ionic strength, as described in the beginning of this section. [e] $\sigma_{Fit} = (U/N)^{1/2}$, eq IV.16.

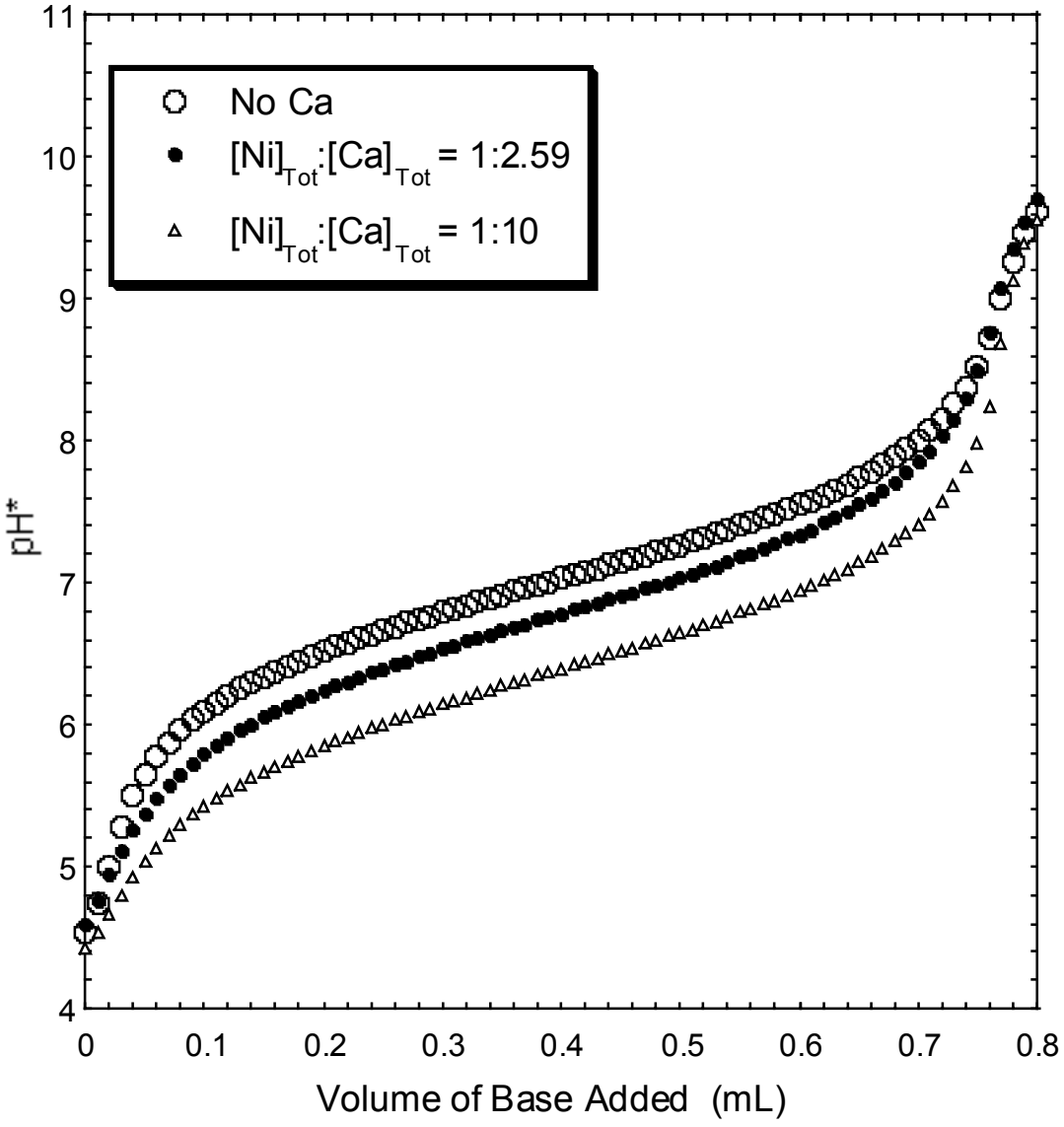


Figure IV.12. Potentiometric titration curves for various stoichiometric ratios of calcium-nigericin in 80% methanol-water at 25 ^{o}C. Each solution contained 6.15 mL of 0.93 mM nigericin acid at an ionic strength of 0.05 M Et_4NCl (25 ^{o}C). The titrant is 7.78 mM Me_4NOH with an ionic strength maintained at 0.05 M with Et_4NCl. A solution of 96 mM calcium chloride was added in the required amount to obtain the indicated stoichiometric ratio.

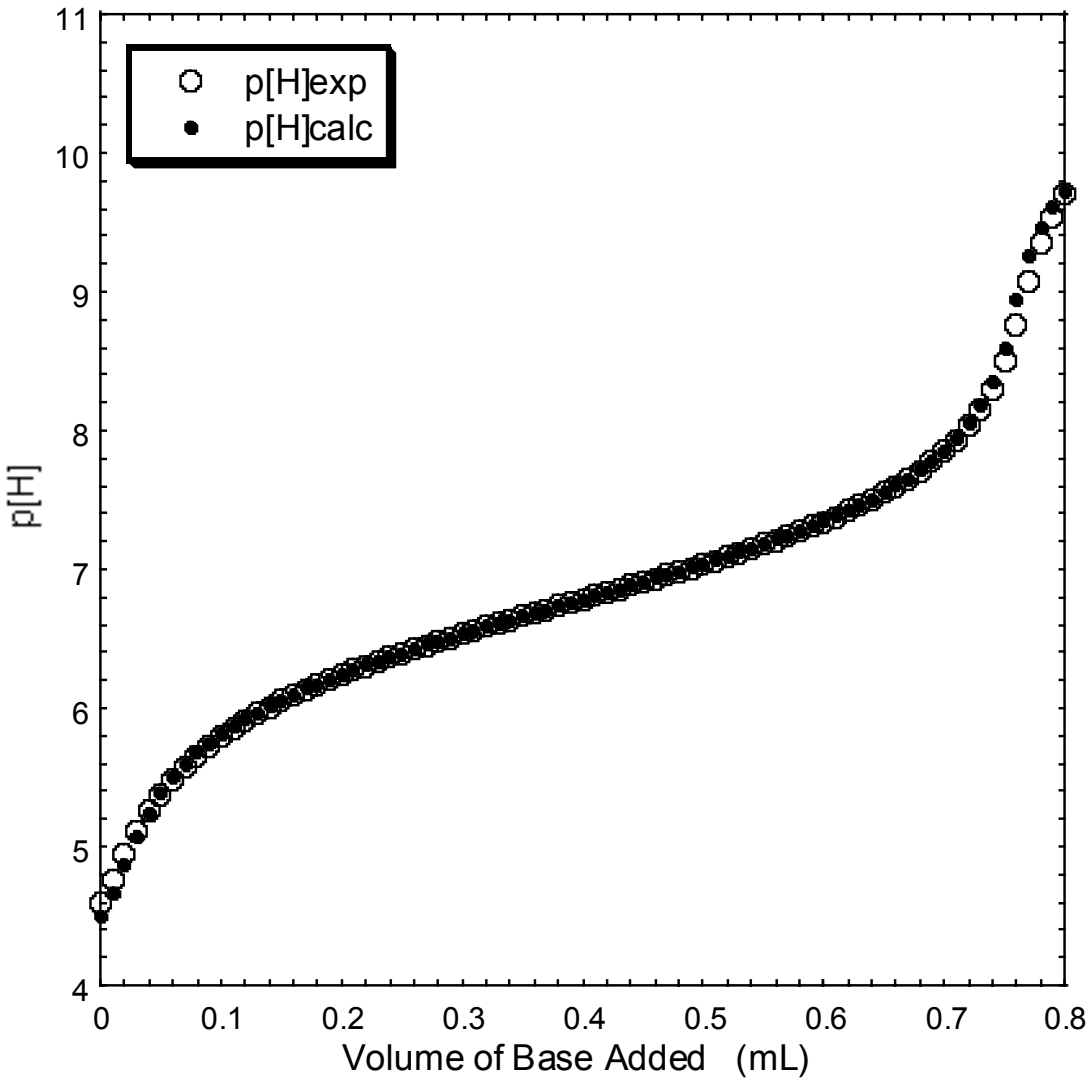


Figure IV.13. A potentiometric titration curve for 6.15 mL of a solution containing 0.93 mM nigericin acid and 2.42 mM calcium chloride at an ionic strength of 0.05 M Et_4NCl (25 ^{o}C). The titrant is 7.78 mM Me_4NOH with an ionic strength maintained at 0.05 M with Et_4NCl. The calculated p[H] values were obtained using the program BEST and refined values of equilibrium constants for the model containing the species listed in Table IV.5.

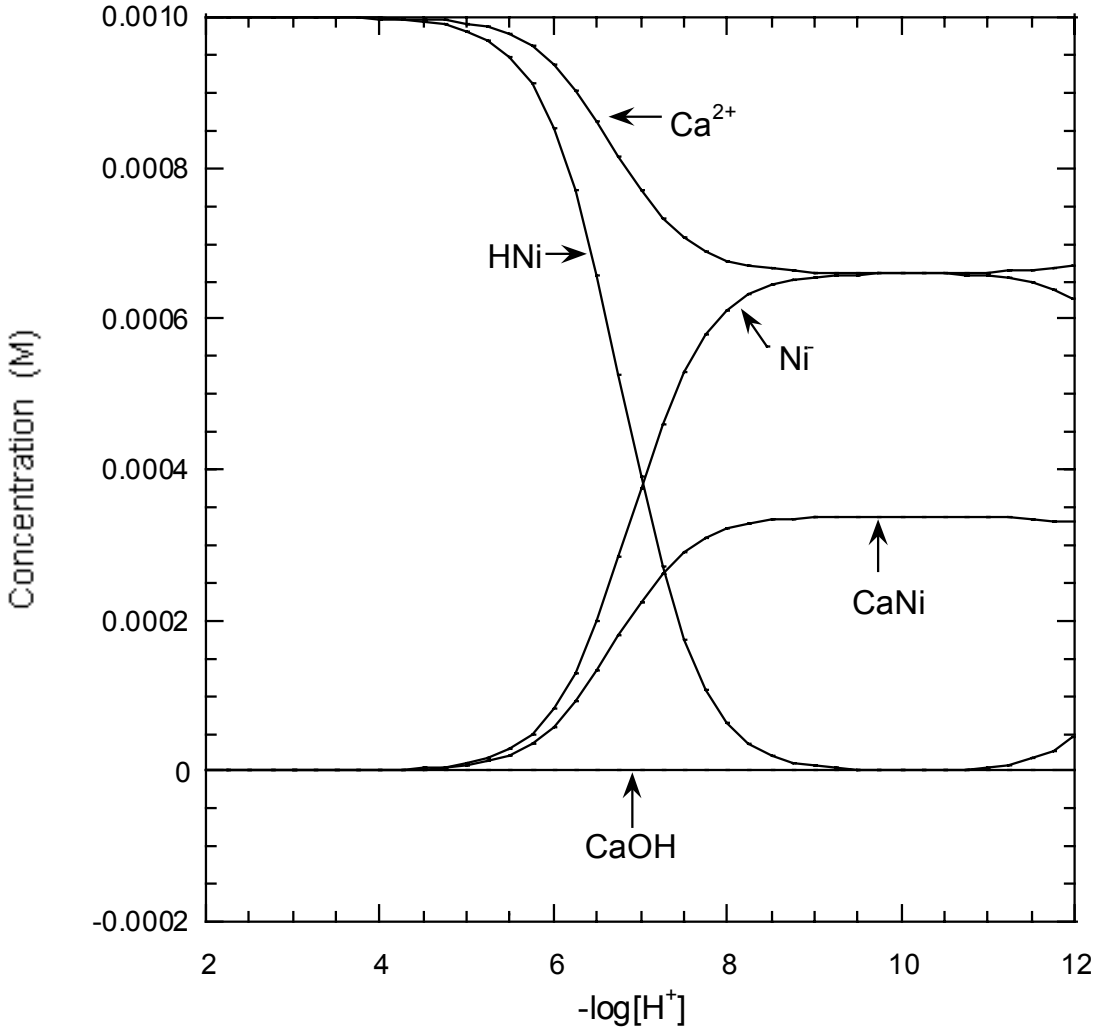


Figure IV.14. Species distribution curves for calcium-nigericin complexes in solution as a function of p[H]. Species concentrations were calculated using the program Comics for 1.0 mM nigericin and 1.0 mM calcium and the average values of the equilibrium constants listed in Table IV.5.

Zinc-nigericin

Different volumes of a solution of standardized zinc perchlorate in 80% methanol-water were added to a solution containing a known concentration of nigericin acid (HNi) to provide ligand-metal ratios ranging from 0.20 to 0.59. The titration procedure was described in Section II.E. Due to the precipitation of zinc-hydroxy complexes, data above pH 7 in all titrations were discarded. During data analysis using the program BEST[3], species such as Zn_2Ni, HZn_2Ni, $ZnNi_2$, $HZnNi_2$, ZnNiOH, and ZnNi were tested. Only ZnNi, ZnNiOH and $HZnNi_2$ produced reasonable constants. Figure IV.15 shows the raw titration data with different Ni/Zn ratios. A titration with the calculated curve obtained using the program BEST is shown in Figure IV.16. The average values of the stability constants for zinc-nigericin complexes were input into the program Comics to generate the species distribution curve shown in Figure IV.17. The calculated values for the stability constant of zinc-nigericin are listed in Table IV.6.

Table IV.6. Log β_X values obtained from potentiometric titrations of nigericin acid (HL) and Zn (II)[a]

Exp. No.	HL-Zn ratio	Identity of complex species X						σ_{fit}[f]
		HL[b]	ZnL[c]	ZnLOH[c,d]	$HZnL_2$[c]	ZnOH[e]	$Zn(OH)_2$[e]	
1	0.20	7.02	2.86	-4.77	12.77	-9.42	-18.2	0.008
2	0.34	7.02	3.18	-4.47	12.95	-9.42	-18.2	0.010
3	0.45	7.02	3.08	-4.59	12.88	-9.42	-18.2	0.006
4	0.59	7.02	2.84	-4.60	12.47	-9.42	-18.2	0.011

[a] 25 ^{o}C, ionic strength 0.05 M (TEAP). [b] The value of log β was fixed during refinement. [c] The value was refined using the program BEST. [d] β_{ZnLOH} is expressed as an acid dissociation constant. [e] Value was fixed during refinement; it was estimated for 80% methanol-water and corrected to 0.05 M ionic strength, as described in the beginning of this section. [f] $\sigma_{Fit} = (U/N)^{1/2}$, eq IV.16.

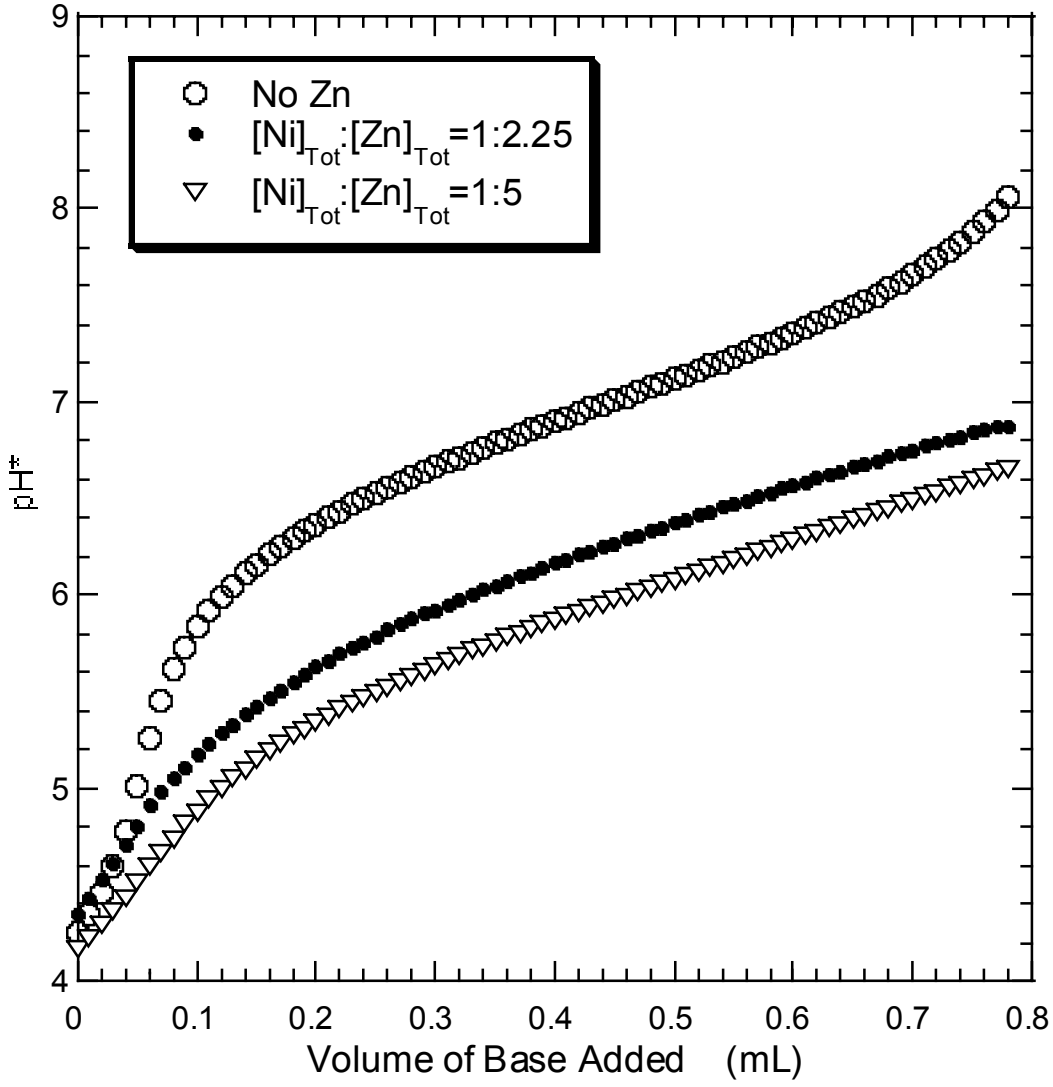


Figure IV.15. Potentiometric titration curves for various stoichiometric ratios of zinc-nigericin in 80% methanol-water at 25 ^{o}C. Each solution contained 7.70 mL of 0.80 mM nigericin acid at an ionic strength of 0.05 M TEAP (25 ^{o}C). The titrant is 7.78 mM Me_4NOH with an ionic strength maintained at 0.05 M with TEAP. A solution of 8.5 mM zinc perchlorate was added in the required amount to obtain the indicated stoichiometric ratio.

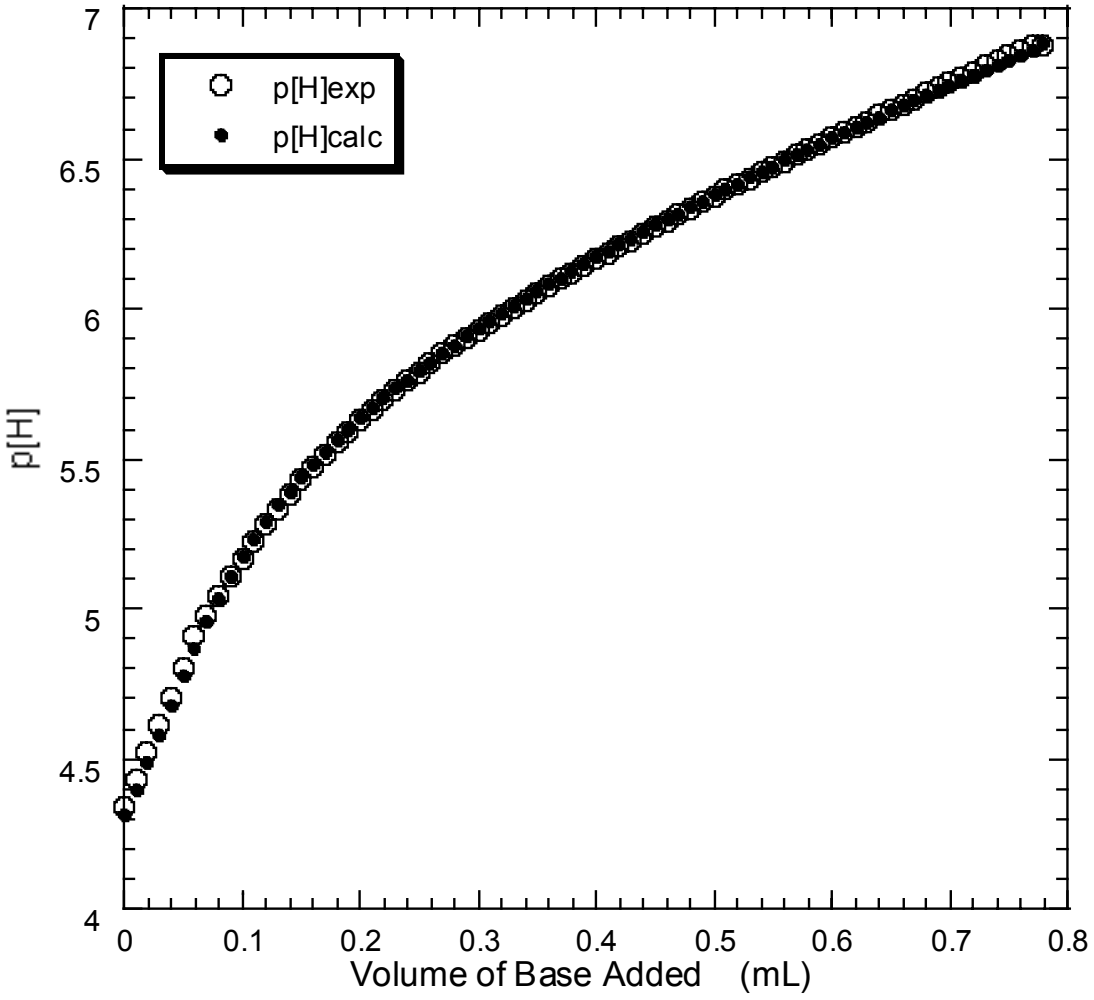


Figure IV.16. A potentiometric titration curve for 7.70 mL of a solution containing 0.80 mM nigericin acid and 1.79 mM zinc perchlorate at an ionic strength of 0.05 M TEAP (25 ^{o}C). The titrant is 7.78 mM Me_4NOH with an ionic strength maintained at 0.05 M with TEAP. The calculated p[H] values were obtained using the program BEST and refined values of equilibrium constants for the model containing the species listed in Table IV.6.

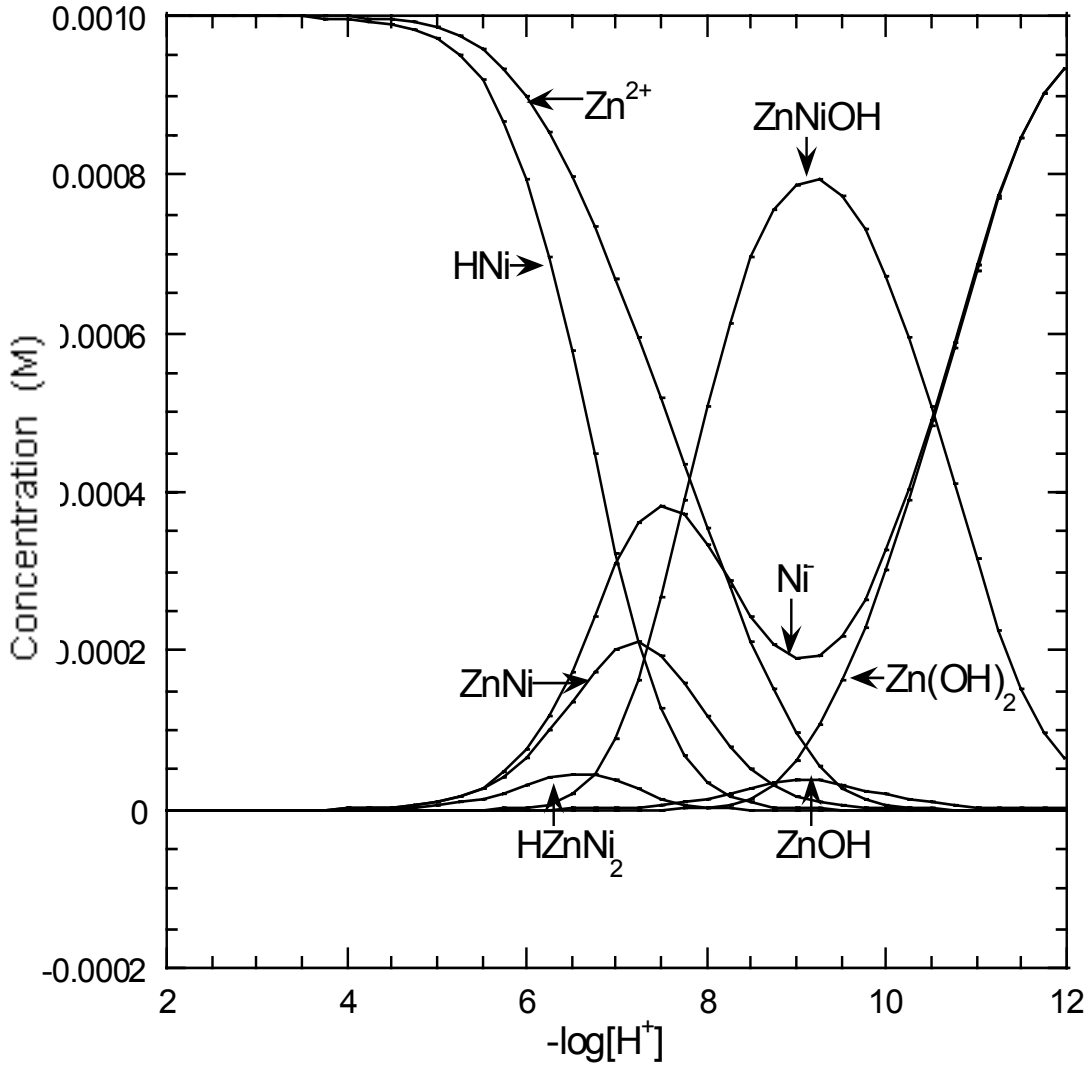


Figure IV.17. Species distribution curves for zinc-nigericin complexes in 80% methanol-water as a function of p[H]. Species concentrations were calculated using the program Comics for 1.0 mM nigericin and 1.0 mM zinc and the average values of the equilibrium constants listed in Table IV.6.

Magnesium-nigericin

Different volumes of a solution of standardized magnesium perchlorate in 80% methanol-water were added to a solution containing a known concentration of nigericin acid (HNi) to provide ligand-metal ratios ranging from 0.37 to 0.94. The titration procedure was described in Section II.E. During data analysis using the program BEST[3], species such as Mg_2Ni, HMg_2Ni, $MgNi_2$, $HMgNi_2$, MgNiOH, and MgNi were tested. Only MgNi, MgNiOH, and $HMgNi_2$ produced reasonable constants. Figure IV.18 shows the raw titration data with different Ni/Mg ratios. A titration with the calculated curve obtained using the program BEST is shown in Figure IV.19. The average values of the stability constants for magnesium-nigericin complexes were input into the program Comics to generate the species distribution curve shown in Figure IV.20. The calculated values for the stability constant of magnesium-nigericin are listed in Table IV.7.

Table IV.7. Log β_X values obtained from potentiometric titrations of nigericin acid (HL) and Mg (II)[a]

Exp. No.	HL-Mg ratio	Identity of complex species X					σ_{fit}[f]
		HL[b]	MgL[c]	$MgLOH$[c,d]	$HMgL_2$[c]	$MgOH$[e]	
1	0.37	7.02	2.50	-	12.55	-11.9	0.024
2	0.45	7.02	2.60	-8.18	12.73	-11.9	0.033
3	0.45	7.02	2.23	-8.41	12.20	-11.9	0.022
4	0.94	7.02	2.50	-8.08	13.03	-11.9	0.023

[a] 25 ^oC, ionic strength 0.05 M (TEAP). [b] The value of log β was fixed during refinement. [c] The value was refined using the program BEST. [d] β_{MgLOH} is expressed as an acid dissociation constant. [e] Value was fixed during refinement; it was estimated for 80% methanol-water and corrected to 0.05 M ionic strength, as described in the beginning of this section. [f] $\sigma_{Fit} = (U/N)^{1/2}$, eq IV.16.

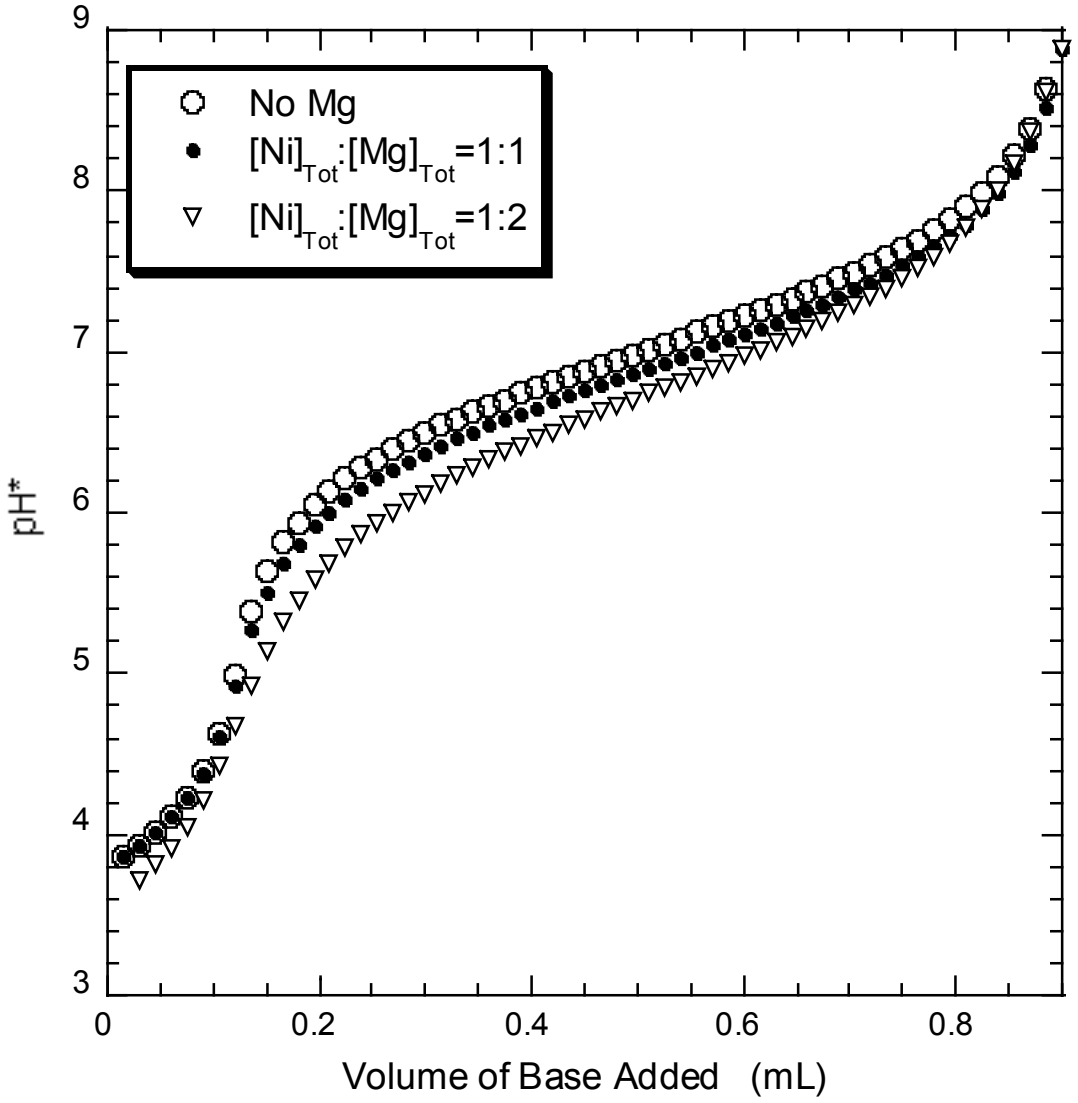


Figure IV.18. Potentiometric titration curves for various stoichiometric ratios of magnesium-nigericin in 80% methanol-water at 25 ^{o}C. Each solution contained 6.10 mL of 0.99 mM nigericin acid at an ionic strength of 0.05 M TEAP (25 ^{o}C). The titrant is 7.78 mM Me_4NOH with an ionic strength maintained at 0.05 M with TEAP. A solution of 0.139 M magnesium perchlorate was added in the required amount to obtain the indicated stoichiometric ratio.

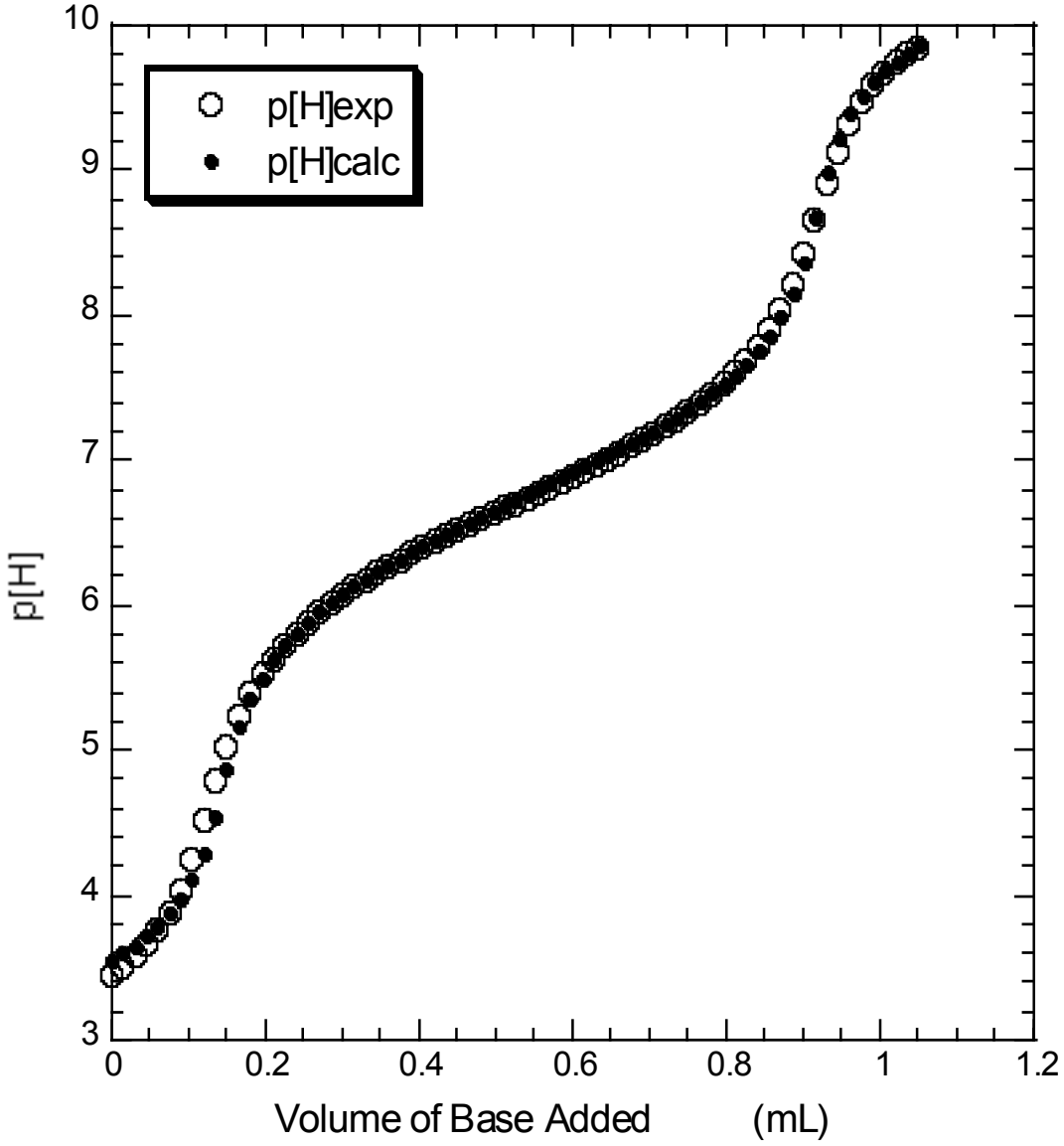


Figure IV.19. A potentiometric titration curve for 6.10 mL of a solution containing 0.99 mM nigericin acid and 2.41 mM magnesium perchlorate at an ionic strength of 0.05 M TEAP (25 ^{o}C). The titrant is 7.78 mM Me_4NOH with an ionic strength maintained at 0.05 M with TEAP. The calculated p[H] values were obtained using the program BEST and refined values of equilibrium constants for the model containing the species listed in Table IV.7.

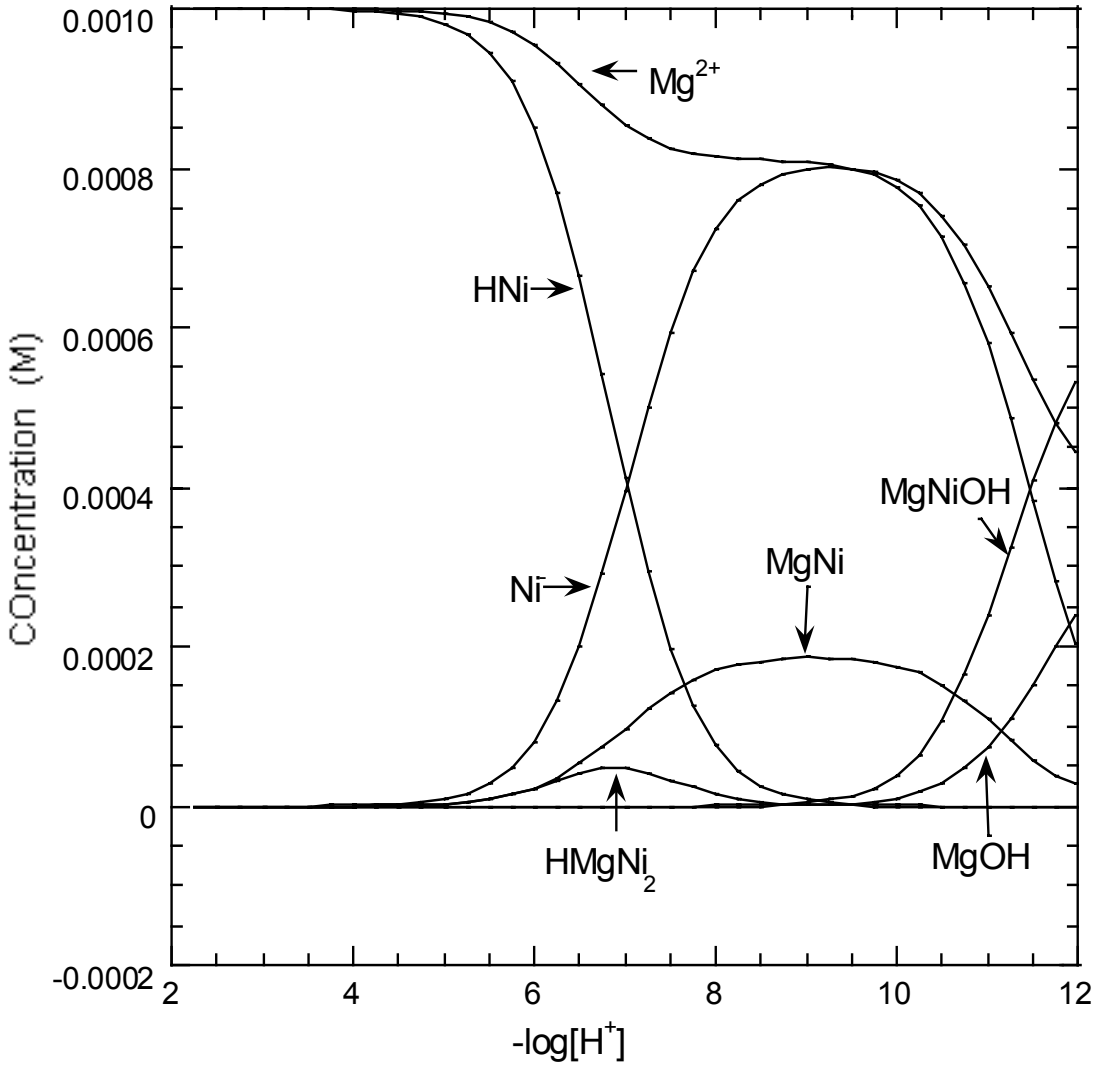


Figure IV.20. Species distribution curves for magnesium-nigericin complexes in 80% methanol-water solution as a function of p[H]. Species concentrations were calculated using the program Comics for 1.0 mM nigericin and 1.0 mM magnesium and the average values of the equilibrium constants listed in Table IV.7.

Lead-nigericin

Different volumes of a solution of standardized lead perchlorate in 80% methanol-water were added to a solution containing a known concentration of nigericin acid (HNi) to provide ligand-metal ratios ranging from 0.877 to 2. The titration procedure was described in Section II.E. Titration data were analyzed using the program BEST[3] that requires the formation constants for lead hydroxide complexes.

Formation constants for lead-hydroxide and lead-methoxide complexes in water[4,6] and in methanol[7] are available in literature but none of the experiments were done in 80% methanol-water. The stability constants for lead–hydroxy or lead-methoxide complexes in 80% methanol-water were estimated based on a study of autoprotolysis constants for different methanol compositions[8]. The results of that study are shown in Figure IV.21. It is clear that the thermodynamic solvent autoprotolysis constant for 80% methanol is closer to the one for water than that for methanol[8]. Therefore, the stability constants for lead-hydroxy complexes are assumed to be equal to those values obtained in water. After the correction for the ionic strength (0.05M), the formation constants of lead-hydroxy complexes in water[6] were expressed in the form of an acid hydrolysis reaction[9] shown in eqs IV.26 and IV.27, as required by the program BEST. Although a number of different lead-hydroxy complexes are possible, defined by eq IV.29, only $Pb(OH)^+$ exits in a significant amount under the experimental conditions used in this work[6,9].

$$x\ Pb^{2+} + y\ OR^- \rightleftharpoons Pb_x(OR)_y^{2x-y} \qquad \beta_{xy} = \frac{[Pb_x(OR)_y^{2x-y}]}{[Pb^{2+}]^x[OR^-]^y} \qquad \text{(IV.29)}$$

where x-y could be 1-1, 1-2, 1-3, 3-4, 3-5, 4-4, 6-8.

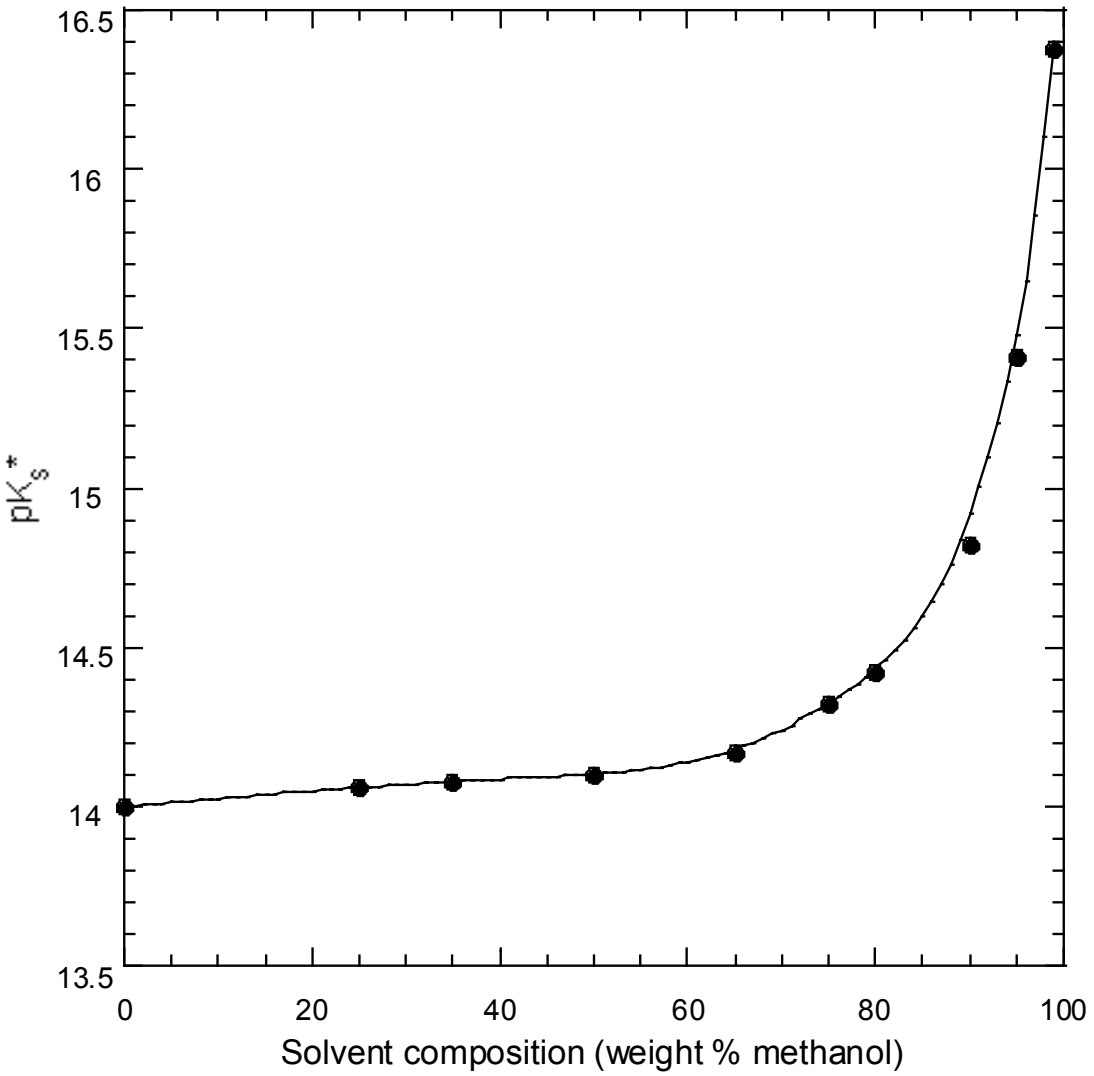


Figure IV.21. Plot of thermodynamic solvent autoprotolysis constants as a function of methanol-water solvent composition[8].

Figure IV.22 shows the raw titration data with different Ni/Pb ratios. In the models for data analysis many species were tested. Only the models containing the species PbNi, Pb_2Ni, $PbNi_2$, and PbNiOH were able to fit the data in a satisfactory manner. The difference between the calculated pH curve based on the model without Pb_2Ni, $PbNi_2$, and PbNiOH and the experimental pH curve indicated the existence of those species in the solutions. Without PbNiOH, the calculated pH curve increased

sharply from pH 7 to pH 10 although the experimental pH curve increased gradually and never reached pH 10. Addition of the species $PbNi_2$ lowered the acidic part of the calculated curve and addition of the species Pb_2Ni increased pH values of the calculated curve in the region pH 5-8. Both PbNiOH and $PbNi_2$ were required to fit all titrations but the species Pb_2Ni was necessary only in the presence of excess lead. Individual titrations with calculated curves obtained using the program BEST are shown in Figures IV.23 and IV.24. Before data analysis all titration curves were cut at pH 8 due to the existence of precipitation. The average values of the stability constants for lead-nigericin complexes were input into the program Comics to generate the species distribution curves for 1.0 mM nigericin and 0.5 mM lead shown in Figure IV.25 or 1.0 mM lead shown in Figure IV.26. The calculated values for the stability constants of lead-nigericin are listed in Table IV.8.

Table IV.8. Log β_X values obtained from potentiometric titrations of nigericin acid (HL) and lead (II) in 80% methanol-water[a]

Exp. No.	HL-Pb ratio	Identity of complex species X						σ_{fit}[f]
		HL[b]	PbL[c]	PbLOH[c,d]	Pb_2L[c]	PbL_2[c]	PbOH[e]	
1	1.54	7.02	7.29	0.313		10.72	-7.96	.022
2	0.877	7.02	6.99	0.260	13.31	10.68	-7.96	.057
3	1	7.02	7.73	0.180	13.57	11.91	-7.96	.047
4	2	7.02	7.88	0.270		12.10	-7.96	.047
5	2	7.02	7.95	0.041		11.46	-7.96	.026

[a] 25 °C, ionic strength 0.05 M (TEAP). [b] The value of log β was fixed during refinement. [c] The value was refined using the program BEST. [d] β_{PbLOH} is expressed as an acid dissociation constant. [e] Value was fixed during refinement; it was estimated for 80% methanol-water and corrected to 0.05 M ionic strength, as described in the text. [f] $\sigma_{Fit} = (U/N)^{1/2}$, eq IV.16.

Titrations in the presence of different metal ions are shown together in Figure V.27. Figure IV.27 shows that adding lead with a 2:1 Ni/Pb ratio moves pH of the nigericin acid solution down ~2 units while adding other divalent metal ions with a 1:1

Ni/Pb ratio doesn't change pH of the nigericin acid solution very much. The complexation constants for different metal-salinomycin complexes are listed in Table V.9.

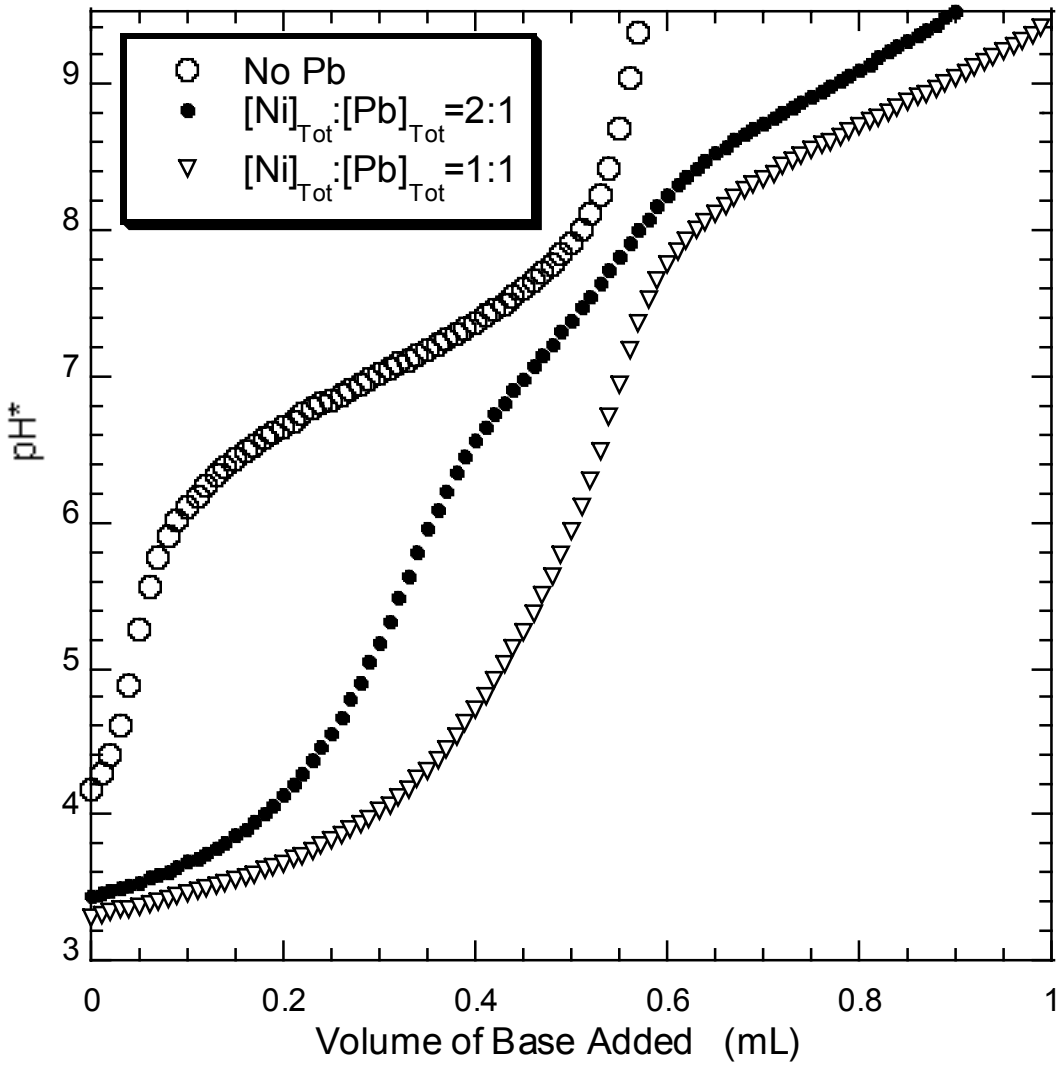


Figure IV.22. Potentiometric titration curves for various stoichiometric ratios of lead-nigericin in 80% methanol-water at 25 ^{o}C. Each solution contained 6.08 mL of 0.77 mM nigericin acid at an ionic strength of 0.05 M TEAP (25 ^{o}C). The titrant is 9.13 mM Me_4NOH with an ionic strength maintained at 0.05 M with TEAP. A solution of 0.0313

M lead perchlorate was added in the required amount to obtain the indicated stoichiometric ratio.

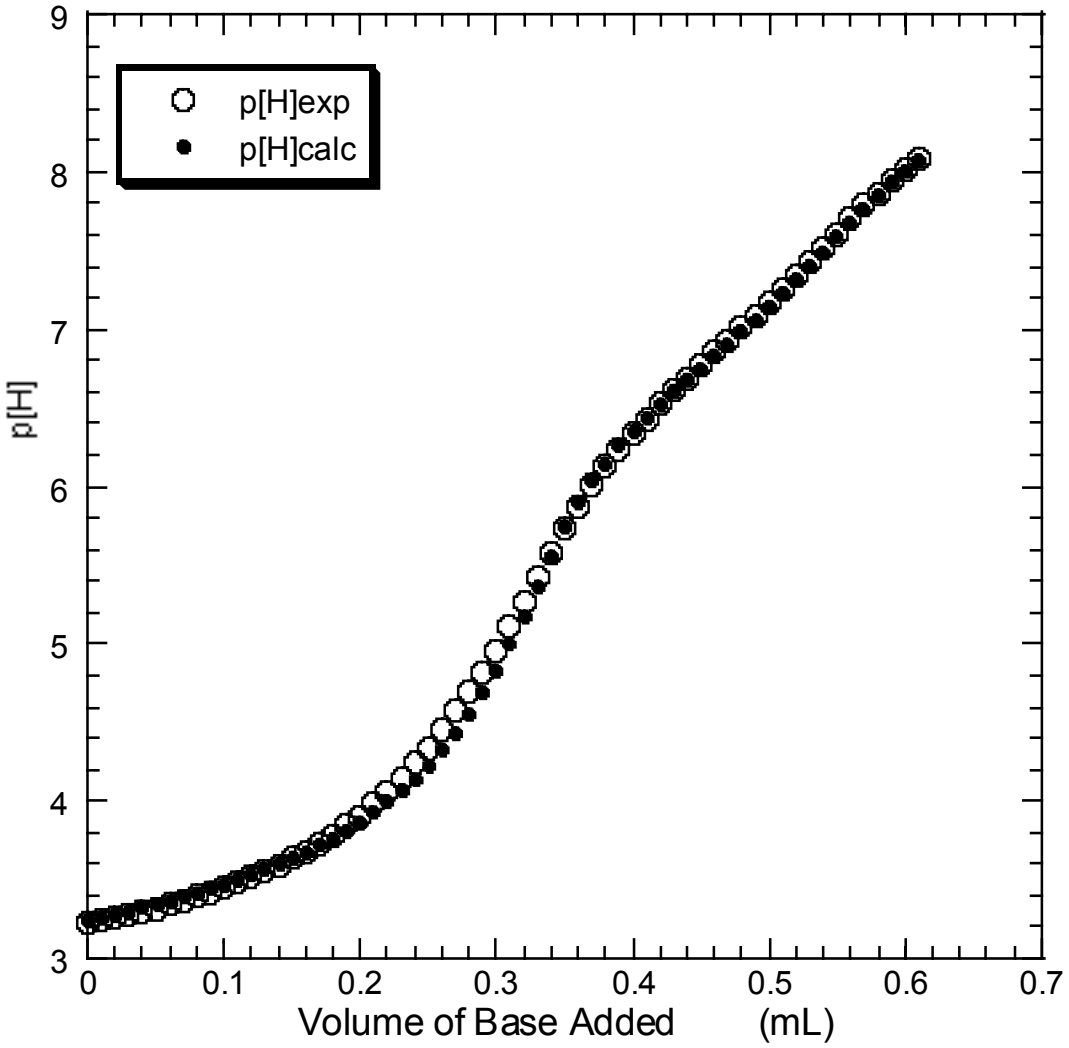


Figure IV.23. A potentiometric titration curve for 6.08 mL of a solution containing 0.77 mM nigericin acid and 0.41 mM lead perchlorate in 80% methanol-water at an ionic strength of 0.05 M TEAP (25 ^{o}C). The titrant is 0.00913 M Me_4NOH with an ionic strength maintained at 0.05 M with TEAP. The calculated p[H] values were obtained using the program BEST and refined values of equilibrium constants for the model containing the species listed in Table IV.7.

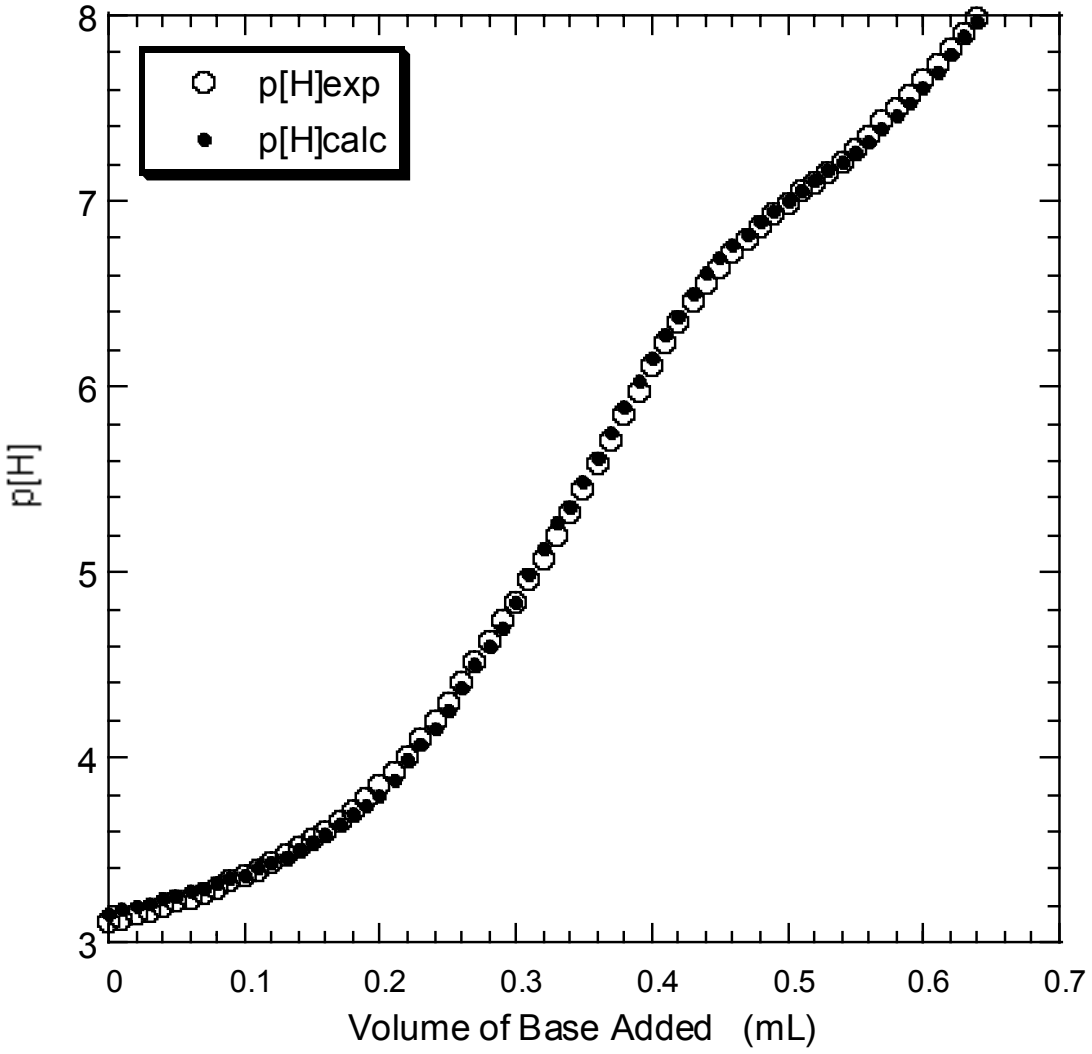


Figure IV.24. A potentiometric titration curve for 5.10 mL of a solution containing 0.6 mM nigericin acid and 0.61 mM lead perchlorate at an ionic strength of 0.05 M TEAP (25 ^{o}C). The titrant is 9.13 mM Me_4NOH with an ionic strength maintained at 0.05 M with TEAP. The calculated p[H] values were obtained using the program BEST and refined values of equilibrium constants for the model containing the species listed in Table IV.7.

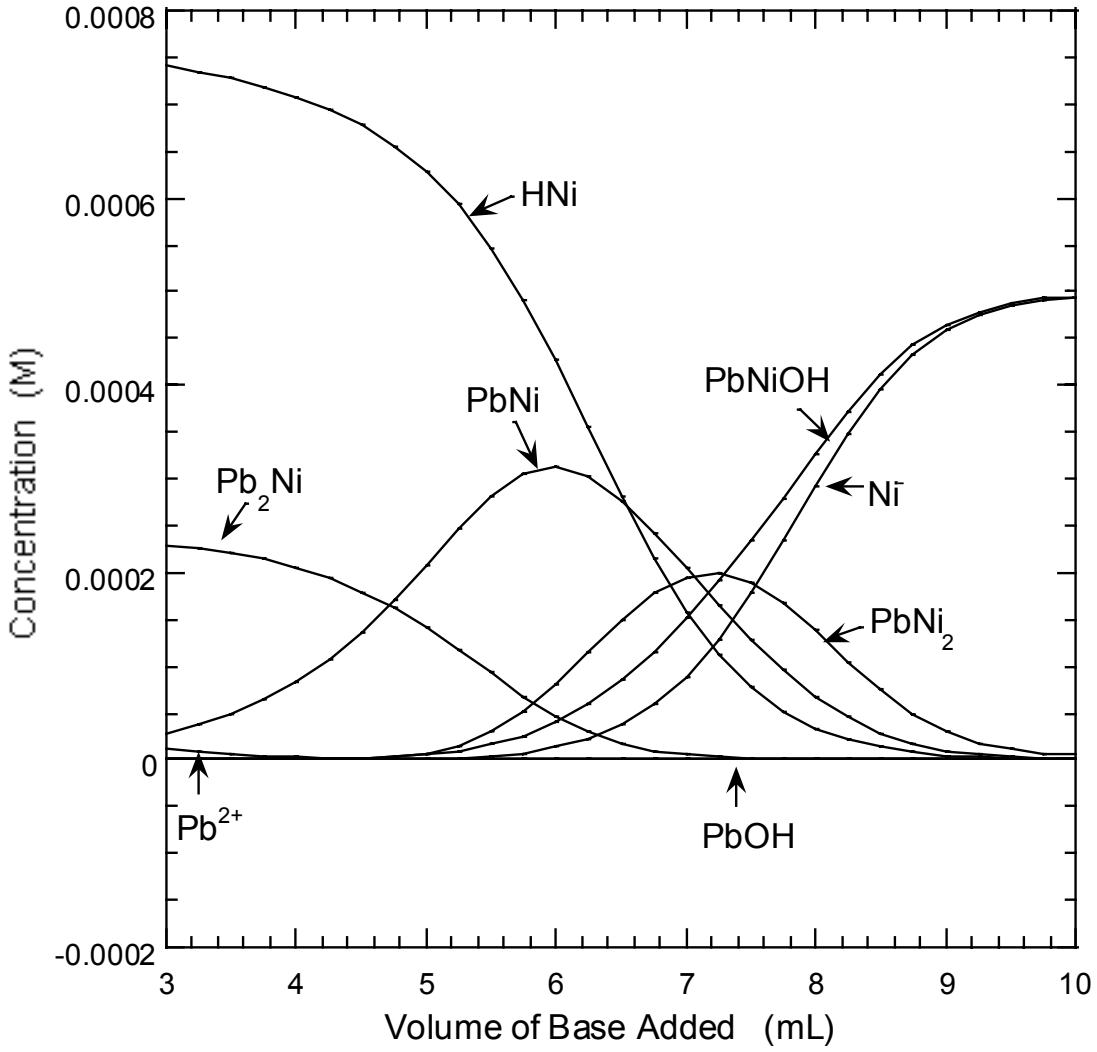


Figure IV.25. Species distribution curves for lead (II)-nigericin complexes in 80% methanol-water solution as a function of p[H]. Species concentrations were calculated using the program Comics for 1.0 mM nigericin and 0.5 mM lead and the average values of the equilibrium constants listed in Table IV.7.

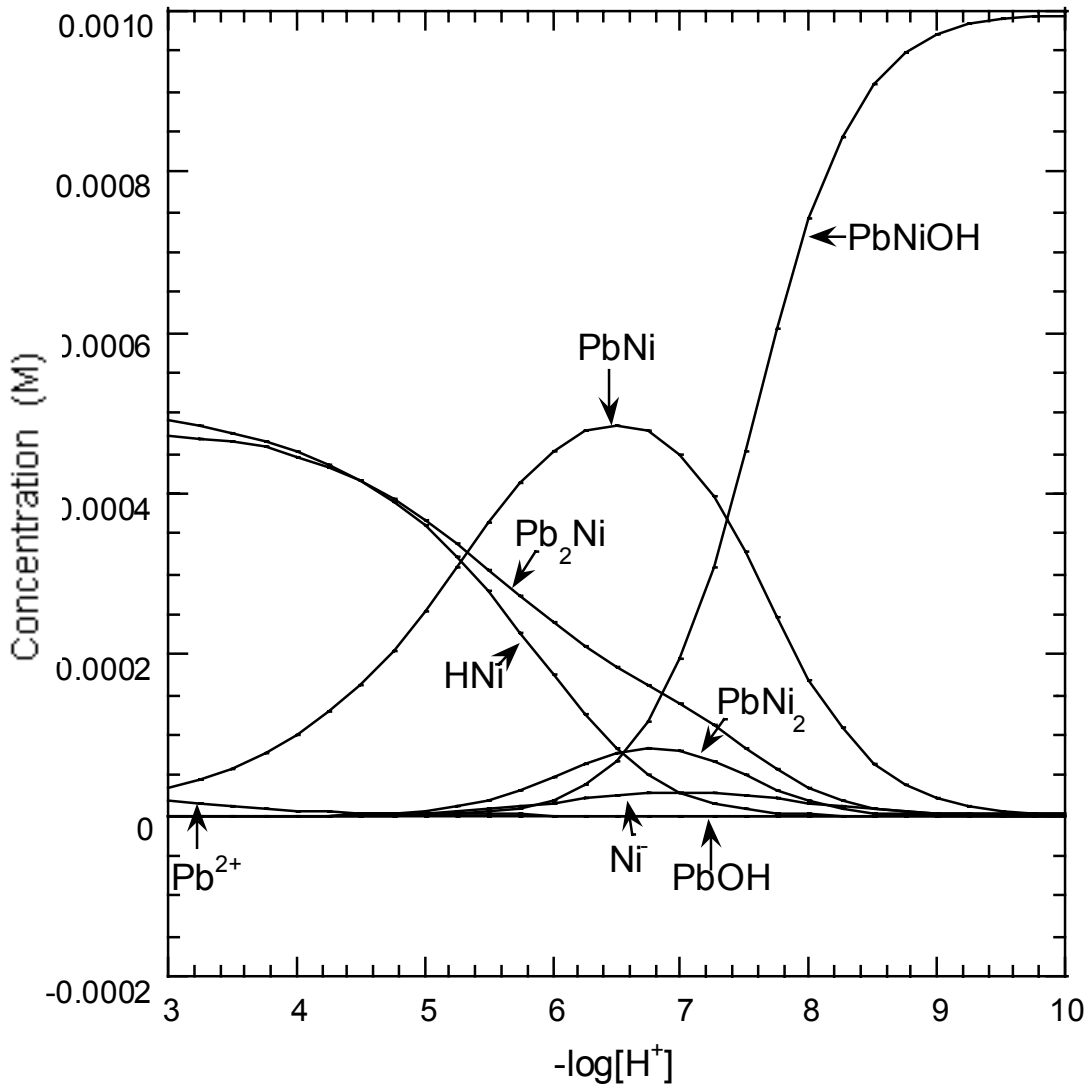


Figure IV.26. Species distribution curves for lead (II)-nigericin complexes in 80% methanol-water solution as a function of p[H]. Species concentrations were calculated using the program Comics for 1.0 mM nigericin and 1.0 mM lead and the average values of the equilibrium constants listed in Table IV.7.

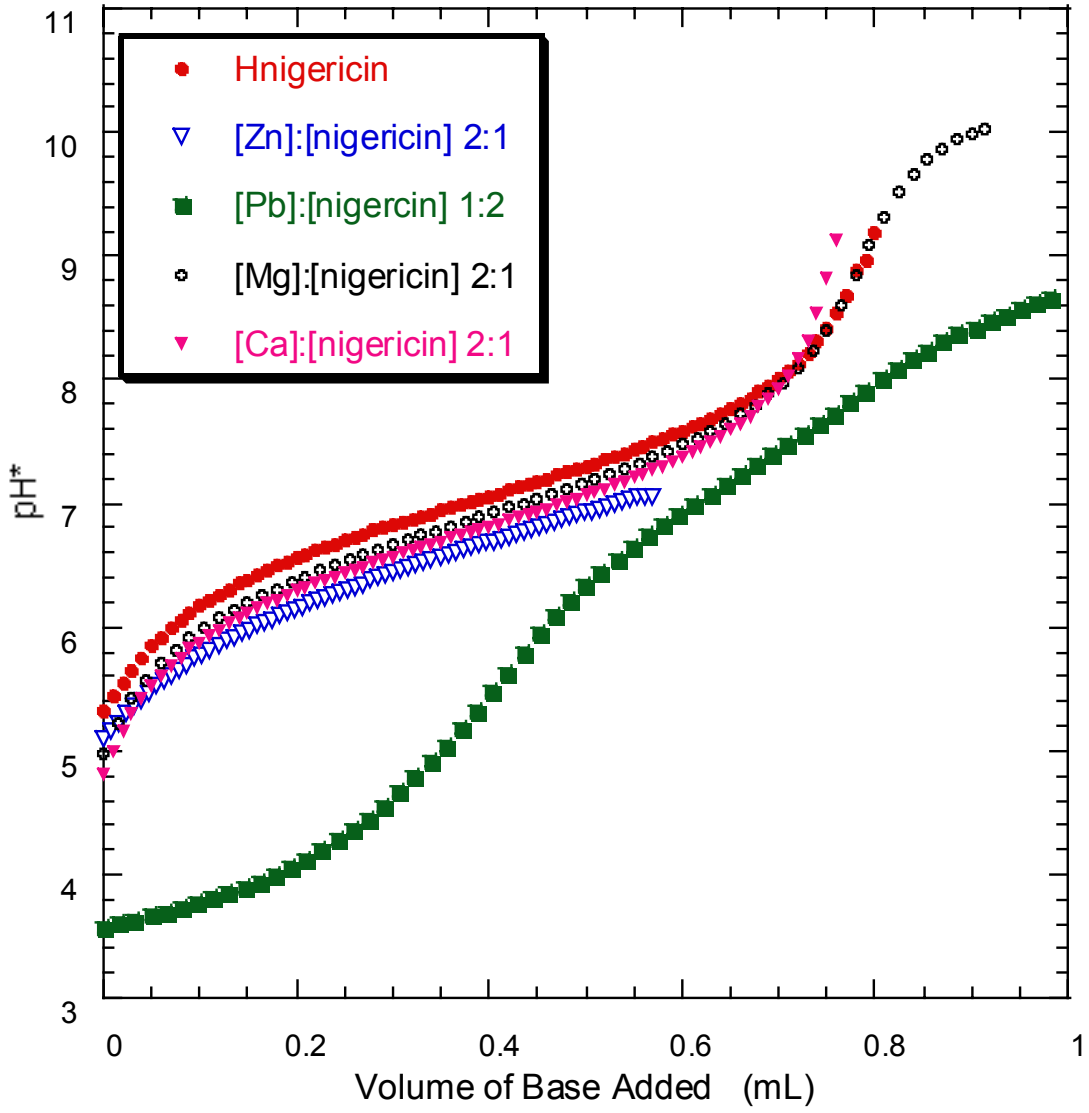


Figure IV.27. Potentiometric titration curves for 6.00 mL of a solution containing 0.7 mM nigericin acid and various metals at the specified stoichiometric ratios and an ionic strength of 0.05 M (25 ^{o}C). The titrant is 0.00778 M Me_4NOH.

Table IV.9. Average values of cumulative equilibrium constants (log β_X) for nigericin with various ions in 80% methanol-water[a]

Ion (M)	Identity of species X [b]				
	ML	ML_2	MLOH[c]	ML_2H	M_2L
H	7.02±0.03	-	-	-	-
Na	2.89±0.07	-	-	-	-
K	3.77±0.21	-	-	13.61±0.12	-
Ca	2.59±0.27	-	-	-	-
Zn	2.99±0.19	-	-4.59±0.18	12.76±0.19	-
Mg	2.46±0.14	-	-8.22±0.19	12.63±0.4	-
Pb	7.57±0.41	11.37±0.65	0.21±0.11	-	13.43±0.13

[a] 25 ^{o}C; ionic strength 0.05 M (TEAP or TEAC). [b] L represents nigericin ligand. [c] β_{MLOH} is expressed as an acid dissociation constant.

IV.F. NMR studies of free nigericin and nigericin complexes.

Peak assignments for sodium nigericin, tetramethylammonium nigericin complexes and nigericin free acid.

NMR is used to identify the ionophore donor atoms involved in metal ion coordination and to gain information about the solution structures for those compounds. The basic principle is that the chemical environment changes for those carbon atoms adjacent to lead-bound oxygen atoms and this results in chemical shift changes between the complexed ionophore and uncomplexed ionophore. Therefore, NMR spectra for complexed ionophores and uncomplexed ionophores (tetraethylammonium salts) in polar (CD_3OD) and nonpolar ($CDCl_3$) solvents were obtained. Carbon chemical shifts were used because peaks in the ^1H NMR spectra overlap too much to assign all H atoms correctly. Although NMR spectra of sodium nigericin and the free acid form of nigericin in several solvents have been reported, new NMR spectra for those compounds were included in this work to minimize errors caused by different instruments and conditions. In the end ^{13}C chemical shifts of the sodium salt, lead complex, and free acid form of nigericin were compared with the nigericin anion (Et_4N^+ salt) to obtain information of the solution structures for the lead complexes.

In Figure IV.28 nigericin is numbered using the scheme proposed by Westley[10]. Proton atoms share the same number with the atom they are attached to while the oxygen atoms have their own numbers.

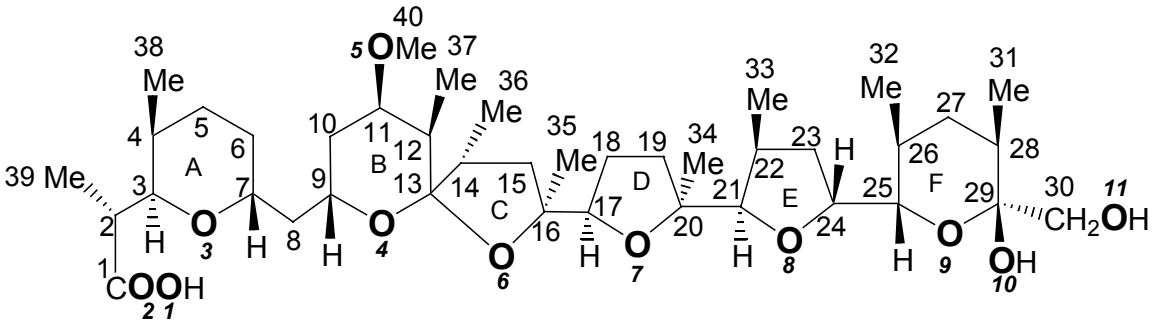


Figure IV.28. Structure of nigericin with numbering schemes for carbon (plain) and oxygen (bold italic) atoms.

^{1}H and ^{13}C spectra were recorded in $CDCl_3$ and CD_3OD for the free acid form, sodium salt, and tetraethyl ammonium salt of nigericin at 25°C (see Figures IV.29 and IV.30). NMR experiments were done in methanol but not in 80% methanol-water because it was shown that NMR spectra obtained in 80% methanol-water resembled those obtained in methanol[9] and it is convenient to compare with the literature values that are available in CD_3OD. Several 2D methods (DEPT, HSQC, HMQC, and HMBC) were used to assign peaks in the NMR spectra because they are more useful than 1D methods in peak assignment. DEPT (Distortionless Enhancement by Polarization Transfer) shows multiplicities of carbon signals very clearly. As shown in Figure IV.31 every peak in the DEPT spectrum is clearly defined. HMQC (Heteronuclear Multiple Quantum Coherence) and HSQC (Heteronuclear Single Quantum Correlation) show only one-bond connections between hydrogen and carbon atoms (see Figure IV.32). HSQC has better resolution than HMQC. HMBC (Heteronuclear Multiple Bond Coherence) shows the correlation between the hydrogen and carbon atoms separated by at least two bonds (see Figure IV.33). Therefore, there can be more correlations for each carbon signal in HMBC spectra than in HMQC and HSQC. In HMBC spectra correlations for tertiary carbon atoms are separated widely from each other. Correlations shown by hydrogen

atoms from CH_3 are extremely strong and possess unique side bands. INADEQUATE is not applied because high solubility is required.

A general procedure is used to assign all the peaks in the ^1H NMR and ^{13}C NMR spectra. First, all peaks in the ^1H NMR (Figure IV.29) and ^{13}C NMR spectra (Figure IV.30) are grouped according to the chemical shift ranges into four categories: the ether or hydroxyl functional group (3.0-5.0 ppm in ^1H NMR and 50-90 ppm in ^{13}C NMR), the carbonyl group (>90 ppm in ^{13}C NMR), the CH_3 group (0-1.0 ppm in ^1H NMR and 0-20 ppm in ^{13}C NMR), and CH and CH_2 unconnected to O (1.0-3.0 ppm in ^1H NMR and 20-50 ppm in ^{13}C NMR). The first peaks identified are C1, C13, C29, and H peak for H40. As shown in Figure IV.30, these first three carbon peaks appear at δ >90 ppm and are far away from other carbon peaks because they are quaternary carbons of the type C=O or O-C-O. C1 is the furthest downfield one. The difference between C13 and C29 is that C13 is coupled to two methyl groups and C29 is coupled to one methyl group. Due to the connection of C40 with O, H40 is the only methyl proton at >3.0 ppm in ^1H NMR with a sharp single peak. The signal for C40 is identified from the correlation with H40 shown by HMQC. Signals for one carbon and several hydrogen atoms (such as C11, H14, H15, H37, H2, H30, H28, H25, H27) can be assigned based on their correlations with C1, C13, C29 and C40 shown in HMBC (see Figure IV.31). From HMQC and HSQC, the corresponding carbon and hydrogen signals are assigned. For example, C13 shows correlations with several hydrogen signals in HMBC. One is in the ether region so it is H11. The assignment of H11 is also confirmed by the correlation with H40 shown in HMBC. Two are in the methyl region so they are H37 and H36 that are assigned after finding the correlation between C11 and H37. C11, C37, and C36 are assigned based on

correlations shown in HMQC or HSQC spectra. For C13, there are two HMBC correlations left in the region for CH or CH_2 unconnected with O. They should be the correlations from H12, H14 and H15. After examination of the correlations shown by H36 and H37 in HMBC spectra, the signal for H14 can be assigned and the other one is H15 because H12 is in a different chemical shift region. Comparison between DEPT spectra and ^{13}C NMR spectra leads to assignment of signals for C16 and C20 that are the remaining quaternary carbons. The correlation with H14 shown in HMBC spectra separates the signal for C16 from the one for C20. Based on all the correlations shown by the known carbon and hydrogen atoms in HMBC and HMQC or HSQC spectra, all carbon peaks and most of H peaks were assigned. When there are two carbon peaks very close to each other, the TRACE function in the NMR software package can obtain the exact frequency of a correlation and then assign the correlation to one of the carbon peaks.

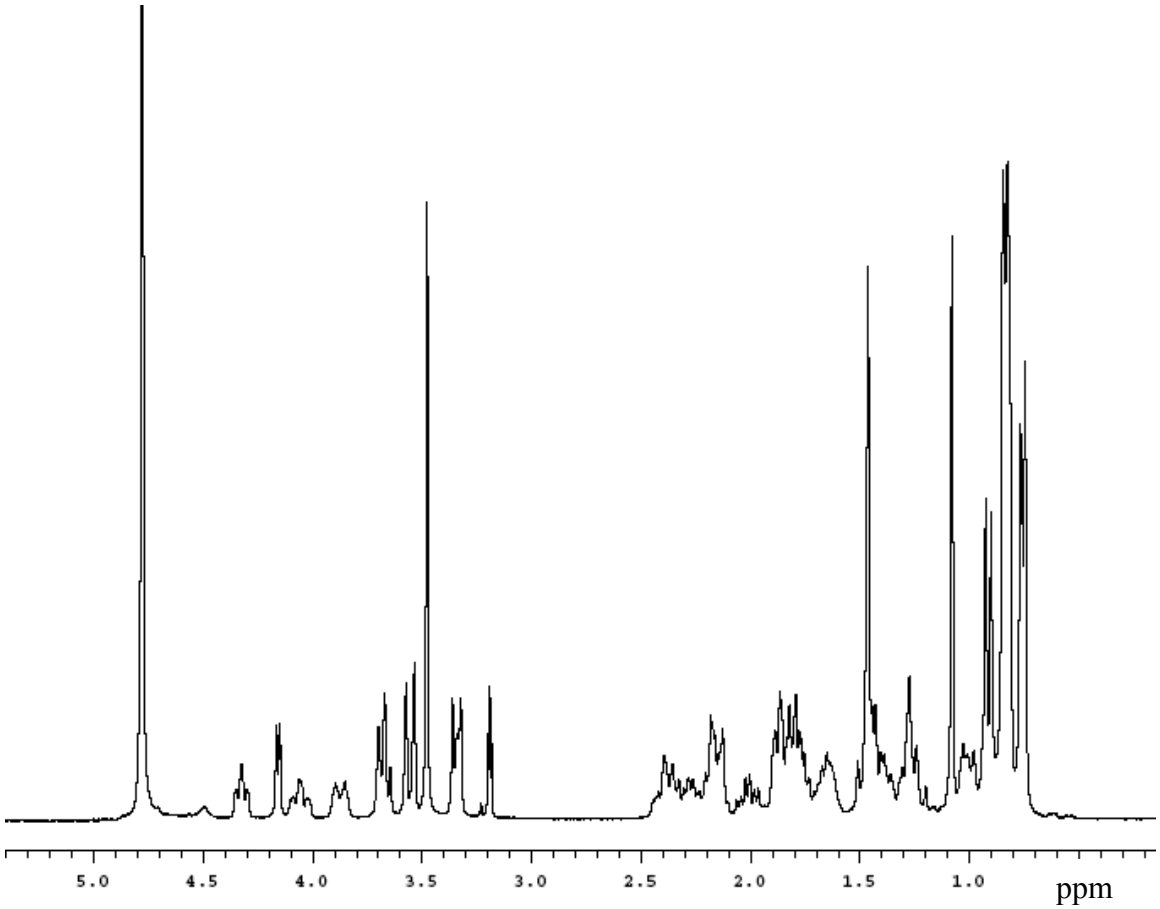


Figure IV.29. ^{1}H NMR spectrum of the sodium-nigericin complex in CD_3OD at 25 ^{o}C.

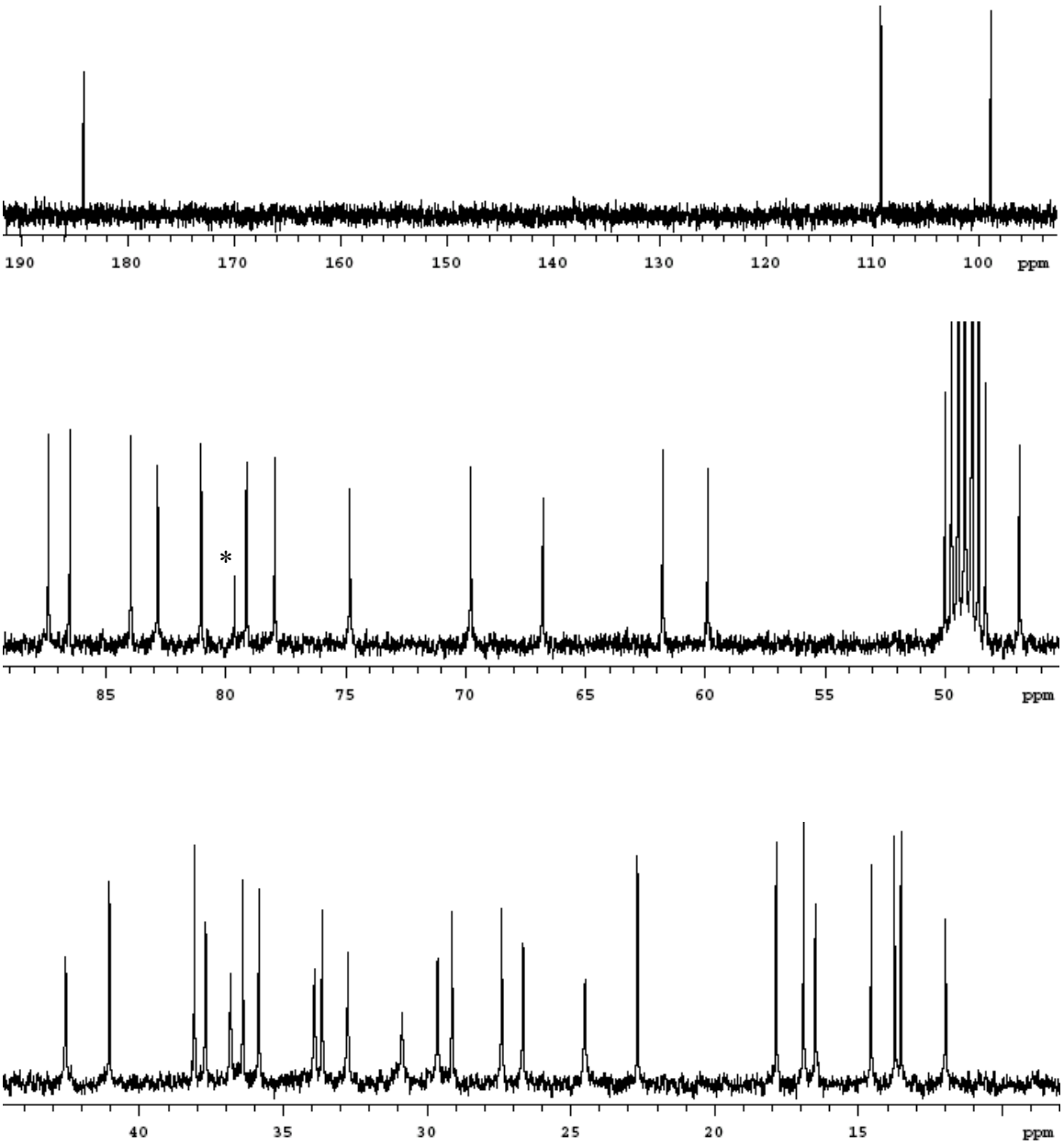


Figure IV.30. ^{13}C NMR spectrum of sodium-nigericin complex in CD_3OD at 25 ^{o}C. The large multiplet at 49 ppm is from CD_3OD. The carbon signal marked by the asterisk mark may result from an unknown impurity.

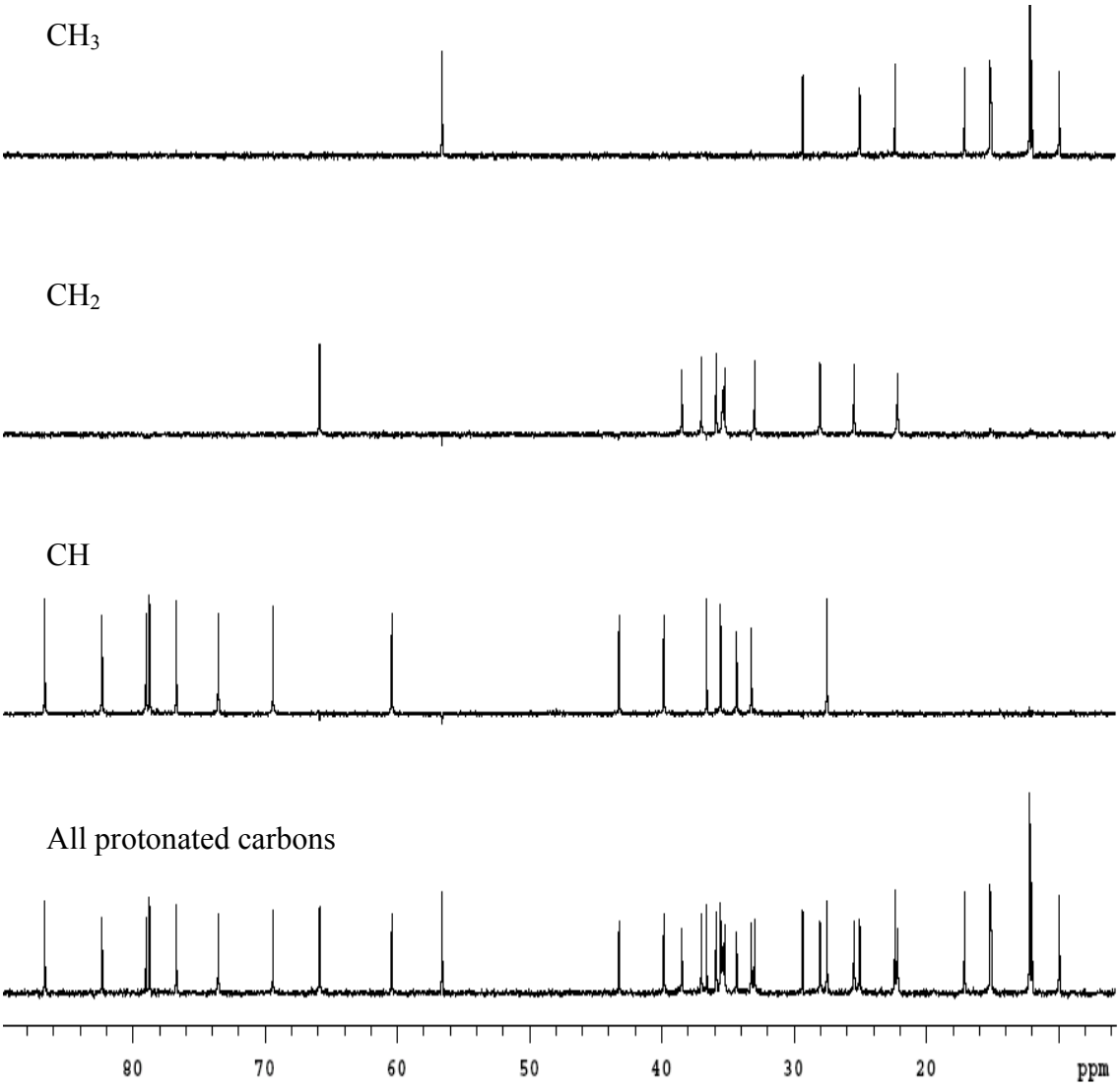


Figure IV.31. DEPT spectrum of the free acid form of nigericin in $CDCl_3$ at 25 ^{o}C. Spectra of carbon atoms with different multiplicities are shown in separate panels.

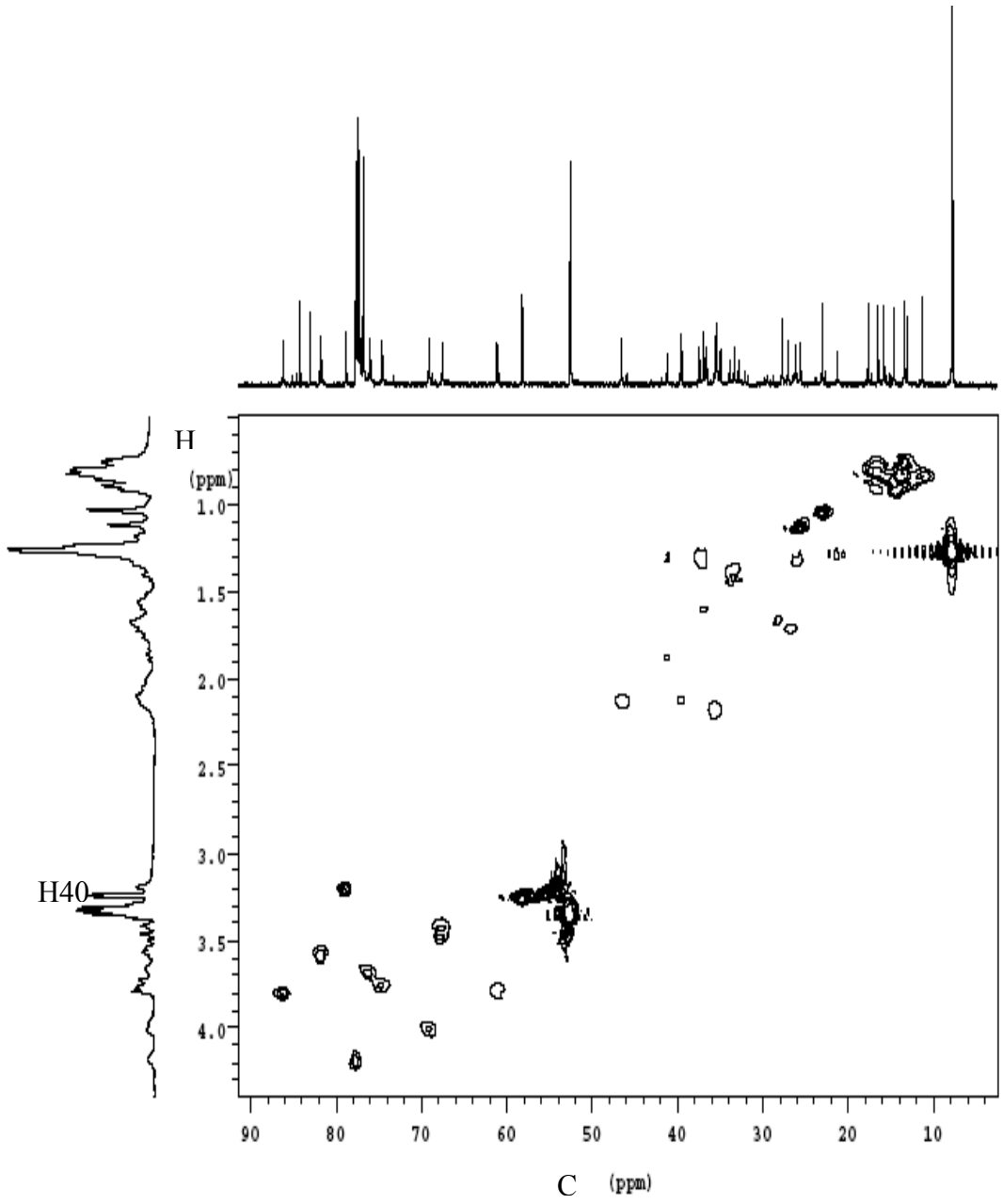


Figure IV.32. HSQC spectrum of the tetraethylammonium salt of nigericin in CD_3OD at 25 ^oC.

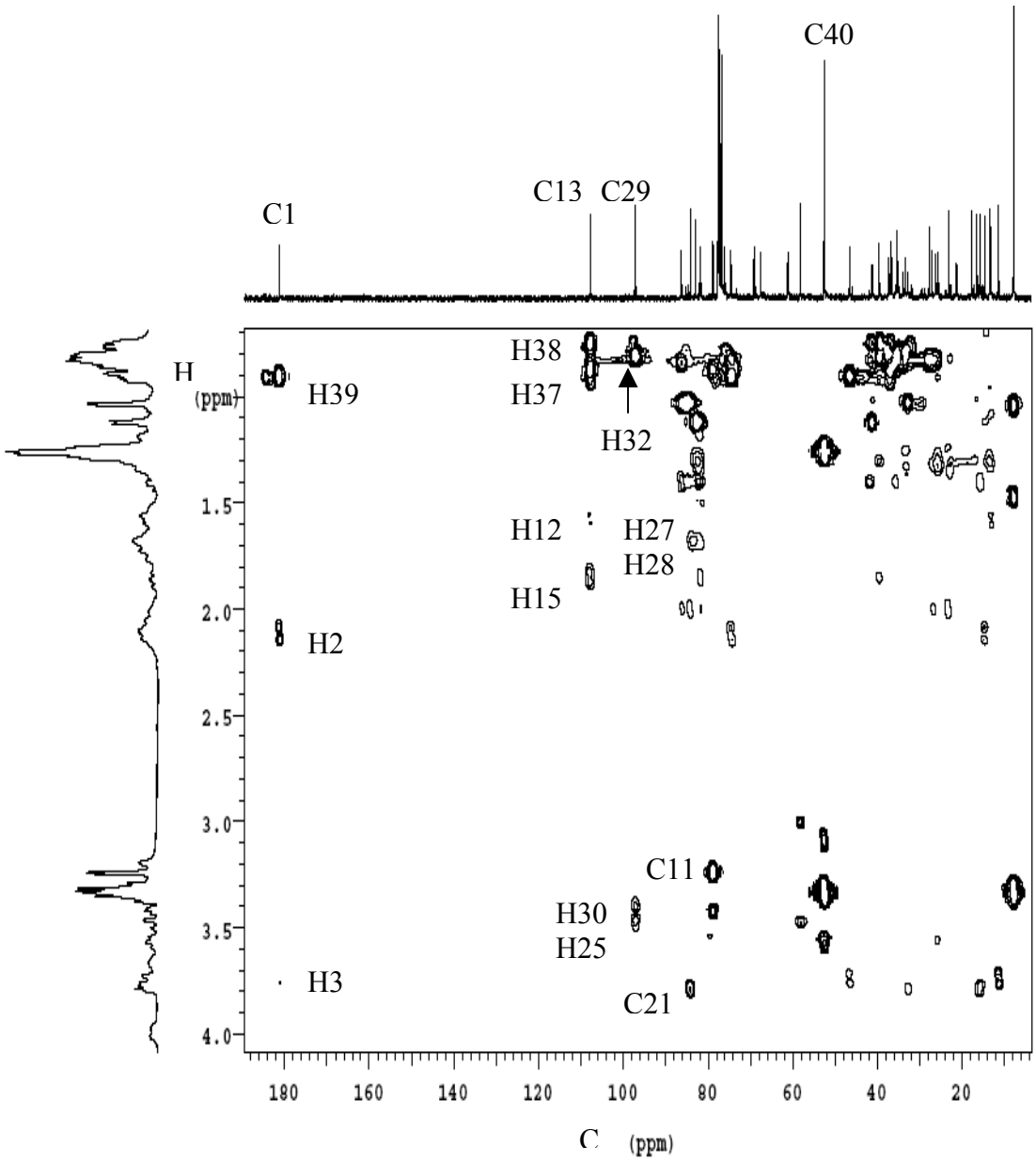


Figure IV.33. HMBC spectrum of the tetraethylammonium salt of nigericin in $CDCl_3$ at 25 ^{o}C.

There is one important phenomenon in peak assignment for these types of natural products. Three bond carbon-proton coupling sometimes shows up in HMBC more intensely than two-bond coupling in this study. That is due to the strained ring systems (five or six-membered heterocycles) present in this type of compound. Whenever there is a W conformation of the bonds between two protons, as shown in Figure IV.34, there is a strong long-range coupling between one proton and the carbon attached to the other proton. Table IV.10 lists carbon atoms where there is substantial difference between three-bond coupling and two-bond coupling.

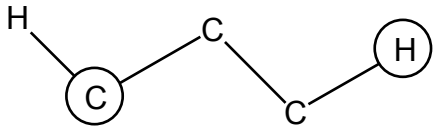


Figure IV.34. Schematic representation of the W type bond conformation.

Table IV.10 The three-bond and two-bond coupling in the HMBC spectrum of the tetraethylammonium salt of nigericin in $CDCl_3$ at 25 ^oC.

carbon #	proton number with three-bond coupling	proton number with two-bond coupling
9	11 (strong)	8 (missing)
11	37, 40 (strong)	10 (weak), 12 (strong)
13	11, 15, 37, 36 (strong)	12 (missing), 14 (strong)
17	15, 19 (strong)	18 (missing)
21	23, 33, 34 (strong)	22 (missing)
25	27, 32 (strong)	26 (weak)
29	25, 27, (strong)	28 (weak), 30 (strong)

Table IV.11-IV.15 lists the experimental chemical shift values for all the carbon and hydrogen atoms of the sodium salt, the free acid form, and tetraethylammonium salt of nigericin in chloroform and methanol. Literature values are available for the sodium salt of nigericin (^{13}C NMR in $CDCl_3$, ^1H NMR in $CDCl_3$ and CD_3OD), and the free acid form of nigericin (^{13}C NMR in $CDCl_3$ and C_6D_6, ^1H NMR in $CDCl_3$, C_6D_6, and CD_3OD) and are

included in Table IV.11. There are minor differences between experimental values with literature values. For the ^{13}C NMR spectra of the sodium salt of nigericin in $CDCl_3$, the assignments of C4 and C35 are reversed compared to those in the literature report. The current experimental values are used because DEPT shows clearly that they are totally different signals (C4 is CH and C35 is CH_3). For the sodium salt of nigericin in CD_3OD, the experimental chemical shifts for H8, H35, and H39 are different than the literature values in methanol but match up with the experimental values in $CDCl_3$ very well. For ^{13}C NMR spectra of the free acid form of nigericin in $CDCl_3$, the experimental values for C24 and C25 switch positions compared with the literature values but match up well with the literature values in C_6D_6. The same behavior was observed for C16 and C17. The experimental values for H36, H26, and H22 of the free acid form of nigericin in methanol are different from the literature values but match up with experimental values in $CDCl_3$. So H22 is the only one in question: however, examination of all the spectra provides evidence indicating the experimental value for H22 is correct.

Table IV.11. ^{1}H and ^{13}C NMR chemical shifts of the sodium salt of nigericin at 25 ^{o}C.

carbon #	carbon connectivity	^{13}C $CDCl_3$ experimental	^{13}C $CDCl_3$ literature[11]	^{1}H $CDCl_3$ experimental	^{1}H $CDCl_3$ literature[12]	^{1}H C_6D_6 literature[12]
1	C=O	184.05	183.9			
2	CH	46.010	45.9	2.33	2.36	2.683
3	CHO	73.311	73.2	3.65	3.675	3.928
4	CH	27.858	29.0	1.72	1.74	1.62
5	CH_2	26.471	26.4	1.40	--	--
6	CH_2	23.707	23.4	1.04,1.97	1.46,1.99	1.97
7	CHO	68.544	68.4	4.04	4.048	4.058
8	CH_2	35.960	35.8	0.87,2.55	0.89,2.588	0.93,2.752
9	CHO	60.537	60.4	4.26	4.283	4.574
10	CH_2	32.244	32.3	0.99,2.30	1.03,2.33	0.8,2.30
11	CHO	79.616	79.5	3.33	3.367	3.065
12	CH	36.896	36.6[a]	1.75	1.78	1.55
13	CO	107.67	107.7			
14	CH	39.746	39.6	2.17	2.18	2.00
15	CH_2	41.874	41.7	1.60,1.77	--	--
16	CO	82.480	82.4[b]			
17	CHO	81.599	81.5	3.60	3.64	3.367
18	CH_2	26.090	25.9	1.78,1.97	1.8	1.70
19	CH_2	29.696	29.6	1.35,2.14	--	1.1,2.41
20	CO	84.924	84.8[b]			
21	CHO	85.354	85.3	4.32	4.345	4.468
22	CH	35.289	35.2	2.24	2.27	1.97
23	CH_2	32.450	32.1	1.40,2.30	1.40,2.37	1.17,2.35
24	CHO	76.992	76.5	4.33	4.358	4.263
25	CHO	76.581	76.9	3.68	3.69	3.889
26	CH	31.984	31.9	1.30	1.32	1.2
27	CH_2	37.347	37.2	1.24,1.32	--	--
28	CH	36.671	36.8[a]	1.49	1.48	1.52
29	CO	97.312	97.2			
30	CH_2OH	67.207	67.2	3.27,3.92	3.30,3.936	3.70,4.279
31	CH_3	16.611	16.4[c]	0.84	0.87	1.163
32	CH_3	17.157	17.0	0.78	0.815	0.696
33	CH_3	16.375	16.2[c]	0.84	0.88	0.655
34	CH_3-CO	23.000	22.8	1.10	1.144	0.903
35	CH_3-CO	29.205	27.7	1.55	1.591	1.798
36	CH_3	13.571	13.4	0.87	0.916	0.948
37	CH_3	13.241	13.0	0.97	1.019	0.95
38	CH_3	11.723	11.6	0.91	0.945	0.970
39	CH_3	14.618	14.4[c]	0.93	0.957	1.153
40	CH_3	59.711	59.5	3.62	3.638	3.724

[a-c] may be interchanged. [d] Literature values for some of hydrogen atoms were not provided by authors, indicated by "--".

Table IV.12. ^{1}H and ^{13}C NMR chemical shifts (ppm) of the sodium salt of nigericin in CD_3OD at 25 ^{o}C.

carbon #	carbon connectivity	^{13}C experimental	^{1}H experimental	^{1}H literature[13]
1	C=O	184.02		
2	CH	46.752	2.14	2.36
3	CHO	74.679	3.56	3.80
4	CH	28.990	1.62	1.81
5	CH_2	27.262	1.38,1.84	--
6	CH_2	24.358	1.01,1.88	--
7	CHO	69.631	3.88	4.12
8	CH_2	36.697	0.90,2.40	1.59,1.93
9	CHO	61.634	4.06	3.97
10	CH_2	33.767	1.44,2.36	2.0
11	CHO	80.893	3.34	3.38
12	CH	36.266	1.66	1.76
13	CO	109.08		
14	CH	40.903	2.18	2.32
15	CH_2	42.420	1.45, 1.83	--
16	CO	83.822		
17	CHO	82.701	3.65	3.87
18	CH_2	26.516	1.80	1.63,1.80
19	CH_2	30.768	1.44,2.01	--
20	CO	86.361		
21	CHO	87.262	4.18	3.84
22	CH	35.705	2.28	2.33
23	CH_2	32.615	2.12,2.18	2.27
24	CHO	79.000	4.33	4.21
25	CHO	77.818	3.68	3.54
26	CH	33.507	1.26	1.45
27	CH_2	37.553	1.26	
28	CH	37.943	1.78	1.86
29	CO	98.785		
30	CH_2OH	66.621	3.34,3.54	3.33,3.49
31	CH_3	16.772	0.83	0.88
32	CH_3	17.718	0.75	0.94
33	CH_3	16.356	0.83	0.88
34	CH_3-CO	22.535	1.07	1.17
35	CH_3-CO	29.496	1.46	1.19
36	CH_3	13.607	0.82	1.01
37	CH_3	13.377	0.91	0.98
38	CH_3	11.834	0.84	0.96
39	CH_3	14.413	0.84	1.05
40	CH_3	59.761	3.48	3.33

[a] Literature values for some of hydrogen atoms were not provided by authors, indicated by "--".

Table IV.13. ^{1}H and ^{13}C NMR chemical shifts (ppm) of the free acid form of nigericin in $CDCl_3$ at 25 ^{o}C.

carbon #	carbon connectivity	^{13}C experimental	^{13}C literature[14]	^{1}H experimental	^{1}H literature[13]
1	C=O	177.45	177.5		
2	CH	44.203	44.2	2.30	2.32
3	CHO	72.866	72.9	3.75	3.78
4	CH	27.442	28.9	1.78	1.75
5	CH_2	26.030	26.1	1.46,1.78	--
6	CH_2	23.381	23.4	1.1,1.98	1.97,2.07
7	CHO	68.995	69.0	4.05	4.07
8	CH_2	35.314	35.8	0.6,2.49	0.90,2.51
9	CHO	60.232	60.4	4.12	4.16
10	CH_2	31.699	32.6	0.8,1.38	0.98,2.20
11	CHO	77.973	79.3	3.34	3.35
12	CH	35.715	36.9	1.65	1.73
13	CO	108.18	108.2		
14	CH	38.930	39.0	2.04	2.07
15	CH_2	42.505	42.5	1.58,1.73	--
16	CO	81.474	82.4		
17	CHO	82.385	81.5	3.49	3.52
18	CH_2	25.700	25.7	1.64,1.92	1.65,1.78
19	CH_2	30.612	30.7	1.34	--
20	CO	83.437	83.4		
21	CHO	85.780	85.3	4.0	4.02
22	CH	35.109	35.4	2.23	2.23
23	CH_2	32.215	32.2	2.22	1.42,2.30
24	CHO	77.172	74.5	4.36	4.37
25	CHO	74.383	78.0	3.95	3.98
26	CH	32.515	31.8	1.27	1.32
27	CH_2	37.362	37.4	1.38	
28	CH	37.112	37.2	1.74	1.67
29	CO	96.992	97.0		
30	CH_2OH	68.259	68.3	3.45	3.48,3.52
31	CH_3	16.301	16.4	0.91	0.88
32	CH_3	17.312	17.3	0.83	0.68
33	CH_3	15.605	16.3	0.87	0.88
34	CH_3-CO	22.655	22.7	1.1	1.12
35	CH_3-CO	27.938	27.5	1.39	1.42
36	CH_3	13.096	13.2	0.86	0.94
37	CH_3	13.246	13.1	0.90	1.02
38	CH_3	10.792	10.8	0.905	0.93
39	CH_3	13.041	15.6	1.15	1.05
40	CH_3	57.383	57.4	3.33	3.35

[a] Literature values for some of hydrogen atoms were not provided by authors, indicated by "--".

Table IV.14. ^{1}H and ^{13}C NMR chemical shifts (ppm) of the free acid form of nigericin in CD_3OD and C_6D_6 at 25 ^{o}C.

carbon #	carbon connectivity	^{13}C CD_3OD experimental	^{1}H CD_3OD experimental	^{1}H CD_3OD literature[13]	^{1}H C_6D_6 literature[15]	^{13}C C_6D_6 literature[15]
1	C=O	179.46				177.1
2	CH	44.716	2.26	2.36	2.57	44.5
3	CHO	75.032	3.72	3.80	3.97	73.4
4	CH	29.011	1.72	1.81	1.48	28.4
5	CH_2	29.518	1.45	--	1.35,1.8	26.4
6	CH_2	23.665	1.2, 1.84	~1.95	0.98,1.98	23.9
7	CHO	70.892	4.02	4.12	4.07	68.9
8	CH_2	37.371	1.33, 2.20	1.59,1.93	1.02,2.74	36.1
9	CHO	61.906	3.88	3.97	4.52	60.9
10	CH_2	36.749	1.5	2.0,~1.20	0.85,2.26	32
11	CHO	80.229	3.28	3.38	3.13	77.5
12	CH	37.027	1.8	1.76	1.67	37.6
13	CO	109.08				108.7
14	CH	41.335	2.24	2.32	2.12	39.5
15	CH_2	39.962	2.02	--	1.77,1.86	43.0
16	CO	85.812				82.0
17	CHO	83.820	3.76	3.87	3.54	82.9
18	CH_2	26.954	1.4, 1.85	~1.63,1.80	1.59,2.0	26.3
19	CH_2	34.475	1.10	--	1.31,2.41	31.3
20	CO	85.502				83.8
21	CHO	88.135	3.74	3.84	4.22	86.3
22	CH	35.818	1.80	~2.33	2.02	35.5
23	CH_2	36.894	1.82, 2.1	2.27	1.28,2.38	32.6
24	CHO	80.496	4.10	4.21	4.40	78.3
25	CHO	78.184	3.42	3.54	4.36	74.8
26	CH	34.719	1.78	1.45	1.28	33.0
27	CH_2	38.504	1.24, 1.32	--	1.72,1.0	38.3
28	CH	38.096	1.64	1.86	1.84	37.3
29	CO	98.842				97.9
30	CH_2OH	67.370	3.28, 3.38	3.33,3.49	3.98,4.04	69.5
31	CH_3	16.663	0.78	0.88	1.37	16.8
32	CH_3	18.590	0.84	0.94	0.7	17.2
33	CH_3	16.602	0.91	0.88	0.81	15.7
34	CH_3-CO	23.871	1.11	1.17	1.07	22.9
35	CH_3-CO	26.534	1.06	1.19	1.86	27.9
36	CH_3	13.668	0.77	1.01	1.08	13.3
37	CH_3	13.496	0.88	0.98	1.10	13.4
38	CH_3	11.447	0.85	0.96	0.83	10.9
39	CH_3	13.668	0.95	1.05	1.04	13.1
40	CH_3	58.113	3.22	3.33	3.56	57.6

[a] Literature values for some of hydrogen atoms were not provided by authors, indicated by "--".

Table IV.15. ^{1}H and ^{13}C NMR chemical shifts (ppm) of the tetraethylammonium salt of nigericin in CD_3OD and $CDCl_3$ at 25 ^{o}C.

carbon #	carbon connectivity	^{13}C $CDCl_3$ experimental	^{1}H $CDCl_3$ experimental	^{13}C CD_3OD experimental	^{1}H CD_3OD experimental
1	C=O	181.32		184.32	
2	CH	46.561	2.13	47.239	2.20
3	CHO	74.560	3.76	75.591	3.75
4	CH	27.719	1.67	29.046	1.70
5	CH_2	26.111	1.32	29.317	1.40
6	CH_2	21.265	1.28	22.722	1.16, 1.31
7	CHO	69.107	4.0	70.569	4.10
8	CH_2	36.576	2.05	37.719	2.04
9	CHO	61.145	3.80	62.211	3.81
10	CH_2	33.873	1.40,2.12	36.858	1.26, 1.84
11	CHO	78.839	3.21	80.479	3.33
12	CH	35.462	1.56	37.023	2.26
13	CO	107.83		109.14	
14	CH	39.506	2.12	41.300	2.32
15	CH_2	41.202	1.30, 1.88	40.388	1.28, 2.04
16	CO	83.003		85.546	
17	CHO	81.729	3.58	83.824	3.79
18	CH_2	27.039	1.71	27.063	1.76
19	CH_2	32.805	1.43, 2.02	35.650	1.50
20	CO	84.211		85.636	
21	CHO	86.220	3.82	88.050	3.79
22	CH	35.362	2.19	35.721	1.69
23	CH_2	34.961	1.2, 1.71	36.648	1.56
24	CHO	77.430	4.20	80.479	4.16
25	CHO	75.982	3.68	78.170	3.49
26	CH	33.319	1.44?	34.735	1.38
27	CH_2	37.424	1.33	38.486	1.29, 1.40
28	CH	36.890	1.6	38.100	1.83
29	CO	97.073		98.876	
30	CH_2OH	67.545	3.43, 3.49	67.364	3.33, 3.44
31	CH_3	16.493	0.80	16.593	0.83
32	CH_3	17.648	0.80	18.531	0.83
33	CH_3	15.786	0.85	16.668	0.95
34	CH_3-CO	23.041	1.04	23.784	1.13
35	CH_3-CO	25.604	1.14	26.227	1.08
36	CH_3	13.376	0.77	13.563	0.89
37	CH_3	13.102	0.85	13.668	0.89
38	CH_3	11.307	0.84	11.585	0.81
39	CH_3	14.638	0.92	14.369	0.92
40	CH_3	58.168	3.25	58.130	3.28
1’	CH_3 (Et_4N^+)	7.776	1.34	7.714	1.24
2’	CH_2 (Et_4N^+)	52.515	3.33	53.328	3.23

NMR peak assignments in nigericin-lead complexes

The lead-nigericin complex (1:2) (Ni_2Pb) used in NMR measurements was prepared by the reaction of lead oxide and the free acid form of nigericin in methanol. The composition of the complex was determined using AA and commercial elementary analysis. The lead-nigericin complex was dissolved (5 mg Ni_2Pb) in 0.5 mL CD_3OD followed by centrifugation or 10 mg Ni_2Pb in 0.5 mL distilled $CDCl_3$. The spectra (^1H NMR, ^{13}C NMR, HMBC, and HSQC) of the lead-nigericin complex in both solvents were obtained at 25 ^oC. As shown in Figures IV.35, IV.36, IV.39, and IV.40, ^1H and ^{13}C NMR peaks of the lead-nigericin complex obtained in $CDCl_3$ are less well resolved than those obtained in CD_3OD although the lead-nigericin complex has higher solubility in $CDCl_3$. Both H and C signals for the lead-nigericin complex in two solvents are broader than those for the free acid form and other salts of nigericin. This phenomena was also observed in NMR studies of the lead-monensin complex, where one set of broad signals was seen at 25 ^oC and two sets of sharper peaks were obtained at –40 ^oC[9]. The broader signals can be explained as the average value for two sets of signals produced by two different nigericin ligands, as found in NMR studies of monensin-calcium and lasalocid-calcium systems[16]. On the other hand the two nigericin ligands are identical. Due to the limited solubility of the lead-nigericin complex, no acceptable DEPT spectrum was obtained.

Part of the HSQC spectrum (10-30 ppm) shown in Figure IV. 38 were not resolved well for the lead-nigericin complex in $CDCl_3$, while the HSQC spectrum in CD_3OD shown in Figure IV.41 provided excellent data. Therefore, the HMBC spectrum shown in Figure IV.37 is used to identify chemical shifts of hydrogen atoms attached to

those carbons in the upfield region of the HSQC spectrum obtained in $CDCl_3$. The same strategy for peak assignment is almost the same as the one applied to the free acid form and other salts of nigericin. All peaks in ^{1}H NMR and ^{13}C NMR were not only grouped based on adjacent functional groups, but also were compared to their counterparts for the free acid form, sodium salt, and tetraethylammonium salt of nigericin. Carbon atoms in the lead-nigericin complex should have chemical shifts close to those in other salts or free acid form of nigericin because it was found that chemical shifts of carbon atoms in monensin changed 0-4 ppm upon lead complexation [9]. But some chemical shifts for several hydrogen atoms are still hard to determine, such as H4, H5, and H6. Figures IV.35-IV.42 list all spectra for the lead-nigericin complexes in $CDCl_3$ and CD_3OD. ^{1}H and ^{13}C chemical shifts are listed in Table IV.16.

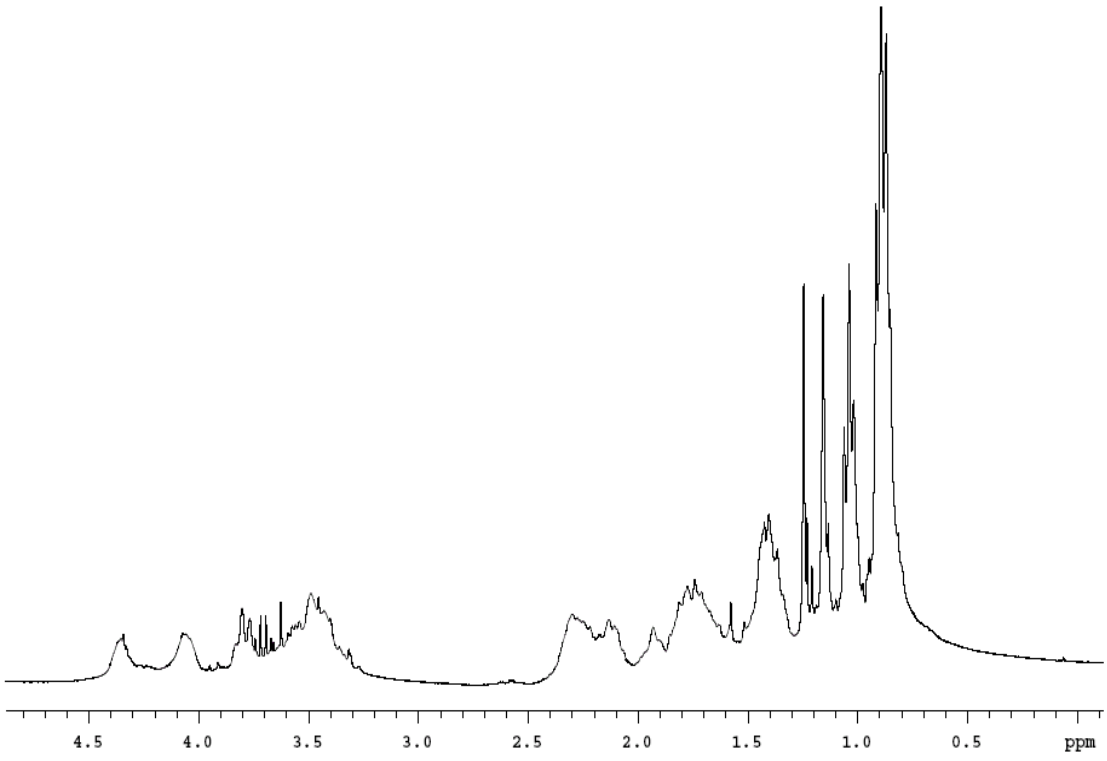


Figure IV.35. ^{1}H NMR spectrum of the lead-nigericin (1:2) complex in $CDCl_3$ at 25 ^{o}C.

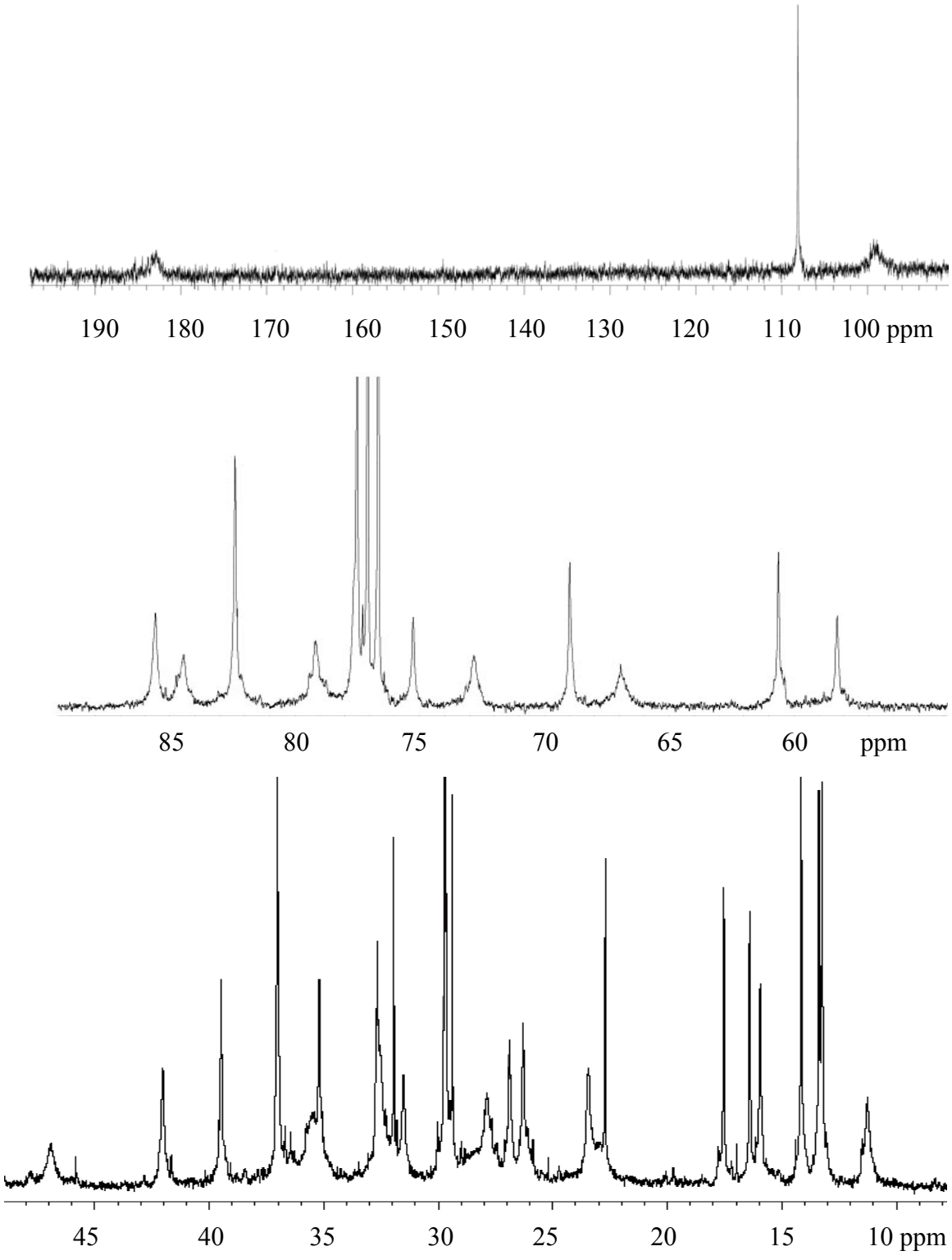


Figure IV.36. ^{13}C NMR spectrum of the lead-nigericin (1:2) complex in $CDCl_3$ at 25 ^{o}C.

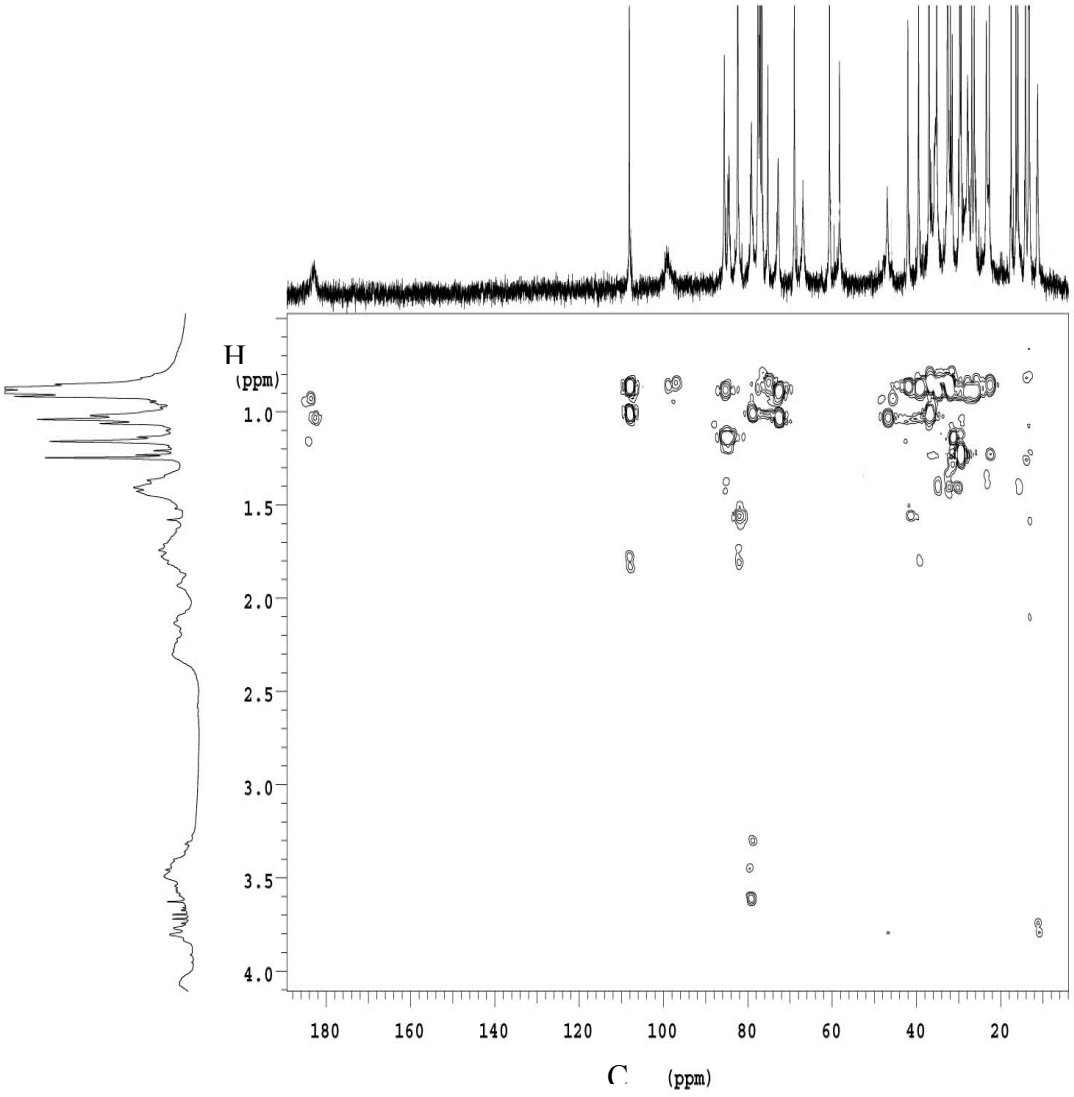


Figure IV.37. HMBC spectrum of the lead-nigericin (1:2) complex in $CDCl_3$ at 25 ºC.

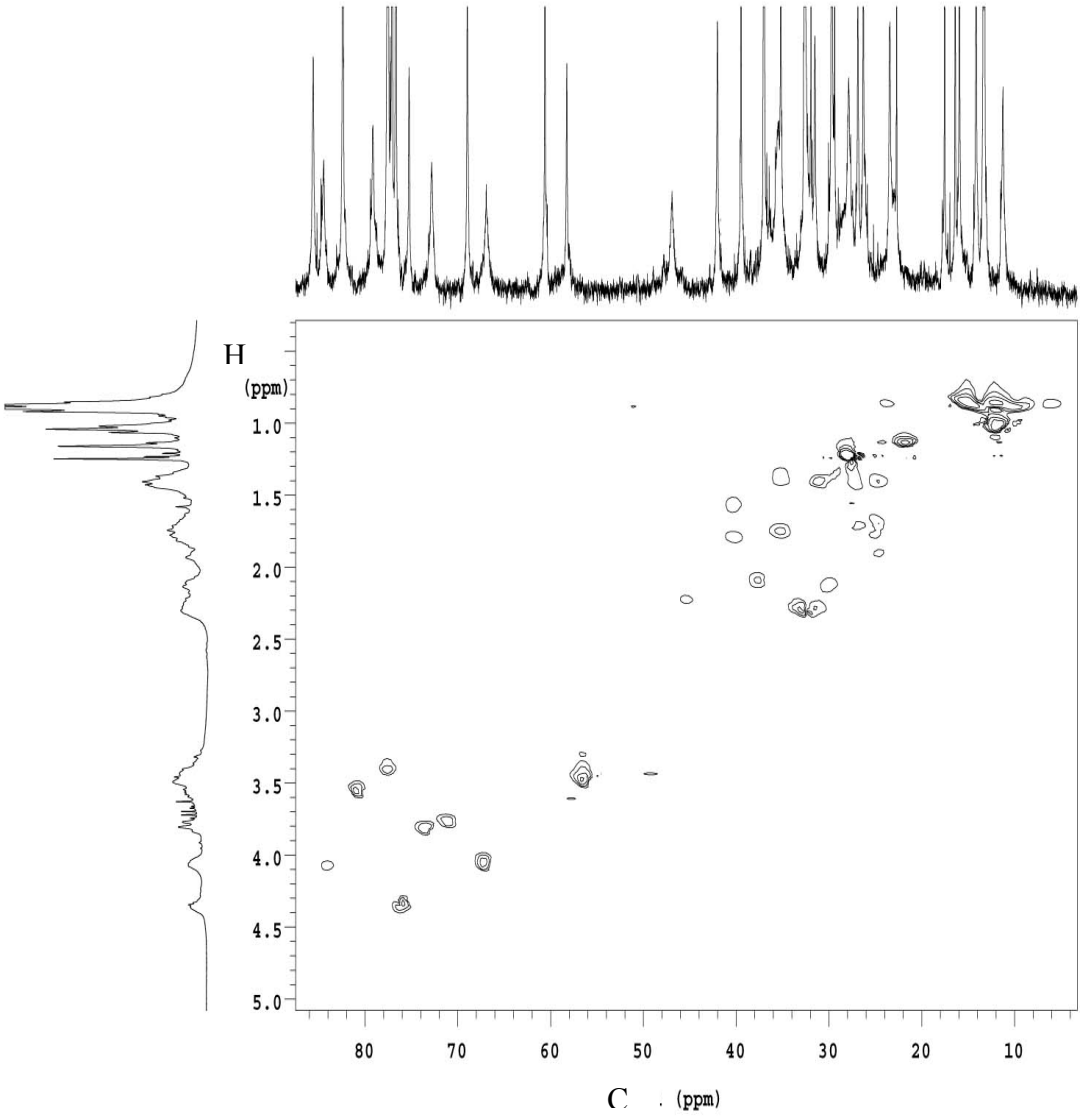


Figure IV.38. HSQC spectrum of the lead-nigericin (1:2) complex in $CDCl_3$ at 25 ^oC

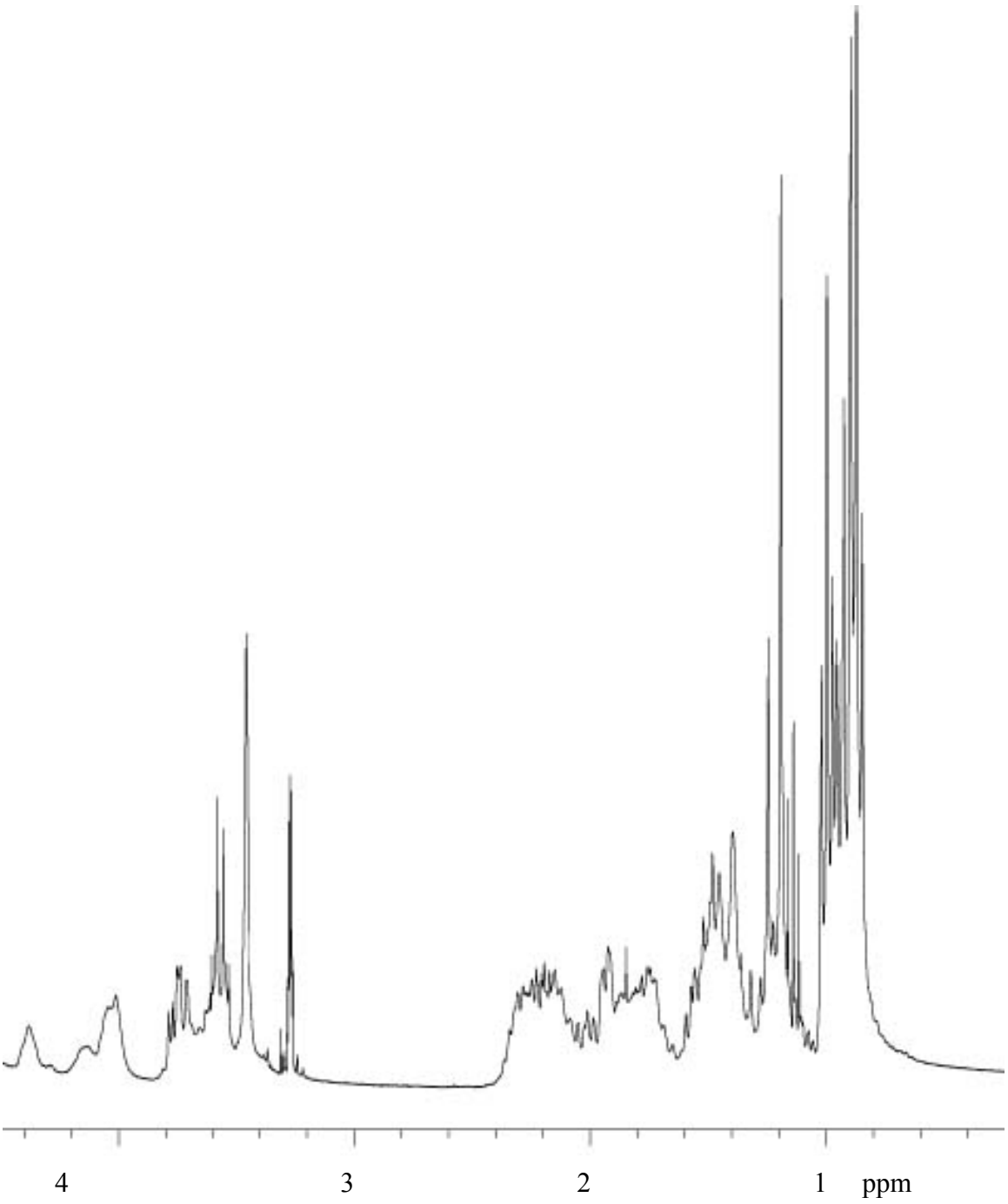


Figure IV.39. ^{1}H NMR spectrum of the lead-nigericin (1:2) complex in CD_3OD at 25 ^{o}C.

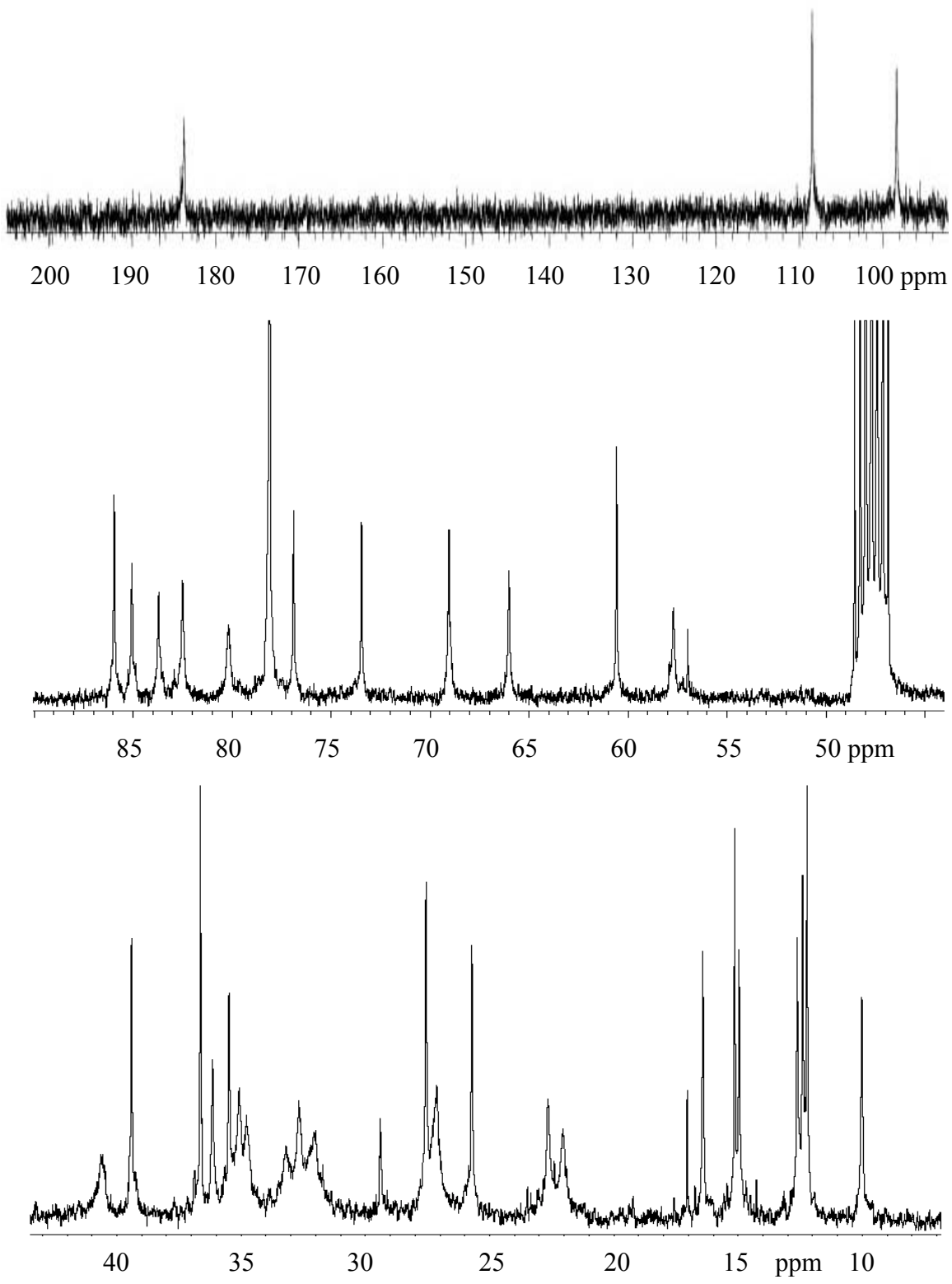


Figure IV.40. ^{13}C NMR spectrum of the lead-nigericin (1:2) complex in CD_3OD at 25 ^{o}C.

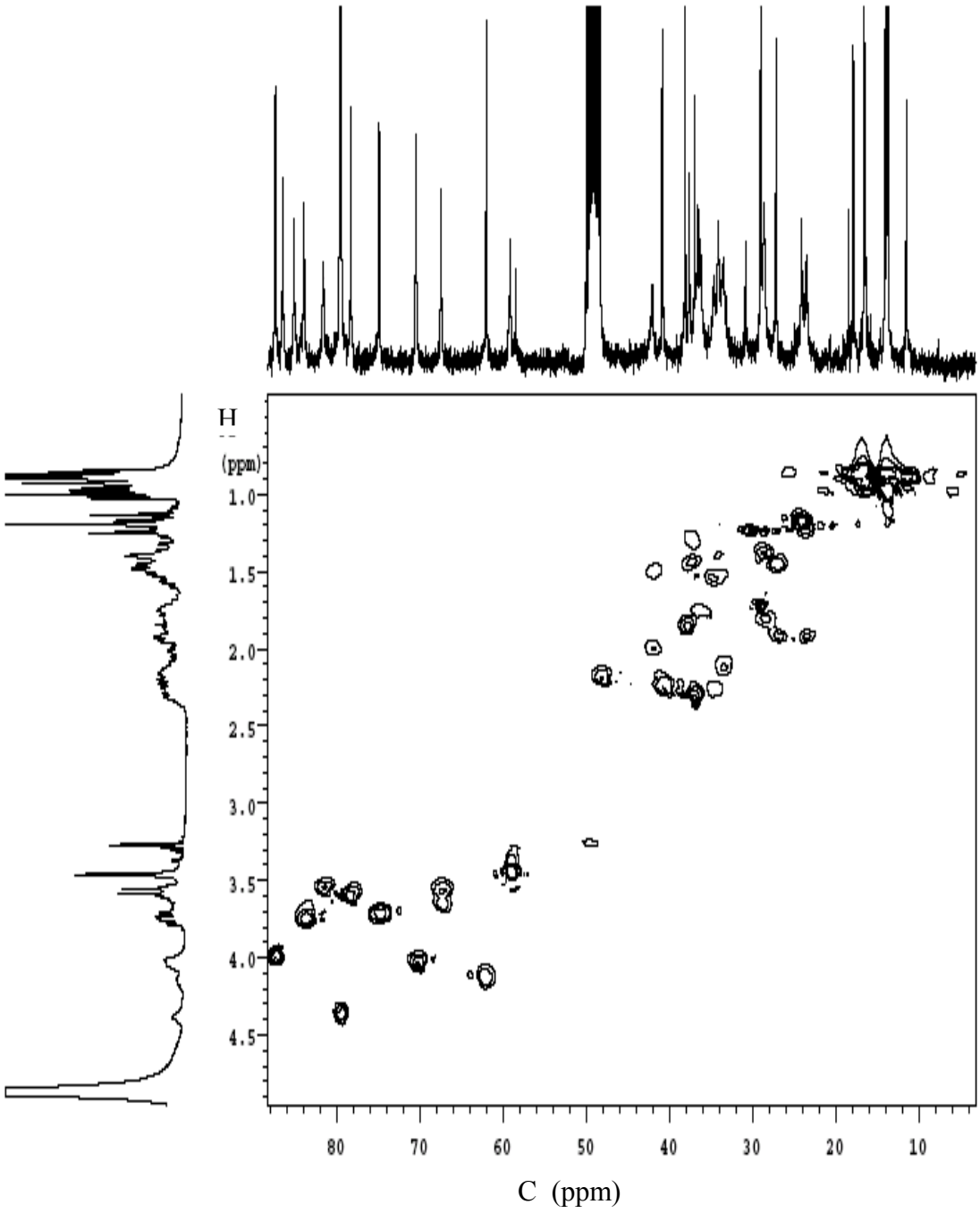


Figure IV.41. HSQC spectrum of the lead-nigericin (1:2) complex in CD_3OD at 25 ^oC.

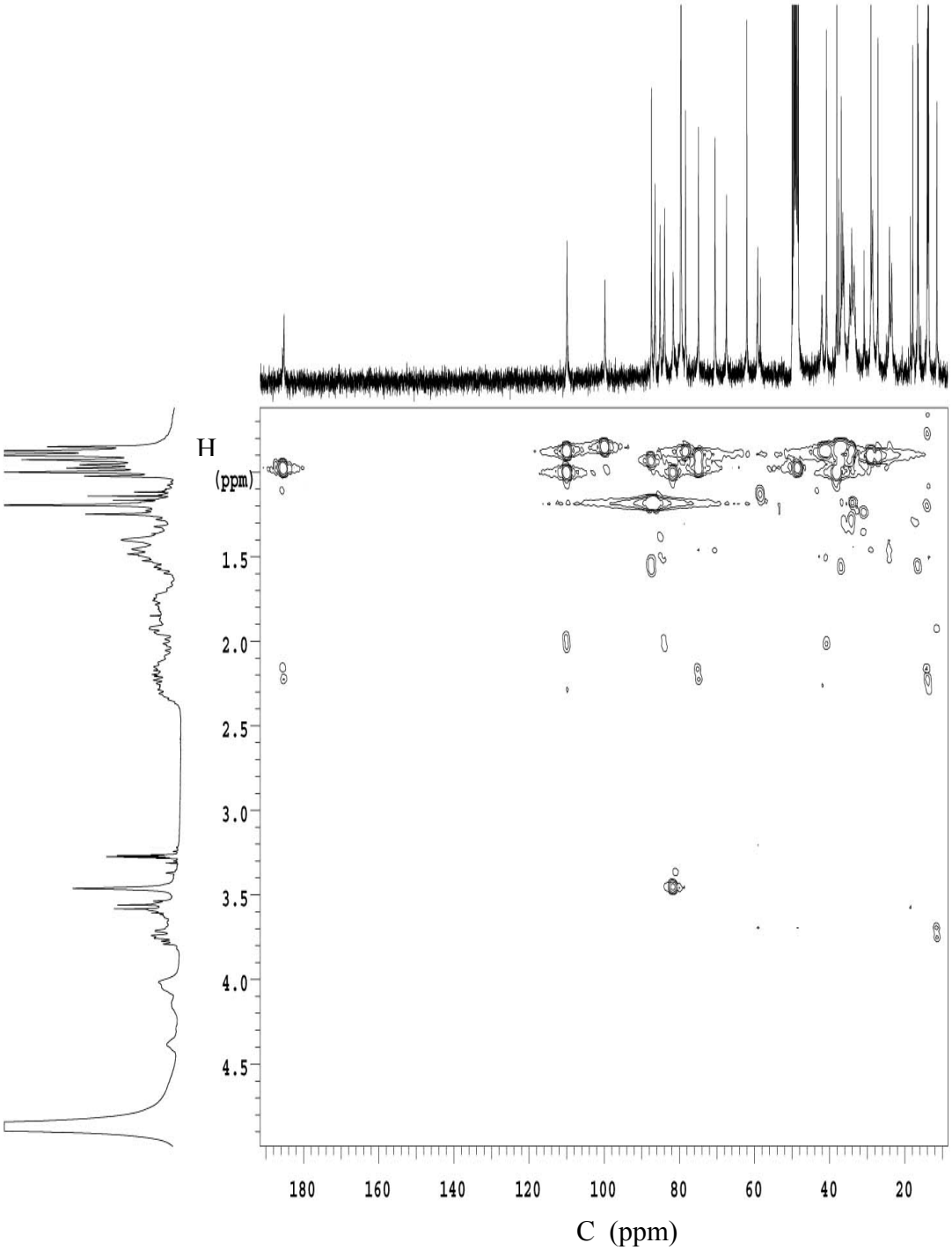


Figure IV.42. HMBC spectrum of the lead-nigericin (1:2) complex in CD_3OD at 25 ^oC.

Table IV.16. ^{1}H and ^{13}C NMR chemical shifts (ppm) of nigericin-lead (2:1) complexes in CD_3OD and $CDCl_3$ at 25 ^{o}C using a Varian 300 MHz spectrometer.

carbon #	carbon connectivity	^{13}C $CDCl_3$ experimental	^{1}H $CDCl_3$ experimental	^{13}C CD_3OD experimental	^{1}H CD_3OD experimental
1	C=O	183.75		185.22	
2	CH	46.832	2.22	48.200	2.2
3	CHO	72.742	3.78	74.913	3.71
4	CH	27.796		29.020	1.39
5	CH_2	26.809		27.171	1.44, 1.92
6	CH_2	23.351		23.494	1.92
7	CHO	68.897	4.05	70.495	4.03
8	CH_2	35.500	2.25	38.097	2.29
9	CHO	60.541	4.25	62.032	4.15
10	CH_2	31.441	2.12	33.465	2.12
11	CHO	79.076	3.42	81.648	3.54
12	CH	36.947	1.78	38.097	1.87
13	CO	108.04		109.94	
14	CH	39.396	2.08	40.867	2.26
15	CH_2	41.946	1.58, 1.80	42.028	1.50, 2.0
16	CO	82.313		85.158	
17	CHO	82.313	3.54	83.957	3.74
18	CH_2	26.208	1.70, 1.78	28.586	1.80
19	CH_2	29.632	1.24	30.849	1.23
20	CO	84.369		86.513	
21	CHO	85.510	4.07	87.408	4.0
22	CH	35.112	2.25	36.943	2.32
23	CH_2	32.490	2.25	34.667	1.54, 2.26
24	CHO	77.200	4.36	79.558	4.37
25	CHO	75.178	3.82	78.344	3.61
26	CH	32.582	1.40	36.235	1.78?
27	CH_2	36.947	1.40	37.610	1.21, 1.44
28	CH	35.112	1.80	36.535	1.78
29	CO	99.219		99.802	
30	CH_2OH	66.863	3.58	67.458	3.58, 3.65
31	CH_3	16.323	0.88	16.592	0.85
32	CH_3	17.451	0.88	17.874	0.88
33	CH_3	15.863	0.92	16.412	0.93
34	CH_3-CO	22.624	1.17	24.101	1.17
35	CH_3-CO	29.298	1.30	29.020	1.72
36	CH_3	14.067	0.90	14.076	0.87
37	CH_3	13.306	1.04	13.682	1.0
38	CH_3	11.164	0.94	11.473	0.91
39	CH_3	13.159	1.07	13.856	0.97
40	CH_3	58.172	3.46	59.168	3.45

Analysis of NMR data in $CDCl_3$

There is only one set of NMR signals present at room temperature for ^{1}H and ^{13}C resonances. No coupling constants could be obtained at room temperature. This might be caused by the rapid exchange of the two nigericin ligands at room temperature. The two ligands might be bound in an identical fashion. Low temperature can decrease the exchange rate so that two sets of NMR signals might be obtained, which has shown in monensin-lead NMR studies at $-40^{o}C$[9]. No low temperature experiment was carried out in this study due to the limited solubility.

^{13}C chemical shifts of the free acid form, sodium salt, and lead complex of nigericin in $CDCl_3$ were compared with the ones for the nigericin anion (Et_4N^+ salt). The differences of ^{13}C chemical shifts ($\Delta\delta^{13}C$) are defined in Eq IV.30 and plotted in Figure IV.43.

$$\Delta\delta^{13}C = \delta^{13}C(MNi) - \delta^{13}C(Et_4NNi) \qquad (M = H, Na, \text{and } Pb) \qquad (IV.30)$$

The plot for HNi in $CDCl_3$ shows many negative values of $\Delta\delta^{13}C$ in contrast to the behavior observed in CD_3OD where $\Delta\delta^{13}C$ values are close to zero except for C1, C2, C7, C19 and C31. This suggests large conformational change for the protonated ionophore in $CDCl_3$. In a hydrophobic environment nigericin endeavors to shield the hydrophilic oxygen atoms from the solvent. A head-tail bridge is formed by hydrogen bonding to form a pseudo-cyclic conformation. This causes conformational changes at many of the carbon atoms that make up the rings and backbone chain (C8-C29).

The varying patterns of $\Delta\delta^{13}C$ values for the sodium salt and lead complex of nigericin indicate the complexity in associated with metal coordination. Metal coordination changes the chemical environment of the carbon atoms attached to the participating oxygen atoms, which causes ^{13}C signals to shift downfield and produces positive values of $\Delta\delta^{13}C$. Conformational changes cause negative values of $\Delta\delta^{13}C$[17]. So the domination of negative

$\Delta\delta^{13}C$ values in the plot for the sodium salt of nigericin is the outcome of conformational change upon complexation.

The sodium salt and lead complex show a greater number of positive $\Delta\delta^{13}C$ values than the free acid form of nigericin in $CDCl_3$ because of the metal coordination. The pattern of $\Delta\delta^{13}C$ values for NaNi in $CDCl_3$ shown in Figure IV.42 is similar to the one in CD_3OD except for C1 and C5 shown in Figure IV.43. This suggests that the conformational change and atoms involved in coordination to Na^+ are similar in both solvents. The large positive value of $\Delta\delta^{13}C$ in C1 in $CDCl_3$ suggests that the carboxylic group interacts with the solvent in CD_3OD while in $CDCl_3$ it either binds to Na^+ or to H-O10 (or H-O11) by hydrogen bonding. The largest negative values occur at rings D and E indicating the presence of large conformational changes. The solid-state study of sodium nigericin [18] reveals the half chair conformation of ring C, the envelope conformation of rings D and E. These three rings are five-membered rings with O. The stable conformation for tetrahydrofuran rings is the half chair conformation[19]. Therefore, rings D and F have undergo large conformational change resulting in large negative values of $\Delta\delta^{13}C$. But the data from another NMR study in $CDCl_3$[12] showed the half chair conformation of ring D and reported no conformational information for rings C and E. Based on this information, ring D should not have large conformation change and then small negative values of $\Delta\delta^{13}C$ that is not consistent with the results found in this work.

The plot for the lead-nigericin complex in $CDCl_3$ shows fewer positive values of $\Delta\delta^{13}C$, but with greater magnitude, than the corresponding plot in D_3OD. Part of the plot (rings A, C, D, and E) resembles the one for HNi in $CDCl_3$. The lead-nigericin complex adopts similar conformation with HNi in those regions because in chloroform $PbNi_2$ and HNi orient their oxygen atoms inside. The largest values of $\Delta\delta^{13}C$ are for C10, C19 and

C23 in both the sodium salt and lead complex suggesting similar conformational changes in those carbons. Rings D and E might be in an envelope conformation. Data from the NMR[12] and solid-state studies[18] show that O3 in ring A doesn't coordinate with sodium. Similar patterns for ring A in the plots of the sodium salt and the lead complex also suggest that oxygen 3 does not participate in the metal coordination with lead. In the plot of $PbNi_2$ Several large $\Delta\delta^{13}C$ values happen in ring F. The solid-state study shows that ring F doesn't participate in coordination with sodium while in the NMR study[12] an opposite result is reported. Based on the results of the solid-state study[18], the larger $\Delta\delta^{13}C$ values of ring F can be explained well. Large conformational change occurs in ring F when the ring changes its role from only hydrogen bonding in the sodium salt to lead coordination in the lead complex. The positive value of $\Delta\delta^{13}C$ on C29 supports this result. The conclusion made in the NMR study[12] can't explain all of these. Positive $\Delta\delta^{13}C$ values shown for C1, C11, C13, C17, C20, and C29 indicate that O1 (or O2), O5, O6, O7, O9, and O10 are coordinated with lead.

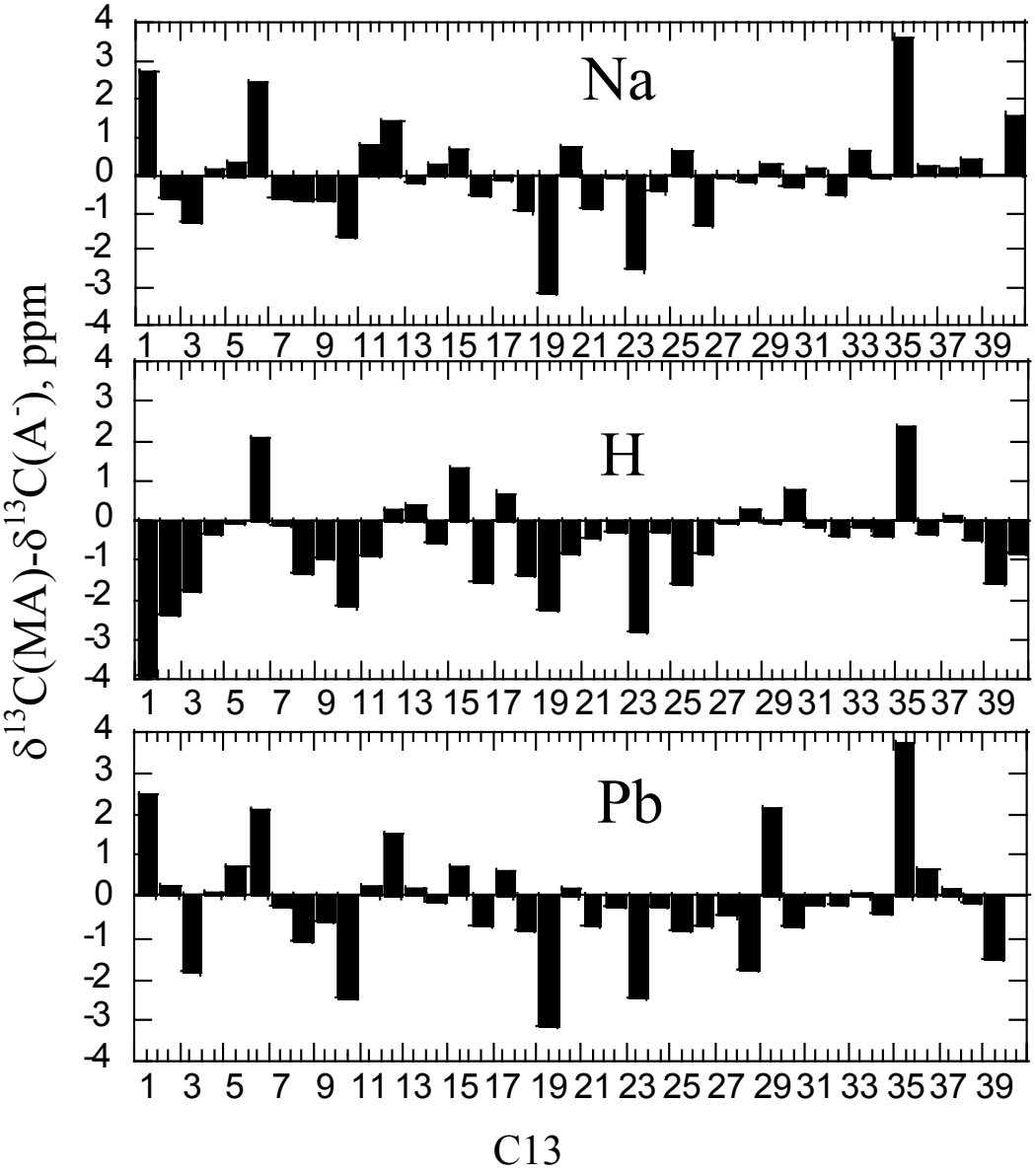


Figure IV.43. Plots of the difference in ^{13}C chemical shifts, $\Delta\delta^{13}C$, between the free acid or complexed forms and the anionic form of nigericin for each carbon atom in $CDCl_3$. Values of $\Delta\delta^{13}C$ were calculated using the experimental ^{13}C chemical shifts listed in Tables IV.10 (Na, top panel), IV.12 (H, middle panel), IV.15 (Pb, bottom panel) and, IV.14 (nigericin anion).

Analysis of NMR Data in CD_3OD

^{13}C chemical shifts of the free acid form, sodium salt, and lead complex of nigericin were compared with the ones for the nigericin anion (Et_4N^+ salt) in CD_3OD. The differences ($\Delta\delta^{13}C$) are plotted in Figure IV.44.

In the case of the free acid form of nigericin where there is no complexation, no significant change was found in values of $\Delta\delta^{13}C$ for most of carbon atoms. The largest changes occur in the carboxylic acid group and the adjacent carbon atoms (C1, C2, and C3). These changes are reasonable after the hydrogen bonding between the carboxyl head and H-O10 or H-O11 is considered. The flexible long chain goes through little conformational change or there is a rapid conformation equilibrium for rings, which shows small $\Delta\delta^{13}C$ values for the rest of carbon atoms. As with the plot in CDCl3, negative values of $\Delta\delta^{13}C$ are prevalent in the plot for the sodium salt of nigericin in CD3OD. For the sodium salt, similar patterns of $\Delta\delta^{13}C$ values in $CDCl_3$ and CD_3OD indicate that the complex has similar conformations in both solvents as described in the section of analysis of NMR data in $CDCl_3$. Large negative values of $\Delta\delta^{13}C$ occur at rings D and E suggesting large conformational change. Rings D and E might be in the envelope conformation as the rings in $CDCl_3$. Large values of $\Delta\delta^{13}C$ appear on all secondary carbons (C5, C6, C10, C15, C18, C19, and C23) on the rings, indicating that on the rings the secondary carbons have the greater flexibility for conformation change. C10, C19 and C23 have the largest chemical shift changes among the whole carbon chain. Small values of $\Delta\delta^{13}C$ suggest that the hinge regions (C7-C8, C16-C17, C20-C21, C24-C25) are so short that only medium conformation changes happen.

In the plot for the lead complex a greater number of positive $\Delta\delta^{13}C$ values are observed than in the plot for the sodium salt. The largest value of $\Delta\delta^{13}C$ is still on C19

indicating the same conformational change as what happens in the sodium salt in both solvents. Ring D might be in the envelope conformation. The rest of larger values occur in ring B. Mild changes are observed in rings C, E, F and the carboxylic acid group. The biggest negative values occur for the same carbons (C5, 10, and 19) in both the sodium salt and lead complexes suggesting similar conformational changes in those carbons. Positive vales of $\Delta\delta^{13}C$ occur at C1, C2, C11, C13, C17, C20, C25, and C29 indicating the role of lead coordination for O1 or O2, and O5, O6, O7, O9, O10 and O11. Similar patterns of $\Delta\delta^{13}C$ in ring A suggest that the same conformational changes occur for ring A in the sodium salt and lead complex. O3 might not be coordinated with lead. Positive values of $\Delta\delta^{13}C$ happen in ring F indicating that ring F is involved in lead coordination.

Compared with NMR data of the lead-monensin complex in CD_3OD, the values of $\Delta\delta^{13}C$ for the lead-nigericin complex in $CDCl_3$ are at least twice as large as the ones in CD_3OD, which suggests that the increased flexibility provided by the longer backbone chain of nigericin allows greater conformational changes and then more oxygen donor atoms might be bound to lead.

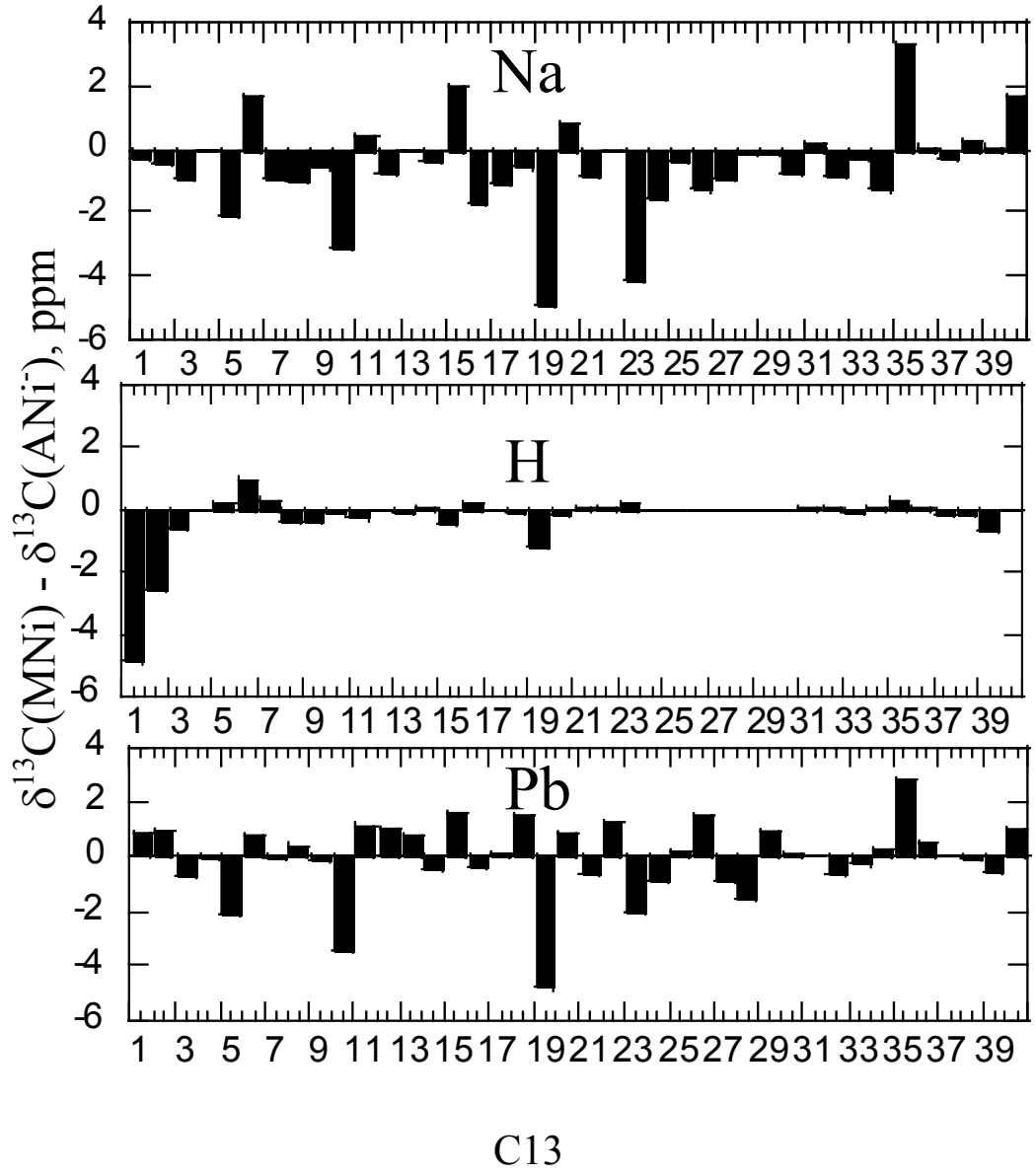


Figure IV.44. Plots of the difference in ^{13}C chemical shifts, $\Delta\delta^{13}C$, between the free acid or complexed forms and the anionic form of nigericin for each carbon atom in CD_3OD. Values of $\Delta\delta^{13}C$ were calculated using the experimental ^{13}C chemical shifts listed in Tables IV.11 (Na, top panel), IV.13 (H, middle panel), IV.15 (Pb, bottom panel) and, IV.14 (nigericin anion).

References

(1) Heusler, K.; Labhart, H.; Loeliger, H.; Ciba, A. G.; Basel, S. *Tetrahedron Lett.* **1965**, *32*, 2847-2854.

(2) Heusler, K.; Loeliger, H.; Woodward, F.; Ciba, A. G.; Basel, S. *Helv. Chim. Acta.* **1969**, *52*, 1495-1516.

(3) Martell, A. E.; Motekaitis, R. J. *Determination and Use of Stability Constants*, 2nd ed.; VCH Publishers: New York, **1992**,

(4) Smith, R. M.; Martell, A. E. *NIST Critically Selected Stability Constants of Metal Complexes Database*, Version 5.0; U.S. Secretary of Commerce, **1998**,

(5) Perrin, D. D.; Sayce, I. G. *Talanta* **1967**, *14*, 833-842.

(6) Sylva, R. N.; Brown, P. L. *J. Chem. Soc., Dalton Trans.* **1980**, 1577-1581.

(7) Palma, M.; Ouahabi, A.; Malfreyt, P.; Juillard, J. *J. Chem. Res., Synop.* **1995**, 404-405.

(8) Taylor, R. W., Ph.D. Thesis, Wayne State University, Detroit, MI, **1973**.

(9) Ivanova, O. G., Ph.D. Thesis, University of Oklahoma, Norman, OK, **2000**.

(10) Westley, J. W. in Polyether Antibiotics: Naturally Occurring Ionophores, Volume 2: Chemistry; Marcel Dekker, Inc.: New York, **1983**, 1-20.

(11) Seto, H.; Otake, N. in Polyether Antibiotics: Naturally Occurring Acid Ionophores, Volume 2: Chemistry; Marcel Dekker, Inc: New York, **1983**, 335-395.

(12) Rodios, N. A.; Anteunis, M. J. O. *Bull. Soc. Chim. Belg.* **1977**, *86*, 917-929.

(13) Rodios, N. A.; Anteunis, M. J. O. *Bull. Soc. Chim. Belg.* **1980**, *89*, 537-550.

(14) David, L.; Ayala, H. L. *J. Antibiot.* **1985**, *38*, 1655-1663.

(15) Berrada, R.; Dauphin, G.; David, L. *J. Org. Chem.* **1987**, *52*, 2388-2391.

(16) Hebrant, M.; Mimouni, M.; Tissier, M.; Pointud, Y.; Juillard, J. *New J. Chem.* **1992**, *16*, 999-1008.

(17) Mimouni, M.; Hebrant, M.; Dauphin, G.; Juillard, J. *J. Chem. Res., Miniprint* **1996**, 1416-1433.

(18) Barrans, P. Y.; Alleaume, M. *Acta Crystallogr., Sect. B* **1980**, *36*, 936-938.

(19) Infarnet, Y.; Duplan, J. C.; Delmau, J.; Huet, J. *C. R. Seances Acad. Sci. Ser. C* **1969**, *269*, 1415-1418.

Chapter V

Results

Studies of lead-salinomycin complexes

V.A Elemental analysis of lead-salinomycin complexes.

Samples of lead-salinomycin (1:2) complexes, prepared using methods described in Section II.B, were submitted to a commercial firm for elemental analysis. The experimental percentages of carbon, hydrogen, and lead obtained are listed in Table V.1 along with the corresponding theoretical values calculated for complexes with varying composition.

Table V.1. Experimental and calculated elemental composition of lead-salinomycin (1:2) complexes[a].

Compound/method	%Pb	%C	%H	%O
Experimental values				
$PbSal_2$ by reaction of PbO with HSal	10.55	61.18	8.76	19.51
Calculated from the specified molecular stoichiometries				
1Pb:2Sal	12.15	59.13	8.09	20.63
1Pb:2Sal:1H_2O	12.01	58.48	8.18	21.33
1Pb:2Sal:2H_2O	11.89	57.87	8.21	22.03

[a] Weight percentage scale (wt/wt) is used. The contents of lead, C and H were determined by Desert Analytics Company. The compounds are considered to only contain Pb, H, C, and O. The equation for %O calculation is (100 - %Pb - %C - %H).

The lead percentage for the lead-salinomycin compound, prepared by the reaction of lead oxide and the free acid form of salinomycin, shows significant deviation from the calculated values but is closest to that for the model with two additional waters of hydration. The experimental carbon percentage is higher than any theoretical values but close to the values for the model without any waters of hydration. The hydrogen percentage is higher than any theoretical values. The experimental oxygen percentage is close to the calculated value for the model without any waters of hydration. Considering

all experimental percentages, the model without waters of hydration best describes the composition of lead-salinomycin complexes made by reaction of lead-oxide and the free acid form of salinomycin. One explanation for the low lead percentage is that the free acid form of salinomycin may degrade during two days reaction in methanol solutions, which could definitely change the lead complexation ability. However, the major peaks in the MS spectra are for lead-salinomycin complexes, as described in Section V.B. In ^{13}C NMR there is only one set of signals, which provides confidence that the compound is pure enough for this study. Other methods were tried to prepare lead-salinomycin complexes. None of these methods produced a product containing higher percentage of lead than the compound made by reaction of lead oxide and the free acid form of salinomycin.

V.B Characterization of the lead-salinomycin complexes by ESI-MS.

ESI-MS was used to characterize the lead-salinomycin complex produced by the reaction of lead oxide and the free acid form of salinomycin. Peak clusters were assigned by comparison of the experimental peak intensities in the cluster to the calculated isotopic pattern.

The lead-salinomycin (1:2) complexes were dissolved in methanol and injected into MicroMass Q-TOF. The positive mode was used and the spectrum is shown in Figure V.1.

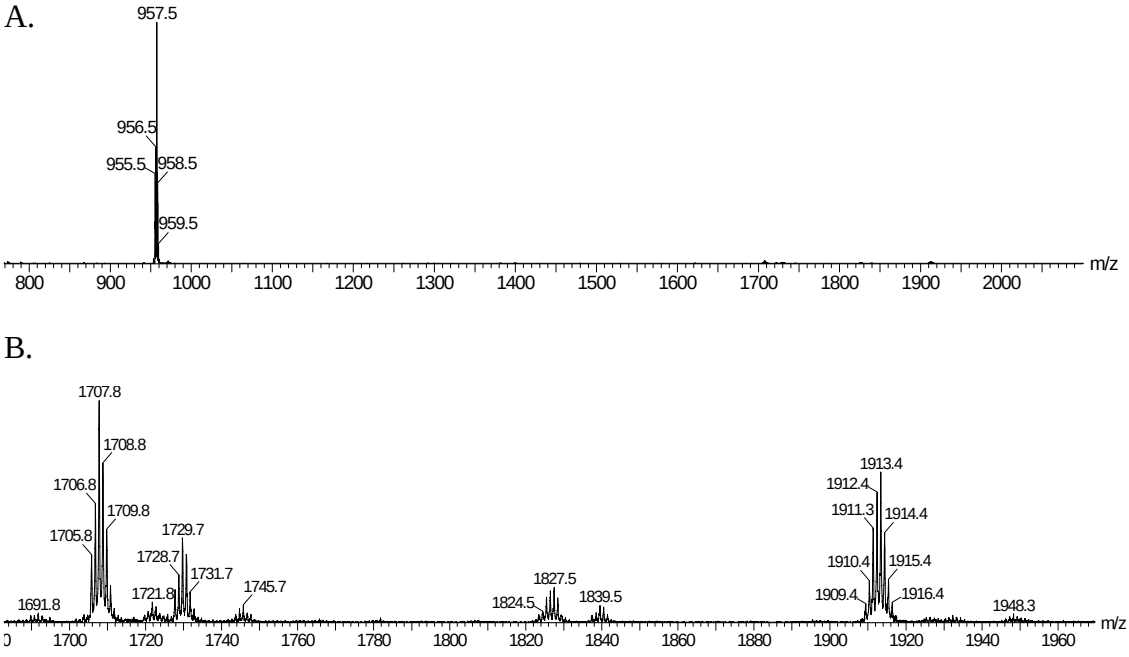


Figure V.1. A. Part of the positive ion ESI-MS for lead-salinomycin complex. Peak clusters for molecular ions having 1:1 (957.5 m/z), 1:2 (1707.7 m/z), and 2:2 (1913.4 m/z) lead-salinomycin stoichiometries are observed. The latter two peaks have low intensities and are expanded as shown in panel B.

Several peak clusters were observed and identified with different lead-salinomycin stoichiometries while there was only one peak cluster was observed in the

ESI-MS spectrum for the lead-nigericin (1:2) complex. Each cluster contained at least five peaks, due to four isotopes of lead and two isotopes of carbon, and was assigned by comparison of the experimental peak intensity pattern to the calculated isotopic pattern of the postulated formula. Important peak clusters were magnified in Figures V.2-V.4 to show the details along with their theoretical counterparts. The lead-salinomycin (1:1) complex (957.5 m/z) was the major peak cluster and accounted for at least 95% of the ion intensity, which indicates the strong interaction of lead and salinomycin. The lead-salinomycin (1:2) $(2sal + H + Pb)^+$ (sal represents the monoanionic form of salinomycin) and (2:2) $(2sal + 2Pb - H)^+$ peak clusters were found at 1707.7 (Figure V.3) and 1913.4 m/z (Figure V.4), respectively. Additional low intensity peak clusters were observed for $(2sal + Pb + Na)^+$ (1729.7 m/z), $(2sal + Pb + K)^+$ (1745.6 m/z), and $(2sal + 2Pb + 2H_2O)^+$ (1949.9 m/z).

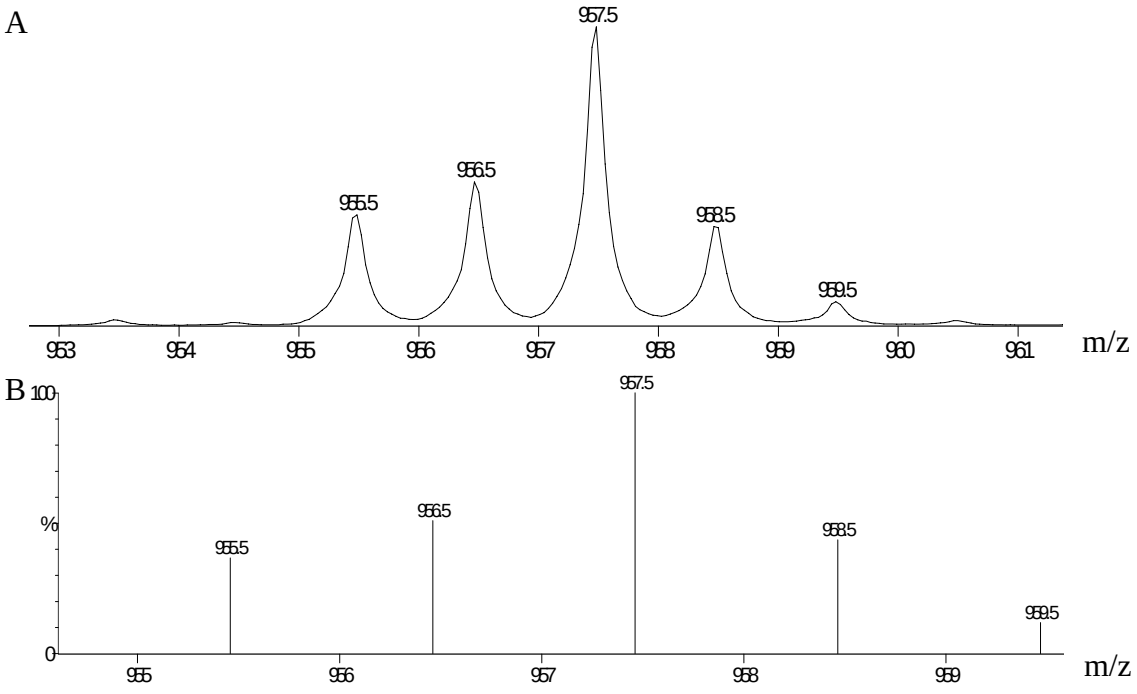


Figure V.2. A. Peaks for the 1:1 lead-salinomycin molecular ion in positive ion ESI-MS. B. The calculated isotopic pattern for $C_{42}H_{69}O_{11}Pb$.

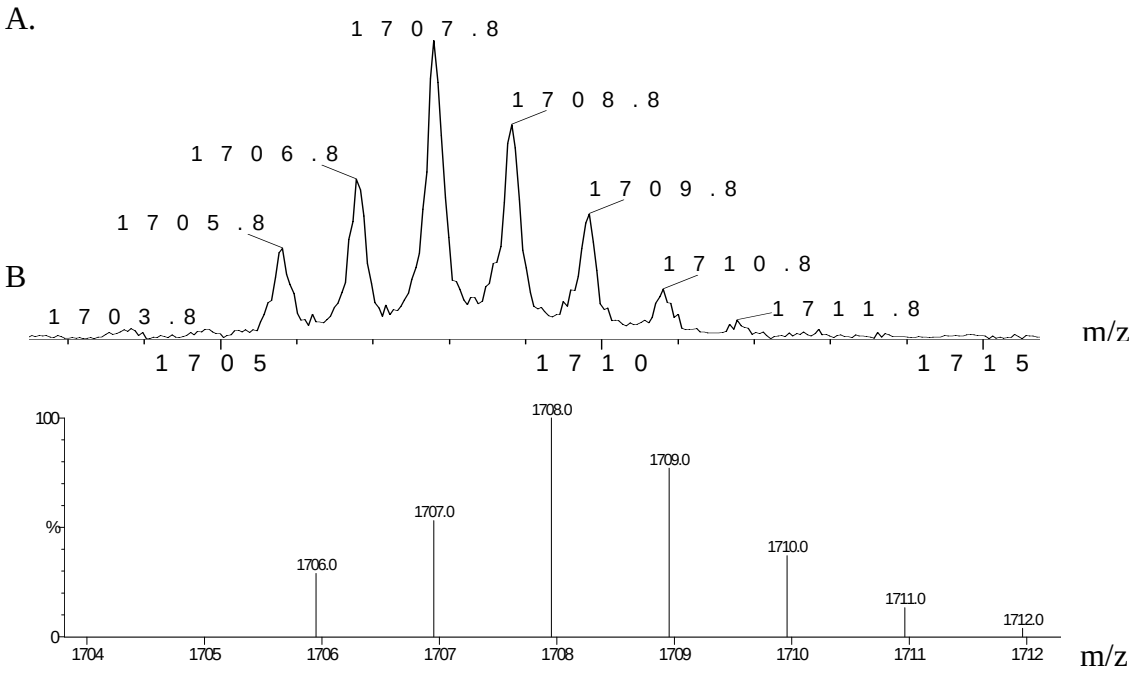


Figure V.3. A. Peaks for the 1:2 lead-salinomycin molecular ion in positive ion ESI-MS. B. The calculated isotopic pattern for $C_{84}H_{139}O_{22}Pb$.

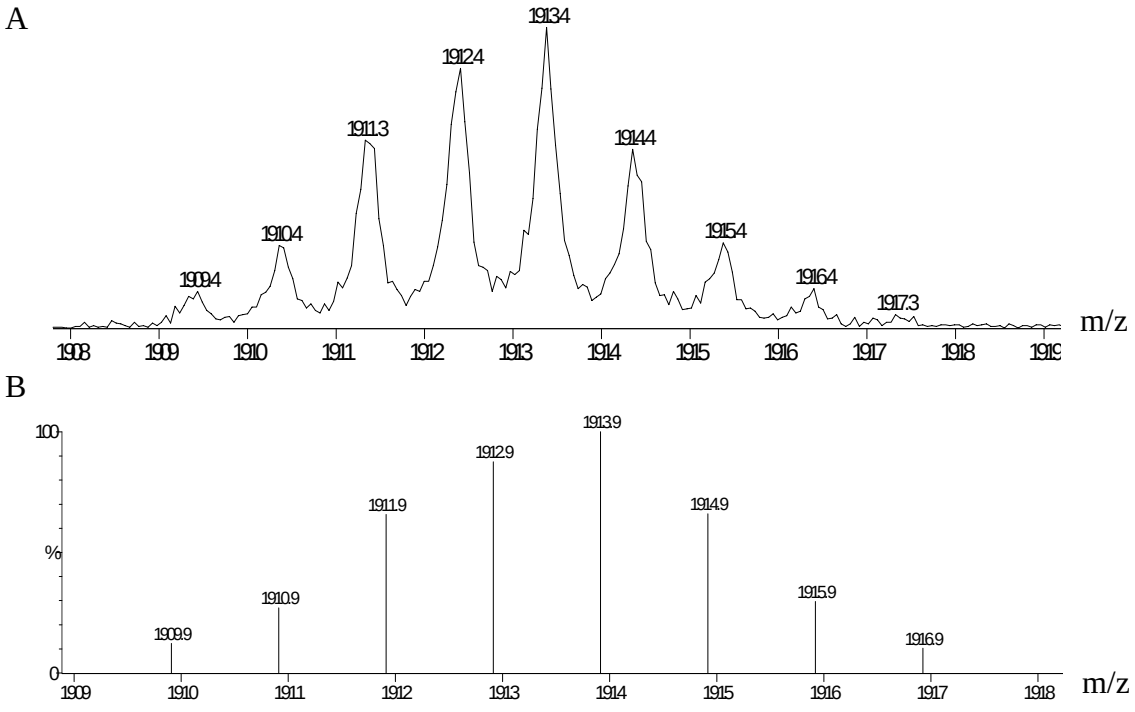


Figure V.4. A. Peaks for the 2:2 lead-salinomycin molecular ion in positive ion ESI-MS. B. The calculated isotopic pattern for $C_{84}H_{137}O_{22}Pb_2$.

V.C UV spectrophotometric studies of lead-salinomycin complexation reactions

Salinomycin does not possess chromophores but the lead-salinomycin complex shows strong signals due to Pb-O charge transfer bands[1,2], that is the basis of the UV studies of the the lead-salinomycin complexation reaction. The experimental details of salinomycin UV studies were described in Section II.E. The purposes of titrations are the same as those for nigericin. The experimental design and calculations are exactly as described in Section IV.C.

Information about the stoichiometry was obtained from the experiment at pH ~6 where the side reaction of salinomycin with protons was negligible. The UV spectrum for the lead-salinomycin titration is shown in Figure V.5. The absorbance at 238 nm was plotted versus the ratio of the total salinomycin to total lead concentrations. The result is shown in Figure V.6. The absorbance behaved in the same way as those in lead-nigericin titrations. Salinomycin forms a lead complex with predominately 1:1 stoichiometry at this pH*.

Data from the experiment at pH ~3 were analyzed as described in Section IV.C. The fitting plot from the last cycle for salinomycin-lead UV titration is shown in Figure V.7. The resulting log value of stability constant for salinomycin-lead (1:1) complex, $\log K_{PbL}$, is 6.977 based on the calculated apparent formation constant K'_{PbL}.

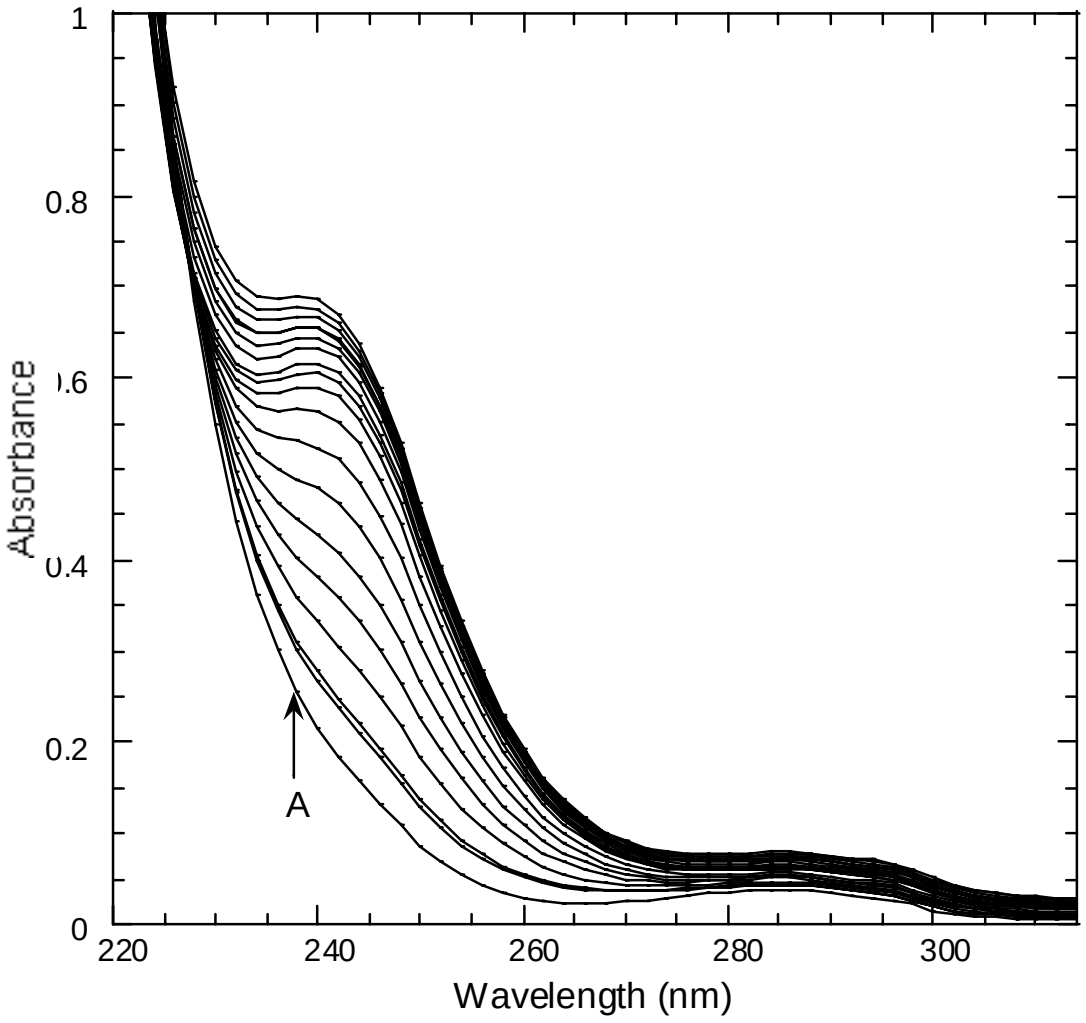


Figure V.5. UV-Vis spectra from the titration of lead perchlorate with salinomycin in 80% methanol-water at 25 ^{o}C. Aliquots (3 or 10 μL) of 0.01 M sodium salinomycin were used to titrate 2.7 mL of a solution containing 0.1 mM lead perchlorate, buffered at pH* 6.3 with 3 mM MES, at an ionic strength of 0.05 M (TEAP). Curve A-$Pb(ClO_4)_2$ alone, no salinomycin added.

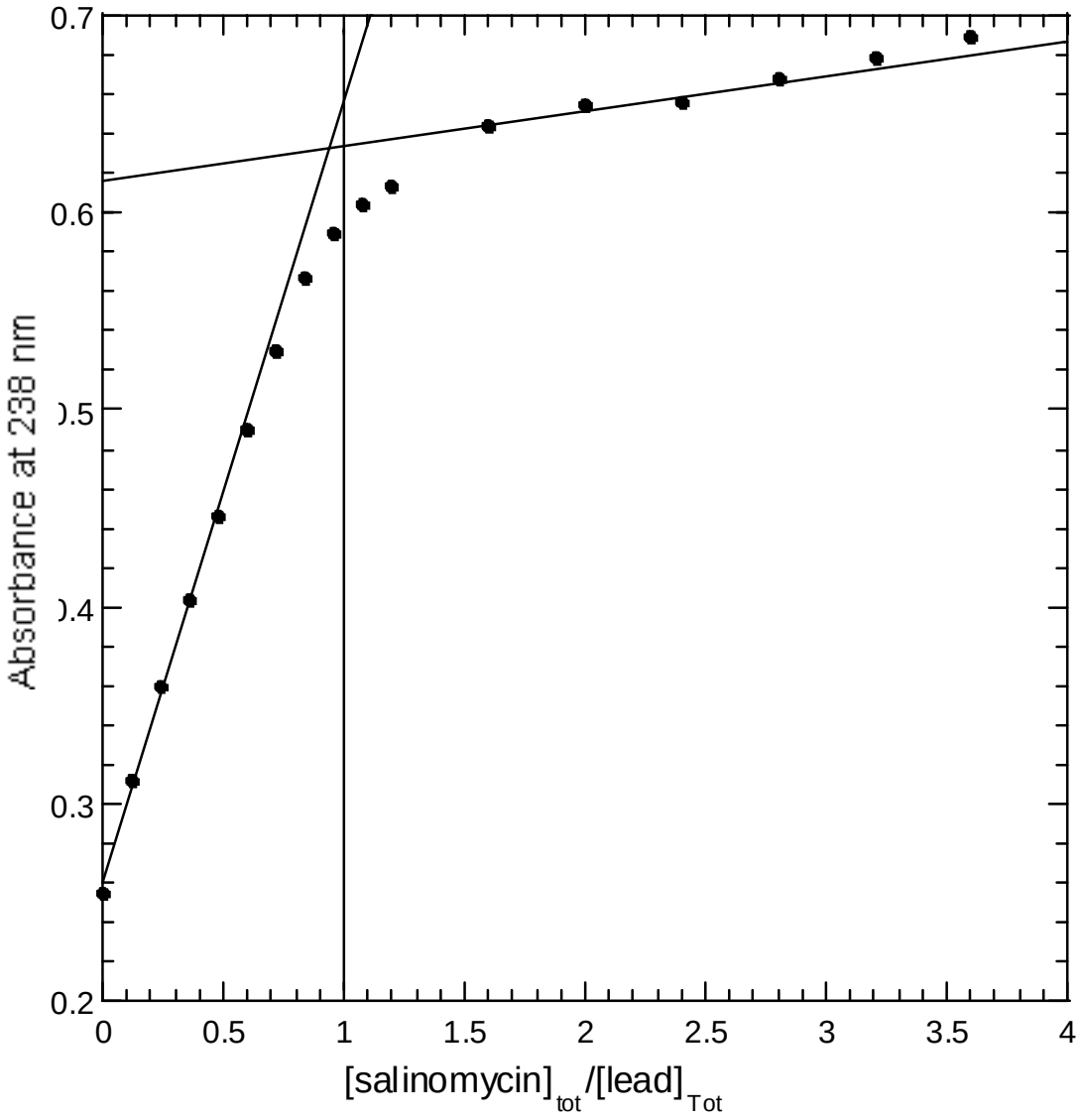


Figure V.6. Plot of the absorbance resulting from each aliquot of sodium salinomycin added versus the ratio of the total salinomycin to total lead concentrations.

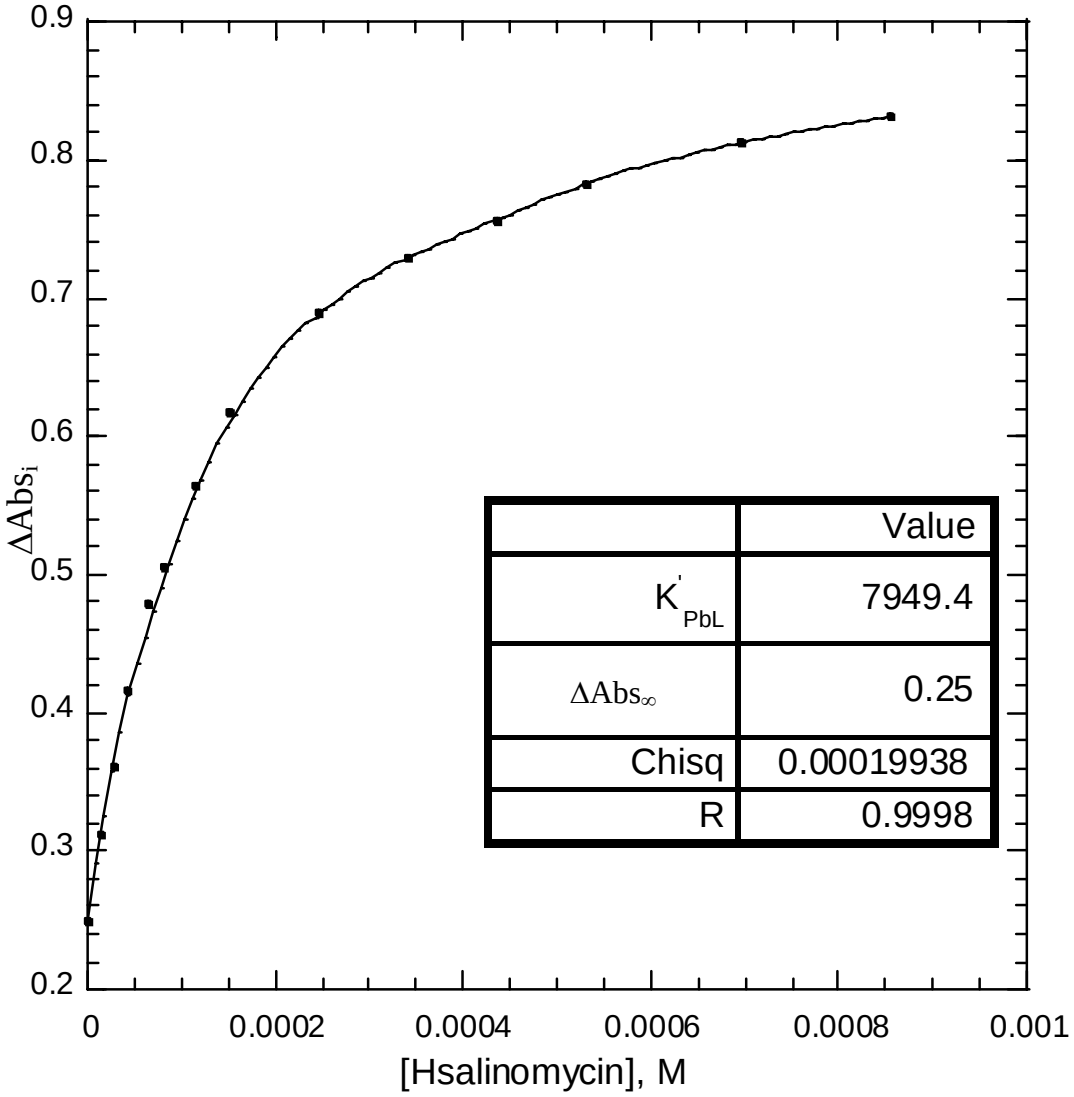


Figure V.7. Change in absorbance at 248 nm as a function of [Hsalinomycin] at pH* 3.177. Aliquots (6 or 10 μL) of 0.01 M salinomycin acid were used to titrate 2.7 mL of a solution containing 0.1 mM lead perchlorate in 80% methanol-water. The titration was done at 25 ^{o}C at an ionic strength of 0.05 M (TEAP). The solid line was calculated from eq IV.12 using the derived parameters listed in the inset table.

V.D The protonation constant for salinomycin in 80% methanol-water determined using potentiometric titrations

The protonation constant for salinomycin was determined using potentiometric and circular dichroism titrations. In potentiometric titrations the free acid form of salinomycin in 80% methanol-water was titrated with a solution of Me_4NOH (I = 0.5M) at 25 ^{o}C as described in Section II.E. A single buffer region appeared in the titration curves indicating only one protonation site in the free acid form of salinomycin. A typical titration curve and the calculated fit are shown in Figure V.8. The titration data was analyzed using the programs PKAS and BEST[3] and the results are listed in Table V.2. The average log value of the protonation constant of salinomycin is 6.49 ± 0.07. This parameter is kept constant during analysis of the titration data for salinomycin-metal complexes, as described in Section IV.D.

Table V.2. Calculated values of the protonation constant for salinomycin in 80% methanol-water[a].

Salinomycin concentration (mM)	Log K_H^C [b]	σ_{fit} [c]
0.618	6.58	0.010
1.01	6.49	0.012
1.01	6.48	0.020
1.01	6.49	0.020
1.18	6.39	0.017

[a] 25 ^{o}C, ionic strength 0.05 M (TEAP). [b] The value was refined using the program BEST. [C] $\sigma_{Fit} = (U/N)^{1/2}$, eq IV.16.

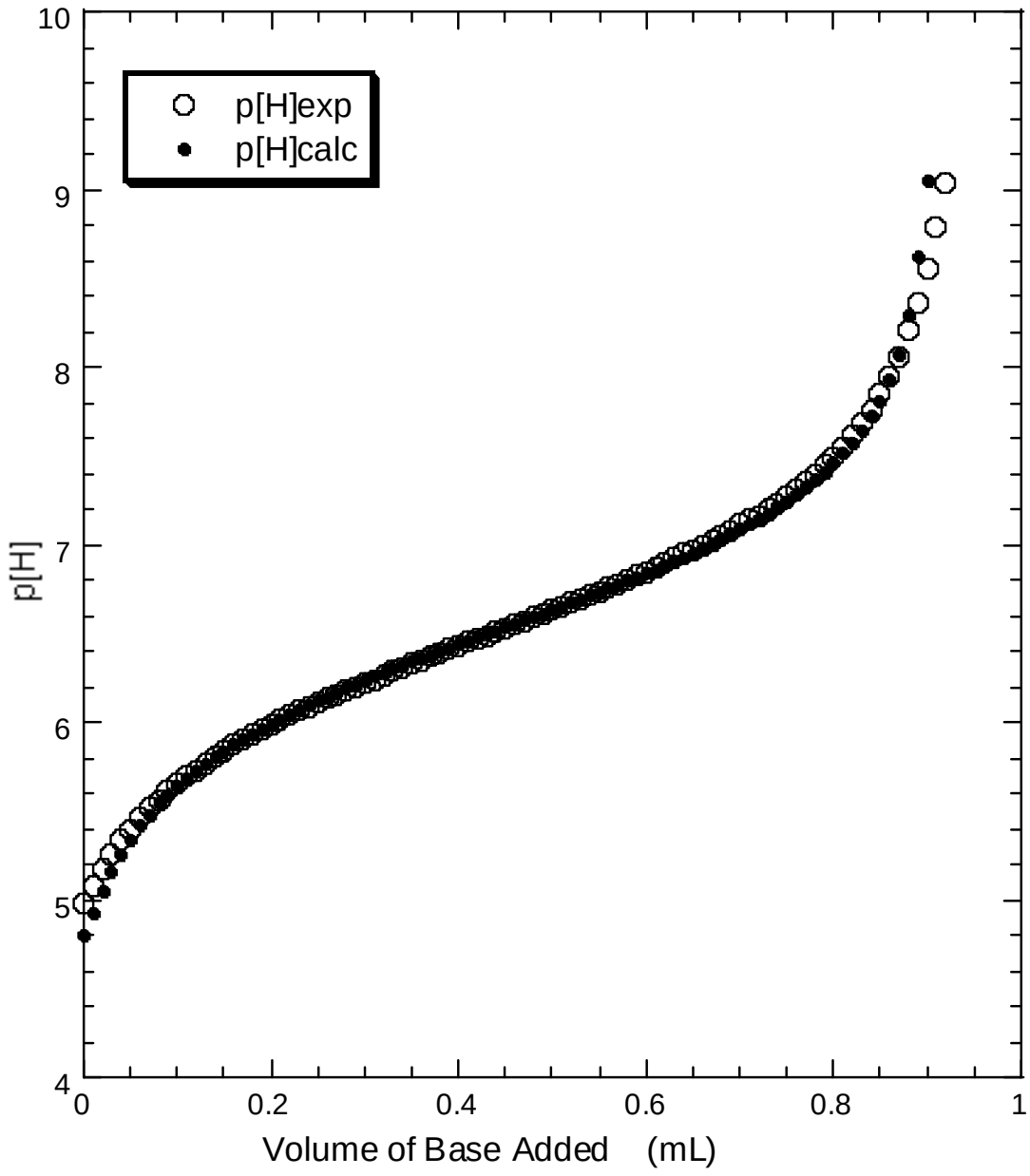


Figure V.8. A potentiometric titration curve for 10.00 mL of a solution containing 1.01 mM salinomycin acid at an ionic strength of 0.05 M TEAP in 80% methanol-water (25 ^{o}C). The titrant is 11 mM Me_4NOH with an ionic strength maintained at 0.05 M with TEAP. The calculated p[H] values were obtained using the program BEST.

The protonation constant for salinomycin in 80% methanol-water determined using CD titrations

The CD spectrum of salinomycin 80% methanol-water shows large negative peaks at 215 and 290 nm as shown in Figure V.9. The intensity of the peak at 215 nm changed markedly with pH. Based on this phenomenon, a CD titration was carried out to obtain the protonation constant of salinomycin in 80% methanol-water for comparison with the volume obtained from potentiometric titrations. A solution of 80% methanol-water was prepared containing 0.647 mM of the free acid form of salinomycin, 5 mM MES and 5 mM HEPES to control pH. The ionic strength was maintained at 0.05 M using TEAP. The solution was adjusted to different pHs using 0.1 M $HClO_4$ and 0.1 M Et_4NOH and CD spectra were recorded after every pH adjustment. The ellipticity values at 215 nm were plotted as a function of pH and were fit to eq V.1 using the non-linear least-squares function in the program Kaleidagraph[4]

$$\Delta Ell_i = \frac{\Delta Ell_L + \Delta Ell_{HL} K_H [H^+]_i}{1 + K_H [H^+]_i} \qquad K_H = \frac{[HL]}{[H^+][L^-]} \qquad \text{(V.1)}$$

where ΔEll_i is the ellipticity value at a given pH, ΔEll_L and ΔEll_{HL} are the limiting ellipticities for the anionic and protonated forms of salinomycin, respectively, and $[H^+]_i$ is the concentration of hydrogen ions at a given pH. A plot of the experimental and calculated curves is shown in Figure V.10. The log value of protonation constant obtained from the fitting is 6.57. This is very close to 6.49, the value determined from the potentiometric titrations.

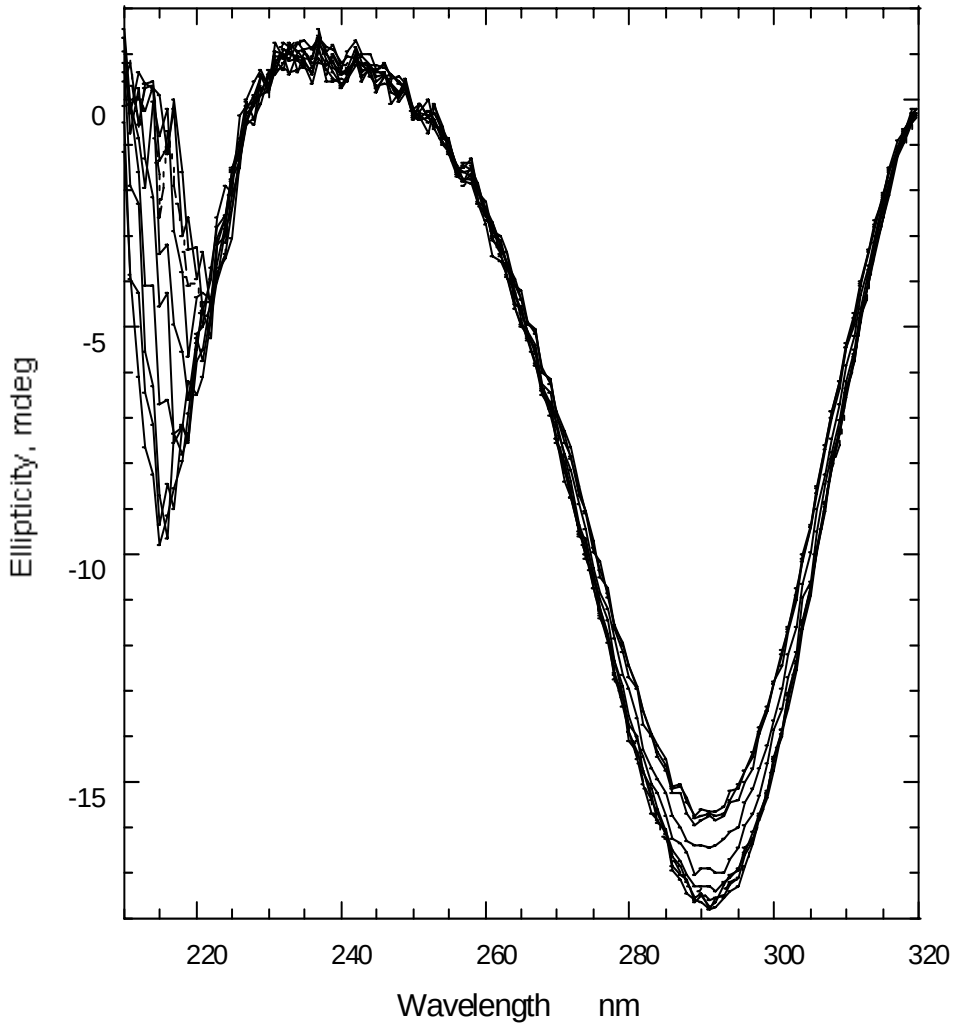


Figure V.9. CD spectra for a solution of 2.7 mL 0.647 mM salinomycin acid containing 5 mM MES and 5 mM HEPES in 80% methanol-water at different pHs using 0.1 M $HClO_4$ and 0.1 M Et_4NOH. The experiment was done at 25^{o}C at an ionic strength of 0.05 M (TEAP).

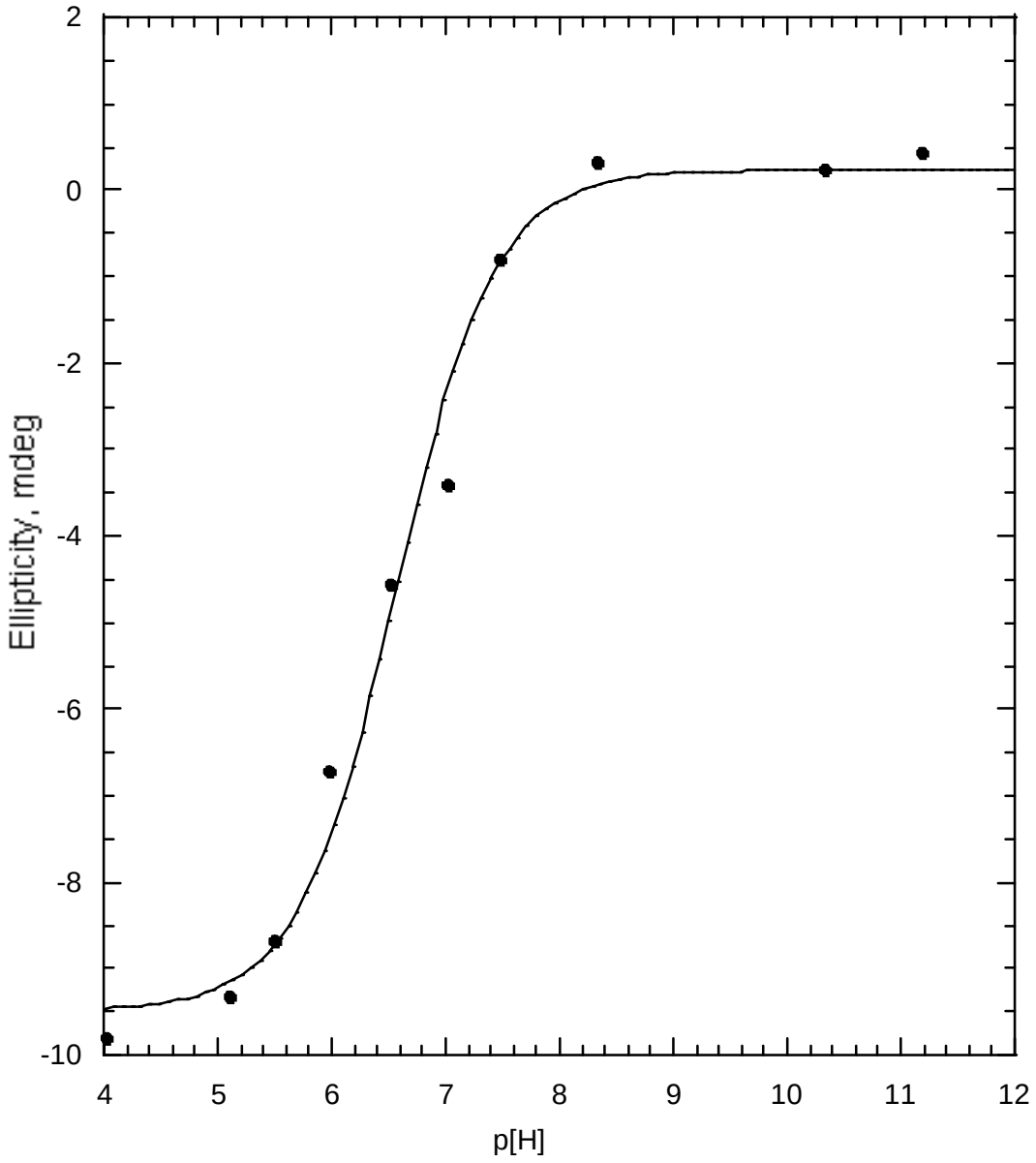


Figure V.10. Plot of the ellipticity values at 215 nm as a function of p[H]. A solution of 2.7 mL 0.647 mM salinomycin acid containing 5 mM MES and 5 mM HEPES in 80% methanol-water was adjusted to different pHs using 0.1 M $HClO_4$ and 0.1 M Et_4NOH. The experiment was done at 25 ^oC at an ionic strength of 0.05 M (TEAP). The solid line was calculated from eq V.1 with parameters ($\log K_H$ = 6.57, ΔEll_L = 0.229, and ΔEll_{HL} = -9.48).

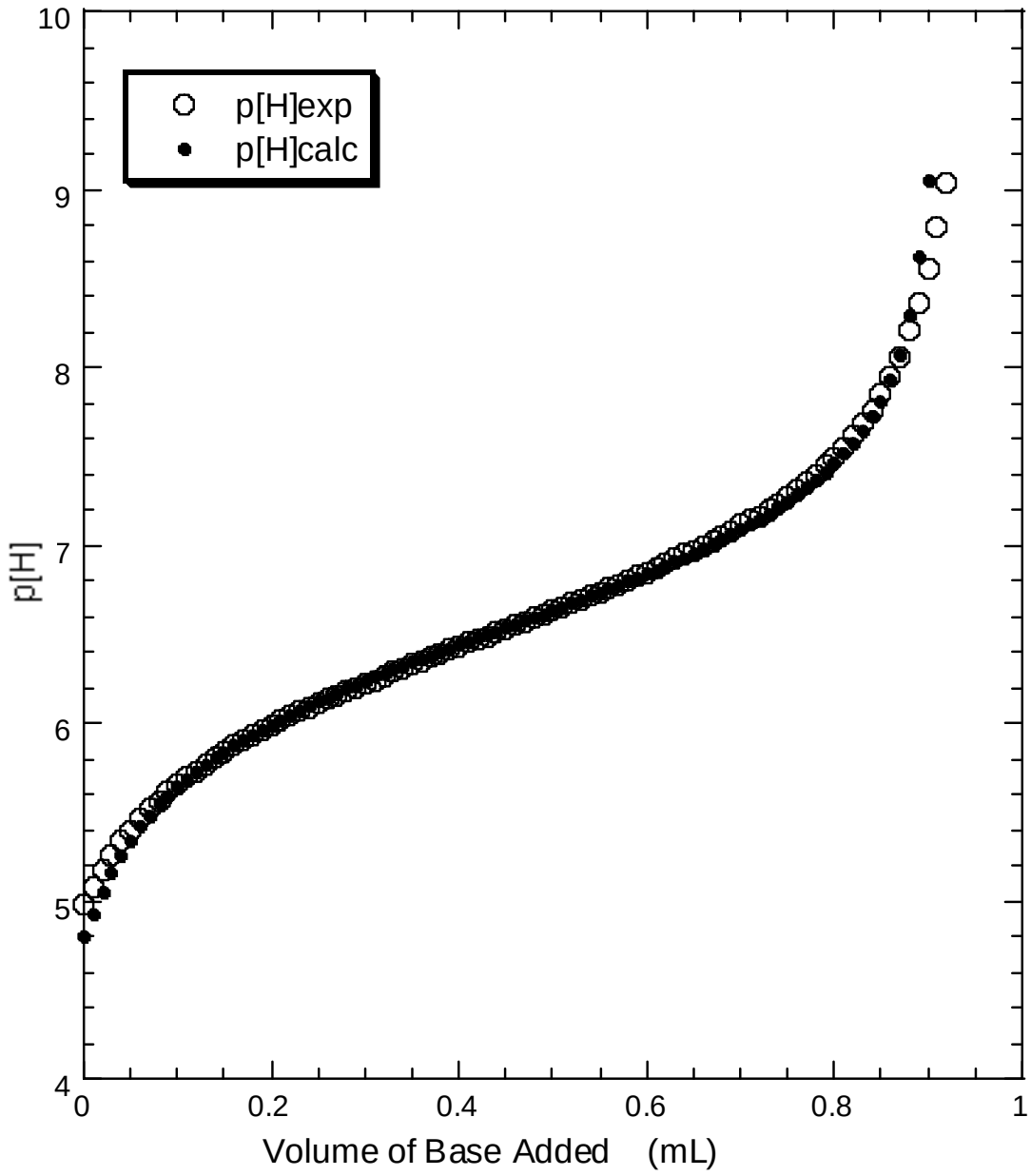
V.E. Potentiometric studies of metal binding

The free acid form of salinomycin in 80% methanol-water was titrated with Me_4NOH solutions in the presence of metal ions as described in Section II.E. Different ratios of salinomycin and metal ions were used to investigate the existence of different complexes as described in Section IV.D. The stability constants of salinomycin complexes of potassium, calcium, zinc, magnesium, and lead were calculated using the program BEST. Protonation constants and stability constants are expressed as overall complexation constants (log β values), as described in Section IV.D.

The protonation constants determined from salinomycin acid titrations without added metal ions and the metal hydrolysis constants were held constant during the refinement. Salinomycin-metal constants were obtained from the refinement. The refinement steps were the same as those described for nigericin in Section IV.D. The values of stability constants obtained from the program BEST were input to the program Comics to calculate species distribution diagrams. Metal complex species were deleted from the model when they accounted for less than 5% of the total ligand or metal concentration.

Sodium-salinomycin

A weighed amount of dry sodium chloride was dissolved in 80% methanol-water and diluted into the desired concentration. Different volumes of sodium chloride solutions were added to a solution containing a known concentration of salinomycin acid (HSal) to provide the desired ligand-metal ratios. The titration procedure was described in Section II.E. After data analysis using the program BEST, the values of log β for sodium-salinomycin (1:1) complexes were found smaller than 2, the lower limit of log β values for potentiometric titrations. It is suspected that sodium doesn't bind with salinomycin strongly enough for accurate measurement of log β. A typical titration curve is fitted with a model excluding sodium ions. The resulting protonation constant for salinomycin from the program is 6.46. The difference is 0.4% between that value and the one from salinomycin acid titrations (6.49). The sigma of the fitting is 0.028. Figure V.11 shows the experimental curve and the calculation curve fitted with the model excluding sodium ions. It is clear that two curves matched up very well. Therefore, Na^+ doesn't bind with significantly salinomycin and at the concentration used acts primarily as an electrolyte in the titrations.



FigureV.11. A potentiometric titration curve for 10.05 mL of a solution containing 1.01 mM salinomycin acid and 0.982 mM NaCl at an ionic strength of 0.05 M (TEAP) in 80% methanol-water (25 ^{o}C). The titrant is 12.8 mM Me_4NOH with an ionic strength maintained at 0.05 M with TEAP. The calculated p[H] values were obtained using the program BEST and refined values of equilibrium constants for the model without sodium ions.

Potassium-salinomycin

A weighed amount of dry potassium chloride was dissolved in 80% methanol-water and was diluted to the desired concentration. Different volumes of potassium chloride solutions were added to a solution containing a known concentration of salinomycin free acid (HSal) to provide ligand-metal ratios ranging from 1.0 to 3.0. The titration procedure was described in Section II.E. During data analysis using the program BEST, species such as K_2Sal, HK_2Sal, $KSal_2$, and KSal were tested. None of these except KSal produced reasonable constants. Figure V.12 shows raw titration data with different Ni/K ratios. Individual titrations are shown in Figures V.13 and V.14 with calculated curves obtained using the program BEST. The average value of the stability constant for KSal was input into the program Comics to generate a species distribution curve shown in Figure V.15. The calculated values of the stability constant of KSal are listed in Table V.3.

Table V.3. Log β_X values obtained from potentiometric titrations of salinomycin acid (HL) and potassium[a]

Exp. No.	HL-K ratio	Identity of complex species X		σ_{fit}[d]
		HL[b]	KL[c]	
1	1.0	6.49	3.29	0.028
2	1.0	6.49	3.32	0.036
3	1.8	6.49	3.28	0.013
4	2.3	6.49	3.39	0.020
5	3.0	6.49	3.44	0.034

[a] 25 ^oC, ionic strength 0.05 M (TEAC). [b] The value of log β was fixed during refinement. [c] The value was refined using the program BEST. [d] $\sigma_{Fit} = (U/N)^{1/2}$, eq IV.16.

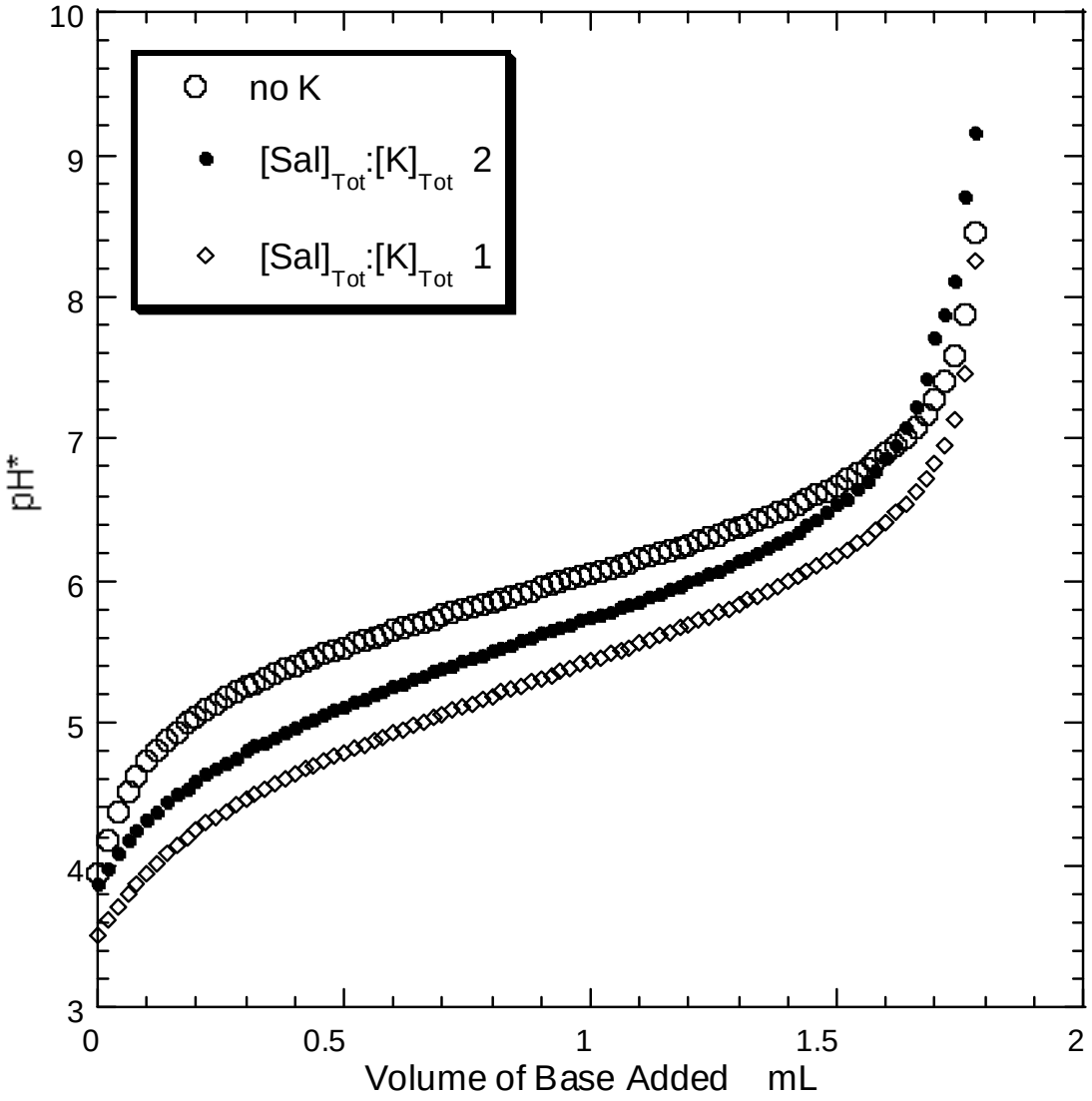


Figure V.12. Potentiometric titration curves for various stoichiometric ratios of potassium-salinomycin in 80% methanol-water at 25 ^{o}C. Each solution contained 5.08 mL of 3.2 mM salinomycin acid at an ionic strength of 0.05 M Et_4NCl (25 ^{o}C). The titrant is 9.3 mM Me_4NOH with an ionic strength maintained at 0.05 M with Et_4NCl. A solution of 0.1075 M potassium chloride was added in the required amount to obtain the indicated stoichiometric ratio.

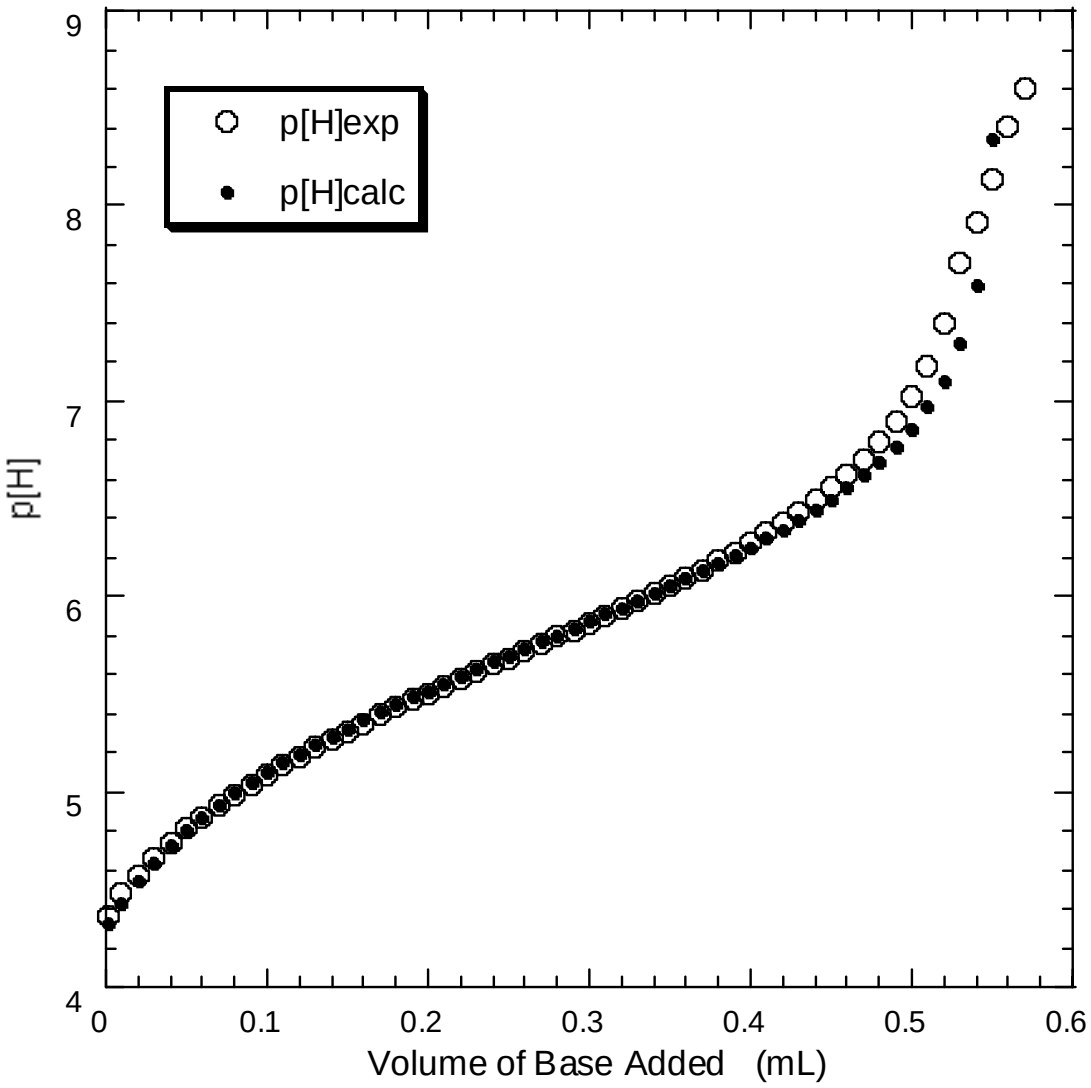


Figure V.13. A potentiometric titration curve for 5.08 mL of a solution containing 3.2 mM salinomycin acid and 1.81 mM potassium chloride at an ionic strength of 0.05 M Et_4NCl (25 ^{o}C). The titrant is 9.3 mM Me_4NOH with an ionic strength maintained at 0.05 M with Et_4NCl. The calculated p[H] values were obtained using the program BEST and refined values of equilibrium constants for the model containing the species listed in Table V.3.

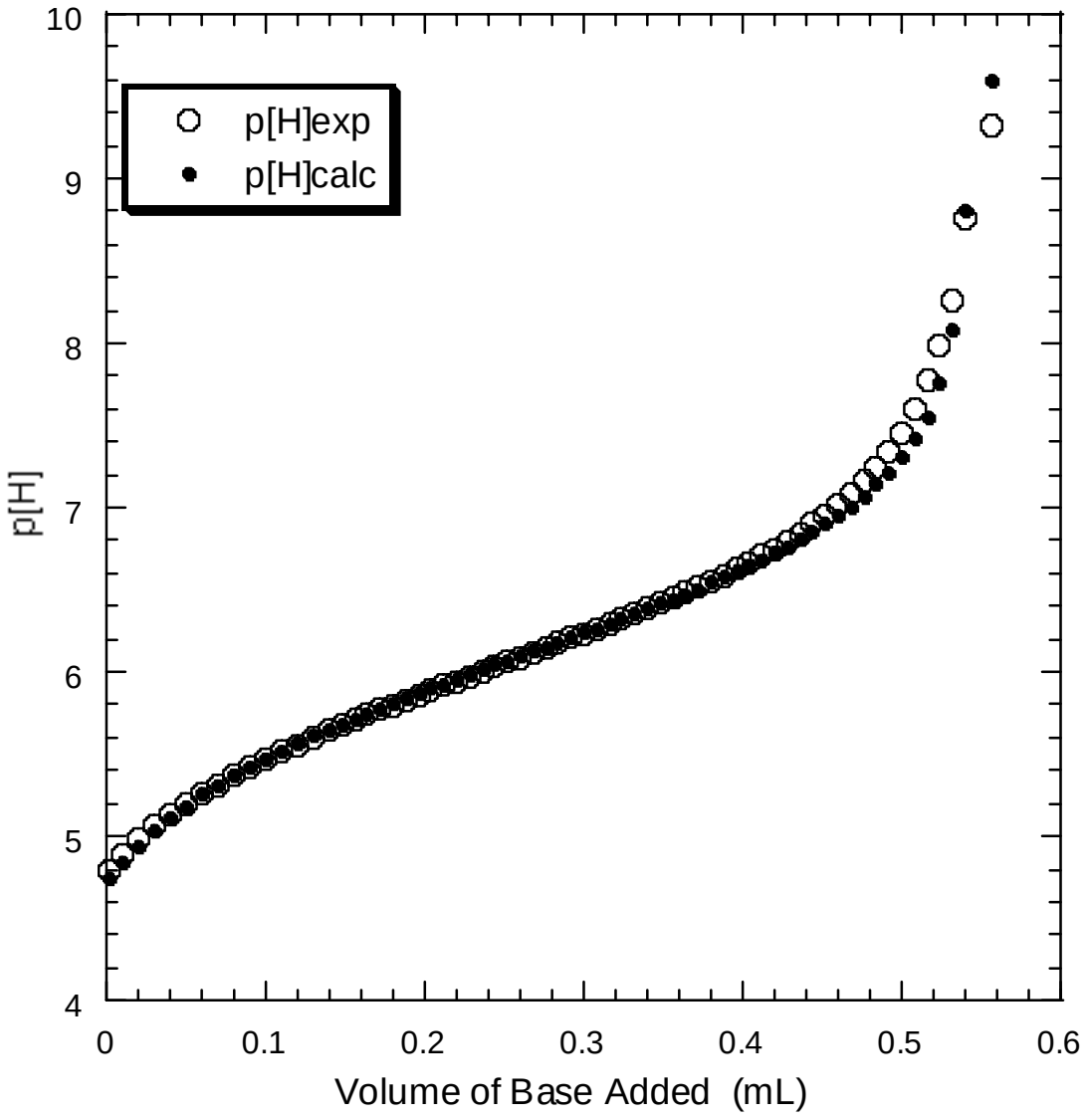


Figure V.14. A potentiometric titration curve for 5.05 mL of a solution containing 1.2 mM salinomycin acid and 1.12 mM potassium chloride at an ionic strength of 0.05 M Et_4NCl (25 ^oC). The titrant is 0.0118 M Me_4NOH with an ionic strength maintained at 0.05 M with Et_4NCl. The calculated p[H] values were obtained using the program BEST and refined values of equilibrium constants for the model containing the species listed in Table V.3.

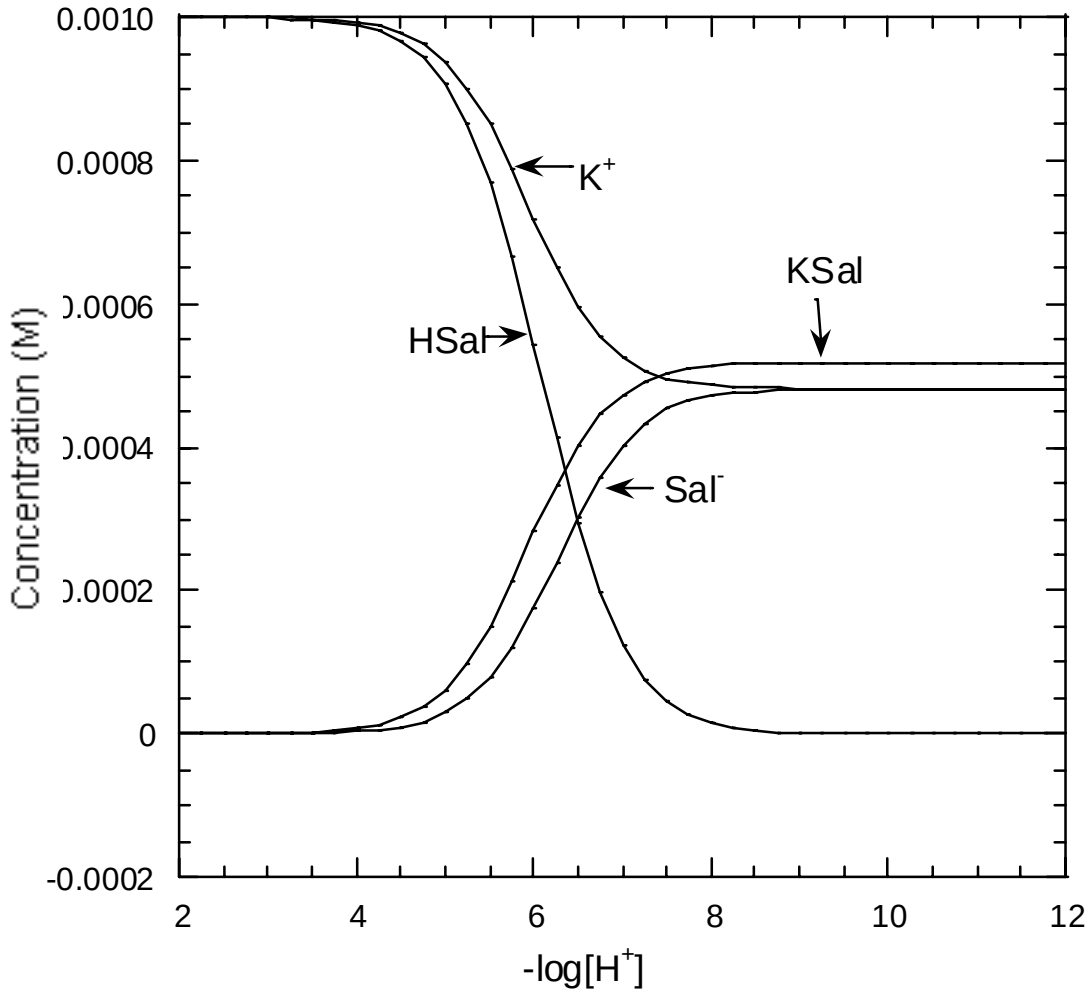


Figure V.15. Species distribution curves for potassium-salinomycin complexes in 80% methanol-water solution as a function of p[H]. Species concentrations were calculated using the program Comics for 1.0 mM salinomycin and 1.0 mM potassium and the average values of the equilibrium constants listed in Table V.3.

Calcium-salinomycin

A solution of standardized calcium chloride in 80% methanol-water was added to a solution with a known concentration of salinomycin acid to provide ligand-metal rations ranging from 0.25 to 2.5. The titration procedure was described in Section II.E. During data analysis using the program BEST, species such as Ca_2Sal, HCa_2Sal, $CaSal_2$, CaSalOH, and CaSal were tested. Only the latter two species were found to exist in solutions at a significant concentration. Figure V.16 shows raw titration data with different Sal/Ca ratios. Individual titrations are shown in Figures V.17 and V.18 with the calculated curves obtained using the program BEST. The average values of the stability constants for calcium-salinomycin complexes were input into the program Comics to generate the species distribution curves shown in Figure V.19. The calculated values of the stability constants of calcium-salinomycin complexes are listed in Table V.4.

Table V.4. Log β_X values obtained from potentiometric titrations of salinomycin acid (HL) and calcium (II)[a]

Exp. No.	HL-Ca ratio	Identity of complex species X				σ_{fit}[f]
		HL[b]	CaL[c]	CaLOH[c,d]	CaOH[e]	
1	0.25	6.49	2.85	-8.08	-13.11	0.008
2	1	6.49	2.64	-7.58	-13.11	0.011
3	2	6.49	2.57	-7.96	-13.11	0.008
4	2.5	6.49	2.31	-7.54	-13.11	0.012

[a]25 ^oC, ionic strength 0.05 M (TEAP). [b]The value of log β was fixed during refinement. [c]The value was refined using the program BEST. [d]β_{CaLOH} is expressed as an acid dissociation constant. [e]The value was fixed during refinement; it was estimated for 80% methanol-water and corrected to 0.05 M ionic strength, as described in Section IV.D. [f]$\sigma_{Fit} = (U/N)^{1/2}$, eq IV.16.

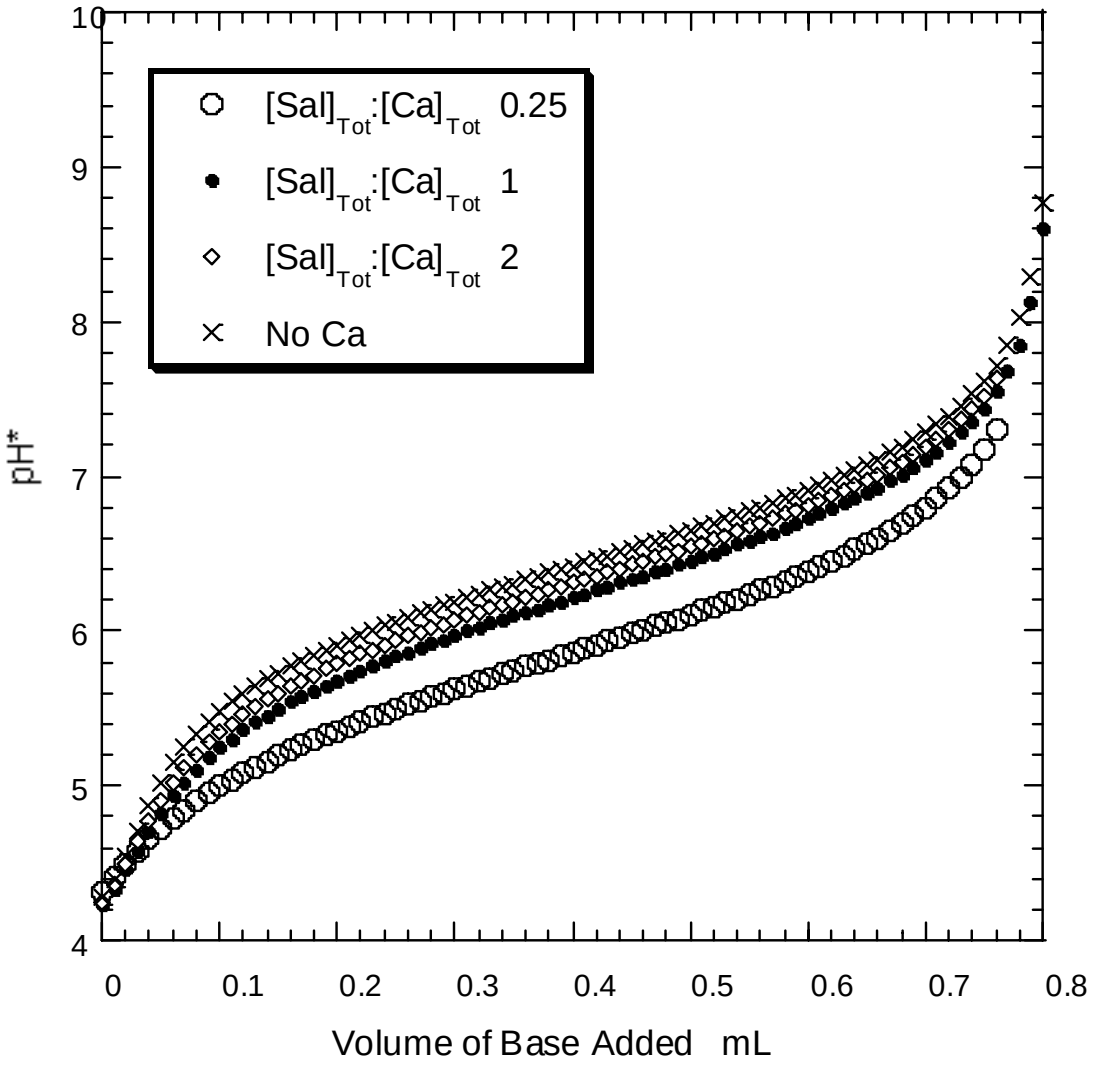


Figure V.16. Potentiometric titration curves for various stoichiometric ratios of calcium-salinomycin in 80% methanol-water at 25 ^{o}C. Each solution contained 5.25 mL of 1.14 mM salinomycin acid at an ionic strength of 0.05 M TEAP (25 ^{o}C). The titrant is 7.78 mM Me_4NOH with ionic strength maintained at 0.05 M with TEAP. A solution of 0.0964 M calcium chloride was added in the required amount to obtain the indicated stoichiometric ratio.

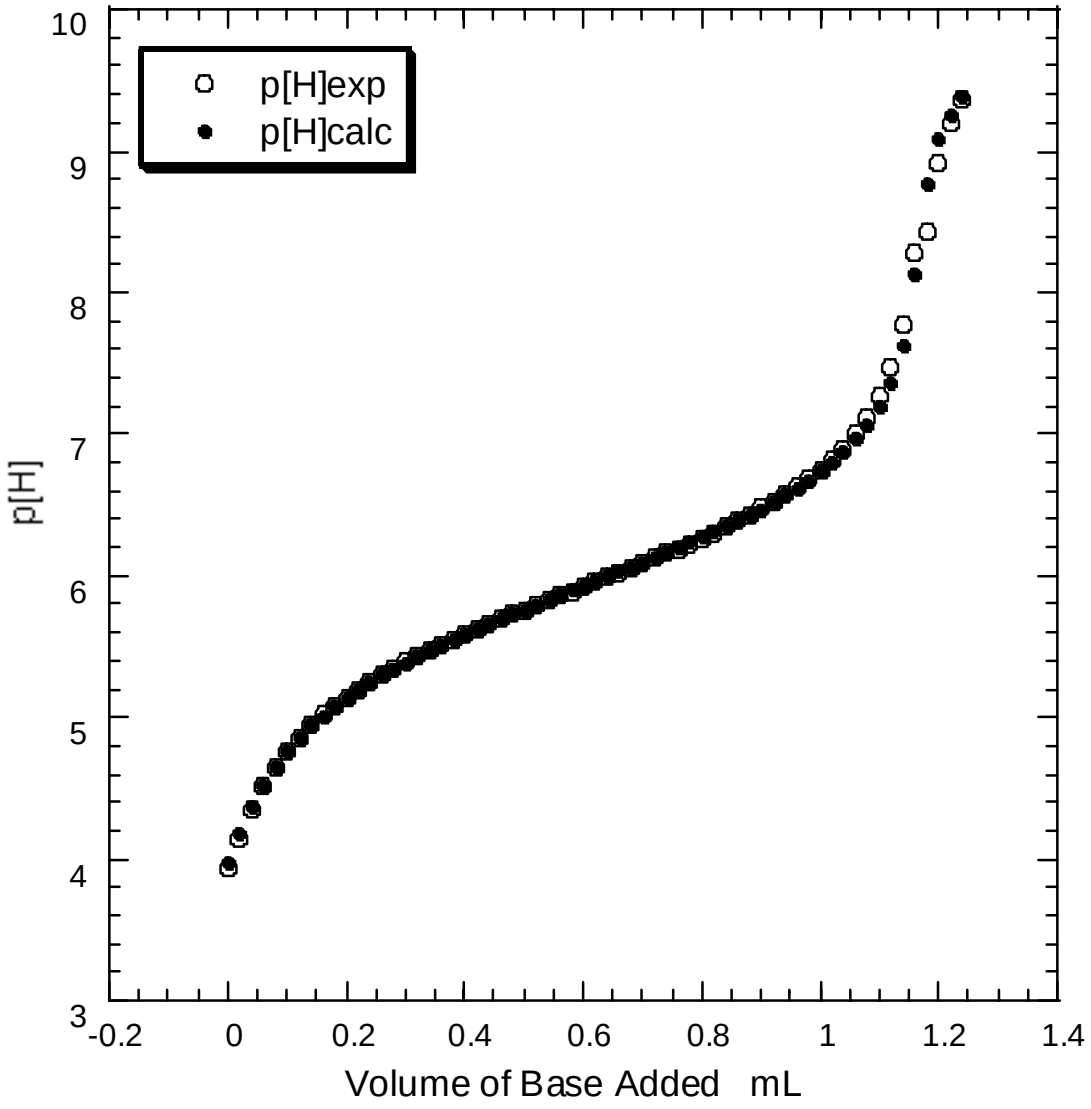


Figure V.17. A potentiometric titration curve for 10.06 mL of a solution containing 1.24 mM salinomycin acid and 0.53 mM calcium at an ionic strength of 0.05 M TEAP (25 ^{o}C). The titrant is 0.0108 M Me_4NOH with ionic strength maintained at 0.05 M with TEAP. The calculated p[H] values were obtained using the program BEST and refined values of equilibrium constants for the model containing the species listed in Table V.4.

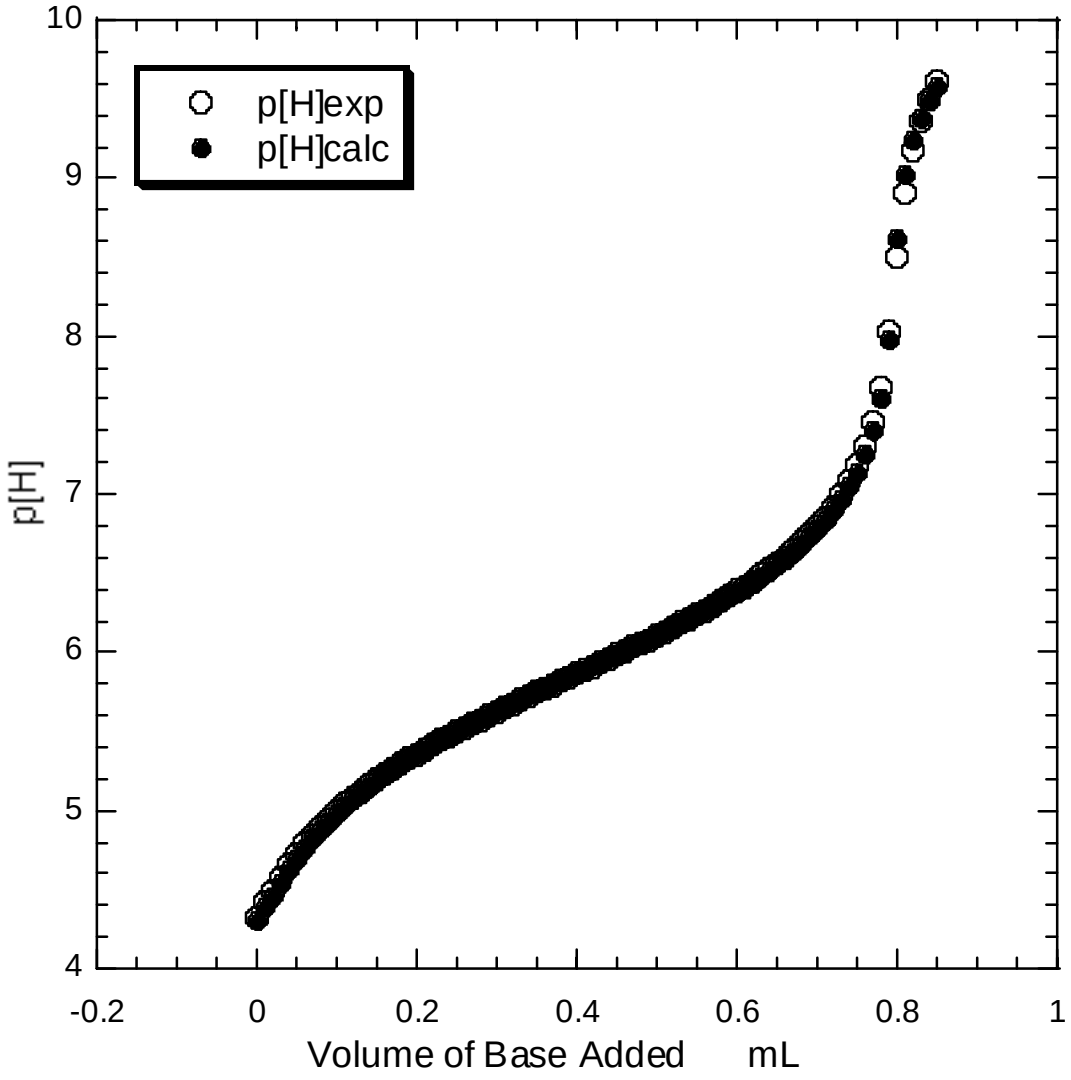


Figure V.18. A potentiometric titration curve for 5.25 mL of a solution containing 1.14 mM salinomycin acid and 4.59 mM calcium at an ionic strength of 0.05 M TEAP (25 ^{o}C). The titrant is 7.78 mM Me_4NOH with an ionic strength maintained at 0.05 M with TEAP. The calculated p[H] values were obtained using the program BEST and refined values of equilibrium constants for the model containing the species listed in Table V.4.

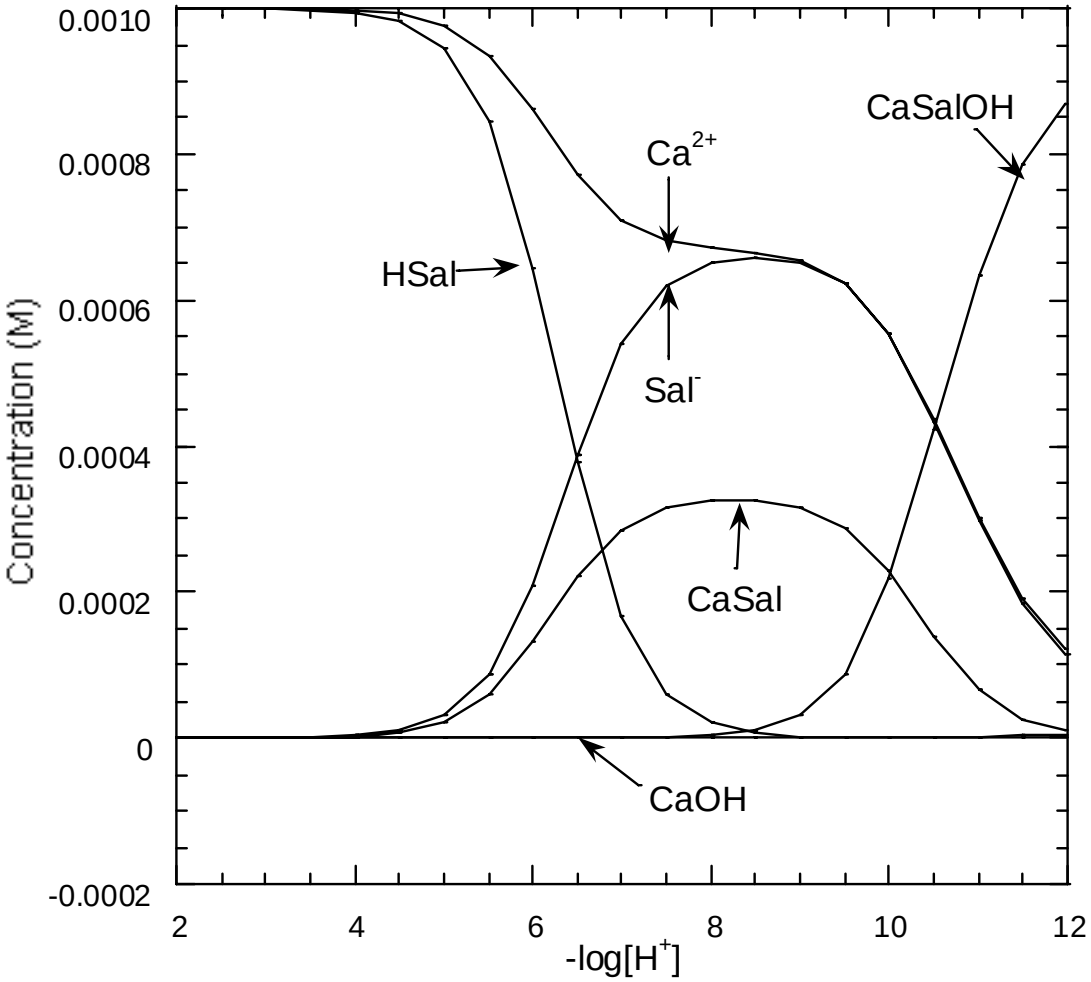


Figure V.19. Species distribution curves for calcium-salinomycin complexes in 80% methanol-water solution as a function of p[H]. Species concentrations were calculated using the program Comics for 1.0 mM salinomycin and 1.0 mM calcium and the average values of the equilibrium constants listed in Table V.4.

Zinc-salinomycin

A solution of standardized zinc perchlorate in 80% methanol-water was added to a solution containing a known concentration of salinomycin acid to provide ligand-metal ratios ranging from 0.5 to 2.52. The titration procedure was described in Section II.E. During data analysis using the program BEST, species such as Zn_2Sal, HZn_2Sal, $ZnSal_2$, ZnSalOH, and ZnSal were tested. Only the latter two species were found to exist in solution at significant concentrations. The stability constant for $Zn(OH)_2$ also was required in the model. Figure V.20 shows raw titration data with different Sal/Zn ratios. Individual titrations are shown in Figures V.21 and V.22 with calculated curves obtained using the program BEST. At pH ~7, zinc ions start to precipitate so all titration data for pH >7 were discarded. The average values of the stability constants for zinc-salinomycin complexes were input into the program Comics to generate the species distribution curves shown in Figure V.23. The calculated values of the stability constants of calcium-salinomycin complexes are listed in Table V.5.

Table V.5. Log β_X values obtained from potentiometric titrations of salinomycin acid (HL) and zinc (II)[a]

Exp. No.	HL-Zn ratio	Identity of complex species X					σ_{fit}[f]
		HL[b]	ZnL[c]	ZnLOH[c,d]	ZnOH[e]	$Zn(OH)_2$[e]	
1	0.5	6.49	2.82	-5.26	-9.42	-18.2	0.022
2	1	6.49	2.52	-5.90	-9.42	-18.2	0.019
3	2.52	6.49	2.30	-5.91	-9.42	-18.2	0.024

[a]25 ^oC, ionic strength 0.05 M (TEAP). [b]The value of log β was fixed during refinement. [c]The value was refined using the program BEST. [d]β_{ZnLOH} is expressed as an acid dissociation constant. [e]The value was fixed during refinement; it was estimated for 80% methanol-water and corrected to 0.05 M ionic strength, as described in Section IV.D. [f]$\sigma_{Fit} = (U/N)^{1/2}$, eq IV.16.

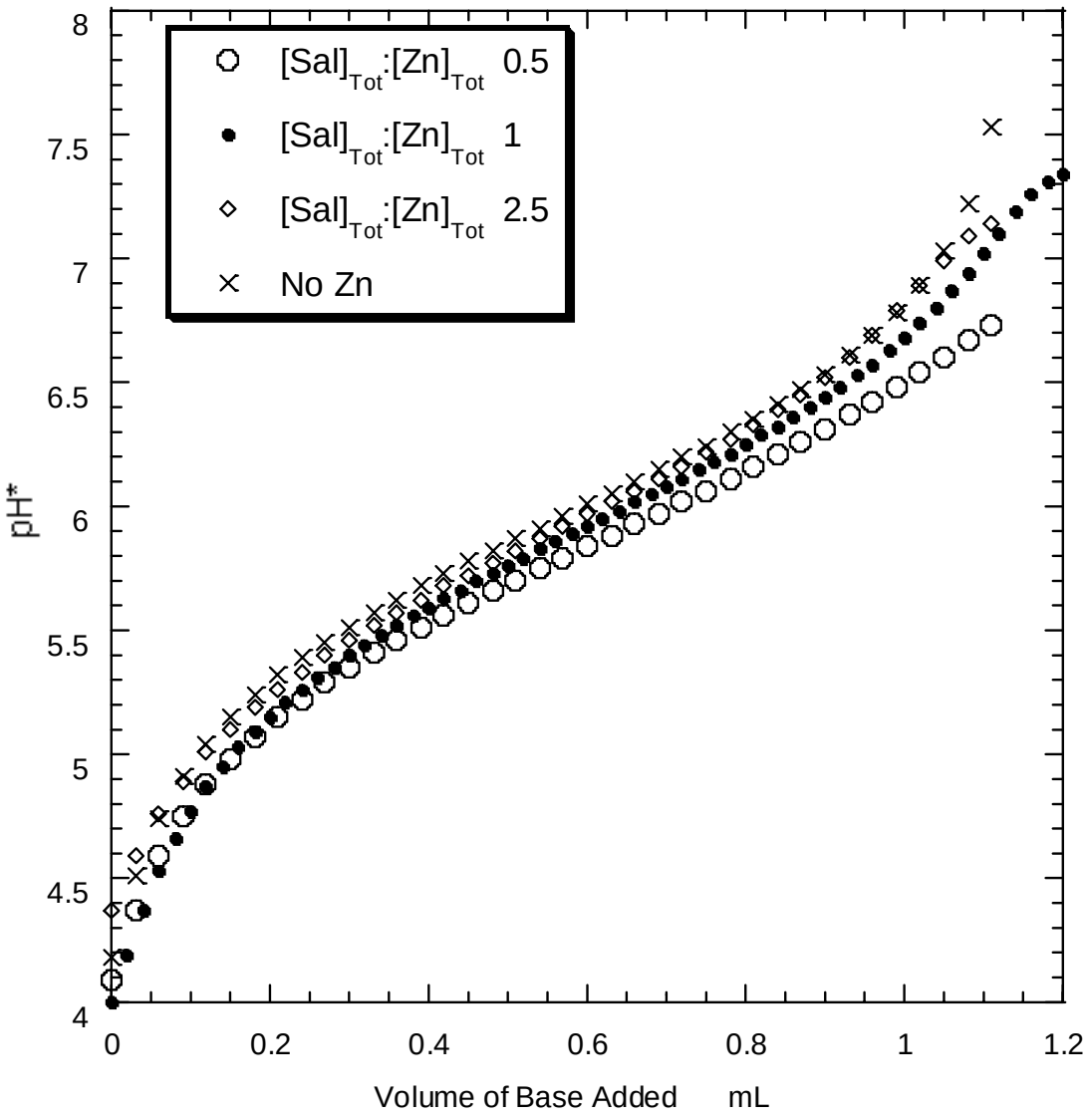


Figure V.20. Potentiometric titration curves for various stoichiometric ratios of zinc-salinomycin in 80% methanol-water at 25 ^{o}C. Each solution contained 10.63 mL of 1.15 mM salinomycin acid at an ionic strength of 0.05 M TEAP (25 ^{o}C). The titrant is 0.0108 M Me_4NOH with ionic strength maintained at 0.05 M with TEAP. A solution of 0.0217

M zinc perchlorate was added in the required amount to obtain the indicated stoichiometric ratio.

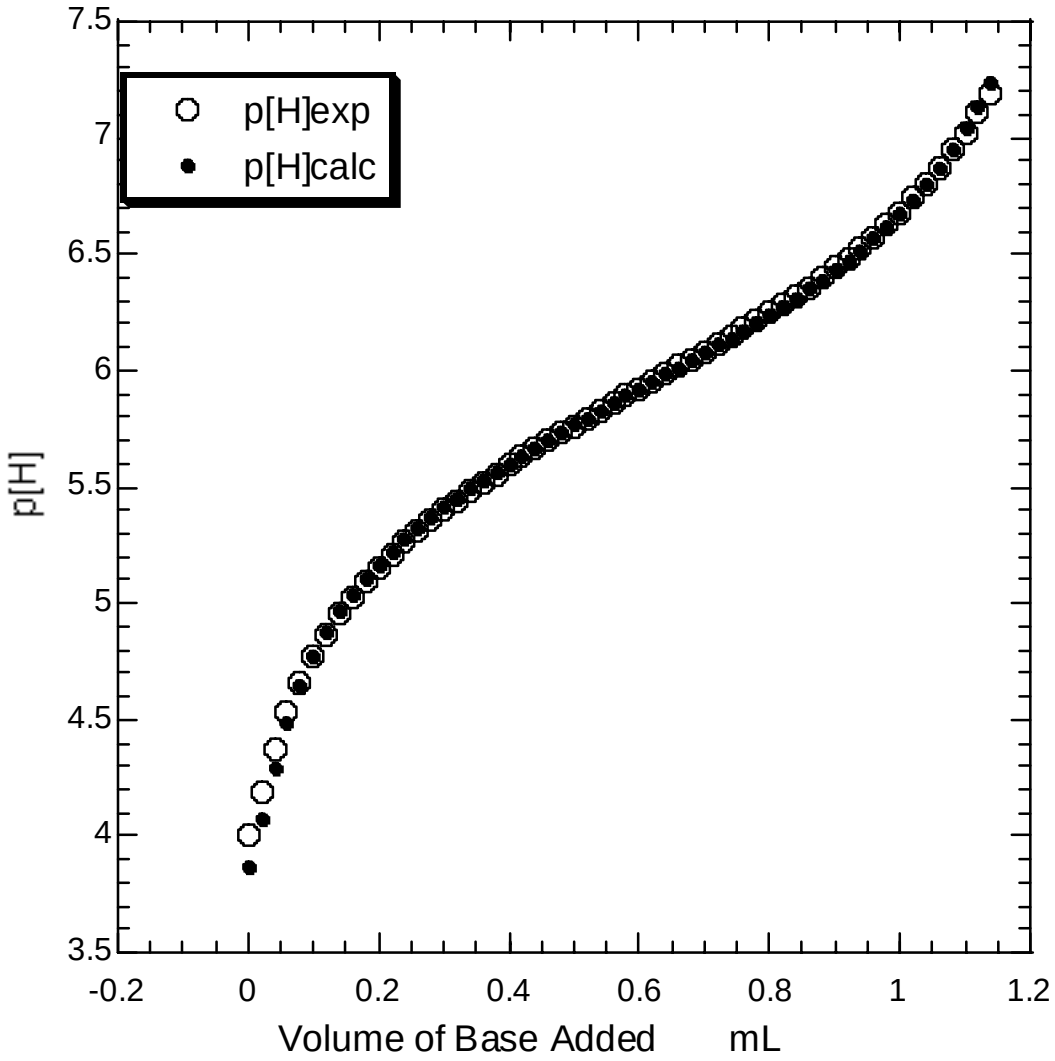


Figure V.21. A potentiometric titration curve for 10.63 mL of a solution containing 1.15 mM salinomycin acid and 1.288 mM zinc perchlorate at an ionic strength of 0.05 M TEAP (25 ^{o}C). The titrant is 0.0108 M Me_4NOH with ionic strength maintained at 0.05 M with TEAP. The calculated p[H] values were obtained using the program BEST and refined values of equilibrium constants for the model containing the species listed in Table V.5.

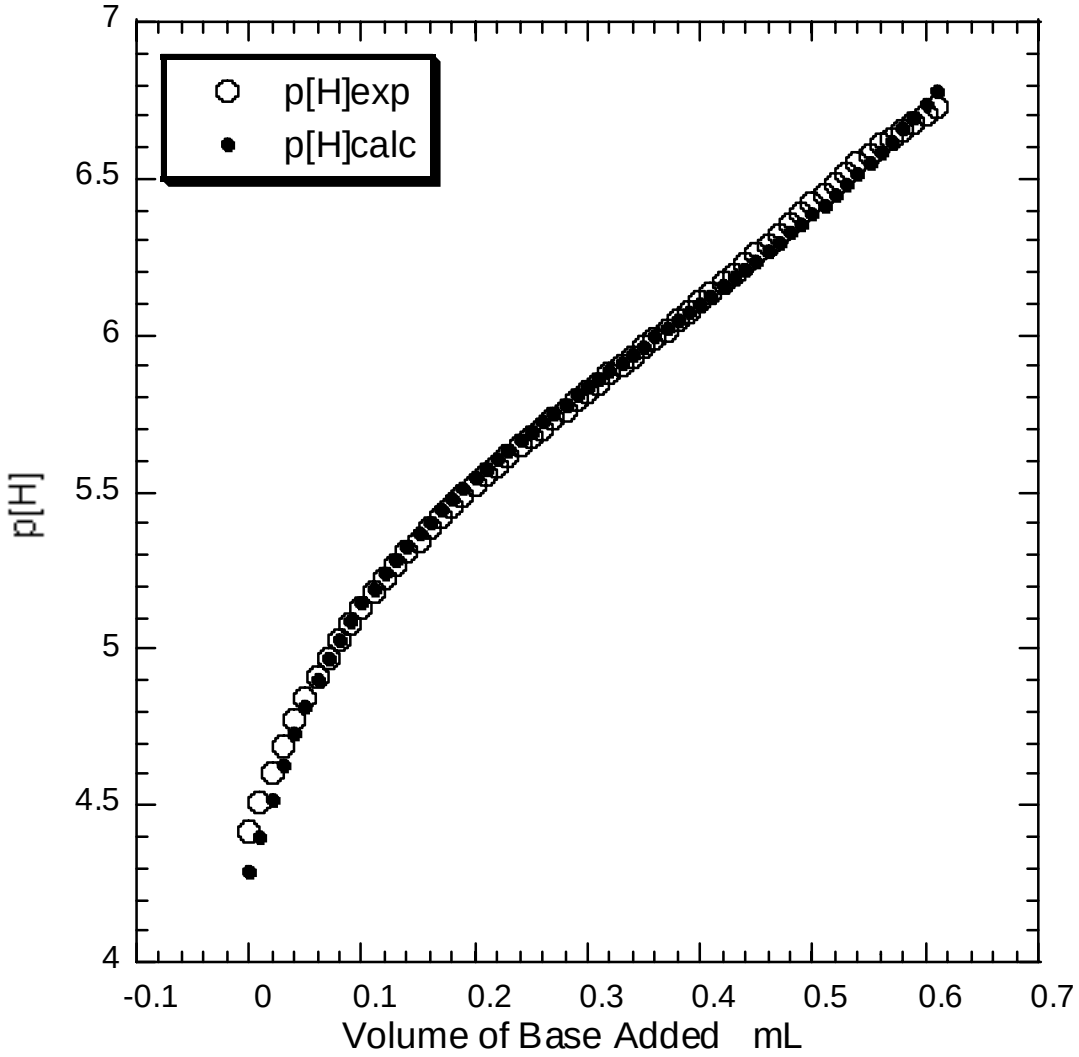


Figure V.22. A potentiometric titration curve for 6.50 mL of a solution containing 0.938 mM salinomycin acid and 1.95 mM zinc perchlorate at an ionic strength of 0.05 M TEAP (25 ^{o}C). The titrant is 0.0108 M Me_4NOH with an ionic strength maintained at 0.05 M

with TEAP. The calculated p[H] values were obtained using the program BEST and refined values of equilibrium constants for the model containing the species listed in Table V.5.

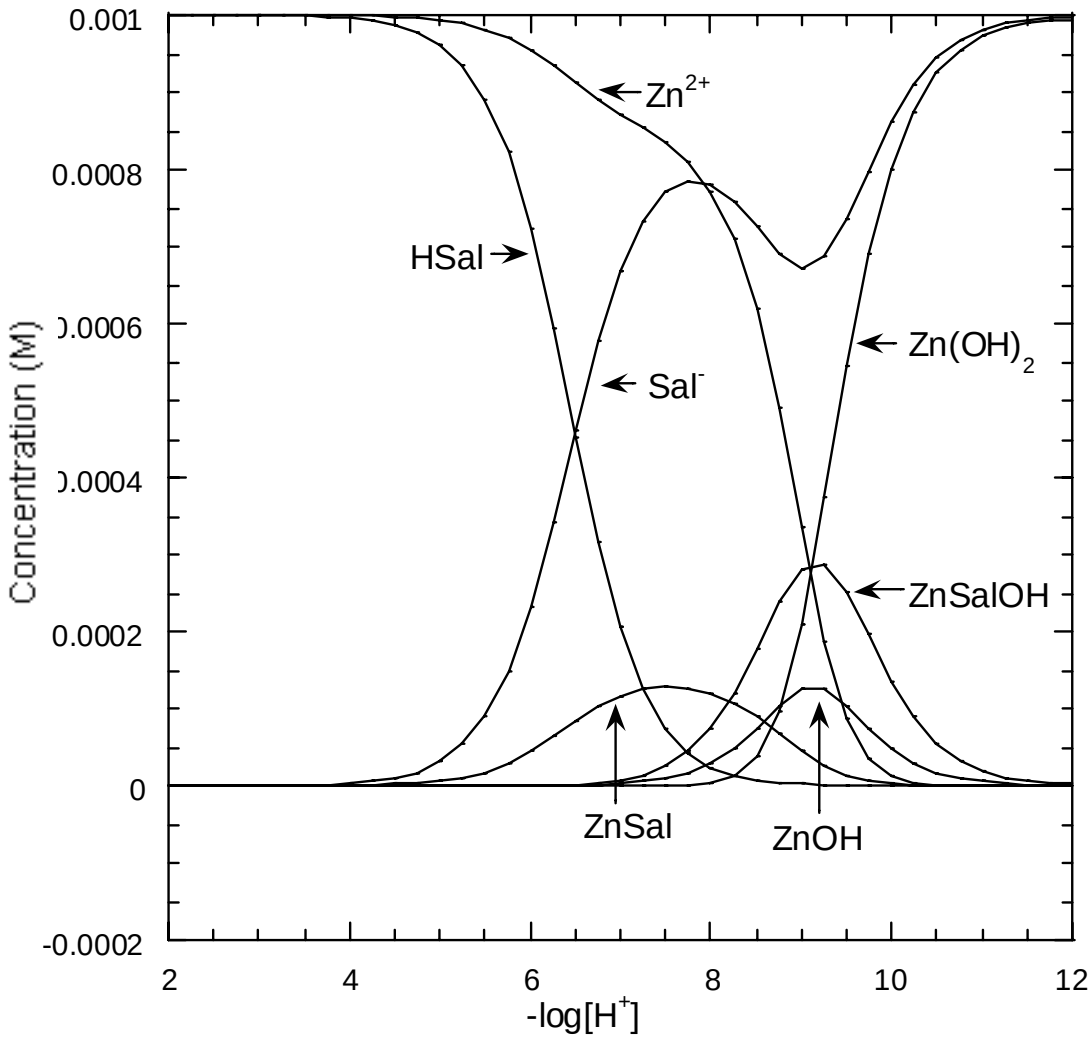


Figure V.23. Species distribution curves for zinc-salinomycin complexes in 80% methanol-water solution as a function of p[H]. Species concentrations were calculated

using the program Comics for 1.0 mM salinomycin and 1.0 mM zinc and the average values of the equilibrium constants listed in Table V.5.

Magnesium-salinomycin

A solution of standardized magnesium perchlorate in 80% methanol-water was added to a solution containing a known concentration of salinomycin acid to provide ligand-metal ratios ranging from 0.22 to 0.30. The titration procedure was described in Section II.E. During data analysis using the program BES, species such as Mg_2Sal, HMg_2Sal, $MgSal_2$, MgSalOH, and MgSal were tested. Only the latter two species were found to exist in solution at significant concentrations. A titration curve is shown in Figure V.24 with the calculated curve obtained using the program BEST. The average values of the stability constants for magnesium-salinomycin complexes were input into the program Comics to generate the species distribution curves shown in Figure V.25. The calculated values of the stability constants of magnesium-salinomycin complexes are listed in Table V.6.

Table V.6. Log β_X values obtained from potentiometric titrations of salinomycin acid (HL) and Mg (II)[a]

Exp. No.	HL-Mg ratio	Identity of complex species X				σ_{fit}[f]
		HL[b]	MgL[c]	MgLOH[c,d]	MgOH[e]	
1	0.22	6.49	2.36	-6.98	-11.9	0.014
2	0.25	6.49	2.75	-7.28	-11.9	0.057
3	0.25	6.49	2.70	-7.14	-11.9	0.040
4	0.30	6.49	2.50	-7.27	-11.9	0.008

[a]25 °C, ionic strength 0.05 M (TEAP). [b]The value of log β was fixed during refinement. [c]The value was refined using the program BEST. [d]β_{MgLOH} is expressed as an acid dissociation constant. [e]The value was fixed during refinement; it was estimated for 80% methanol-water and corrected to 0.05 M ionic strength, as described in Section IV.D. [f]$\sigma_{Fit} = (U/N)^{1/2}$, eq IV.16.

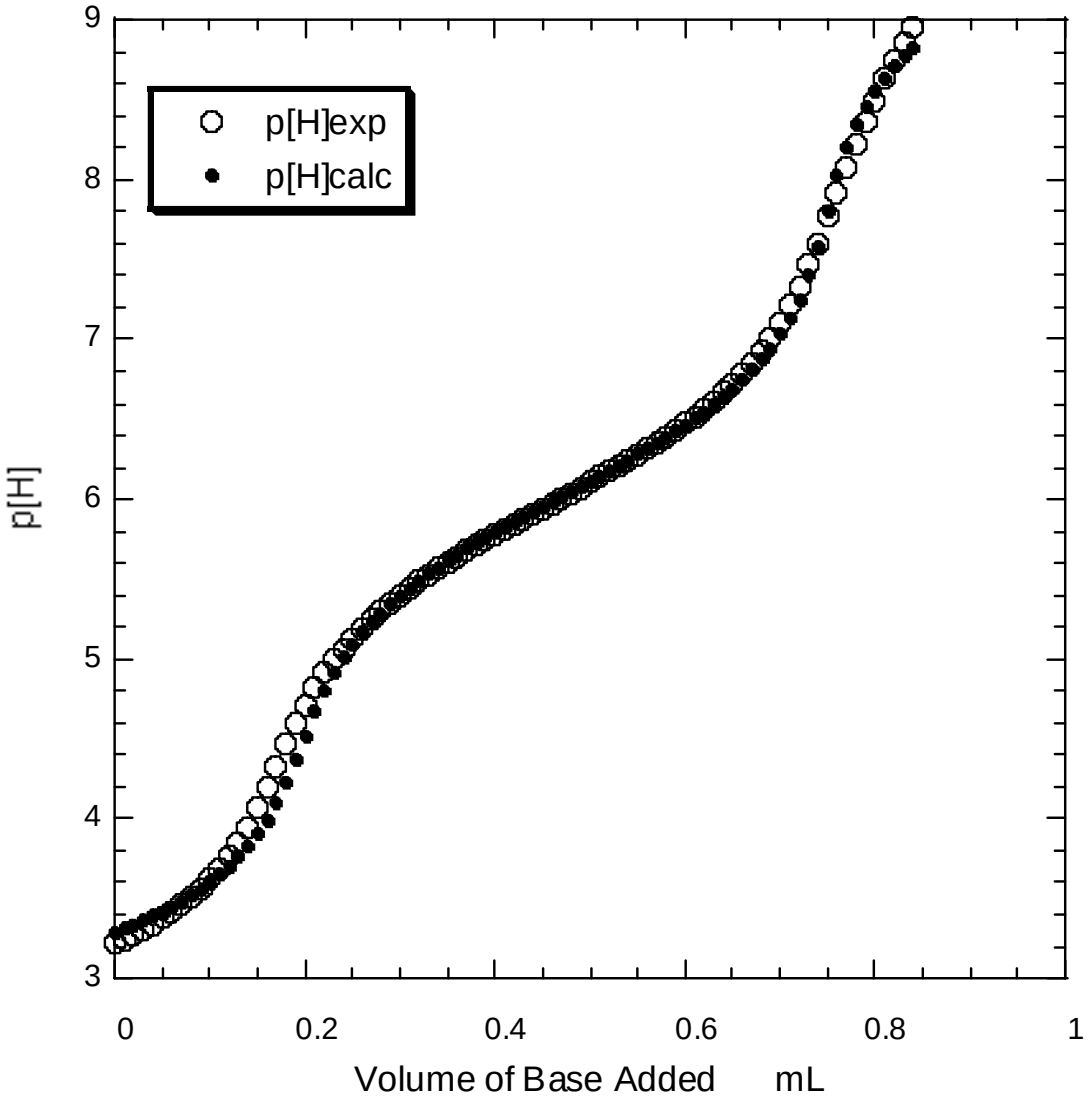

p[H]exp
p[H]calc
p[H]
9
8
7
6
5
4
3
0
0.2
0.4
0.6
0.8
1
Volume of Base Added mL

Figure V.24. A potentiometric titration curve for 6.93 mL of a solution containing 1.09 mM salinomycin acid and 3.54 mM magnesium perchlorate at an ionic strength of 0.05 M TEAP (25 ^{o}C). The titrant is 7.78 M Me_4NOH with an ionic strength maintained at 0.05 M with TEAP. The calculated p[H] values were obtained using the program BEST and refined values of equilibrium constants for the model containing the species listed in Table V.6.

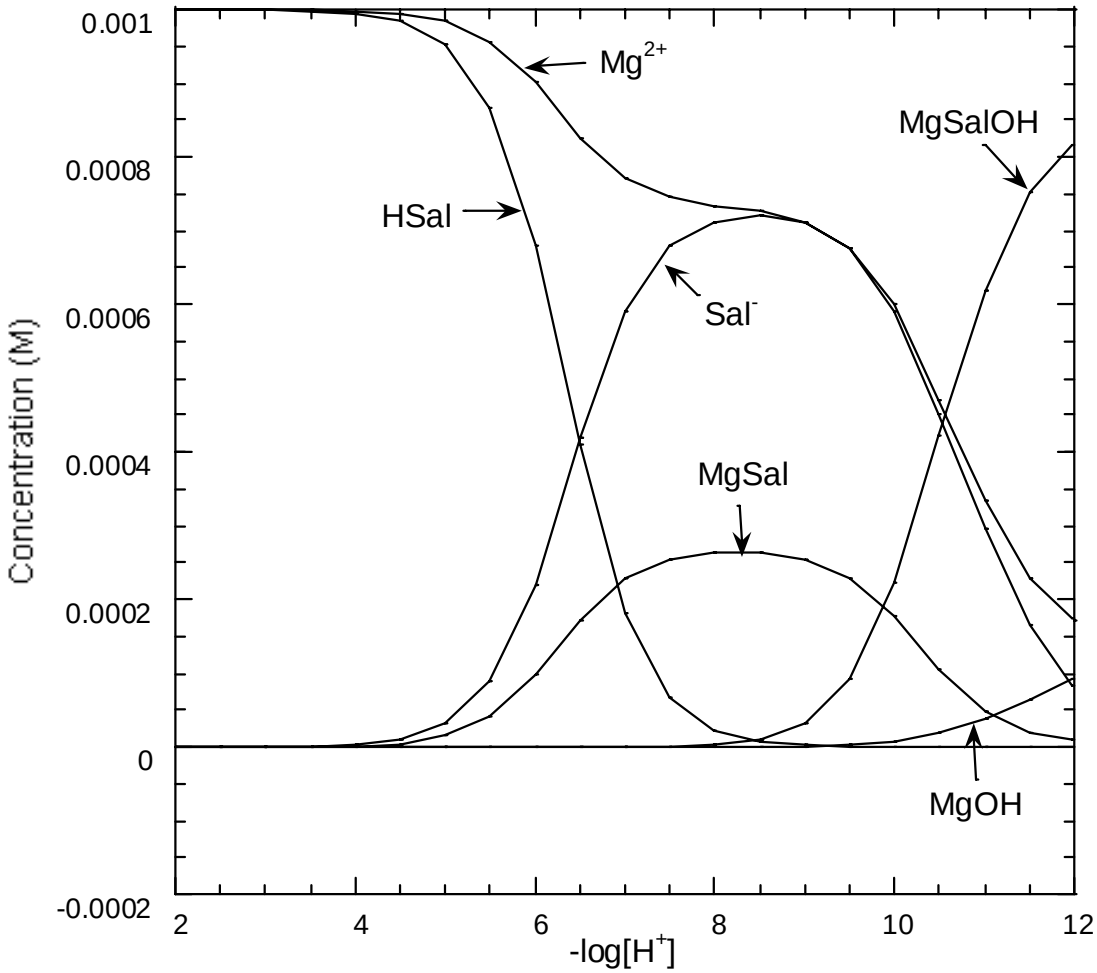


Figure V.25. Species distribution curves for magnesium-salinomycin complexes in 80% methanol-water solution as a function of p[H]. Species concentrations were calculated using the program Comics for 1.0 mM salinomycin and 1.0 mM magnesium and the average values of the equilibrium constants listed in Table V.6.

Lead-salinomycin

A solution of standardized lead perchlorate in 80% methanol-water was added to a solution containing a known concentration of salinomycin acid to provide ligand-metal ratios ranging from 0.6 to 1.8. The titration procedure was described in Section II.E. Figure V.26 shows raw titration data with different Sal/Pb ratios. During data analysis using the program BEST, species such as Pb_2Sal, $PbHSal_2$, $PbSal_2$, PbSalOH, and PbSal were tested. Titration data for pH >8 were not included due to the existence of precipitation. Individual titrations are shown in Figures V.27 and V.28 with the calculated curves obtained using the program BEST. The average stability constants were input into the program Comics to generate species distribution curves for 1.0 mM salinomycin and 0.5 mM lead as shown in Figure V.29 and for 1.0 mM salinomycin and 1.0 mM lead as shown in Figure V.30. The calculated values of the stability constants of lead-salinomycin complexes are listed in Table V.7.

Table V.7. Log β_X values obtained from potentiometric titrations of salinomycin acid (HL) and lead (II) in 80% methanol-water[a]

Exp. No.	HL-Pb ratio	Identity of complex species X							σ_{fit}[f]
		HL[b]	PbL[c]	PbLOH[c,d]	Pb_2L[c]	PbL_2[c]	PbL_2H	PbOH[e]	
1	0.678	6.49	7.13	-0.794	11.28	12.67	17.25	-7.96	.024
2	0.600	6.49	7.05	0.284	11.96	12.78		-7.96	.040
3	0.67	6.49	7.16	0.328	11.59	12.53	18.24	-7.96	.055
4	0.677	6.49	7.05	0.417	11.24			-7.96	.048
5	1.8	6.49	7.20	-0.437	12.81	12.32	18.96	-7.96	.035
6	1.8	6.49	7.31	0.360	11.52	12.48	18.68	-7.96	.044

7	1.8	6.49	7.24	-0.414	12.15	11.58	18.46	-7.96	.035

[a]25 [o]C, ionic strength 0.05 M (TEAP). [b]The value of log β was fixed during refinement. [c]The value was refined using the program BEST. [d]β_{PbLOH} is expressed as an acid dissociation constant. [e]The value was fixed during refinement; it was estimated for 80% methanol-water and corrected to 0.05 M ionic strength, as described in Section IV.D. [f]$\sigma_{Fit} = (U/N)^{1/2}$, eq IV.16.

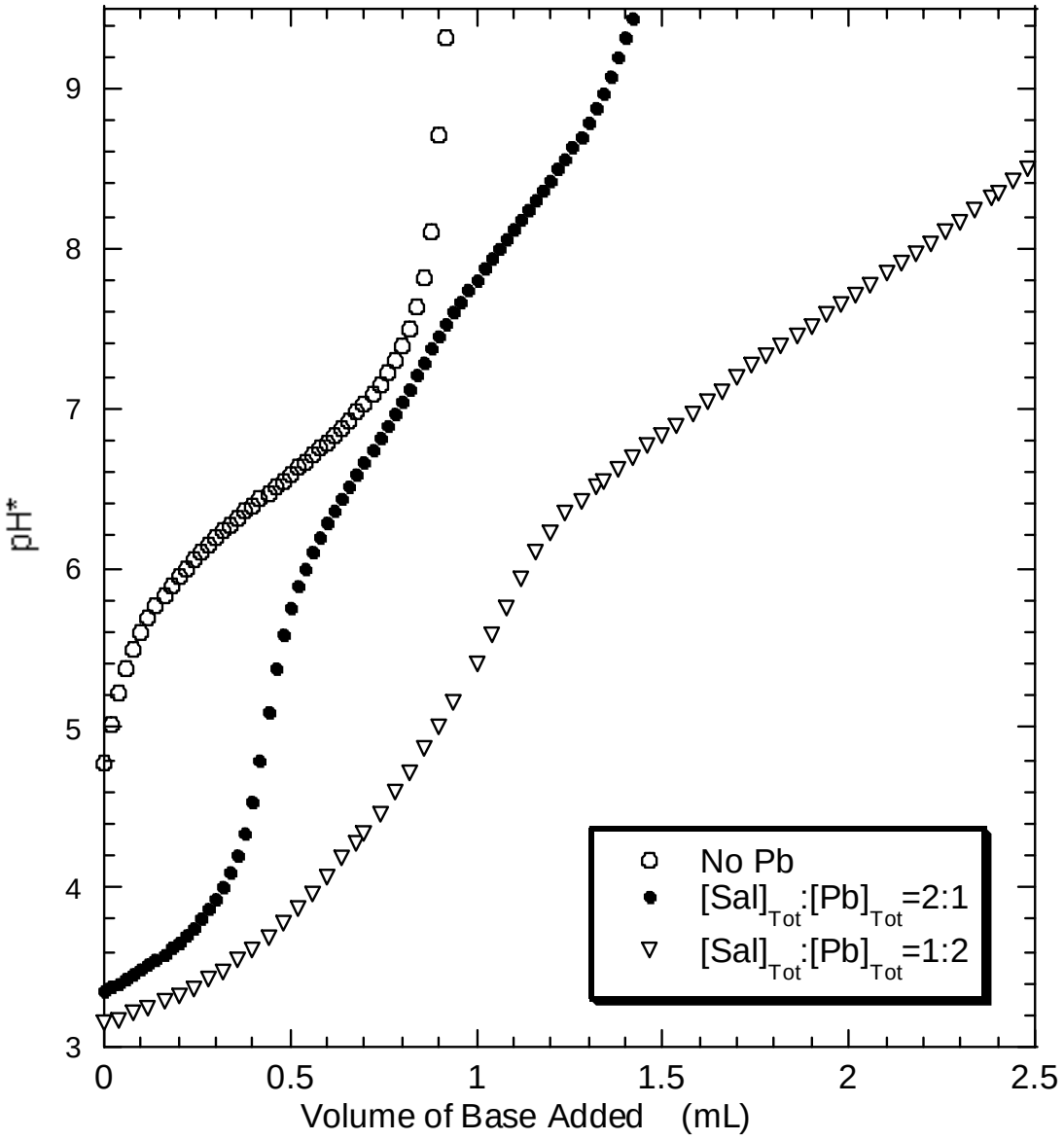


Figure V.26. Potentiometric titration curves for various stoichiometric ratios of lead-salinomycin in 80% methanol-water at 25 ^{o}C. Each solution contained 10.4 mL of 0.9 mM salinomycin acid at an ionic strength of 0.05 M TEAP (25 ^{o}C). The titrant is 0.01 M Me_4NOH with an ionic strength maintained at 0.05 M with TEAP. A solution of 0.0313 M lead perchlorate was added in the required amount to obtain the indicated stoichiometric ratio.

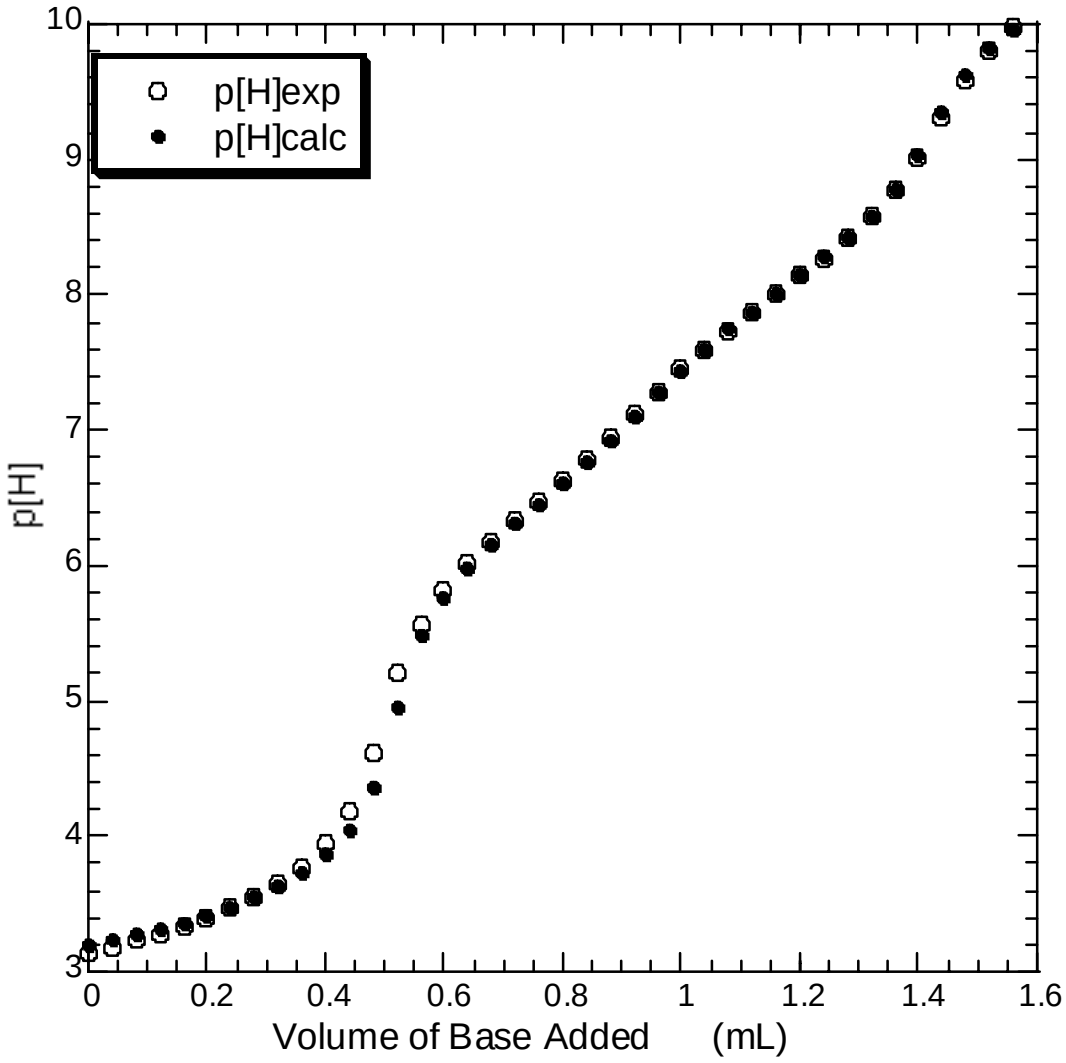


Figure V.27. A potentiometric titration curve for 10.40 mL of a solution containing 0.90 mM salinomycin acid and 0.49 mM lead perchlorate at an ionic strength of 0.05 M TEAP (25 ^{o}C). The titrant is 0.01 M Me_4NOH with ionic strength maintained at 0.05 M with TEAP. The calculated p[H] values were obtained using the program BEST and refined values of equilibrium constants for the model containing the species listed in Table V.7.

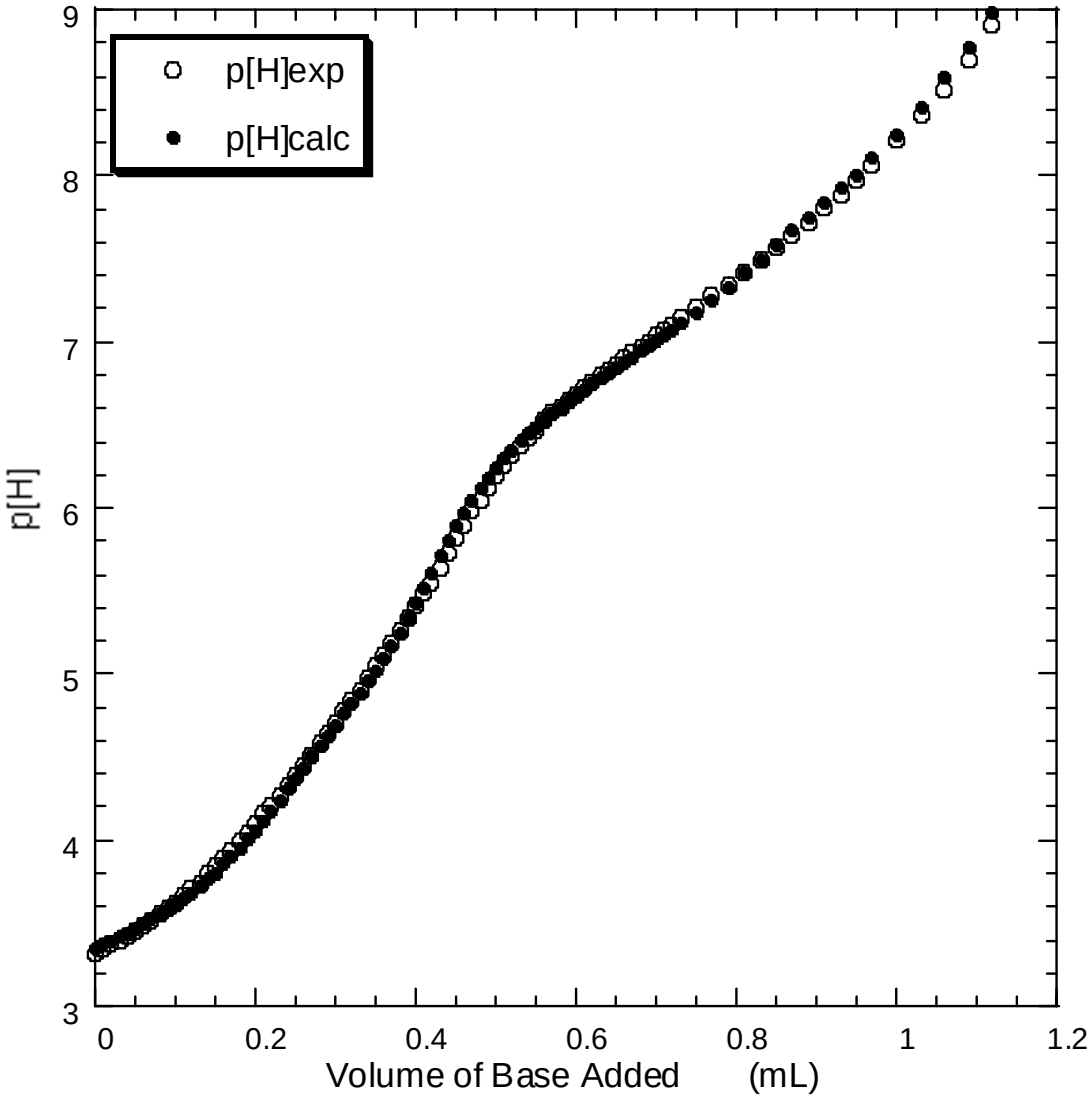


Figure V.28. A potentiometric titration curve for 5.62 mL of a solution containing 0.916 mM salinomycin acid and 1.35 mM lead perchlorate at an ionic strength of 0.05 M TEAP (25 ^{o}C). The titrant is 0.0128 M Me_4NOH with an ionic strength maintained at 0.05 M with TEAP. The calculated p[H] values were obtained using the program BEST and refined values of equilibrium constants for the model containing the species listed in Table V.7.

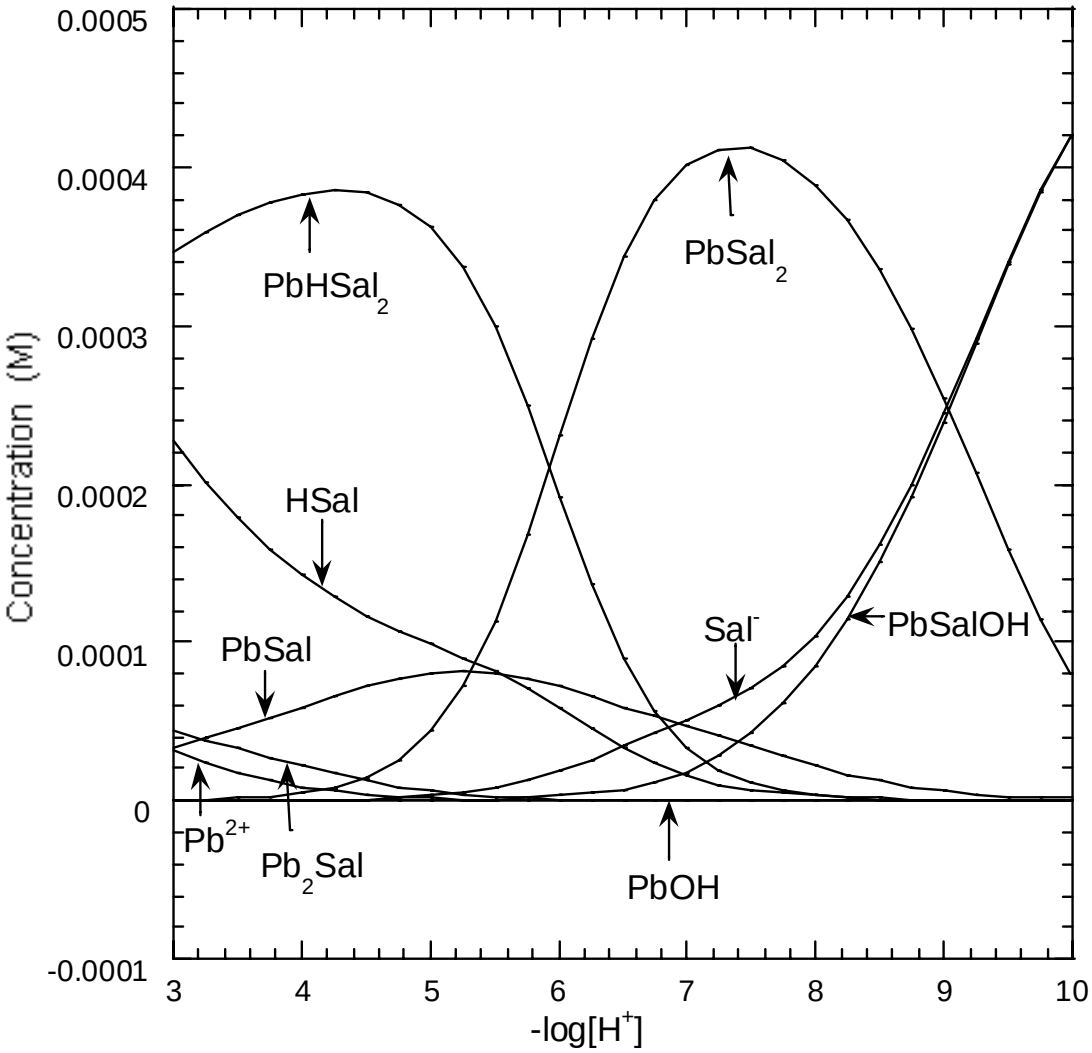


Figure V.29. Species distribution curves for lead-salinomycin complexes as a function of p[H] in 80% methanol-water. Species concentrations were calculated using the program Comics for 1.0 mM salinomycin and 0.5 mM lead and the average values of the equilibrium constants listed in Table V.7.

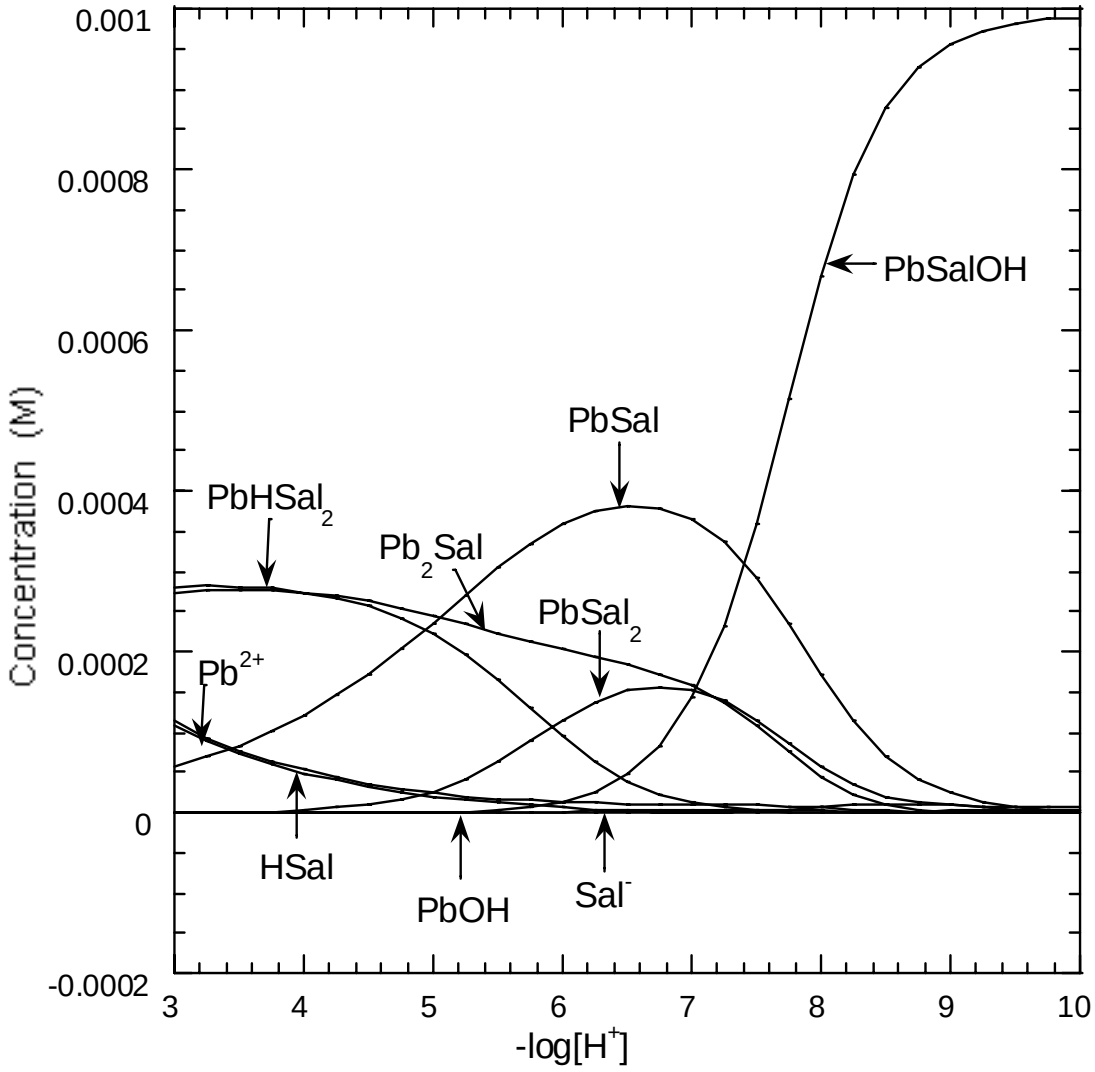


Figure V.30. Species distribution curves for lead (II)-salinomycin complexes in 80% methanol-water solution as a function of p[H]. Species concentrations were calculated using the program Comics for 1.0 mM salinomycin and 1.0 mM lead and the average values of the equilibrium constants listed in Table V.7.

Titrations in the presence of different metal ions are shown together in Figure V.31. As with nigericin, Figure V.28 shows that adding lead with a 2:1 Sal/Pb ratio moves pH of the nigericin acid solution down ~2 units while adding other divalent metal

ions with a 1:1 Sal/Pb ratio doesn't change pH of the salinomycin acid solution very much.

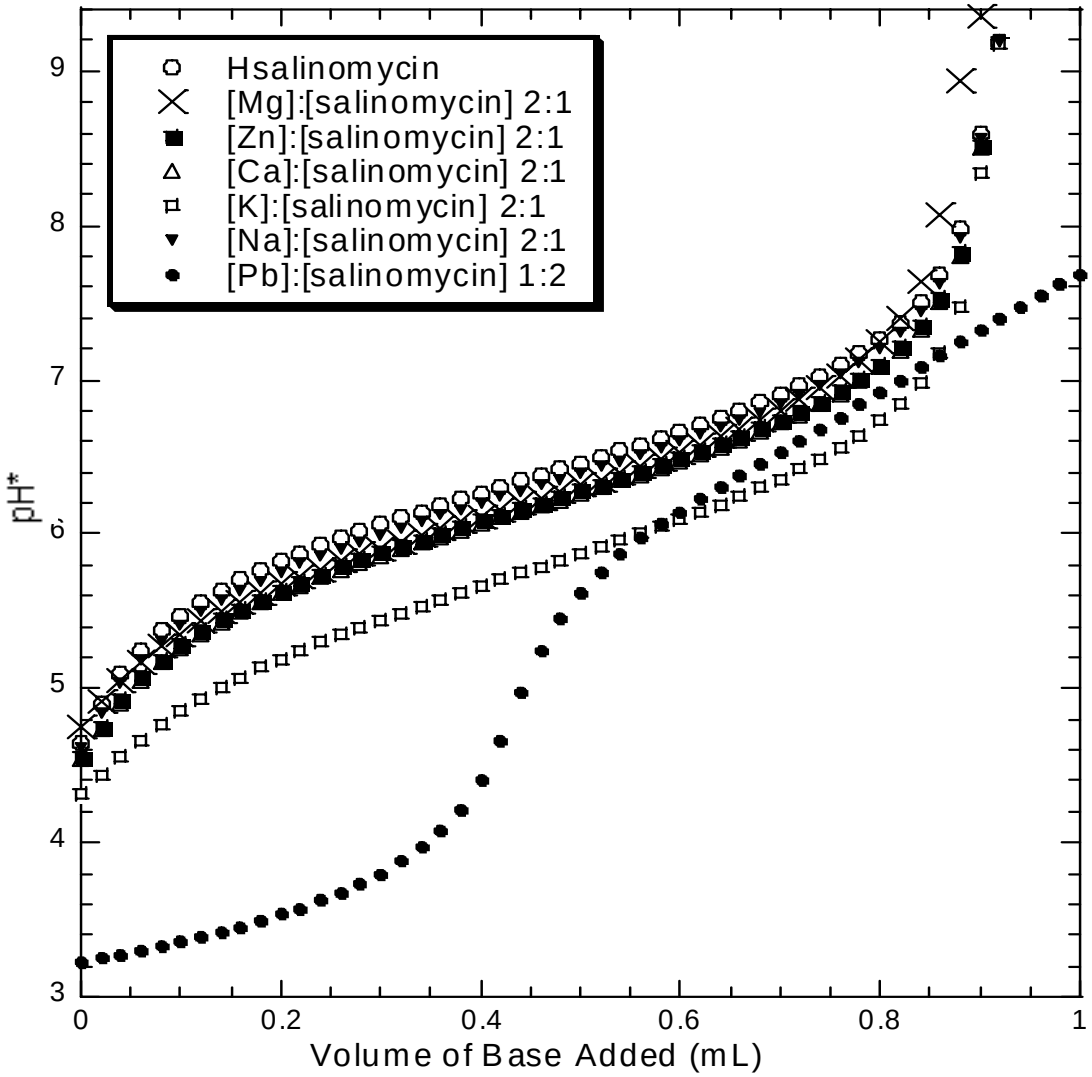


Figure V.31. Potentiometric titration curves for 10.00 mL of a solution containing 0.9 mM salinomycin acid and various metals at an ionic strength of 0.05 M at 25°C. The titrant is 0.01 M Me_4NOH.

The complexation constants for different metal-salinomycin complexes are listed in Table V.8.

Table V.8. Average values of cumulative equilibrium constants (log β_X) for salinomycin with various ions in 80% methanol-water[a]

Ion (M)	Identity of species X [b]				
	ML	ML_2	MLOH[c]	ML_2H	M_2L
H	6.49±0.07	-	-	-	-
Na	-	-	-	-	-
K	3.34±0.1	-	-	-	-
Ca	2.59±0.26	-	-7.79±0.29	-	-
Zn	2.54±0.28	-	-5.69±0.22	-	-
Mg	2.57±0.18	-	-7.17±0.11	-	-
Pb	7.16±0.15	12.39±0.42	-0.26±0.53	18.31±0.65	11.79±1.02

[a] 25°C; ionic strength 0.05 M (TEAP or TEAC). [b] L represents salinomycin ligand.
[c] β_{MLOH} is expressed as an acid dissociation constant.

V.F. NMR studies of free salinomycin and salinomycin complexes.

Peak assignments for the free acid form, sodium salt and tetramethylammonium salt of salinomycin.

NMR spectra were obtained for the free acid form, sodium salt, tetraethylammonium salt, and lead complex of salinomycin in $CDCl_3$ and CD_3OD. As with nigericin, ^{13}C chemical shifts of the sodium salt, lead complex, and free acid form of salinomycin were compared with the salinomycin anion (Et_4N^+ salt) to obtain information about the solution structure for the lead complex. Although NMR spectra of the free acid and sodium salt of salinomycin in several solvents have been reported[5-7], new NMR spectra for those compounds were included in this work to minimize errors caused by different instruments and conditions. The structures of salinomycin and narasin are shown below, using the scheme proposed by Westley[8].

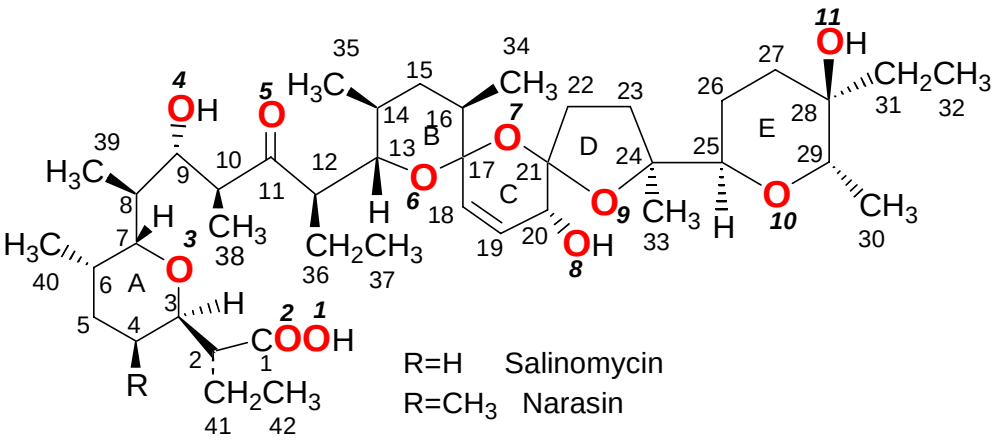


Figure V.32. Structures of salinomycin and narasin molecules with numbering schemes for carbon (plain style) and oxygen (bold italic) atoms.

^1H and ^{13}C spectra were recorded in $CDCl_3$ and CD_3OD for all compounds. 2D NMR (DEPT, HSQC, and HMBC) methods were used to assign peaks in the 1D NMR spectra. The procedure of peak assignment applied to salinomycin is the same as the one described for the nigericin study. NMR spectra of compounds of salinomycin are easier to analyze than those for compounds of nigericin because salinomycin has three more carbons (C11, C18, and C19) in the downfield region (120 ppm-220 ppm) and therefore, provide more correlations in the HMBC spectra. As with nigericin, the three-bond

carbon-proton couplings sometimes appear more intensely than the two-bond couplings in the HMBC spectra of salinomycin compounds, as shown in Table V.9.

Figures V.33-V.36 show spectra of several salinomycin compounds. Tables V.10-V.14 list the ^{1}H and ^{13}C chemical shifts obtained in this work and previously reported for those compounds in several solvents. There are some differences in peak assignments between the values of sodium salinomycin reported and the ones obtained in this work in $CDCl_3$. Two pairs of carbons exchange places (C34 and C35, C36 and C42). All of these carbons atoms have the same multiplicity and are adjacent to each other, or in a similar environment. However, the values obtained in this work match up with the values reported in DMSO[3] and the HMBC spectrum of sodium salinomycin provides strong evidence for the validity of the experimental values.

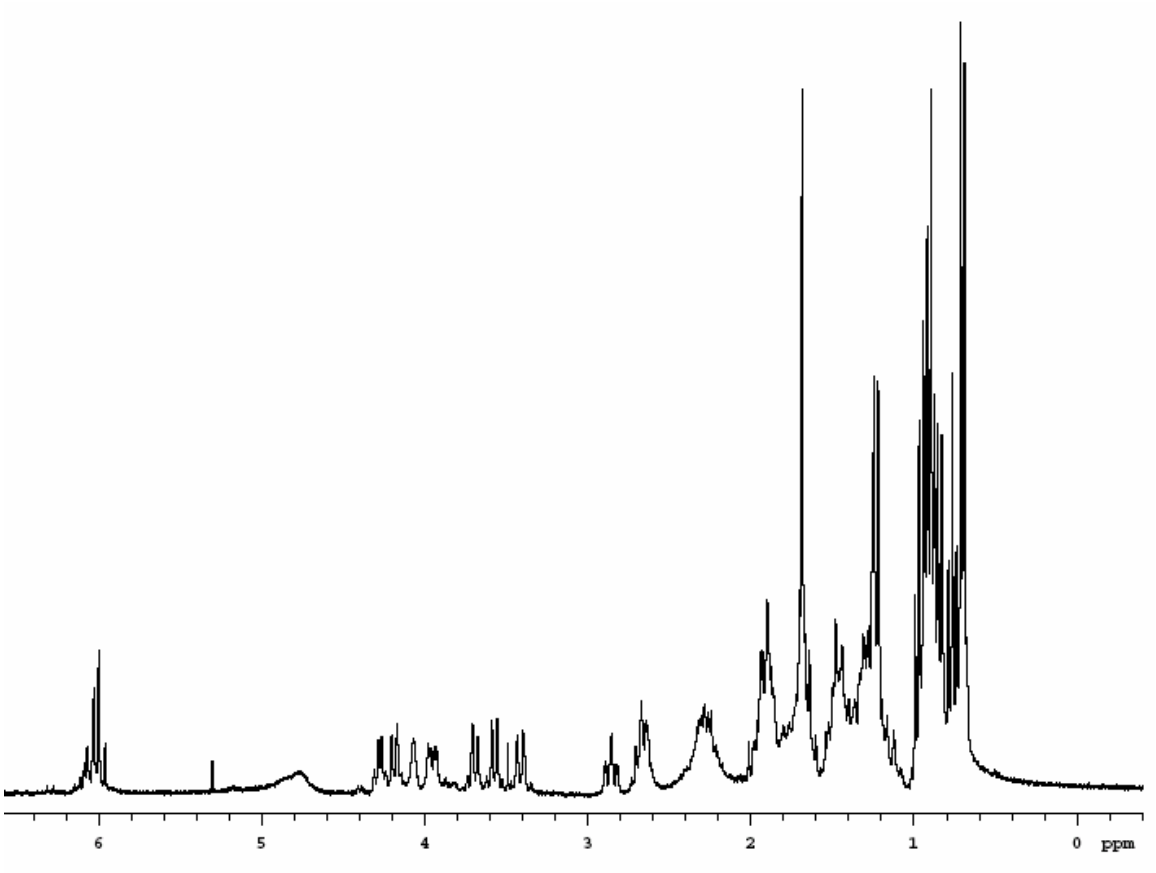


Figure V.33. ^{1}H NMR spectrum of the sodium salt of salinomycin in $CDCl_3$ at 25 ^{o}C.

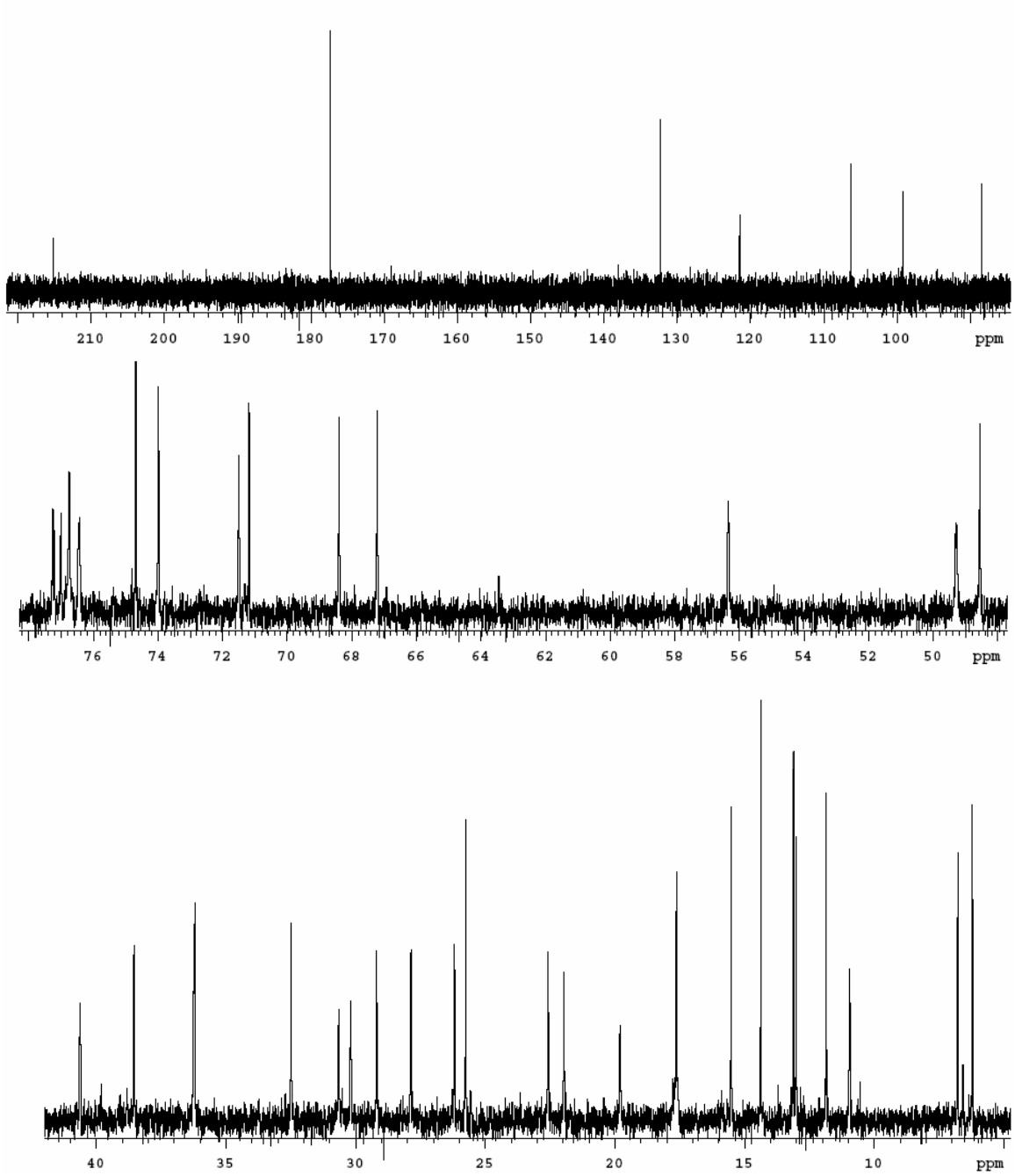


Figure V.34. ^{13}C NMR spectrum of the free acid form of salinomycin in $CDCl_3$ at 25 ^{o}C.

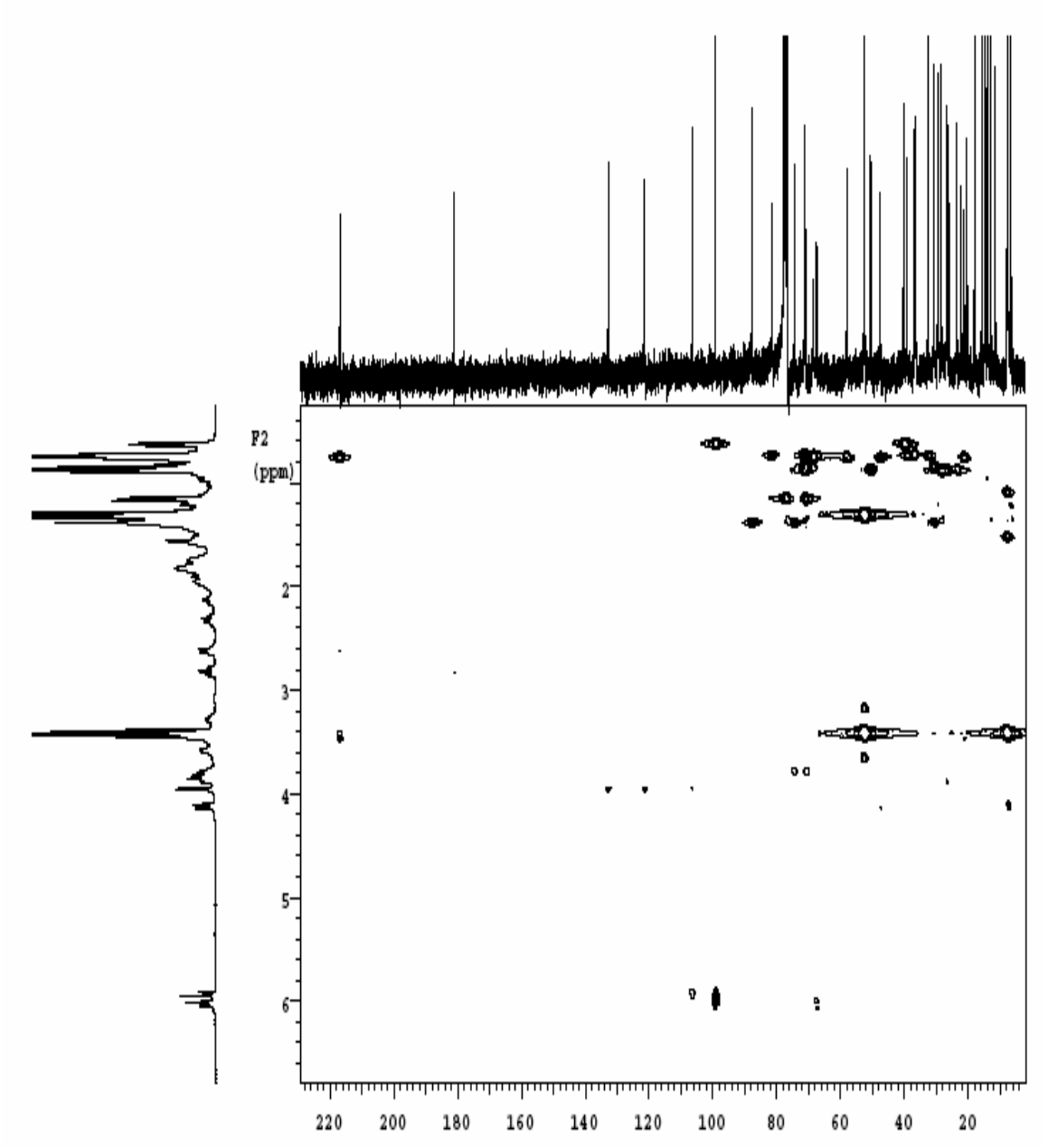


Figure V.35. HMBC spectrum of the tetraethylammonium salt of salinomycin in $CDCl_3$ at 25 ^{o}C.

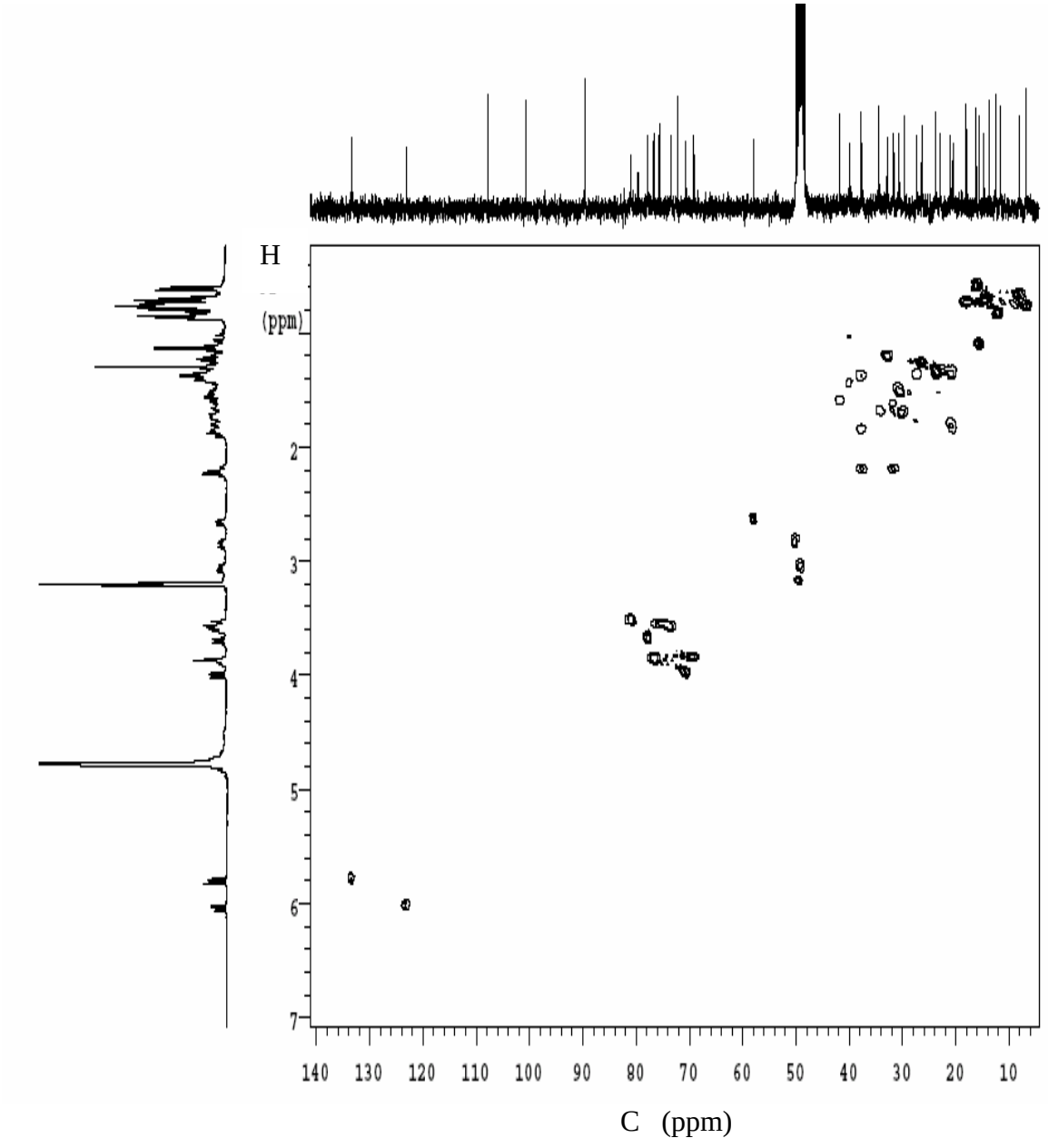


Figure V.36. HSQC spectrum of the free acid form of salinomycin in CD_3OD at 25 ^oC.

Table V.9. Different C-H coupling behavior shown in HMBC spectrum (Figure V.35) of the tetraethylammonium salt of salinomycin in $CDCl_3$ at 25 ^oC.

carbon #	carbon connectivity	three-bond coupling	two-bond coupling	two-bond coupling missing
1	COOH	4	2	
2	CH	42		41
3	CH-O		2, 4	
4	CH_2	40	3	
5	CH_2	3		4
6	CH		40	
7	CH-O	9, 39, 40		6, 8
8	CH		7, 39	
9	CH-O	38, 39 (strong)	10 (weak)	
10	CH		9, 38	
11	C=O	13, 38 (strong)	10, 12 (weak)	
12	CH	37, 10 (strong)	36 (weak)	
13	CH-O	35 (strong)	12 (weak)	
14	CH	12,	35	13, 15
15	CH_2	34, 35		14, 15
16	CH		34	15
17	O-C-O	19, 34	18	16
18	CH=CH	20		19
19	CH=CH	20	18 (weak)	
20	CH-OH	18		19
21	O-C-O	19 (strong)	20 (weak)	22
22	CH_2	20		23
23	CH_2	33		22
24	C-O		23, 25, 33	
25	CH-O	27, 33, 29		26
26	CH_2	33, 30 (strong)	25 (weak)	
28	C-OH	30, 32 (strong)	29, 31	
29	CH-O		30	
30	CH_3	25		29
31	CH_2		32	
32	CH_3		31	
36	CH_2	13 (strong)	12, 37	
37	CH_3	12	36	
38	CH_3		10	
39	CH_3	9		8
40	CH_3	7		6
41	CH_2		2, 42	
42	CH_3		41	

Table V.10. ^{1}H and ^{13}C NMR chemical shifts (ppm) of sodium salinomycin in $CDCl_3$ using a Varian 500 MHz spectrometer and literature values at 25 ^{o}C.

carbon #	carbon connectivity	^{13}C experimental	^{1}H experimental	^{13}C literature[9]	^{1}H literature[6]
1	COOH	184.961		184.8	
2	CH	51.07	2.80	51.1	2.86
3	CH-O	75.871	3.89	75.8	3.94
4	CH_2	19.821	1.40,1.85	19.7	1.89
5	CH_2	26.779	1.40,1.85	26.8	1.41
6	CH	27.952	1.40	28.0	1.78
7	CH-O	71.310	3.73	75.6	3.70
8	CH	35.792	1.4	32.5	1.45
9	CH-O	67.791	4.1	67.8	4.21
10	CH	49.627	2.61	49.6	2.67
11	C=O	217.79		217.6	
12	CH	55.609	2.64	55.5	2.67
13	CH-O	75.470	3.61	71.3	3.54
14	CH	32.360	1.6	35.9	1.71
15	CH_2	38.575	1.46	38.6	1.13, 1.66
16	CH	40.535	1.64	40.6	1.71
17	O-C-O	98.981		99.1	
18	CH=CH	122.048	6.02	122.1	5.99
19	CH=CH	130.638	5.95	130.8	6.05
20	CH-OH	66.559	3.99	66.6	4.05
21	O-C-O	107.010		107.1	
22	CH_2	36.433	1.89,2.30	36.1	1.90, 2.32
23	CH_2	32.462	1.63,1.89	32.5	1.90, 1.90
24	C-O	88.293		88.3	
25	CH-O	74.618	3.5	74.6	3.42
26	CH_2	19.821	1.55,1.86	19.9	1.37, 2.21
27	CH_2	29.234	1.55,1.83	29.1	1.51, 1.73
28	C-OH	70.268		70.5	
29	CH-O	76.446	4.18	76.5	4.29
30	CH_3	14.634	1.21	14.7	1.23
31	CH_2	32.127	1.24	32.1	1.30
32	CH_3	6.444	0.83	6.5	0.90
33	CH_3	27.646	1.63	27.7	1.70
34	CH_3	15.770	0.65	17.6	0.70
35	CH_3	17.519	0.82	15.7	0.89
36	CH_2	15.552	1.28	23.7	1.33, 1.92
37	CH_3	13.104	0.73	12.4	0.76
38	CH_3	12.011	0.79	12.1	0.85
39	CH_3	6.707	0.65	6.8	0.70
40	CH_3	10.677	0.88	10.7	0.92
41	CH_2	23.566	1.20	15.7	1.30, 1.50
42	CH_3	12.397	0.93	13.2	0.96

Table V.11. ^{1}H and ^{13}C chemical shifts (ppm) of sodium salinomycin using a Varian 300 MHz spectrometer and literature values using a 500 MHz spectrometer at 25 ^{o}C.

carbon #	carbon connectivity	^{13}C CD_3OD experimental	^{1}H CD_3OD experimental	^{1}H DMSO literature[7]	^{13}C DMSO literature[7]
1	COOH	184.354			181.50
2	CH	51.958	2.80	2.66	49.68
3	CH-O	77.686	3.82	3.69	75.06
4	CH_2	21.128	1.4,1.82	1.35,1.76	19.66
5	CH_2	27.614	1.3,1.80	1.38,1.79	26.29
6	CH	29.507	1.72	1.71	27.40
7	CH-O	72.945	3.48	3.61	70.39
8	CH	37.277	1.40	1.30	35.60
9	CH-O	69.836	4.18	4.04	66.79
10	CH	50.120	2.75	2.70	48.38
11	C=O	217.815			215.33
12	CH	56.930	2.7	2.67	54.86
13	CH-O	77.191	3.50	3.56	75.69
14	CH	33.942	1.68	1.67	32.02
15	CH_2	39.723	1.06,1.56	1.11,1.62	38.14
16	CH	41.788	1.60	1.61	39.98
17	O-C-O	100.326			98.31
18	CH=CH	124.191	6.12	6.03	122.04
19	CH=CH	131.740	5.88	5.73	130.42
20	CH-OH	67.667	3.97	3.99	65.04
21	O-C-O	107.736			105.92
22	CH_2	37.432	1.82,2.14	1.82,2.12	35.97
23	CH_2	33.060	1.82,1.94	1.79,1.91	31.88
24	C-O	89.354			87.40
25	CH-O	75.655	3.65	3.41	73.75
26	CH_2	21.510	1.32,1.8	1.27,2.13	19.31
27	CH_2	30.400	1.52,1.56	1.47,1.51	28.70
28	C-OH	72.110			69.32
29	CH-O	77.854	4.05	4.00	75.69
30	CH_3	15.103	1.15	1.17	14.45
31	CH_2	32.788	1.25	1.20	31.59
32	CH_3	6.867	0.82	0.83	6.22
33	CH_3	27.812	1.52	1.56	26.81
34	CH_3	16.210	0.64	0.65	15.63
35	CH_3	17.906	0.82	0.85	17.33
36	CH_2	17.784	1.2,1.35	1.28,1.84	15.72
37	CH_3	13.613	0.73	0.73	12.85
38	CH_3	13.332	0.76	0.74	12.48
39	CH_3	7.483	0.665	0.63	6.69
40	CH_3	11.453	0.85	0.86	10.81
41	CH_2	24.442	1.32	1.15,1.31	23.04
42	CH_3	12.997	0.86	0.82	12.36

Table V.12. ^{1}H and ^{13}C experimental chemical shifts (ppm) of the free acid form of salinomycin using a Varian 500 MHz spectrometer and literature values in $CDCl_3$.

carbon #	carbon connectivity	^{13}C experimental	^{1}H experimental	^{13}C literature[5]	^{1}H literature[6]
1	COOH	177.283		177.2	
2	CH	48.554	2.65	48.9	2.90
3	CH-O	74.5	4.0	74.9	3.98
4	CH_2	19.482	0.64,1.6	20.1	1.93
5	CH_2	25.937	1.6	26.4	1.60
6	CH	27.604	1.66	28.0	1.83
7	CH-O	70.87	3.44	75.2	3.64
8	CH	36.097	1.25	32.6	1.47
9	CH-O	68.134	3.91	68.7	4.16
10	CH	49.014	2.65	49.2	2.75
11	C=O	215.453		214.5	
12	CH	56.162	2.37	56.5	2.63
13	CH-O	77.196	3.55	71.7	3.88
14	CH	32.335	1.64	36.5	1.72
15	CH_2	38.413	0.85,1.4	38.6	1.09, 1.61
16	CH	40.368	1.5	40.7	1.71
17	O-C-O	98.96		99.2	
18	CH=CH	121.136	5.90	121.6	5.98
19	CH=CH	132.098	5.85	132.4	6.03
20	CH-OH	67.072	3.75	67.2	3.98
21	O-C-O	106.015		106.4	
22	CH_2	36.013	1.75,2.15	36.2	2.09, 2.40
23	CH_2	29.859	1.60,2.05	30.2	1.84, 2.23
24	C-O	88.174		88.5	
25	CH-O	73.723	3.75	73.7	3.93
26	CH_2	21.722	1.50	21.9	1.54, 1.62
27	CH_2	29.051	1.56	29.3	
28	C-OH	71.231		70.9	
29	CH-O	76.22	3.65	77.2	3.83
30	CH_3	14.138	0.99	14.5	1.24
31	CH_2	30.601	1.20	30.6	1.32, 1.39
32	CH_3	5.964	0.61	6.3	0.89
33	CH_3	25.508	1.23	25.8	1.48
34	CH_3	15.288	0.41	17.9	0.70
35	CH_3	17.399	0.59	15.6	0.90
36	CH_2	17.487	1.3,1.8	22.7	1.39, 1.93
37	CH_3	12.775	0.48	11.9	0.76
38	CH_3	12.86	0.51	12.8	0.81
39	CH_3	6.469	0.47	7.0	0.72
40	CH_3	10.608	0.65	11.2	0.94
41	CH_2	22.359	1.30	16.6	1.40, 1.54
42	CH_3	11.606	0.67	13.2	0.95

Table V.13. ^{1}H and ^{13}C experimental chemical shifts (ppm) of the free acid form of salinomycin using a Varian 500 MHz spectrometer in CD_3OD.

carbon #	carbon connectivity	^{13}C	^{1}H
1	COOH	179.501	
2	CH	50.01	2.83
3	CH-O	76.695	3.85
4	CH_2	20.997	1.34
5	CH_2	27.345	1.34,1.72
6	CH	29.694	1.7
7	CH-O	73.485	3.56
8	CH	37.804	1.37
9	CH-O	70.641	3.98
10	CH	49.32	3.05
11	C=O	217.418	
12	CH	57.940	2.64
13	CH-O	81.007	3.5
14	CH	34.420	1.67
15	CH_2	39.986	1.0,1.42
16	CH	41.755	1.59
17	O-C-O	100.616	
18	CH=CH	123.029	6.04
19	CH=CH	133.394	5.8
20	CH-OH	69.166	3.84
21	O-C-O	107.764	
22	CH_2	37.623	1.84,2.19
23	CH_2	31.656	1.66,2.18
24	C-O	89.643	
25	CH-O	75.647	3.54
26	CH_2	23.006	1.50
27	CH_2	30.595	1.54
28	C-OH	72.257	
29	CH-O	77.816	3.67
30	CH_3	15.605	1.10
31	CH_2	32.878	1.2
32	CH_3	6.834	0.76
33	CH_3	26.404	1.26
34	CH_3	16.165	0.58
35	CH_3	18.041	0.74
36	CH_2	20.530	1.80
37	CH_3	13.696	0.72
38	CH_3	14.744	0.72
39	CH_3	8.143	0.66
40	CH_3	11.687	0.82
41	CH_2	23.781	1.32
42	CH_3	12.441	0.82

Table V.14. ^{1}H and ^{13}C NMR chemical shifts (ppm) of tetraethylammonium salt of salinomycin in CD_3OD and $CDCl_3$ at 25 ^{o}C (experimental values).

carbon #	carbon connectivity	^{13}C $CDCl_3$	^{1}H $CDCl_3$	^{13}C CD_3OD	^{1}H CD_3OD
1	COOH	180.854		183.505	
2	CH	50.322	2.82	51.786	2.80
3	CH-O	76.429	3.89	77.623	3.8
4	CH_2	20.087	1.38, 1.82	21.311	1.37
5	CH_2	26.568	1.38	27.512	1.28, 1.8
6	CH	28.137	1.74	29.661	1.72
7	CH-O	70.966	3.83	72.857	3.72
8	CH	36.573	1.42	37.884	1.44
9	CH-O	68.291	4.13	70.708	4.17
10	CH	47.286	3.26	49.23	2.94
11	C=O	216.642		217.051	
12	CH	57.791	2.62	57.933	2.72
13	CH-O	81.305	3.44	80.800	3.25
14	CH	32.322	2.0	34.840	1.71
15	CH_2	38.943	1.43	40.173	1.0, 1.44
16	CH	40.017	1.72	41.815	1.62
17	O-C-O	98.972		100.683	
18	CH=CH	121.178	6.00	123.322	6.06
19	CH=CH	132.538	5.95	133.200	5.80
20	CH-OH	67.289	3.95	69.447	3.86
21	O-C-O	106.261		107.684	
22	CH_2	36.199	1.94, 2.30	37.550	1.90, 2.18
23	CH_2	30.520	1.79, 2.13	31.823	1.66, 2.18
24	C-O	87.592		89.256	
25	CH-O	74.190	3.58	75.554	3.49
26	CH_2	21.910	1.42, 1.52	22.786	1.30, 1.54
27	CH_2	29.051	1.56	30.595	1.54
28	C-OH	70.699		72.270	
29	CH-O	76.777	3.78	77.883	3.74
30	CH_3	14.521	1.15	15.471	1.12
31	CH_2	30.520	1.27	32.818	1.24
32	CH_3	6.305	0.84	6.848	0.78
33	CH_3	25.854	1.38	26.310	1.29
34	CH_3	15.542	0.62	16.185	0.60
35	CH_3	17.785	0.73	18.541	0.76
36	CH_2	21.015	1.82	20.577	1.80
37	CH_3	13.533	0.75	13.516	0.75
38	CH_3	14.094	0.75	14.830	0.75
39	CH_3	7.226	0.72	7.949	0.66
40	CH_3	11.231	0.86	11.927	0.76
41	CH_2	23.264	1.40	24.401	1.17, 1.31
42	CH_3	12.632	0.86	13.002	0.84
1' (Et_4N^+)	CH_2	52.338	3.42	53.342	3.20
2' (Et_4N^+)	CH_3	7.553	1.30	7.715	1.18

NMR peak assignments in the lead-salinomycin (1:2) complex

The lead-salinomycin (1:2) complex ($PbSal_2$) was prepared using the reaction of lead oxide and the acid form of salinomycin in methanol and the elemental composition was confirmed by commercial elementary analysis. The lead-salinomycin (1:2) complex (5 mg $PbSal_2$) was dissolved in 0.5 mL CD_3OD or (10 mg $PbSal_2$) in distilled $CDCl_3$. Solids were removed by centrifugation. The spectra (^1H NMR, ^{13}C NMR, HMBC, and HSQC) of the lead-salinomycin (1:2) complex in both solvents were obtained at 25^oC using a Varian 300 MHz spectrometer. As found for the lead-nigericin (1:2) complex, ^1H and ^{13}C NMR peaks of the lead salinomycin complex obtained in $CDCl_3$ have lower resolution than those in CD_3OD although the lead complex has higher solubility in $CDCl_3$ than in CD_3OD. Both ^1H and ^{13}C peaks for the lead-salinomycin (1:2) complex in both solvents are broader than those for the free acid form of salinomycin and the other salts of salinomycin.

The strategy for peak assignment is the same as the one applied to the lead nigericin complex. All spectra of the lead-salinomycin complex are shown in Figures V.37-V.44. Due to the limited solubility of the lead complex, no acceptable DEPT spectrum was obtained. Some peaks in the upfield regions in the HSQC spectrum were not well resolved for the lead salinomycin complex in $CDCl_3$, as shown in Figure V.40. Therefore, HMBC is used to identify chemical shifts for hydrogen atoms attached to those carbons in the upfield regions of the HSQC spectrum obtained in $CDCl_3$. HMBC is also used to obtain chemical shifts for the quaternary carbon atoms C1 and C11 that do not appear in ^{13}C NMR as shown in Figure V.38. The ^1H and ^{13}C chemical shifts obtained in $CDCl_3$ and CD_3OD are listed in Table V.15.

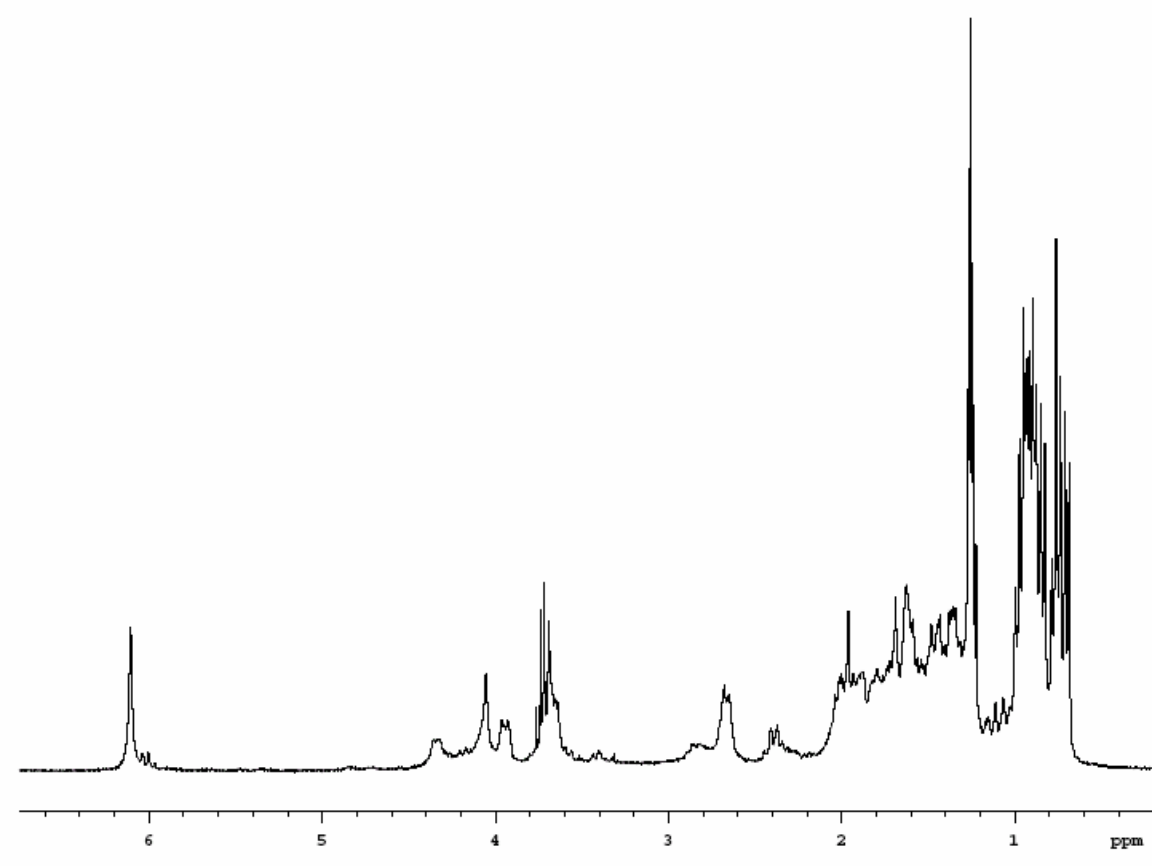


Figure V.37. ^{1}H NMR spectrum of the lead-salinomycin (1:2) complex in $CDCl_3$.

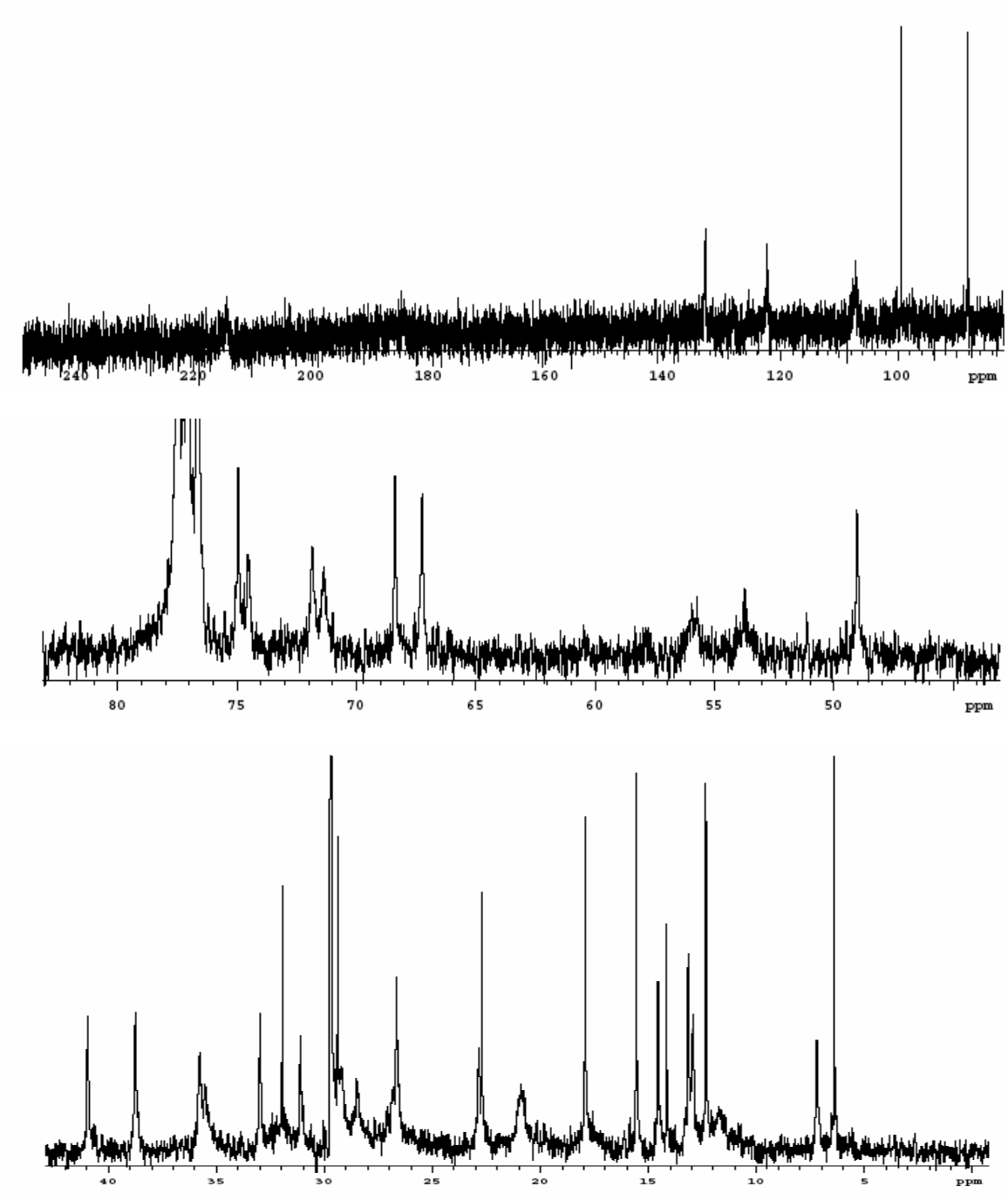


Figure V.38. ^{13}C NMR spectrum of the lead-salinomycin (1:2) complex in $CDCl_3$.

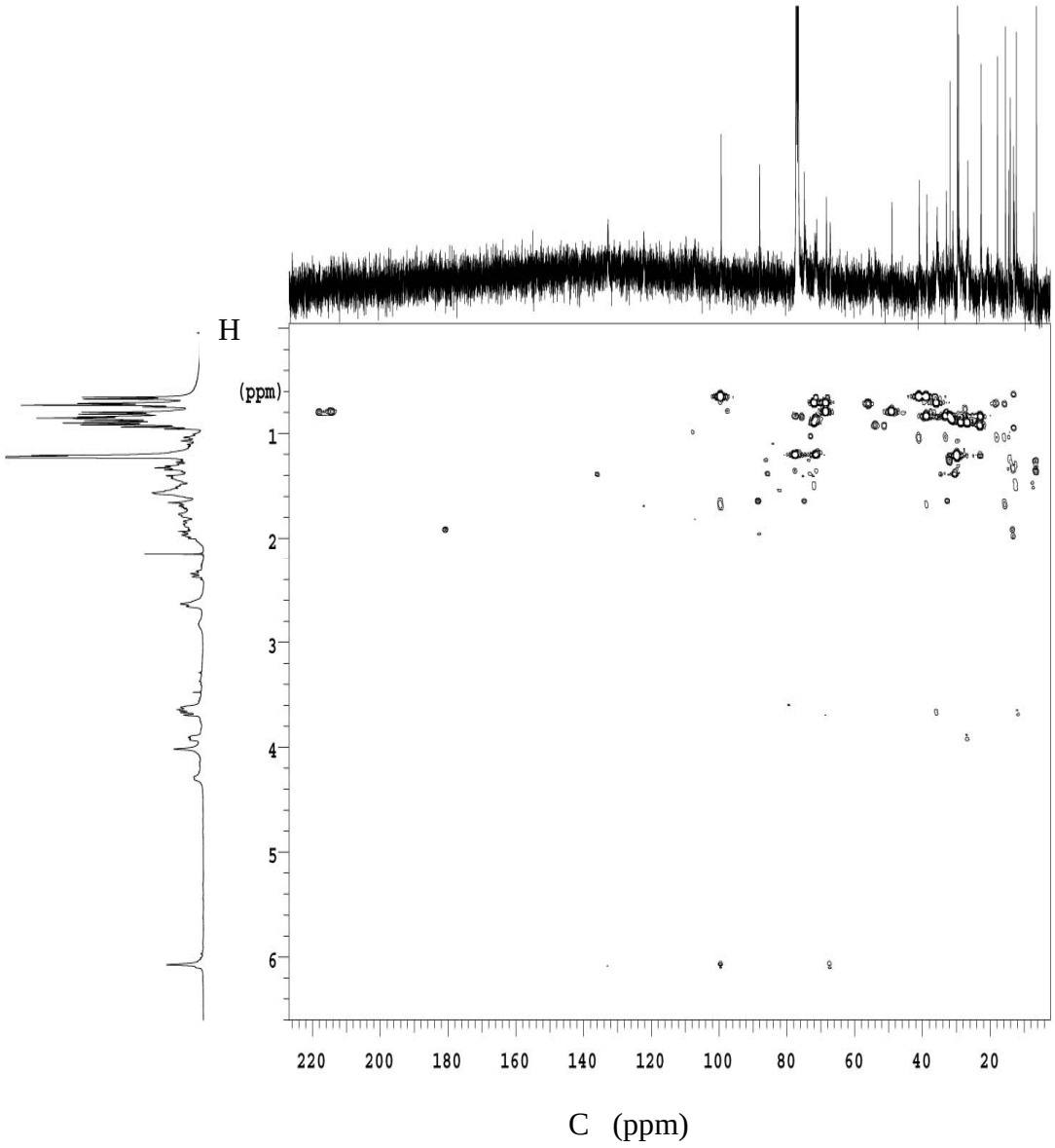


Figure V.39. HMBC spectrum of the lead-salinomycin (1:2) complex in $CDCl_3$.

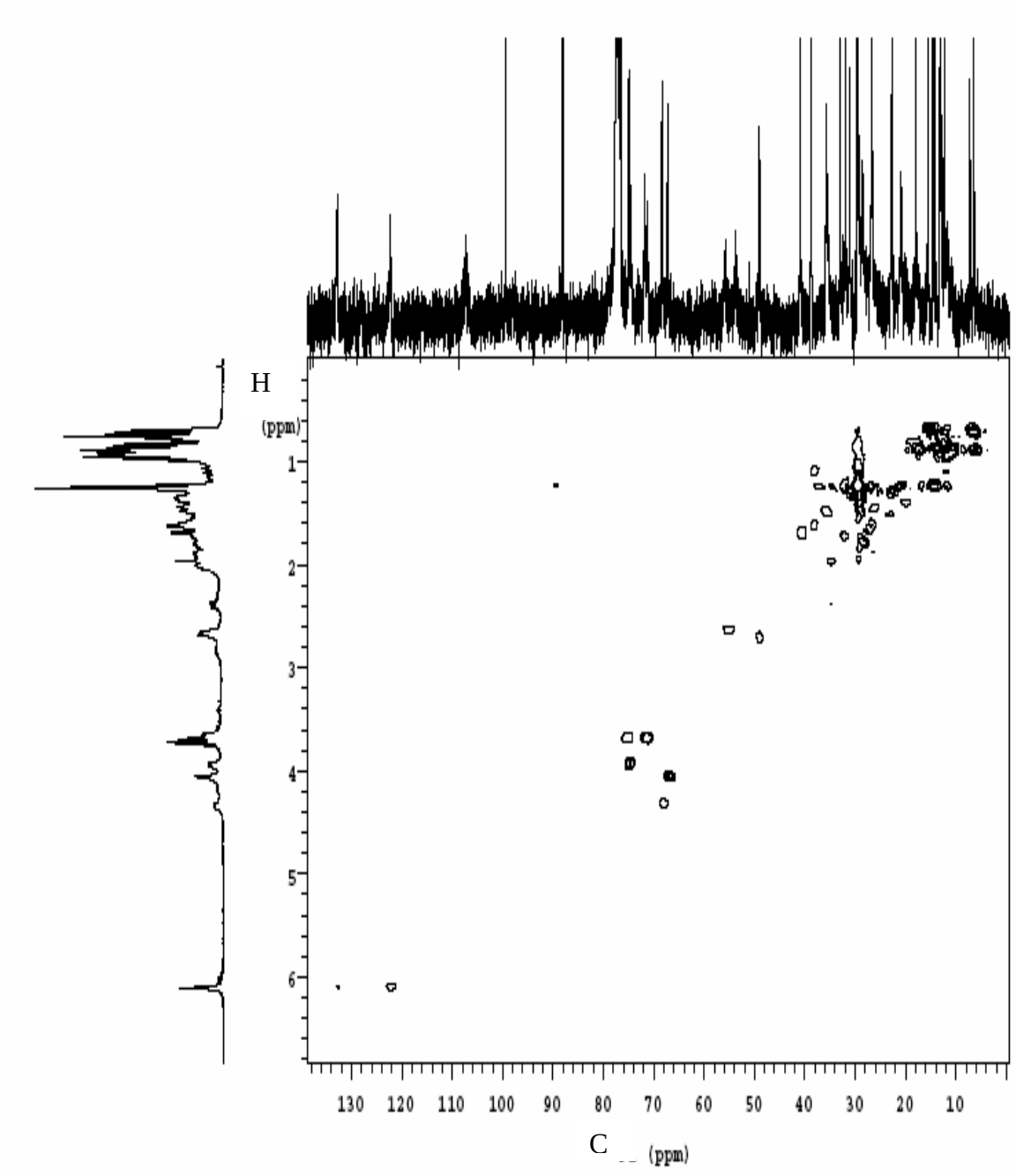


Figure V.40. HSQC spectrum of the lead-salinomycin (1:2) complex in $CDCl_3$.

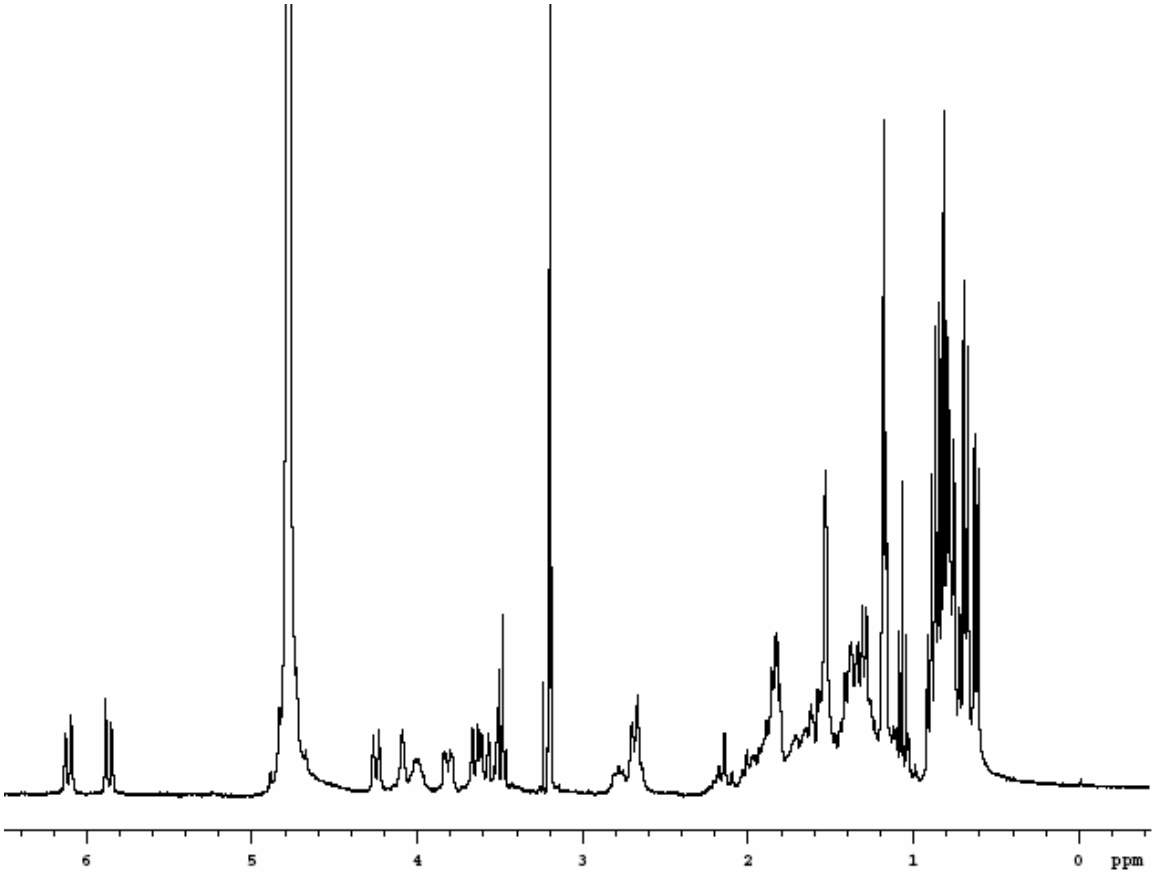


Figure V.41. ^{1}H NMR spectrum of the lead-salinomycin (1:2) complex in CD_3OD.

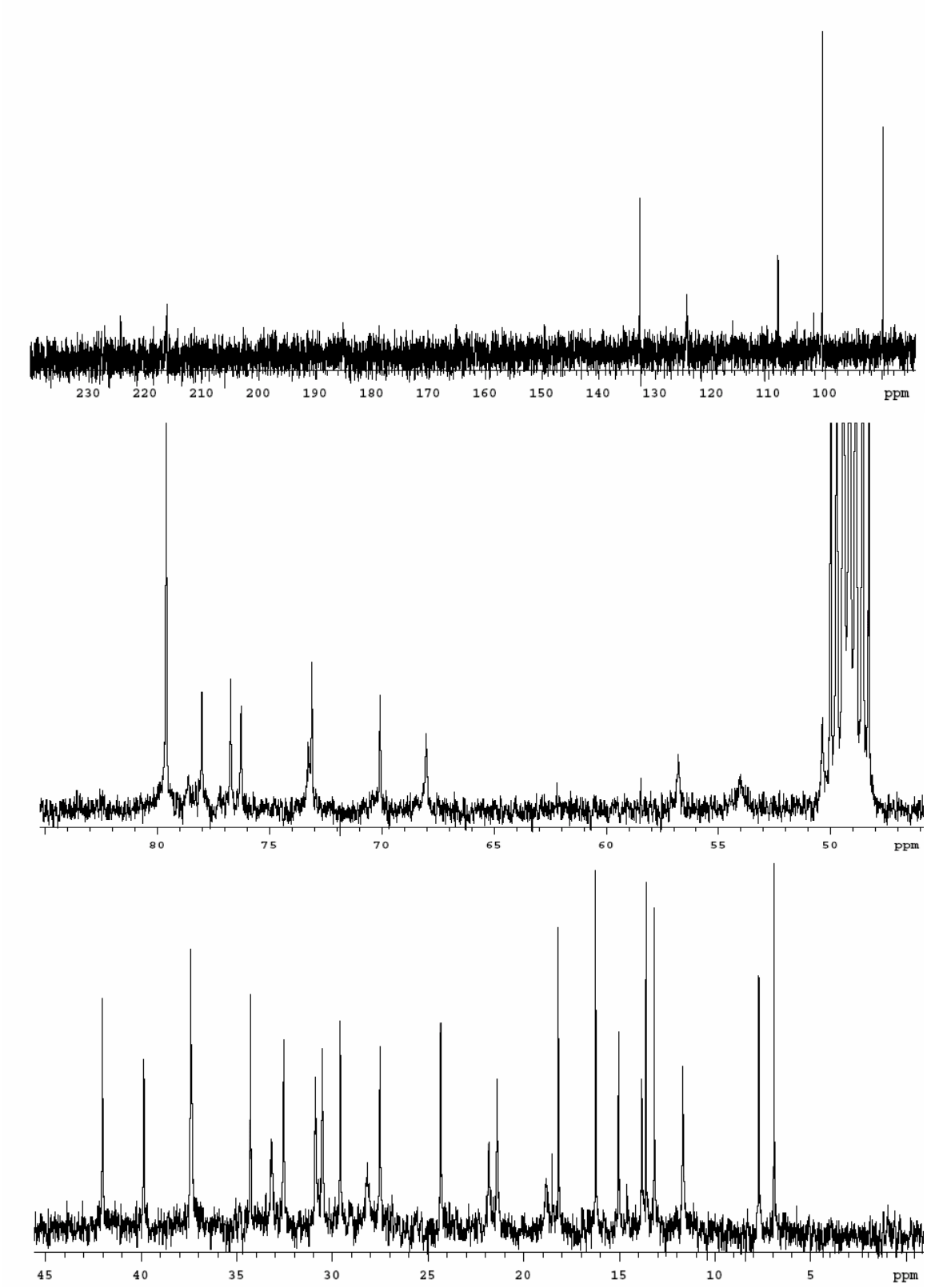


Figure V.42. ^{13}C NMR spectrum of the lead-salinomycin (1:2) complex in CD_3OD.

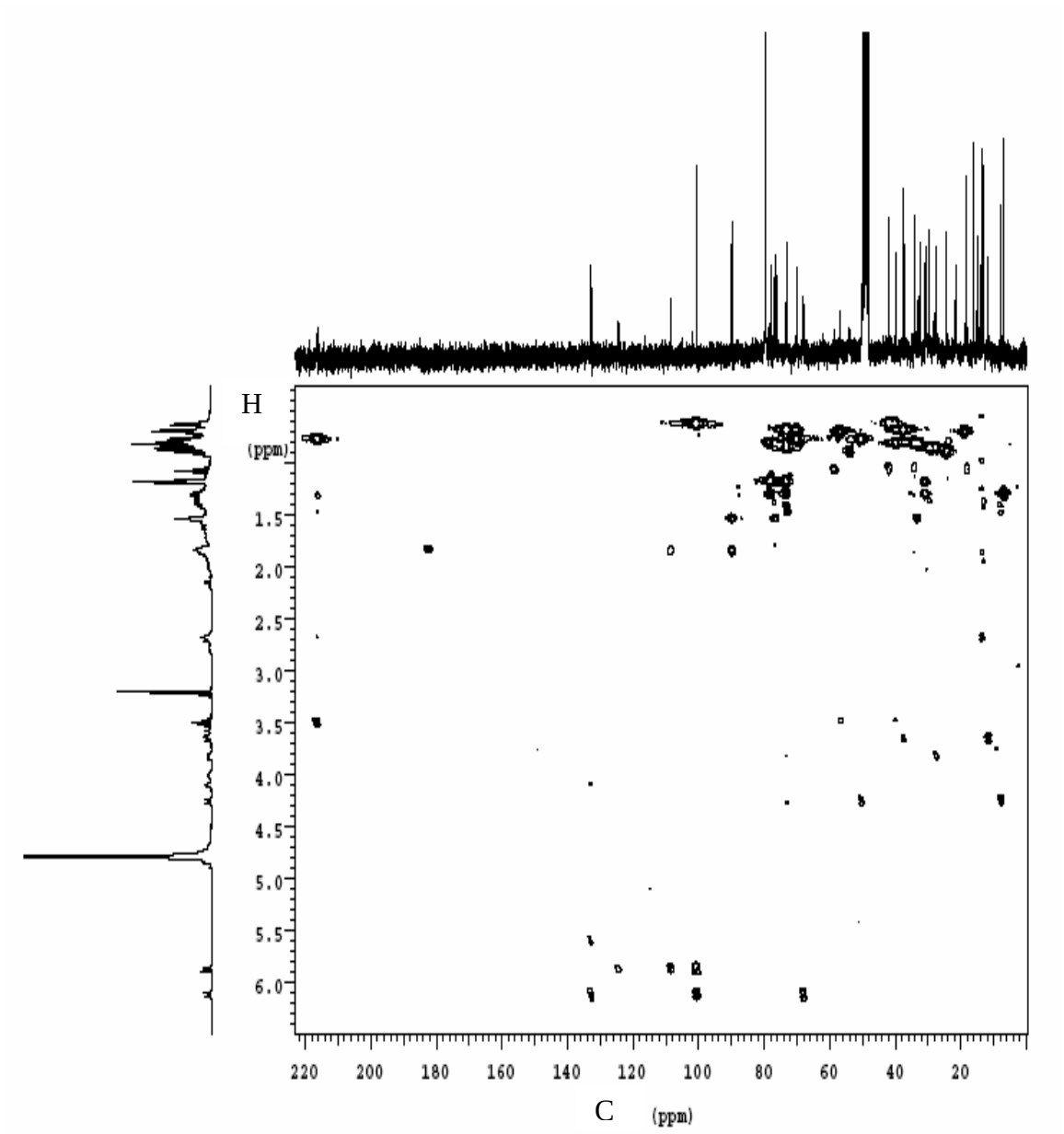


Figure V.43. HMBC spectrum of the lead-salinomycin (1:2) complex in CD_3OD.

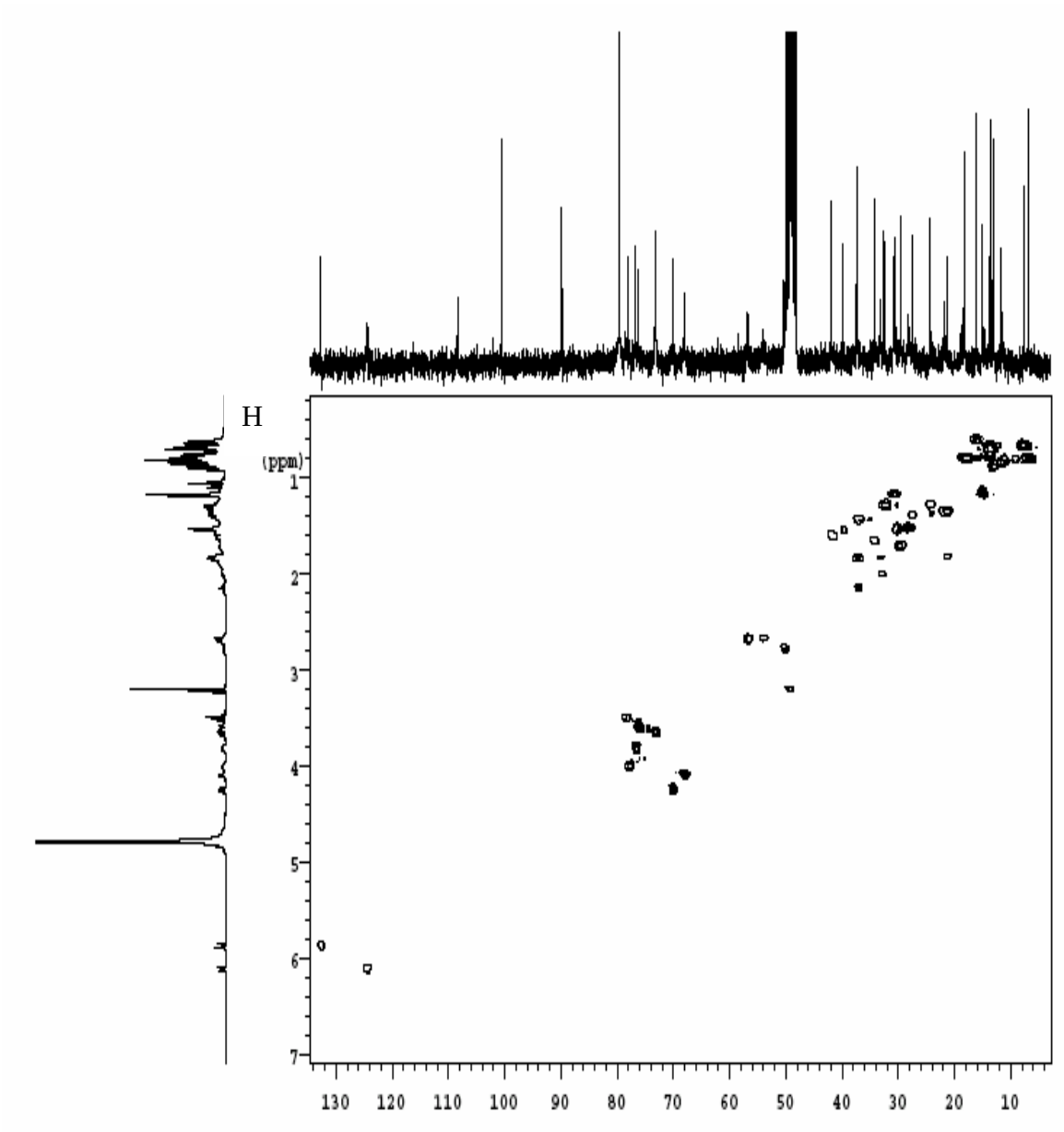


Figure V.44. HSQC spectrum of the lead-salinomycin (1:2) complex in CD_3OD.

Table V.15. ^{1}H and ^{13}C NMR chemical shifts (ppm) of the lead-salinomycin (1:2) complex in CD_3OD and $CDCl_3$ at 25 ^{o}C (experimental values) using a Varian 300-MHz spectrometer.

carbon #	carbon connectivity	^{13}C $CDCl_3$	^{1}H $CDCl_3$	^{13}C CD_3OD	^{1}H CD_3OD
1	COOH	181		183.846	
2	CH	53.673	2.62	54.036b	2.66
3	CH-O	74.904	3.90	76.742	3.82
4	CH_2	20.875	1.50	20.398	1.39, 1.80
5	CH_2	26.622	1.4,1.80	27.518	1.34, 1.80
6	CH	28.464	1.75	29.601	1.71
7	CH-O	71.814	3.66	73.124	3.64
8	CH	35.726	1.5	37.001	1.44
9	CH-O	68.337	4.28	70.081	4.25
10	CH	48.981	2.70	50.365	2.78
11	C=O	216.50		216.290	
12	CH	55.669	2.63	56.806	2.68
13	CH-O	77.207	3.99	78.611	4.00
14	CH	32.942	1.70	34.286	1.65
15	CH_2	38.716	1.02,1.60	39.866	1.04, 1.54
16	CH	40.918	1.67	42.029	1.60
17	O-C-O	99.406		100.583	
18	CH=CH	122.292	6.06	124.457	6.10
19	CH=CH	132.825	6.06	132.780	5.85
20	CH-OH	67.195	4.01	68.032	4.09
21	O-C-O	107.288		108.398	
22	CH_2	35.426	1.75,1.9	37.423	1.83, 2.14
23	CH_2	31.067	1.40,1.9	33.225	1.82, 2.00
24	C-O	88.026		89.877	
25	CH-O	74.504	3.62	76.281	3.58
26	CH_2	22.817	1.64	22.826	1.52
27	CH_2	29.679	1.26	30.902	1.18
28	C-OH	71.333		73.160	
29	CH-O	77.207	3.61	78.030	3.51
30	CH_3	14.514	1.20	15.044	1.17
31	CH_2	31.908	1.20	32.551	1.28
32	CH_3	6.365	0.85	6.921	0.81
33	CH_3	29.345	1.20	28.186	1.52
34	CH_3	15.516	0.75	16.245	0.80
35	CH_3	17.885	0.65	18.201	0.61
36	CH_2	17.885	1.50	18.515	1.30, 1.86
37	CH_3	14.114	0.7	13.829	0.67
38	CH_3	13.119	0.70	13.609	0.76
39	CH_3	7.173	0.7	7.722	0.66
40	CH_3	12.298	0.92	11.687	0.85
41	CH_2	22.670	0.9,1.45	24.348	1.27, 1.34
42	CH_3	12.906	0.80	13.182	0.88

Analysis of NMR Data in CD_3OD

The lead-salinomycin-lead (1:2) complex shows only one broad set of NMR signals at room temperature for ^{1}H and ^{13}C resonances. No low temperature experiment was carried out in this study due to the limited solubility of the complex.

The ^{13}C chemical shift differences ($\Delta\delta^{13}C$) between the free acid form, sodium salt and the lead complex of salinomycin and salinomycin anion (Et_4N^+) in CD_3OD as defined in eq IV.30 were used to obtain information about the conformation changes and possible donor atoms involved in complexation in those compounds.

$$\Delta\delta^{13}C = \delta^{13}C(MNi) - \delta^{13}C(Et_4NNi) \qquad (M = H, Na, \text{and } Pb) \qquad (IV.30)$$

The data are plotted in Figure V.45. As found for the values of $\Delta\delta^{13}C$ of the acid form of nigericin and monensin A in CD_3OD, there is no significant change in values of $\Delta\delta^{13}C$ for most of the backbone carbon chain of HSal except that the carboxyl head group and adjacent atoms (C1-C3) have the largest value of $\Delta\delta^{13}C$ (1-4 ppm). One oxygen atom in the carboxylic acid group forms a head-tail hydrogen bond with O11, which explains the large value of $\Delta\delta^{13}C$ for C1.

The sodium salt salinomycin has show significant chemical shift changes throughout the carbon chain indicating that this salinomycin ligand is required to undergo great conformational changes to coordinate the central metal ion. Negative values of ($\Delta\delta^{13}C$) are prevalent in the plot for the sodium salt as shown in Figure V.30. This is similar to the pattern observed with the sodium salts of nigericin and monensin A. X-ray data show that only four oxygen atoms coordinate the central sodium atom (O2, O5, O9, and O10)[7]. The same oxygen atoms could be involved in sodium coordination in the solution. C1 and C11 show significant positive values of $\Delta\delta^{13}C$ indicating that O donor

atoms 1 (2) and 5 coordinated to sodium. Positive $\Delta\delta^{13}C$ values found for C3, C7, C24, and C25 are associated with donor atoms O3, O9 and O10. The largest negative value of $\Delta\delta^{13}C$ at C13 indicates that large conformation change takes place at C13.

As with nigericin and monensin, there are a greater number of positive peaks in the plot for the lead complex than the one for the sodium salt of salinomycin. The ranges of $\Delta\delta^{13}C$ values for lead-salinomycin (1:2) (-2.5 to 2.5 ppm) and lead-nigericin (1:2) (-5 to 3 ppm) complexes are much larger than those observed for lead-monensin (1:2) complexes (-1.5 to 1.0 ppm). One reason may be that salinomycin and nigericin are longer than monensin.

Positive values of $\Delta\delta^{13}C$ on C1 and C2 provide indicate that O1 or O2 are involved in the lead coordination. Positive values of $\Delta\delta^{13}C$ at C7, C21, C24, C25, C28, and C29 suggest the participation of O3, O9, 10, and O11 in lead coordination. O7 and O9 cannot be involved in lead coordination at the same time.

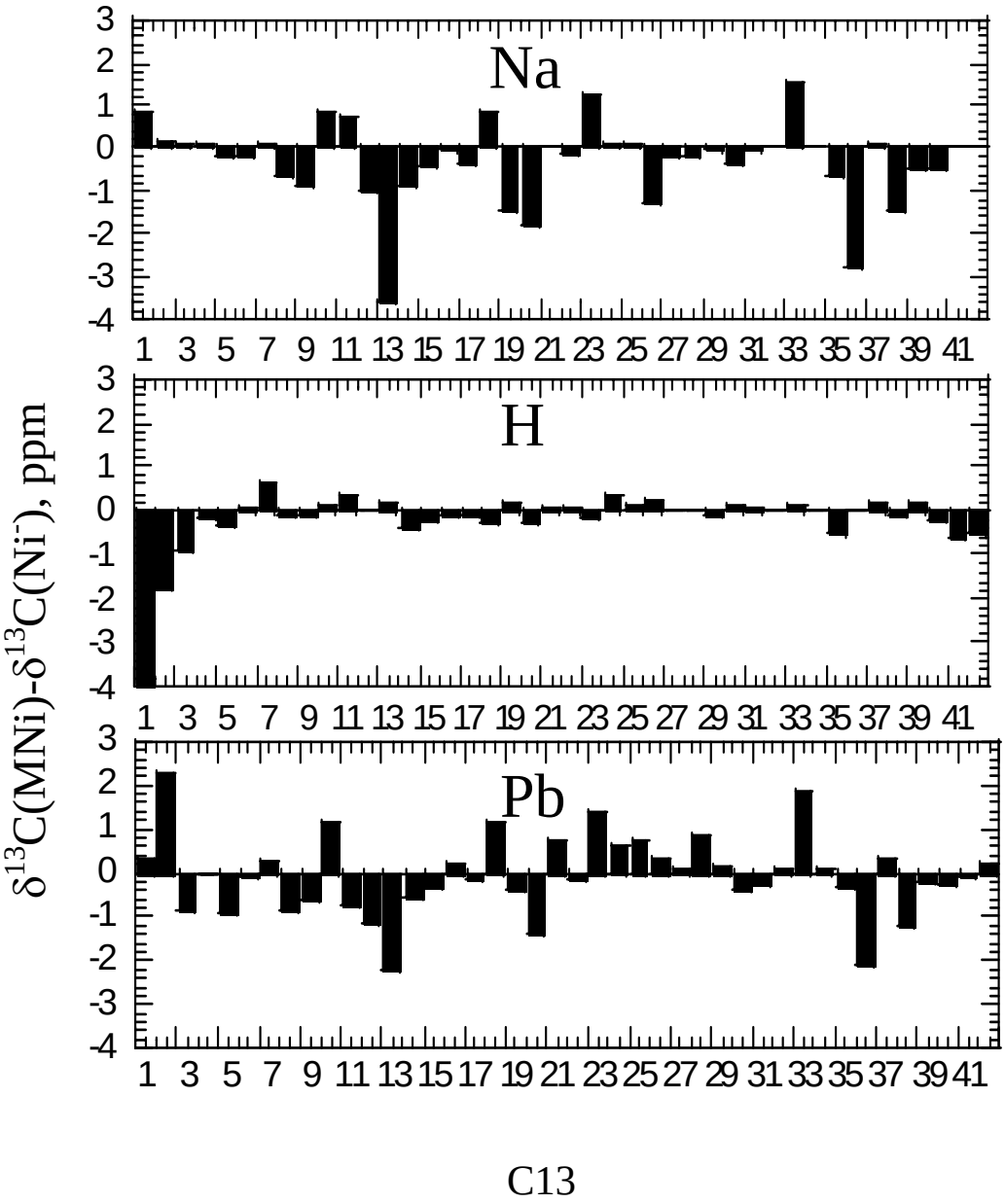


Figure V.45. Plots of the difference in ^{13}C chemical shifts, $\Delta\delta^{13}C$, between the free acid or complexed forms and the anionic form of salinomycin for each carbon atom in CD_3OD. Values of $\Delta\delta^{13}C$ were calculated using the experimental ^{13}C chemical shifts listed in Tables V.11 (Na, top panel), V.13 (H, middle panel), V.15 (Pb, bottom panel) and, V.14 (salinomycin anion).

Analysis of NMR data in $CDCl_3$

The ^1H and ^{13}C NMR signals are broader than their counterparts in methanol. ^{13}C chemical shift differences ($\Delta\delta^{13}C$) between the free acid form, sodium salt and lead complex of salinomycin and the salinomycin anion (Et_4N^+) in $CDCl_3$ are used to determine potential donor atoms in the lead-salinomycin (1:2) complex and values of $\Delta\delta^{13}C$ for all carbon atoms are shown in Figure V.46.

The plot of HSal is dominated by negative peaks, particularly for the region C7-C12, while there are far fewer changes in the plot of HSal in CD_3OD. This suggests that a large conformation change occurs in $CDCl_3$. The large negative values of $\Delta\delta^{13}C$ indicate that the flexible hinge region (C7-C13) undergoes a significant conformation change. Large negative values of $\Delta\delta^{13}C$ occur for the atoms of the carboxylic acid group. This suggests that a large conformation change occurs to form head-tail hydrogen bond.

Similar patterns of the values of $\Delta\delta^{13}C$ are found in plots for the sodium salt of salinomycin in CD_3OD and $CDCl_3$. Small values of $\Delta\delta^{13}C$ changes are observed in ring A. The flexible hinge region (C7-C13) is characterized by larger values of $\Delta\delta^{13}C$ for C10-C13. C13 possesses the largest value of $\Delta\delta^{13}C$ (-6ppm), indicating a large conformation change because it is the connection between the flexible hinge region and the tricyclic ring system (B-C-D). Values of $\Delta\delta^{13}C$ in the rest of carbon chain also show similar patterns to their counterparts in CD_3OD. Positive values of $\Delta\delta^{13}C$ at C1, C11, C21, C24, and C25 indicate that sodium atom in $CDCl_3$ is coordinated with O1 or O2, O5, O9, and O10. Theoretical calculations combined with 2D NMR spectroscopy in $CDCl_3$ draw the same conclusion[7].

As with nigericin, the salinomycin lead complex has the greater number of positive peaks in $CDCl_3$ than in CD_3OD. The pattern of $\Delta\delta^{13}C$ values at C7-C13 except C11 is similar to the sodium salt of salinomycin in the same solvent. This suggests that the conformation change in the hinge region of the lead salinomycin complex similar to the one in the sodium salt. In the lead-salinomycin complex, O5 might not be coordinated with lead, which explains the small negative value of $\Delta\delta^{13}C$ in C11. The values of $\Delta\delta^{13}C$ for the region C17-C29 is predominantly positive. The occurrence of positive values found for C1, C7, C9, C17, C21, C24, C25, C28, and C29 suggests the involvement of O1 or O2, O3, O6 or O7, O9, O10, and O11 in lead coordination.

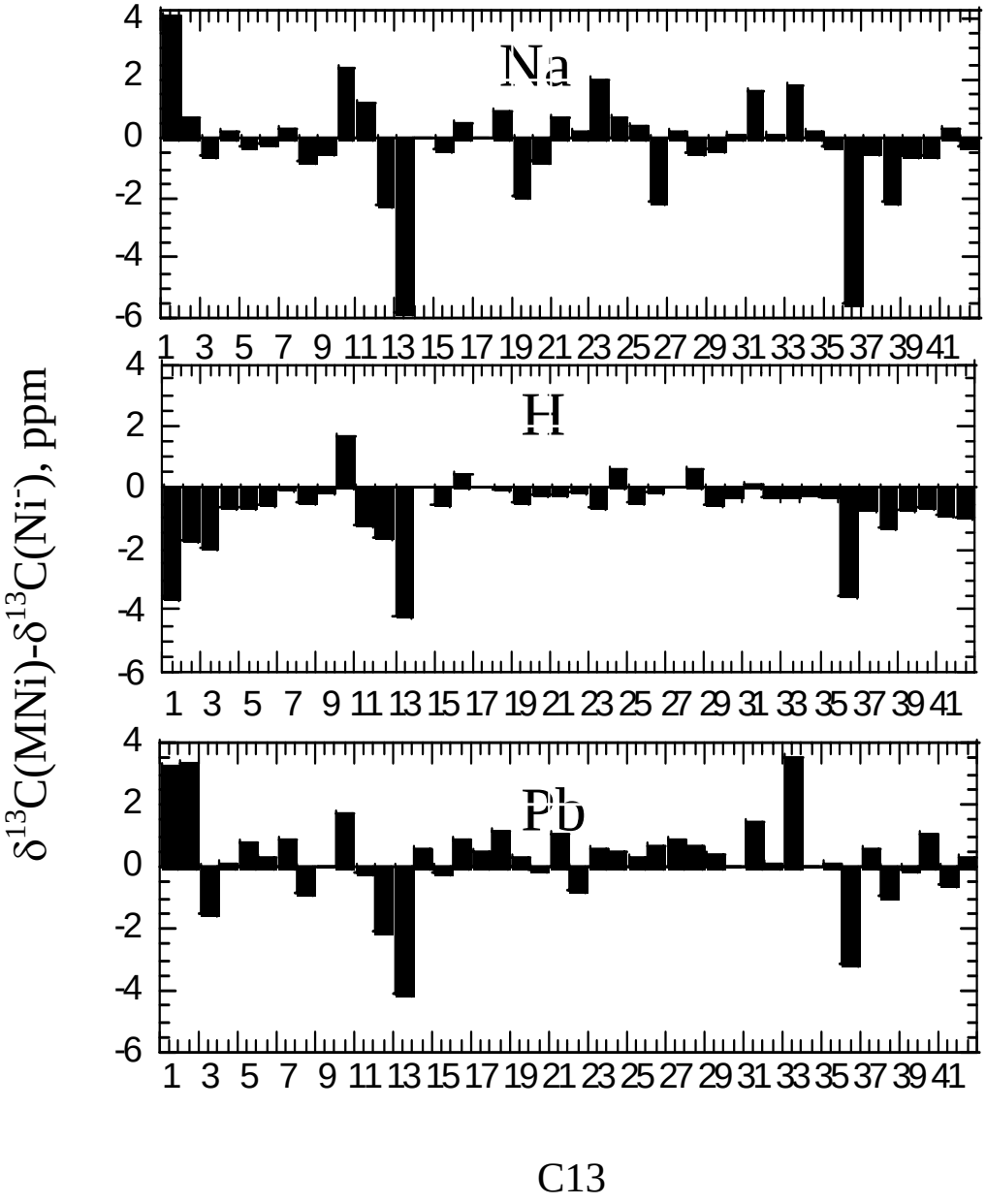


Figure V.46. Plots of the difference in ^{13}C chemical shifts, $\Delta\delta^{13}C$, between the free acid or complexed forms and the anionic form of salinomycin for each carbon atom in $CDCl_3$. Values of $\Delta\delta^{13}C$ were calculated using the experimental ^{13}C chemical shifts listed in Tables V.10 (Na, top panel), V.12 (H, middle panel), V.15 (Pb, bottom panel) and, V.14 (salinomycin anion).

References

(1) Heusler, K.; Labhart, H.; Loeliger, H.; Ciba, A. G.; Basel, S. *Tetrahedron Lett.* **1965**, *32*, 2847-2854.

(2) Heusler, K.; Loeliger, H.; Woodward, F.; Ciba, A. G.; Basel, S. *Helv. Chim. Acta.* **1969**, *52*, 1495-1516.

(3) Martell, A. E.; Motekaitis, R. J. *Determination and Use of Stability Constants*, 2nd ed.; VCH Publishers: New York, **1992**,

(4) KaleidaGraph; 3.5 ed.; Synergy Software, **1990**.

(5) Seto, H.; Yahagi, T.; Miyazaki, Y.; Ôtake, N. *J. Antibiot.* **1977**, *30*, 530-532.

(6) Anteunis, M. J. O.; Rodios, N. A. *Bull. Soc. Chim. Belg.* **1981**, *90*, 715-735.

(7) Paulus, E. F.; Kurz, M.; Matter, H.; Vertesy, L. *J. Am. Chem. Soc.* **1998**, *120*, 8209-8221.

(8) Westley, J. W. in Polyether Antibiotics: Naturally Occurring Ionophores, Volume 2: Chemistry; Marcel Dekker, Inc.: New York, **1983**, 1-20.

(9) Seto, H.; Miyazaki, Y.; Fujita, K.-I.; Otake, N. *Tetrahedron Lett.* **1977**, *28*, 2417-2420.

Chapter VI

Discussion

Polyether ionophores have been widely utilized as agriculture additives. Their ion transport selectivity has great applications in broad fields. Metal ions at various concentrations play a vital role in biological systems. Some of their functions have been studied while the others remain unknown, especially for those metals present at extremely small concentrations[1]. Changing a metal concentration selectively, using ionophores, is the first step in studies of biological functions of metals. Recently studies show the extremely high selectivity of some ionophores for lead over other divalent cations[2,3]. The basis of their transport ion selectivity is the focus of the research described in this dissertation. Understanding the mechanism of metal ion transport will open new fields of application and improve design of new ionophores for designated ions. To reach this goal requires the information about the stoichiometry, structure, equilibria, and identity of the ionophore species involved in transport. Transport studies provide information about identities of the transporting species. The equilibrium constants for the major reactions and the structures of several metal complexes were determined and were used to explain the transport data obtained in vesicle studies.

VI. A. Isolation and characterization of the lead complexes with the polyether ionophores nigericin and salinomycin

The composition of possible ionophore-lead complexes is important for identification of the transporting species and further determination of the transport mode. These lead complexes are required for the structural studies.

Isolation of complexes and their elemental analysis.

Lead-ionophore (1:2) complexes were prepared using several methods and the composition of the products was determined by elemental analysis. The most successful method was the reaction of lead oxide and the free acid form of nigericin or salinomycin in methanol. The experimental values of elemental composition provided by that method are closest to the theoretical values. For the method of back-extraction using aqueous lead nitrate solutions, lead tends to remain in the acidic aqueous phase. The reaction of lead acetate and the free acid form of nigericin or salinomycin in acetone results in an acidic acetone solution. After water and chloroform are added, the lead and acetic acid partition into the aqueous phase. Although there is no water in the reaction using lead carbonate, the reaction itself produces water and carbon dioxide that keep the solution acidic and lead does not bind with nigericin or salinomycin well under acidic conditions. It is difficult to make the solutions slightly basic without precipitation of lead.

The elemental percentages for the lead-nigericin (1:2) complex correspond well with the calculated values for the model containing three waters of hydration, as shown in Table IV.1. The lead-salinomycin complex shows some deviation from the theoretical values, especially in the lead percentage as shown in Table V.1. The majority of the

complex is still lead-salinomycin (1:2) complex because the experimental lead percentage is 88.7% of the theoretical value for the model with three additional waters of hydration. The low lead percentage can be explained in several ways. Degradation studies show that salinomycin solutions at pH ~4 are stable for ~9 hours at room temperature. The reaction using lead oxide requires stirring for two days at room temperature. Some of salinomycin may have decomposed so less amount of lead is reacted with salinomycin. Another reason for the low lead percentage is the solubility of lead-salinomycin (1:2) complex. The solubility of lead-salinomycin (1:2) complex is less than 10 mg in 1 mL methanol. In addition, there is the possibility that the lead-salinomycin (1:2) complex blocks the active surface of lead-oxide and prevents the stoichiometric reaction.

Characterization of complexes by mass spectrometry.

ESI-MS was used to characterize the lead-ionophore (1:2) complexes. In the MS spectra of the lead-salinomycin complex, there are peak clusters representing the lead-salinomycin (1:1) and (1:2) complexes. The lead-nigericin (1:2) complex only shows peak clusters for the lead-nigericin (1:1) complex because instrumental conditions were changed. Under the same instrumental conditions used for the lead-nigericin complex, the lead-salinomycin complex produced no peaks corresponding to the lead-salinomycin (1:2) complex. The presence of peak clusters associated with sodium and potassium ion adducts is expected due to contamination of sodium and potassium ions in the MS instrument. It is clear that salinomycin and nigericin have great affinity for lead because lead-ionophore (1:1) complexes dominate the MS spectra. The ESI-MS results also suggest the possibility of the formation of lead-ionophore (1:2) complexes in solution.

VI. B. Protonation constants of salinomycin and nigericin.

Protonation and deprotonation reactions occur on both sides of the membrane and compete with the metal ion complexation reactions. Thus, the protonation constants are required for explanation of metal transport by ionophores in biological systems. The values obtained in 80% methanol-water have been shown previously to represent those in biological membrane systems[4-7].

The protonation constant of nigericin was only obtained by potentiometric titrations because nigericin does not give usable signals in the UV or CD spectra. The mean log value of the protonation constant is 7.02 ± 0.03. This is close to the literature value reported in 30% dioxane-H_2O (v/v) (6.93) as shown in Table VI.1.

Table VI.1. Literature values of the protonation constants of nigericin in various organic solvents and heterogeneous media at 25°C.

log K_H	method	solvent system
6.93	potentiometry	dioxane-H_2O 30%(v/v)[8]
8.45	potentiometry	ethanol 90%[8]
7.76	potentiometry	dioxane-H_2O 45%(v/v)[8]
10.2	voltammetry	methanol[9]
6.25	potentiometry	bilayer lipid vesicles[10]

Measurements done in bilayer lipid membrane give a value for nigericin (logK_H = 6.25) similar to the one obtained in 80% methanol-water (log K_H = 7.02). The difference between these two values can be explained by the different ionic strengths used in these two systems. This supports the idea that 80% methanol-water is a good replacement for biological membranes. The value reported in 45% dioxane-water (v/v) is also close to the experimental value in this work. The literature value for nigericin reported in methanol is three orders larger than the experimental value. This change has been found in studies for other ionophores and acetic acid as shown in Table VI.2. Potentiometric

titrations in 90% ethanol-water produced a value larger than the experimental value by 1.4 orders of magnitude. All these differences in log K_H are largely due to variations in solvent polarity.

Table VI.2. Protonation constants of ionophore antibiotics and acetic acid in different solvent systems at 25°C (ionic strength = 0 M).

compound	log K_H	
	80% methanol-water	methanol
monensin A	7.20[11]	10.24[12]
lasalocid	5.21[11]	8.23[13]
A23187	8.04[5]	10.7[14]
acetic acid	6.57[15]	9.52[16]

The mean value of log protonation constant of salinomycin is 6.49 ± 0.07, which is close to the value (6.57) obtained by circular dichroism. Therefore, salinomycin in different protonation stages has distinct CD signals, which could be valuable in studies of salinomycin in phospholipid membranes. It is surprising that there are no literature reports about the protonation constant of salinomycin.

Based on Table VI.2 nigericin, monensin, and salinomycin have similar protonation constants that are close to the one for acetic acid because the carboxylate group is the only functional group in all those ionophores and acetic acid that can be protonated. The protonation constant for salinomycin is closest to the value for acetic acid. The protonation constant for nigericin in 80% methanol-water is close to that for monensin due to the structural similarity. Both nigericin and monensin are weaker acids than salinomycin. As with monensin, significant fractions of salinomycin and nigericin are in a protonated form at physiological pH. This is important because both the protonated and unprotonated forms are required in the transport cycle.

VI.C. Complexation constants of metal ions with nigericin and salinomycin.

Complexation constants of metal ions with nigericin and salinomycin were obtained using the program BEST[17] to analyze the titration data. All constants were expressed as overall formation or acid hydrolysis constants, as shown in Tables IV.8 and V.8. For ML (1:1) complexes, the overall constant is the same as the first stepwise complexation constant, K_{ML}. The overall hydrolysis constant for the ternary hydroxy complex, β_{MLOH}, and the formation constant for 1:1 ionophore-lead complex, β_{ML}, are used to calculate the stepwise complexation constant, K_{MLOH}, based on eqs VI.1-VI.3.

$$ML^+ + OH^- \rightleftharpoons MLOH \qquad K_{MLOH} = \frac{[MLOH]}{[ML^+][OH^-]} \qquad \text{(VI.1)}$$

$$\beta_{MLOH} = \frac{[MLOH][H^+]}{[M^{2+}][L^-]} \qquad \text{(VI.2)}$$

$$\beta_{ML} = \frac{[ML^+]}{[M^{2+}][L^-]} \qquad \text{(VI.3)}$$

Therefore, $K_{MLOH} = \frac{\beta_{MLOH}}{\beta_{ML} K_S}$ ($\log K_S = 14.05$) (VI.4)

Or $\log K_{MLOH} = \log \beta_{MLOH} - \log \beta_{ML} + pK_S$ (VI.5)

The average experimental values for the overall complexation constants of nigericin with metal ions and the stepwise equilibrium values for MNiOH are listed in Table VI.3. The formation constant for $PbNi^+$ measured using potentiometric titrations ($\log K_{ML} = 7.57$) matches well with the values obtained from UV-Vis titrations ($\log K_{ML} = 7.58$).

Table VI.3. Average values of overall complexation constants of nigericin with metal ions in 80% methanol-water at 25°C.

ion (M)	average values of log β_X or log K_X for the complex species X				
	ML	ML_2	MLOH	ML_2H	M_2L
H^+	7.02±0.03	-	-	-	-
Na^+	2.89±0.07	-	-	-	-
K^+	3.77±0.21	-	-	13.61±0.12	-
Ca^{2+}	2.59±0.27	-	-	-	-
Zn^{2+}	2.99±0.19	-	6.47±0.18[a]	12.76±0.19	-
Mg^{2+}	2.46±0.14	-	3.37±0.19[a]	12.63±0.4	-
Pb^{2+}	7.57±0.41	3.8±0.65	6.69±0.11[a]	-	5.86±0.13

[a] the equilibrium constant is expressed as shown in eq VI.1.

The formation constant for $PbNi^+$ is the largest one for ML type complexes and is 3.8 orders of magnitude larger than the constant for KNi and ~4.5 orders of magnitude larger than the values for the remaining metal ions studied. The formation constant for $PbNi_2$ is 3.77 orders of magnitude smaller than the formation constant for $PbNi^+$. This means that $PbNi_2$ is not significant when the ligand concentration is smaller than 10^{-5} M. Formation of ternary hydroxy complexes, MLOH, is significant because a neutral species is formed. The value of K_{MLOH} for Mg^{2+} is small and the MgNiOH species will be negligible at pH <9.5. The value of K_{MNiOH} for Zn^{2+} and Pb^{2+} are significantly larger than Mg^{2+}. However, the formation constant for ZnNi is so small that formation of ZnNiOH is negligible. Only for lead is the species PbNiOH formed in significant amounts at the concentrations and pH found in biological systems. No complexation constants for MNi_2 are obtained for other divalent cations except Pb^{2+}. Other species are proposed for some cations such as MNi_2H for K^+, Zn^{2+}, and Mg^{2+} and Pb_2Ni. Concentrations of these species are not significant at the physiological pH and concentrations of ionophores usually employed in biological systems (less than 10^{-6} M).

Values for complexation constants of metal ions with nigericin in different solvents and heterogeneous media are listed in Table VI.4. Absolute values of K_{ML} in

different solvents are difficult to compare because the values are affected by the solvent properties such as dielectric constants and polarity[18]. But K_{ML} values for a given ion follow the same trend as the solvent varies. This is known for the complexation constants of A23187 from 60% methanol to 100% methanol[5]. As shown in Table VI.4, most of literature values show a trend (K^+>Na^+) except in two experiments where values for NaNi and KNi are similar. There is only one report about complexation between nigericin and divalent cations (log K_{ML} 5.53 for Mg^{2+}, 5.43 for Ca^{2+}, 5.14 for Sr^{2+}, and 5.66 for Ba^{2+})[19]. Although the literature values reported in ethanol are different than the experimental values in 80% methanol-water, the trends for both sets are the same. In ethanol and 80% methanol-water, the formation constants for the divalent cations are close to each other. In ethanol the complexation constants for divalent cations are 4-5 times smaller than the ones for monovalent cations such as sodium[19]. In 80% methanol the complexation constants are for divalent cations 2-3 times smaller than the one for sodium. Although the order of complexation constants for CaNi and MgNi switched places in ethanol and 80% methanol-water, the complexation constants for both species in the same solvent are close to each other.

Table VI.4. Values of the complex formation constants of nigericin with monovalent cations in various organic solvents and heterogeneous media at 25°C.

solvent	Log K_{ML}								
	Li^+	Na^+	K^+	Rb^+	Cs^+	Tl^+	Mg^{2+}	Ca^{2+}	Pb^{2+}
methanol[20]		4.38	5.17			64			
dioxane/H_2O 45%(v/v)[21]	4.16	3.91	3.70	3.70	3.82	65			
bilayer lipid vesicles[22]		1.34	1.98			66			
ethanol[19]		6.17	6.14	6.08	5.977	6.39	5.53	5.43	
80% methanol-water[a]		2.89	3.77				2.46	2.59	7.57

[a] obtained in this work

All stepwise complexation constants obtained for salinomycin with metal ions are listed in Table VI.5. The formation constants for $PbSal^+$ measured using potentiometric titrations (log K_{ML} = 7.16) matched well with the values obtained from UV-Vis titrations (log K_{ML} = 6.98).

Table VI.5. Average values for overall complexation constants of salinomycin with metal ions in 80% methanol-water.

ion (M)	average values of log β_X or log K_X for the complex species X				
	ML	ML_2	MLOH[c]	ML_2H	M_2L
H^+	6.49±0.07	-	-	-	-
Na^+	-	-	-	-	-
K^+	3.34±0.1	-	-	-	-
Ca^{2+}	2.59±0.26	-	3.67±0.29[a]	-	-
Zn^{2+}	2.54±0.28	-	5.82±0.22[a]	-	-
Mg^{2+}	2.57±0.18	-	4.32±0.11[a]	-	-
Pb^{2+}	7.16±0.15	5.23±0.42	6.63±0.53[a]	4.66±0.65	4.63±1.02

[a] the equilibrium constant is expressed as shown in eq VI.1.

As with nigericin, $PbSal^+$ possesses the largest complexation constant among the MSal complexes determined. The complexation constant for $PbSal^+$ is about 4.6 orders larger than the values for other divalent cations, and 3.82 orders larger than that for KSal. The complexation constant for PbSalOH is larger than that for ZnSalOH by a factor of 10 and 2-3 orders of magnitude larger than the values for other divalent cations. The formation constant for $ZnSal^+$ is so small that formation of ZnSalOH is negligible. So are the species of MSalOH for the remaining divalent cations. Other types of lead-salinomycin complexes ($PbSal_2$, Pb_2Sal, and $PbSal_2H$) were included in the model used to fit the titration data. The formation constants for those species are about 2 orders of magnitude smaller than the value for $PbSal^+$. All these lead species except $PbSal^+$ and PbSalOH are negligible at the physiological pH and concentrations of ionophores employed in biological systems (less than 10^{-6} M).

It is concluded that the major lead species with salinomycin and nigericin has 1:1 ligand/metal composition for the metal and ionophore concentrations less than 10^{-4} M. This is consistent with the results from the UV-Vis and CD titrations.

Comparing the protonation constants and complexation constants of nigericin, salinomycin, and monensin listed in Table VI.6, shows that these ionophores show similar patterns for these values. The values for the lead complexes are the largest among the metal ions tested. The remaining divalent cations form complexes with similar complexation constants. The ternary hydroxy complexes for zinc and lead are the most stable ones among the same type of complexes. The other divalent cations either don't form MLOH or produce very weak complexes.

Table VI.6. The protonation constants and overall formation constants for nigericin, salinomycin and monensin[2] with several metals obtained in 80% methanol-water.

complex (X)	average values of log β_X or log K_X for the complex species X		
	nigericin	salinomycin	monensin
HL	7.02	6.49	6.83
NaL	2.89	<2	5.0
KL	3.77	3.34	3.76
CaL	2.59	2.59	3.10
ZnL	2.99	2.54	3.74
MgL	2.46	2.57	3.16
PbL	7.57	7.16	7.25
ZnLOH	9.46	8.36	10.41
PbLOH	14.26	12.39	14.35

There are also many differences between these ionophores. Salinomycin is the strongest acid among these ionophores. Nigericin is a slightly weaker acid than monensin. However, they only vary by a factor of 3.4. Nigericin possesses the largest complexation constant for the PbL^+ complex required to form a ternary hydroxy compound, PbLOH. Salinomycin has the smallest complexation constant for PbL^+. The equilibrium constant for PbNiOH is smaller than the value for PbMonOH. The

differences between the values for lead-monensin and lead-nigericin complexes are small and cancel each other. So the overall formation constants for PbNiOH and PbMonOH are extremely close to each other. Even salinomycin has an overall formation constant for PbSalOH close to PbNiOH and PbMonOH. But the overall constants for nigericin and salinomycin complexes with the other divalent cations are smaller than those of the same type for monensin by 0.5-2.2 orders of magnitude. The overall constant for ZnNiOH is smaller than the value for ZnMonOH by a factor of 10. ZnSalOH is 100 times weaker than ZnMonOH. Therefore, the initial transport rates of Zn^{2+} by nigericin and salinomycin are smaller than that by monensin. For the monovalent cations, the equilibrium constants for KNi, KSal and KMon are similar. But nigericin and salinomycin behave totally differently from monensin when sodium is considered. Monensin forms a stronger complex with sodium than other monovalent cations, while the sodium complex of salinomycin is very weak (log K_{ML}<2) and the equilibrium constant for NaNi is as small as those for the divalent cation-nigericin (1:1) complexes except $PbNi^{+}$.

VI.D. NMR Studies of ligand conformation and binding in lead complexes having 1:2 lead-ionophore stoichiometry.

As described in Sections IV.F and V.F, monensin, salinomycin, and nigericin share a number of common features regarding the patterns of chemical shift changes upon complexation with sodium and lead, suggesting that nigericin and salinomycin compounds adopt conformations similar to the corresponding monensin compounds. NMR spectra of the lead-nigericin (1:2) and lead-salinomycin (1:2) complexes were obtained in two different solvents. In each solvent only one set of signals was present in these spectra. The chemical shifts should be average values for two ligands, which was found in monensin-lead studies at room tempreture[11]. After examination of ^{13}C chemical shift differences between nigericin anions (Ni^-, Et_4N^+) and the free acid form of nigericin, sodium and lead complexes in methanol ($\Delta\delta^{13}C$), O1 or O2, O4, O5, O6, O7, O9 or O10, and O11 are possible donor atoms for coordination with lead. It is impossible to differentiate between O1 and O2 because the double bond is conjugated within O1, O2 and C1 and the bond C1-C2 rotates. Sometimes O1 and O2 can bind in a bidentate fashion. From structural point of view, it is clear that O4 cannot be coordinated with lead at the same time as O5 and O6. O5 is in the opposite side of the same ring with O4. The conformational limit on the spiroketal rings prevents O4 and O6 to bind with lead at the same time. It is possible that O4 is not involved in lead coordination and the positive value at C13 is caused by the metal coordination of O6. Because O5 is coordinated with lead, O4 cannot be one of the donor atoms and O6 should be coordinated with lead. Positive values appear in C25 and C29, suggesting that O9and O10 could be involved in lead coordination. It is impossible that O9 and O10 in the same ligand are coordinated

with lead simultaneously due to steric constraints. There is less chance for O9 to be coordinated with lead because the value of $\Delta\delta^{13}C$ is very small for O9 while O10 has a large $\Delta\delta^{13}C$ value. O11 could be coordinated with lead. This patterns appear for the terminal pyran ring in crystal structures of the sodium, potassium, and silver salts of monensin[23-25].

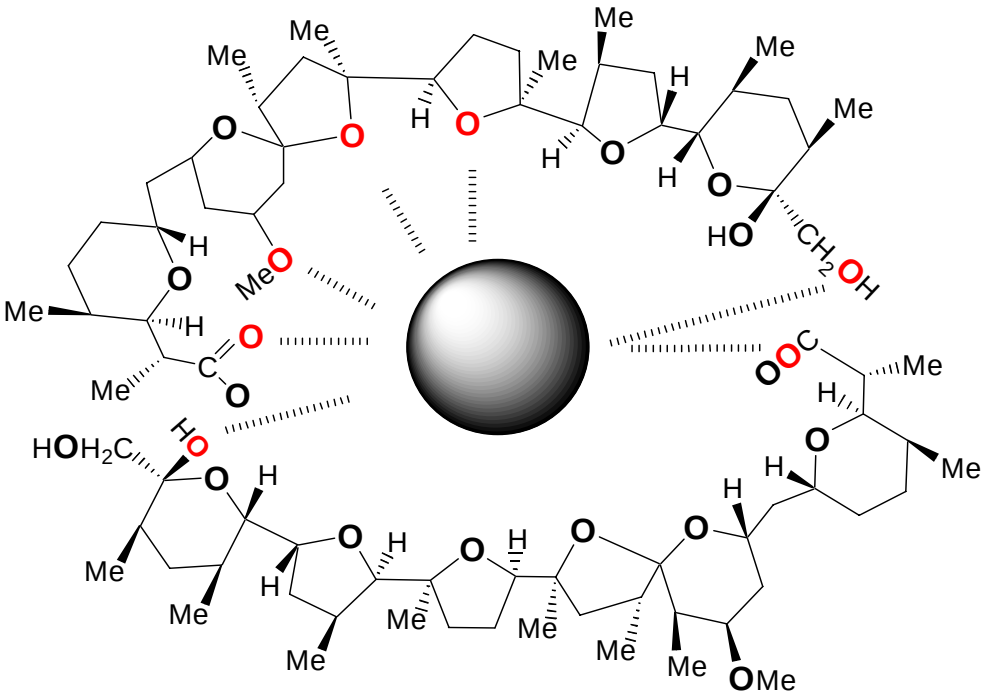


Figure VI.1. Schematic diagram of possible nigericin coordination in the lead (II) complex in methanol based on ^{13}C chemical shift data.

For the lead-nigericin complex in chloroform, positive values of $\Delta\delta^{13}C$ found for C1, C11, C13, C17, C20, and C29 indicate that O1 or O2, O4, O5, O6, O7, O9 and O10 could be coordinated with lead. Similar to the situation found in methanol, O4 is not involved in lead complexation because O5 is coordinated with lead. O9 could not be coordinated with lead because O10 from the same ligand is coordinated with lead. To identify the exact oxygen atoms in the two ligands requires more evidence related to germinal proton coupling constants and the dihedral angles, which were achieved in

nigericin sodium salt[26]. However, the low solubility and broader NMR signals of the lead-nigericin (1:2) complex prevents these assignments for ^{1}H NMR spectra.

Lead-salinomycin (1:2) complex

The lead-salinomycin (1:2) complex might donate O1 or O2, O3, O7, O9, O10, and O11 after analysis of chemical shift change in methanol, as described in Section V.F. As noted for nigericin it is obvious that O7 and O9 cannot be coordinated with lead at the same time. Because O9 is definitely coordinated with lead, O7 is not involved in lead coordination.

For NMR data in chloroform the positive values found for C1, C7, C17, C21, C24, C25, C28, and C29 indicate that O1 or O2, O3, O6 or O7, O9, O10, and O11 are possibly coordinated with lead, as described in Section V.F. There are several pairs of oxygen atoms that are not able to bind at the same time, such as O10 and O11, O6, O9, and O7. Because O9 is definitely coordinated with lead, O7 is not involved in lead coordination and O6 is coordinated with lead.

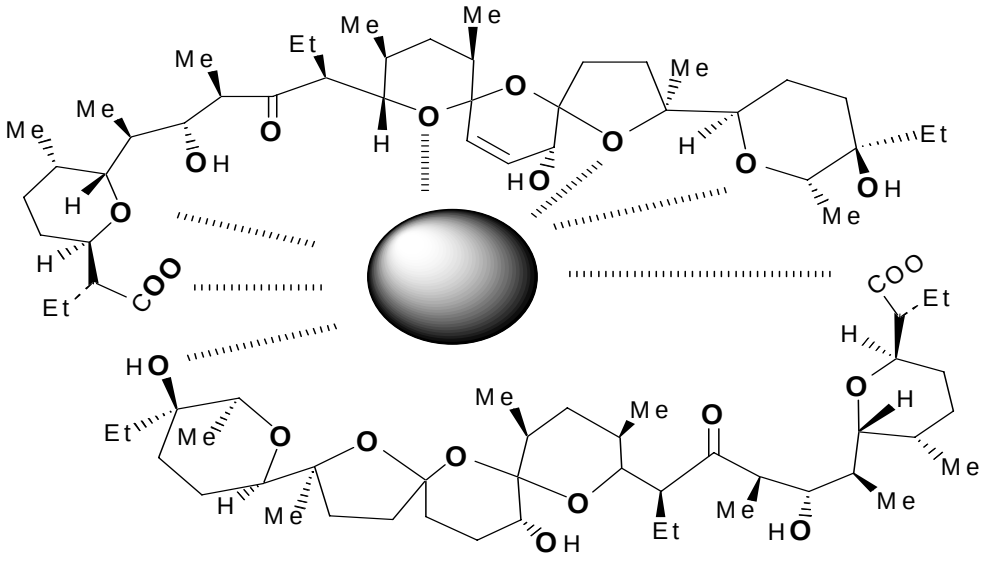


Figure VI.2. Schematic diagram of possible salinomycin coordination in the lead(II) complex in chloroform based on 13C chemical shift data.

VI.E. Discussion of the lead transport data and the results of the present study compared with monensin and ionomycin.

The cation transport selectivities of monensin, ionomycin and nigericin have been studied thoroughly. Figure VI.3 shows the transport of lead and other divalent cations by these three ionophores.

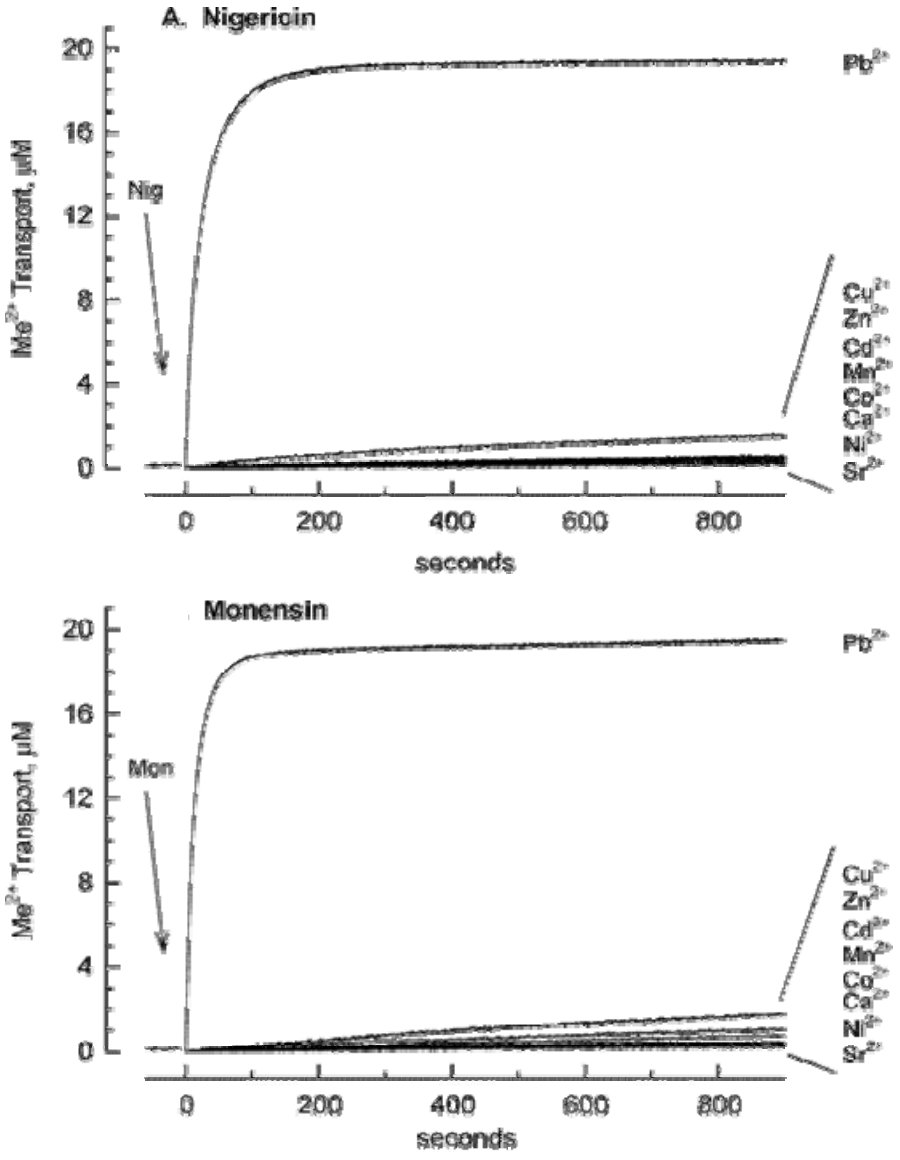


Figure VI.3. Selectivity trends for membrane transport of divalent cations by nigericin, monensin and ionomycin at pH 7.0 using phospholipid vesicles[3].

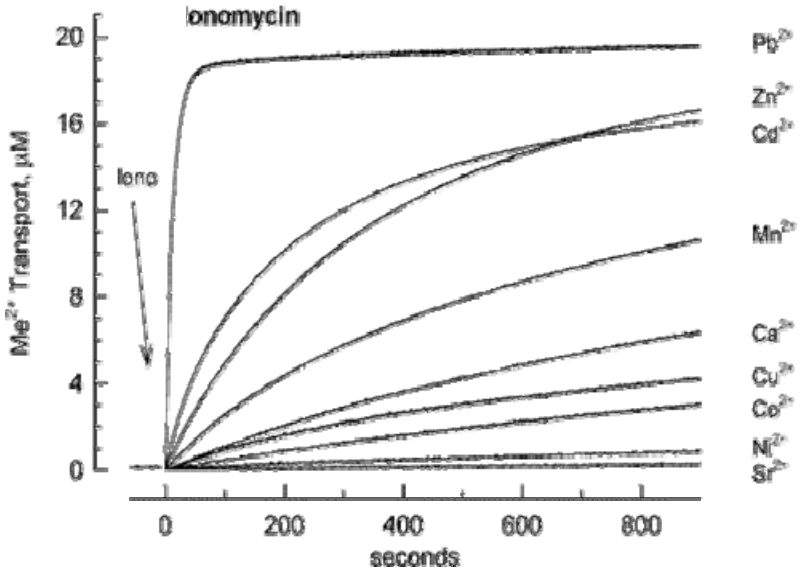


Figure VI.3. (continued) Selectivity trends for membrane transport of divalent cations by nigericin, monensin and ionomycin at pH 7.0 using phospholipid vesicles[3].

Under the conditions employed all three ionophores have high selectivity for lead, compared to other divalent cations. The transport selectivities for lead over calcium can be expressed as S values defined by eq VI.6.

S = (initial rate of Pb transport)/(initial rate of Ca transport) (VI.6)

Among these three ionophores the highest selectivity for lead transport relative to calcium was found for monensin (3340) and nigericin (2890) is slightly lower. Ionomycin has the lowest selectivity (100). The overall selectivity of nigericin is better than that of monensin when all the divalent cations studied are considered. Nigericin doesn't transport Cu^{2+}, Zn^{2+}, and Cd^{2+} as well as monensin. Plots of log transport rate vs log of the free lead concentration and log rate vs log of the ionophore concentration, shown in Figures VI.4 and VI.5, possess slopes close to 1, suggesting that the main lead transport species has a 1:1 stoichiometry, ionophore:cation, for all three ionophores.

Ionomycin has the highest efficiency (absolute rate) for lead transport among all three ionophores.

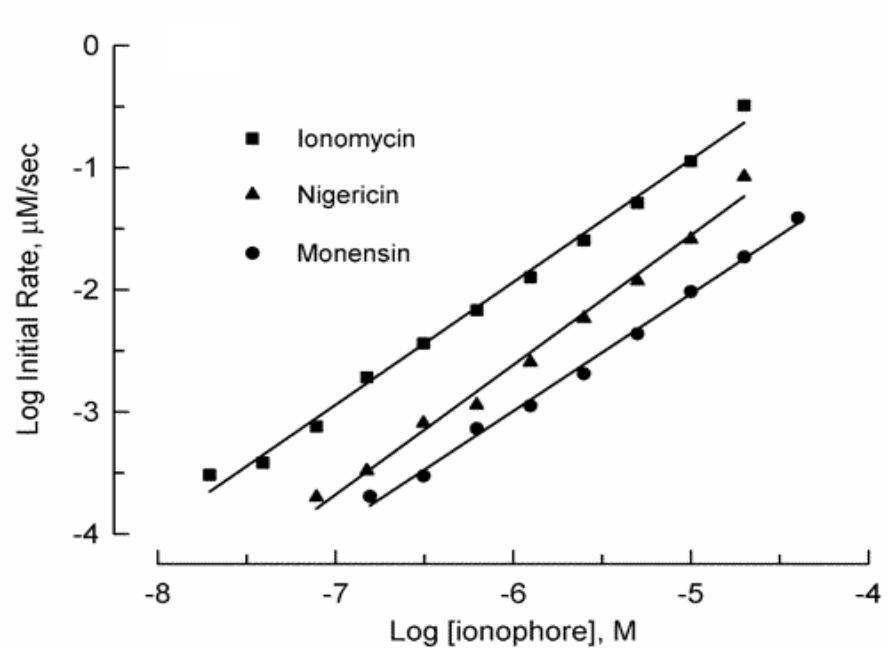


Figure VI.4. Dependence of Pb^{2+} transport across POPC membranes by three ionophores on the concentrations of ionophores using phospholipid vesicles[3].

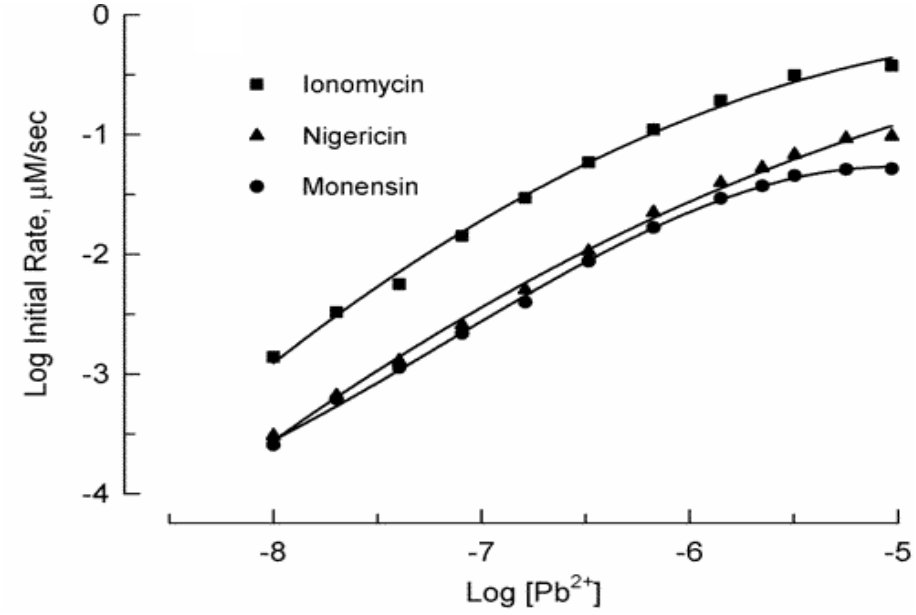


Figure VI.5. Dependence of Pb^{2+} transport across POPC membranes by three ionophores on the concentration of free Pb^{2+} using phospholipid vesicles[3].

As the pH is varied, the concentrations of all species are changed and the transport rates of lead by ionophores are affected. To determine the pH dependence of the transport rate of lead, transport studies were done at different pHs at fixed concentrations of ionophore and free lead as shown for nigericin in Figure VI.6.

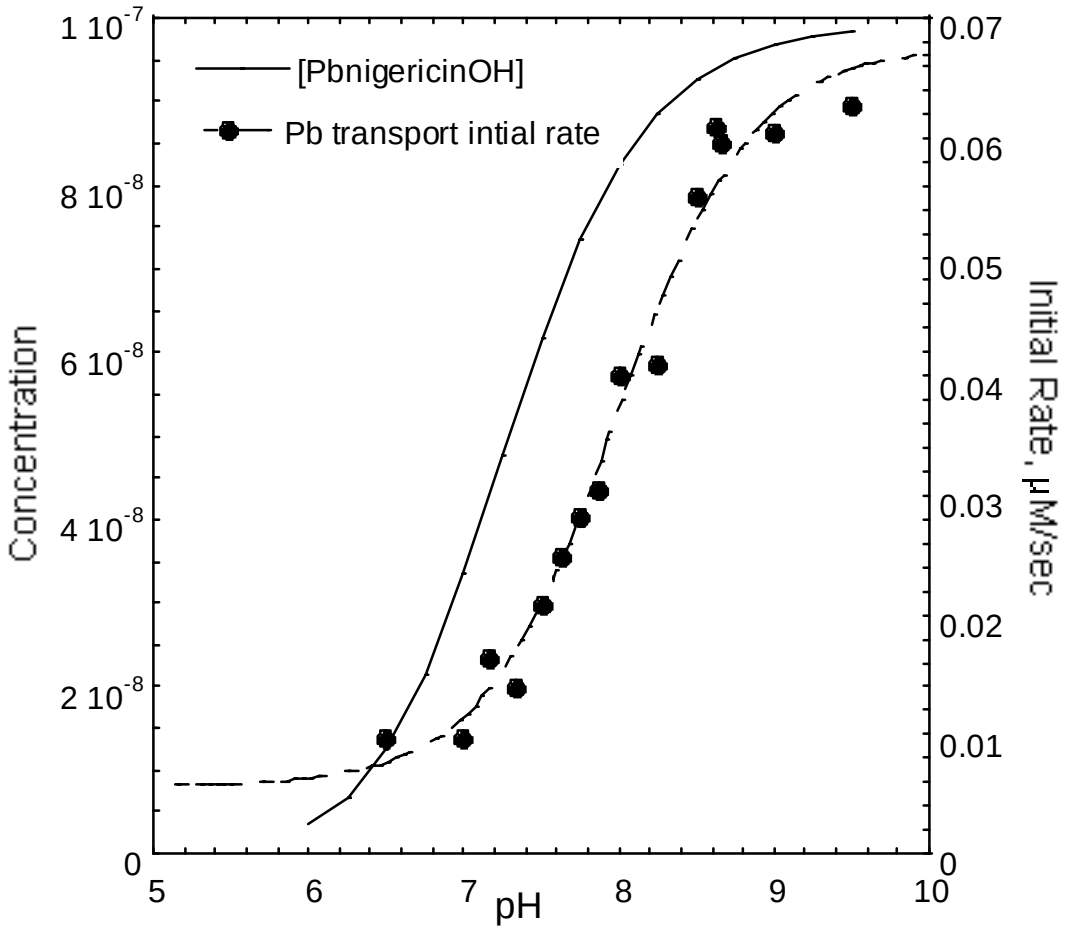


Figure VI.6. Dependence of Pb^{2+} transport by nigericin on external pH[3].

The lead transport rate increases with pH over the range of 6.5-9 and with a half maximal value obtained around 7.94. Similar pH studies of lead transport by ionomycin and monensin showed similar behavior with half maximal rates at pH 7.88 and 7.80. It is concluded that monensin is ionized in that pH range and the formation of the ternary

hydroxy species PbMonOH improves the transport rate further. The structural similarity of monensin and nigericin should lead to similar transport species for nigericin. The membrane potential did not arise when no methods were taken to dissipate the membrane potential, indicating that neutral species play a major role in lead transport by nigericin. When the membrane potential was collapsed, the initial rate of lead transport increased slightly, indicating that the electrogenic mode contributes only a small portion of the lead transport. Therefore, a mixed mode is applied when the membrane potential is dissipated while the electroneutral mode is the only mode when the membrane potential is against the direction of metal transport.

All of these results from transport studies can be explained well by complexation information of ionophores with lead. The protonation and complexation values for nigericin with lead listed in Table IV.7 were input into the program Comics[27] to produce the species distribution curve calculated at an ionophore concentration that is typical of those used in biological systems. As shown in Figure VI.7, the concentrations of 2:1 and 1:2 lead-nigericin complexes were negligible. $PbNi^+$ has the highest concentration among all the species at the physiological pH and could be the major transport species. But the relationship of the concentration of $PbNi^+$ and pH values is totally different from the relationship of lead transport rate and pH values, indicating that $PbNi^+$ is not the major transport species. There is additional evidence supporting the hypothesis that the major transport mode is electroneutral. Rapid lead transport remains when the membrane potential is not collapsed[3]. PbNiOH is the only neutral species present in a significant amount at pH ~7. The concentrations of NiPbOH are plotted vs pH in the same panel with the nigericin transport data in Figure VI.6. It is clear that concentrations of PbNiOH

are affected by pH in the same way as the rate of lead transport by nigericin. The ternary hydroxyl species, PbNiOH is primarily responsible for Pb transport by nigericin, at least under conditions where an electroneutral mechanism is required. Those two curves in Figure VI.6 do not overlap each other because the complexation constants obtained in 80% methanol-water may differ slightly from corresponding values of the membrane-bound ionophores.

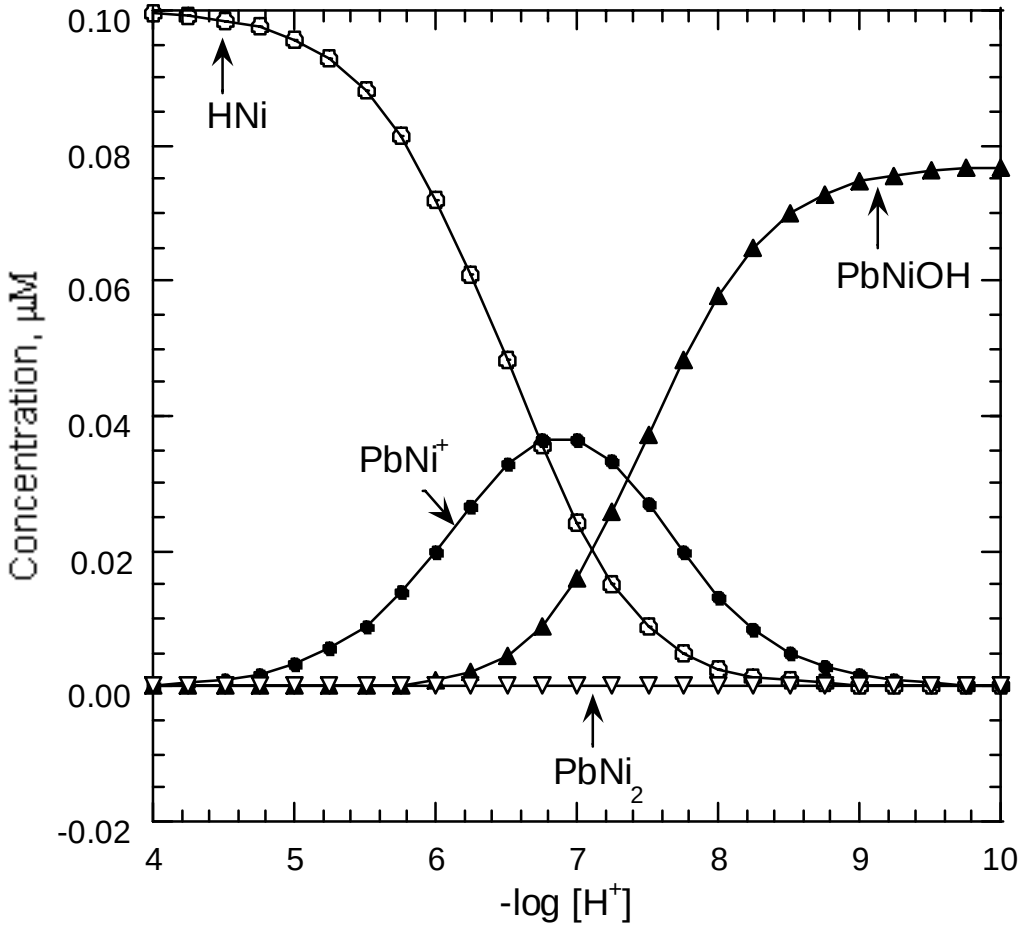


Figure VI.7. Species distribution curves for lead-nigericin complexes as a function of p[H] in 80% methanol-water. Species concentrations were calculated using the program Comics for 0.1 μM nigericin and 0.1 μM lead using the values listed in Table IV.7.

The ability to form the ternary hydroxy complex provides an explanation of the high selectivity for lead over other divalent cations. Other divalent cations such as Ca^{2+} cannot form the ternary hydroxyl complex required for transport by the electroneutral mode. What is also important is that $CaNi^{+}$ is not formed at the concentrations of nigericin and the metal ion used for transport (less than 10^{-6} M) because K_{CaNi} is only ~10^{3}. Among the other divalent cations only Zn^{2+} forms significant amounts of the ternary hydroxy species, ZnNiOH. This may explain the higher initial transport rates for Zn^{2+} compared to Ca^{2+}. Because the overall constant for ZnNiOH is smaller than the value for PbNiOH by approximately 5 orders of magnitude, Pb^{2+} can be transported with high selectivity. Similar behavior was observed with monensin, but nigericin has a better overall selectivity for lead over other divalent cations. This might be explained by the fact that the overall constants for nigericin complexes with divalent cations are smaller than those of the same type for monensin by 0.5-2.2 orders of magnitude. The overall constant for ZnNiOH is smaller than the value for ZnMonOH by a factor of 10. Therefore, the initial transport rate of Zn^{2+} by nigericin is smaller than that by monensin. All these complexation constants match up well with the selectivity of nigericin and monensin for lead over other divalent cations.

Application of monensin in the treatment of lead-intoxication was tested using rats fed with lead salts. Monensin was shown to reduce lead accumulation in several organs and tissues. It also accelerated the excretion of lead that was accumulated previously and produced this effect without depleting the organs of zinc or copper ions[2]. Nigericin should behave in the same way as monensin and could be a better candidate because nigericin has a better overall selectivity for lead than monensin.

For salinomycin there is only one transport experiment shown in Figure VI.8.

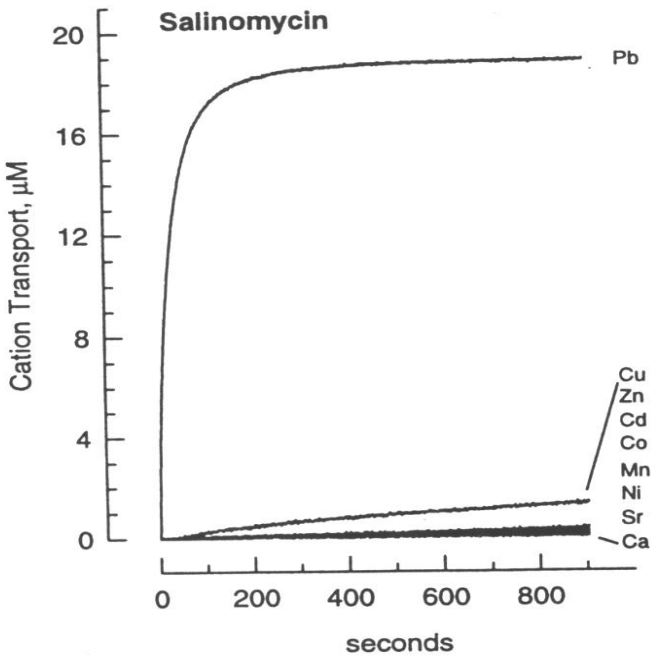


Figure VI.8. Selectivity trends for membrane transport of divalent cations by salinomycin at pH 7.0 using phospholipid vesicles[28].

The concentration and pH dependence of transport rate are not available. The transport selectivity of salinomycin for lead over calcium is 3030 close to the values for nigericin and monensin, which can be explained in the same way with nigericin and monensin. Figure VI.9 shows $PbSal^+$ and PbSalOH are the only prevalent species containing lead at the concentration of salinomycin (≤1.0 μM) used in biological systems. $PbSal^+$ is several orders more stable than the same type of complexes formed by other divalent cations. Other divalent cations, Ca^{2+} and Mg^{2+}, don't produce the ternary hydroxy complexes at the physiological pH and Zn^{2+} only forms a weak species. Based on the conclusions drawn for nigericin and monensin, the ternary hydroxy complex, PbSalOH, should play a major role in lead transport by salinomycin. All of these factors are consistent with the observed high transport selectivity of salinomycin for lead. As with nigericin, the overall

selectivity of salinomycin for lead shown in Figure VI.8 is better than that of monensin because species containing salinomycin and other metal ions except Pb^{2+} are less stable than the similar monensin complexes. Salinomycin, as one of the three commercial feed additives has lower toxicity towards animals than nigericin. With the same selectivity for lead as nigericin, salinomycin could be a better candidate than nigericin in applications for treatment of lead intoxication.

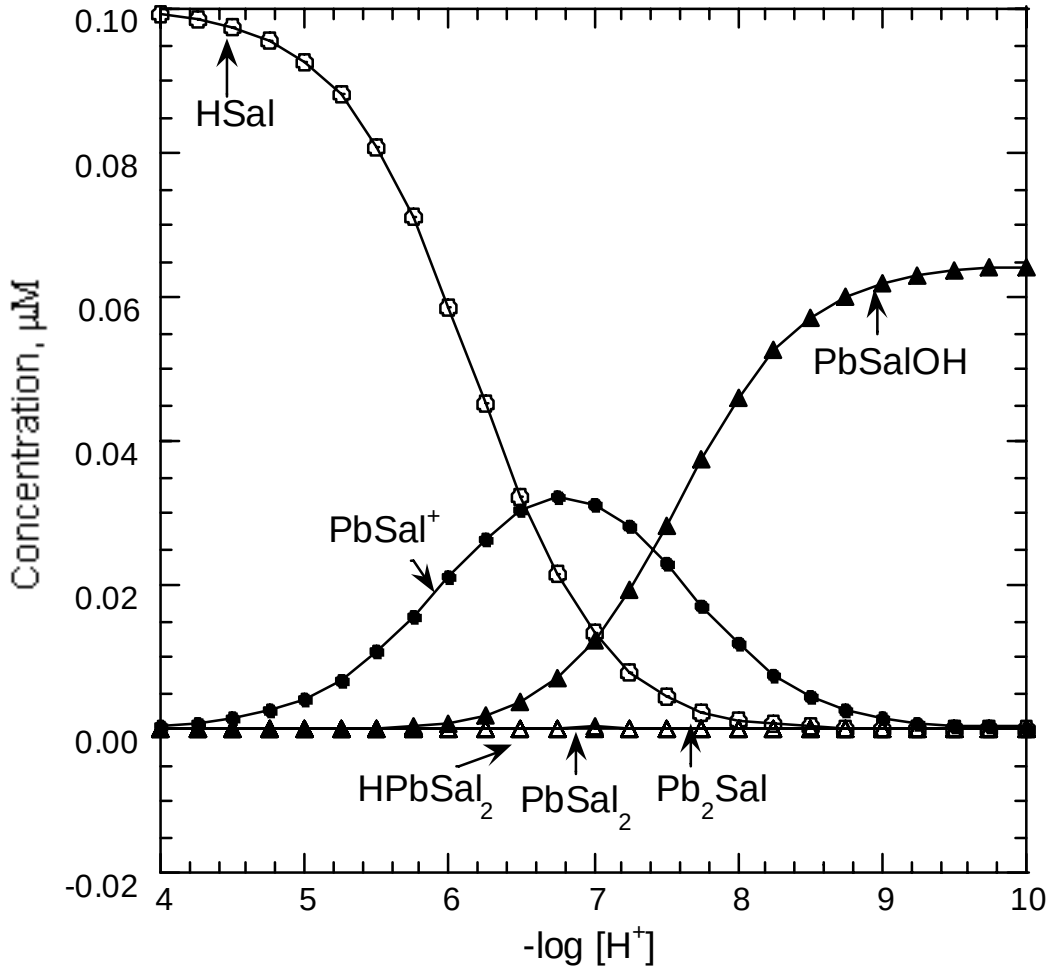


Figure VI.9. Species distribution curves for lead-salinomycin complexes as a function of p[H] in 80% methanol-water. Species concentrations were calculated using the program Comics[27] for 0.1 μM salinomycin and 0.1 μM lead using the values listed in Table V.7.

References

(1) Frausto da Silva, J. J. R.; Williams, R. J. P. *The Biological Chemistry of the Elements: the Inorganic Chemistry of Life*; Oxford University Press Inc.: New York, **2001**,

(2) Hamidinia, S. A.; Shimelis, O. I.; Tan, B.; Erdahl, W. L.; Chapman, C. J.; Renkes, G. D.; Taylor, R. W.; Pfeiffer, D. R. *J. Biol. Chem.* **2002**, *277*, 38111-38120.

(3) Hamidinia, S. A.; Tan, B.; Erdahl, W. L.; Chapman, C. J.; Taylor, R. W.; Pfeiffer, D. R. *Biochemistry* **2004**, *43*, 15956-15965.

(4) Chapman, C. J.; Puri, A. K.; Taylor, R. W.; Pfeiffer, D. R. *Biochemistry* **1987**, *26*, 5009-5018.

(5) Kauffman, R. F.; Taylor, R. W.; Pfeiffer, D. R. *Biochemistry* **1982**, *21*, 2426-2435.

(6) Taylor, R. W.; Chapman, C. J.; Pfeiffer, D. R. *Biochemistry* **1985**, *24*, 4852-4859.

(7) Taylor, R. W.; Pfeiffer, D. R.; Chapman, C. J.; Craig, M. E.; Thomas, T. P. *Pure Appl. Chem.* **1993**, *65*, 579-584.

(8) Toro, M.; Arzt, E.; Cerbon, J.; Alegria, G.; Alva, R.; Meas, Y.; Estrada-O, S. *J. Membr. Biol.* **1987**, *95*, 1-8.

(9) Sabela, A.; Koryta, J.; Valent, O. *J. Electroanal. Chem.* **1986**, *204*, 267-272.

(10) Antonenko, Y. N.; Yaguzhinsky, L. S. *Biol. Membr.* **1988**, *5*, 718-727.

(11) Ivanova, O. G., Ph.D. Thesis, University of Oklahoma, Norman, OK, **2000**.

(12) Pointud, Y.; Pierzo, C.; Tissier, C.; Juillard, J. *J. Chim. Phys. Phys.-Chim. Biol.* **1985**, *82*, 891-897.

(13) Bolte, J.; Demuynck, C.; Jeminet, G.; Julliard, J. *Can. J. Chem.* **1982**, *60*, 981-989.

(14) Tissier, C.; Juillard, J.; Boyd, D. W.; Albrecht-Gary, A. M. *J. Chim. Phys.* **1985**, *82*, 899-906.

(15) Rorabacher, D. B.; MacKellar, W. J.; Shu, F. R.; Bonavita, M. *Anal. Chem.* **1971**, *43*, 561-573.

(16) Shedlovsky, T.; Kay, R. L. *J. Phys. Chem.* **1956**, *60*, 151-155.

(17) Martell, A. E.; Motekaitis, R. J. *Determination and Use of Stability Constants*, 2nd ed.; VCH Publishers: New York, **1992**,

(18) Painter, G. R.; Pressman, B. C. *Top. Curr. Chem.* **1982**, *101*, 84-110.

(19) Cornelius, G.; Gartner, W.; Haynes, D. H. *Biochemistry* **1974**, *13*, 3052-3057.

(20) Lutz, W. K.; Wipf, H. K.; Simon, W. *Helv. Chim. Acta.* **1970**, *53*, 1741-1746.

(21) Alva, R.; Lugo-R., J. A.; Arzt, E.; Cerbon, J.; Rivera, B., E.; Toro, M.; Estrada-O *J. Bioenerg. Biomembr.* **1992**, *24*, 125-129.

(22) Riddell, F. G.; Tompsett, S. T. *Biochim. Biophys. Acta* **1990**, *1024*, 193-197.

(23) Barrans, P. Y.; Alleaume, M.; Jeminet, F. *Acta Crystallogr., Sect. B* **1982**, *38*, 1144-1147.

(24) Walba, D. M.; Hermsmeier, M.; Haltiwanger, R. C.; Noordik, J. H. *J. Org. Chem.* **1986**, *51*, 245-249.

(25) Pangborn, w.; Duax, W.; Langs, D. *J. Am. Chem. Soc.* **1987**, *109*, 2163-2166.

(26) Pointud, Y.; Tissier, M.; Juillard, J. *J. Solution Chem.* **1983**, *12*, 473-483.

(27) Smith, R. M.; Martell, A. E. *NIST Critically Selected Stability Constants of Metal Complexes Database*, Version 5.0; U.S. Secretary of Commerce, **1998**,

(28) Pfeiffer, D. R. Ohio State University, Columbus, OH; Taylor, R. W. University of Oklahoma., Norman, OK *Personal Communications* **1999-2005**.